Trace elements variations in polar ice during the late quartenary with special emphasis on cosmic fallout

Paolo Gabrielli

LABORATOIRE DE GLACIOLOGIE ET GEOPHYSIQUE DE L'ENVIRONNEMENT
(UMR CNRS-UNIVERSITE JOSEPH FOURIER 5183)

DIPARTIMENTO DI SCIENZE AMBIENTALI
(UNIVERSITÁ CA'FOSCARI DI VENEZIA)

VARIATION DES ELEMENTS PRESENTS A L'ETAT DE TRACES DANS LES GLACES POLAIRES PENDANT LA FIN DU QUATERNAIRE, NOTAMMENT EN LIAISON AVEC LES RETOMBEES DE MATIERE EXTRATERRESTRE

VARIAZIONE DEGLI ELEMENTI IN TRACCIA NEL GHIACCIO POLARE DURANTE IL TARDO QUATERNARIO CON PARTICOLARE ATTENZIONE RIGUARDO AL FLUSSO DI MATERIALE COSMICO

TRACE ELEMENTS VARIATIONS IN POLAR ICE DURING THE LATE QUATERNARY WITH SPECIAL EMPHASIS ON COSMIC FALLOUT

Paolo GABRIELLI

Thèse de doctorat de l'Université Joseph Fourier - Grenoble (France)
(Arrêtés ministériels du 5 Juillet 1984 et 30 mars 1992)
en cotutelle avec l'Università Ca'Foscari di Venezia (Italia)

Spécialité : Doctorat en Sciences de la Terre et de l'Univers

Specialità: Dottorato in Scienze Ambientali

Soutenance: Grenoble, 26 Octobre 2004

Composition du jury :

M.	Freddy ADAMS	Président du Jury
M.	Bernard MARTY	Rapporteur
M.	Eric WOLFF	Rapporteur
M.	Gabriele CAPODAGLIO	Examinateur
M.	John PLANE	Examinateur
M.	Carlo BARBANTE	Directeur de thèse
M.	Claude BOUTRON	Directeur de thèse

Singularly, when I received the message that Carlo Barbante left on my answer machine in April 2001, I was at the Venice airport, coming back from a meeting for Safety Health and Environment managers, held by my ex company in Paris. I thank Carlo for that telephone call and then for constantly following and supporting me during these three years.

I'm particularly grateful also to Claude Boutron because, although predicting the three hardest years of my life at the beginning of this PhD, he continuously transferred to me the enthusiasms of his scientific impetus that allowed me to face this challenge in the best conditions.

I thank very much Freddy Adams, Gabriele Capodaglio, Bernard Marty, John Plane and Eric Wolff for accepting of being part of my PhD commission. I want to thank John Plane also for his fundamental and rigorous scientific support during all the PhD period.

I'm grateful also to Petru Jitaru, Frédéric Planchon and Paul Vallelonga for their scientific collaboration and their important direct contribution in the redaction of this manuscript. I want to thank also Paul Crutzen, Sungmin Hong, Jean Robert Petit and Kevin Rosman for their kind scientific assistance and collaboration.

I warmly thank the "ICP SFMS snow team" components of the laboratory of Paolo Cescon at the University Ca'Foscari of Venice and in particular Warren Cairns, Giulio Cozzi, Vania Gaspari and Anita Varga, not only for their highly professional help but also for their friendly support. I want to thank also the components of the "Mercury team" of the LGGE in Grenoble, Aurelien Dommergue, Christophe Ferrari,

Pierre Alexis Gauchard and Sonia Nagorsky for their friendly help and important scientific collaboration.

A special thank to Sophie Bernard, Olivier Magand, Estelle Poutou and Nico for their great hospitality during the final part of my PhD and to Marco Benedetti, Marco Favaro and Silvia for their hospitality in Venice during these three years. I want to thank also all the other friends and colleagues of the LGGE and in particular Gilles Aymoz, Olivier Alemanni, Jean Philippe Ballestrieri, Hervé Bonnaveira, Jean Francois Chemin, Danièle Cordier, Robert Delmas, Barbara Delmonte, Gael Durand, Paul Duval, Jean-Luis Gabarre, Francisco Ferron, Michel Fily, Dimitry Khvorostyanov, Gerhard Krinner, Alain Manouvrier, Jacques Meyssonnier, Marie Christine Mieulet, Michelle Poinsot, Dominique Raynaud, Jocelyne Roquemora, Delphine Six, Sophie Seguinel.

I want to thank all the components of the EPICA Science and Drilling teams, the people of logistic from ENEA and all the friends and colleagues working with me in Dome C during the season 2002/2003.

Finally, I want to thank Natascia that immediately believed in this project, encouraging me to accept this challenge and then patiently waiting. This manuscript is dedicated to her.

INDEX

RÉSUMÉ

L' analyse des éléments traces dans les carottes de glace profondes provenant des régions polaires apportent de précieuses informations environnementales sur les sources naturelles de ces éléments, le transport longue distance de ces éléments et les mécanismes de dépôts des aérosols au cours du Quaternaire récent (les dernières centaines de milliers d'années).

Dans cette étude, nous avons mesuré de nombreux éléments traces (Li, Mg, V, Cr, Mn, Co, Cu, As, Rb Sr, Cd, Ba, Ir, Pt, Hg (incluant MeHg et Hg^{2+}), Pb (et les isotopes du Pb), Bi et U) dans diverses sections de trois carottes de glace profondes qui ont été forées en Antarctique et au Groenland dans le cadre de programmes internationaux: la carotte de Dome C/EPICA (derniers ~220,000 ans), la carotte de Vostok (derniers ~410,000 ans) et la carotte de GRIP (derniers ~100,000 ans). Les analyses ont été réalisées en salle blanche par spectrométrie de masse à secteur magnétique couplée à un plasma induit (ICP-SFMS), par spectrométrie de masse à ionisation thermique (TIMS) et par spectrométrie de masse à temps de vol couplée à un plasma induit.

Les résultats obtenus pour Ir et Pt montrent des preuves des retombées passées des produits de vaporisation et de recondensation des poussiéres météoritiques, vers les calottes polaires. Les flux de retombées des dérivé de poussiéres météoritiques ont été utilisés pour estimer le taux d'accrétion passés des particules interplanétaires sur le planète Terre. Le but étant également d'identifier d'ancients changements de la circulation atmosphérique Antarctique telle qu'une plus forte subsidence vers le plateau Antarctique de l'Est au cours des périodes climatiques froides.

Cette étude confirme aussi que les poussières crustales ont été des supports de transport privilégié pour de nombreux éléments traces vers l'Antarctique au cours des périodes climatiques les plus froides. En particulier pour le Pb, l'approche isotopique indique d'une part une source géographique unique pour les poussières d'origine crustale et d'autre part une contribution significative provenant du volcanisme. Finalement, l'analyse des espèces du Hg montre des concentrations plus fortes d'environ un ordre de grandeur que les données précédemment publiées, indiquant ainsi l'importance des phénomènes de dépôts au cours des derniers âges glaciaires.

RIASSUNTO

Lo studio degli elementi in traccia nelle carote di ghiaccio polari fornisce importanti informazioni ambientali, riguardanti le sorgenti naturali di aerosol ed i relativi processi globali di trasporto e di deposizione durante il tardo Quaternario (ultime centinaia di migliaia di anni).

Nell'ambito di questo lavoro sono stati analizzati diversi elementi in traccia (Li, Mg, V, Cr, Mn, Co, Cu, As, Rb, Sr, Cd, Ba, Ir, Pt, Hg (con MeHg e Hg2+), Pb (con i suoi isotopi), Bi and U) in vari campioni di ghiaccio appartenenti a tre carote prelevate in Antartide e in Groenlandia nell'ambito di diversi programi internazionali: la carota di EPICA a Dome C, (ultimi ~220,000), la carota di Vostok (ultimi ~410,000) e la carota di GRIP (ultimi ~100,000). Le analisi sono state compiute in laboratori a contaminazione controllata mediante la tecnica analitica della spettrometria di massa accoppiata induttivamente ad una sorgente al plasma (ICP-SFMS), della spettrometria di massa a ionizzazione termica (TIMS) e della spettrometria di massa a tempo di volo accoppiata induttivamente ad una sorgente al plasma (ICP-TO-SFMS)

Attraverso l'analisi di iridio e platino è stata rilevata la presenza nel ghiaccio preistorico della Groenlandia e dell'Antartide dei prodotti di vaporizzazione e ricondensazione dei meteoroidi, il cosiddetto "meteoric smoke", depositatosi in passato sulle calotte polari. La determinazione di questo flusso ha permesso di stimare l'input globale del particellato di origine cosmica ed ha consentito di individuare antiche variazioni nella circolazione atmosferica dell'Antartide ed in particolare di un rafforzamento dei processi di subsidenza sul plateau antartico durante i periodi climatici più freddi.

Questo studio conferma inoltre che, in generale, il principale vettore degli elementi in traccia in Antartide durante le ere glaciali, è stato il particolato di origine crostale. In particolare lo studio degli isotopi del piombo rafforza l'idea di un'unica sorgente di polvere continentale suggerendo inoltre un possibile e significativo contributo vulcanico. Infine, la determinazione delle specie del mercurio ha messo in luce concentrazioni di circa un ordine di grandezza superiori rispetto a quanto riportato precedentemente, indicando l'importanza dei processi di deposizione durante le ere glaciali.

ABSTRACT

The determination of trace elements in deep polar ice cores provides important environmental information concerning natural sources, long-range transport and deposition processes of the aerosol during the late Quaternary (last few hundred thousands years).

In this work, we have measured various trace elements (Li, Mg, V, Cr, Mn, Co, Cu, As, Rb, Sr, Cd, Ba, Ir, Pt, Hg (including MeHg and $Hg2^{+}$), Pb (including Pb isotopes), Bi and U) in various sections of three deep ice cores which were drilled in Antarctica and Greenland as part of international programmes: the Dome C/EPICA ice core (past ~220 kyr), the Vostok ice core (past ~410 kyr) and the GRIP ice core (past ~100 kyr). The analyses were performed by Inductively Coupled Plasma Sector Field Mass Spectrometry, Thermal Ionization Mass Spectrometry and Inductively Coupled Plasma Time of Flight Sector Field Mass Spectrometry, in clean room conditions.

The results obtained for Ir and Pt shows evidence of the past fallout of vaporization and re-condensation products of meteoroids, the "meteoric smoke", to the polar ice caps. The meteoric smoke influx was used to estimate the past accretion rate of interplanetary dust particles to the Earth and to identify ancient changes in the Antarctic atmospheric circulation such as an enhanced subsidence onto the East Antarctic plateau during cold climatic stages.

This study confirms also that crustal dust was the main carrier of various trace elements to East Antarctica during the coldest climatic stages. In particular, lead isotopes systematic supports the idea of a single dust source area and suggests a significant contribution from volcanoes. Finally, mercury species determination highlights concentrations higher by about one order of magnitude than values previously reported, indicating the importance of deposition processes during the last glacial ages.

I OBJECTIVES OF THIS STUDY

This study is aimed at assessing and deciphering natural variations of atmospheric trace elements in Greenland and Antarctic ice during the last few climatic cycles. The ice samples considered here are valuable sections of three deep international ice cores drilled in Greenland at Summit (GRIP) and in East Antarctica at Dome C and Vostok, with special emphasis on the EPICA/Dome C ice core, which reached a depth of 3190 m in January 2003, covering eight glacial cycles [*Epica community members*, 2004].

The principal objective of this study is the evaluation of the natural variations of two platinum group elements (PGEs), Ir and Pt, in the three above mentioned polar ice cores during the last few climatic cycles. These elements, highly enriched in chondritic meteorites [*Anders and Grevesse*, 1989], are taken as proxy of cosmic material and in particular of the fallout of the meteoric smoke particles which originate in the mesosphere (~ 50 – 90 km of altitude) as ablation products of meteoroids and interplanetary dust particles (IDPs) [*Hunten et al.*, 1980]. Our work aims at estimating the accretion rate of cosmic material vaporized in the mesosphere and whether there is a relationship between cosmic fallout fluxes of IDPs and past climate changes in the Earth's system [*Muller and MacDonald*, 1995].

By studying the meteoric smoke fallout fluxes to Greenland and Antarctica, poorly known processes concerning the global transport of aerosol particles from the upper layers of the atmosphere down to the surface of the polar ice caps can also be investigated. Moreover, the contribution from terrestrial natural sources such as continental dust and volcanic emissions to Ir and Pt fluxes will be evaluated in order

to obtain a preliminary overview of the global geochemical processes driving the occurrence of these metals in the Earth's system.

The second objective is the determination of various other trace elements in Antarctic ice such as Li, Mg, V, Cr, Mn, Co, Cu, As, Rb, Sr, Cd, Ba, Hg, Pb, Bi and U in order to study the natural sources and the processes of transport and deposition of tropospheric aerosol to the East Antarctic plateau during the last few climatic cycles. A particular attention is devoted to the study of Pb isotopes which could allow to better identify source areas of aeolian particles found in ancient ice and could help to distinguish different kinds of natural sources by discriminating for instance between crustal and volcanic contributions. Finally, the evaluation of Hg and its species, such as Hg^{2+} (inorganic mercury) and MeHg (methylmercury), will aim at determining possible variations in oceanic paleoproductivity and Hg deposition processes during the last few climatic cycles.

II STRUCTURE AND CONTENTS OF THE THESIS

CHAPTER 1: INTRODUCTION

In this chapter introductive information about the study of the trace elements in snow and ice cores are given. A short historical note is reported with special emphasis on the previously published studies concerning Ir and Pt in polar snow and ice. Moreover, this chapter illustrates the general scientific context of the investigations of cosmic material ablating in the mesosphere and subsequently accreting to Earth. Finally, we give a general overview of the Antarctic and Greenland drilling sites, the ice core sections considered in this work and the analytical procedures.

CHAPTER 2: PAST FALLOUT OF METEORIC SMOKE TO THE POLAR ICE CAPS

This chapter is based on three articles describing the study of Ir and Pt, which were used as tracers of cosmic material fallout to the Greenland and Antarctic ice caps during the last few climatic cycles.

The first article describes in detail the new analytical methodology which we have developed during this thesis for the determination of Ir an Pt concentrations at ultra low levels in unfiltered melted samples of polar ice. It is based on inductively coupled plasma sector field mass spectrometry (ICP-SFMS) coupled with a micro-flow nebulizer and desolvation system together with a pre-concentration procedure. This article was recently published in the *Journal of Analytical Atomic Spectrometry, 19, 831-837, 2004.*

The second article presents the results obtained from the measurement of Ir and Pt in various sections of the 3029 m deep Greenland ice core drilled as part of the European program Greenland Ice Core Project GRIP [*Dansgaard et al.*, 1993], dated from ~0.7 to 128 kyr BP. Results reveal the signature of meteoroid ablation products, known as meteoric smoke particles and provide important information regarding the transport of meteoric smoke from the mesosphere to the surface of the polar ice caps. This article was submitted to "*Nature*" in May 2004. The version presented here is the revised version, which was sent to *Nature* in August 2004.

The third article presents two records of Ir and Pt obtained from the analysis of various sections of two deep Antarctic ice cores: the new 3190 m Dome C/EPICA ice core [*Epica community members*, 2004], and the 3623 m Vostok ice core [*Petit et al.*, 1999]. The sections, which were analysed, were from the upper 2193 m of the Dome C/EPICA ice core (age from 0.6 to 217 kyr BP) and from the upper 2751 m of the Vostok ice core (age from 4.6 to 237 kyr BP). These records show a meteoric smoke fallout strongly associated with past low temperatures, evidencing subsidence of cold air masses from the upper troposphere of East Antarctica during the coldest climatic stages. This article will be submitted soon to "*Science*".

CHAPTER 3: TRACE ELEMENTS VARIATION IN EAST ANTARCTICA DURING THE LATE QUATERNARY.

This chapter is based on two articles describing the results obtained from the measurement of various trace elements in the Dome C/EPICA and Vostok cores during the last two (Dome C) and four (Vostok) climatic cycles.

The first article illustrates the measurement of Li, V, Cr, Mn, Co, As, Rb, Sr, Ba, Bi and U in Vostok ice dated from ~4,6 to ~410 kyr years BP. We show that

concentrations were highly variable, with low values during warm periods and much higher values during the coldest stages of the last four ice ages. The contribution from the different possible natural sources such as rock and soil dust, sea salt aerosol and volcanic emissions are discussed for each metal. This article has just been submitted to "*Earth and Planetary Science Letter*".

The second article deals with the determination of Li, Mg, Cr, Mn, Co, Cu, As, Rb, Cd, Ba and Bi in samples from the new Dome C/EPICA ice core, down to the depth of 2193 m. It is shown that during the ~220 kyr spanned by this record, concentrations were highly variable, with low values during warm periods and high values during cold periods, matching remarkably well the insoluble dust concentration profile obtained in the same core. This article will be submitted soon to "*Atmospheric Environment*".

CHAPTER 4: LEAD ISOTOPES IN EAST ANTARCTIC ICE DURING THE LAST TWO CLIMATIC CYCLES

This chapter, made of a single article, presents the results obtained by measuring ^{204}Pb, ^{206}Pb, ^{207}Pb, ^{208}Pb in the EPICA/Dome C ice core samples extending back to ~220 kyr BP. It is the longest time series of Pb isotopes ever reported from an ice core. The data show that Pb isotopic ratios in Antarctic ice varied in parallel with changing climate, and can be explained by changing mixtures of crustal and volcanic lead. This article has been submitted for publication in "*Geophysical Research Letters*".

CHAPTER 5: DETERMINATION OF TOTAL MERCURY AND MERCURY SPECIES IN EAST ANTARCTICA OVER THE LAST TWO CLIAMATIC CYCLES

This chapter is made of two articles, devoted to the investigation of Hg and Hg species in Antarctic ice.

The first article presents the new analytical method, which we have developed for the direct determination of Hg in polar snow and ice. It is based on the use of Inductively Coupled Plasma Sector Field Mass Spectrometry (ICP-SFMS). The potential of this new method was illustrated by successfully measuring Hg in various snow and ice samples from Antarctica and the Arctic. This article has been published in *Journal of Analytical Atomic Spectrometry, 19, 823-830, 2004.*

The second article reports the determination of total Hg, methylmercury (MeHg) and inorganic mercury (Hg^{2+}) obtained from the analysis of various sections of the upper 2138 m of the Dome C/EPICA ice core back to ~210 Kyr. The measurements were performed using an original method developed at the Department of Chemistry of the University of Antwerpen (Solid-phase Microextraction and Multicapillary Gas Chromatography Hyphenated to Inductively Coupled Plasma-Time-of-Flight-Mass Spectrometry). Levels of mercury species much higher than concentrations previously obtained, were recorded during the last glacial age, highlighting the importance of enhanced processes of Hg deposition during this period. This article has been prepared for submission to "*Nature*".

CHAPTER 6: CONCLUSIONS AND PERSPECTIVES.

In this last chapter the most innovative scientific knowledge produced by this work is summarised, together with the most promising perspectives for future investigations, with special focus on the analytical aspects that will need to be further addressed for the determination of ultra low concentrations of Ir and Pt in polar ice.

1 INTRODUCTION

1.1 Trace element studies in snow and ice

1.1.1 Pioneering heavy metals studies

The history of the study of trace elements, especially heavy metals, in polar snow and ice started in the 1960s when Clair Patterson, a geochemist at the Department of Earth and Planetary Sciences of the California Institute of Technology (Caltech) was the first to accurately determine lead in snow and ice dated from the last few centuries and collected in North West Greenland and in West Antarctica [*Murozumi et al.*, 1969]. When he became interested in snow and ice, Clair Patterson was already a famous scientist [*Bertsh Mc Grayne*, 2002; *Nriagu*, 1999]. He had already given the first accurate determination of the age of the Earth [*Patterson*, 1956; *Patterson et al.*, 1955], pioneered the concept of contamination control in handling environmental samples [*Patterson and Settle*, 1976] and been one of the very first to realize that humankind was polluting the global environment for lead especially because of the extensive use of the lead additives for gasoline which were discovered in the early 1920s by Thomas Midgely [*Nriagu*, 1990].

In the course of his study of the extent of lead pollution, Clair Patterson realized that he needed to determine past changes in the occurrence of this metal in atmospheric archives such us dated snow and ice deposited in the Greenland and Antarctic ice caps. It led him and his co-workers M. Murozumi and T.J. Chow to develop highly innovative ultra clean procedures to collect snow samples in remote areas in Greenland and Antarctica, and to pioneer ultra sensitive techniques to

accurately determine lead in these very valuable samples by isotope dilution with thermal ionization mass spectrometry. It especially allowed them to obtain the very first data on changes in lead concentrations in Greenland snow and ice from 800 years BC to the mid-1960s [*Murozumi et al.*, 1969]. These data conclusively showed for the first time that natural lead concentrations in Greenland ice were extremely low 800 years BC (~ 1 ppt). They also documented a very spectacular increase of lead concentrations in Greenland snow from the Industrial Revolution onward, up to concentrations of ~ 200 ppt in the mid-1960s [*Murozumi et al.*, 1969]. A large part of this tremendous increase was observed after the 1930s and was clearly linked with the ever-increasing use of lead additives in gasoline especially in the US. This famous paper played a major role in the phasing out of lead additives.

Later, Clair Patterson was the first to be able to analyse accurately lead and other trace elements in deep ice cores whose outside had been highly contaminated during drilling operations [*Ng and Patterson*, 1981]. This was achieved by developing sophisticated procedures which allowed to decontaminate the contaminated core sections by chiselling successive veneer layers of ice in progression from the outside to the centre, without transferring the enormous contamination present on the outside to the inner core. This major step allowed for the accurate analysis of lead and several other trace elements in a few sections from the Camp Century Greenland ice core and the Byrd Antarctic ice core, allowing to confirm that natural lead concentrations in polar ice were extremely low [*Ng and Patterson*, 1981].

1.1.2 The Patterson's heritage

Outside Caltech, the first efforts to determine trace elements in polar snow and ice were made by M. Vosters, F. Hanappe and Edward Picciotto at the University of Brussels and by Claude Boutron, Martin Echevin and Claude Lorius at the Laboratoire de Glaciologie in Grenoble. Despite the fact that they made considerable efforts to reduce contamination problems and develop ultra-sensitive analytical techniques, the data they obtained for Antarctic and Greenland snow were not totally reliable and were still in positive error because of not fully solved contamination problems, especially for heavy metals. Just to give an example, lead concentrations in surface Antarctic snow published by Boutron and Lorius in the 1970s [*Boutron and Lorius*, 1979] were about one order of magnitude higher than the values, which were obtained later using improved decontamination procedures.

At that time, it became rapidly obvious that the only way to improve the situation was to work directly with Clair Patterson. This was achieved by Claude Boutron who went to Caltech for rather long time periods to learn about the ultra-clean procedures, which were used in the clean laboratory at Caltech. During these stays, Claude Boutron and Clair Patterson were the first to obtain data on past changes in lead and other heavy metals in Antarctic ice during the last climatic cycle, through the analysis of various sections of the 905 m Dome C core and the 2083 m Vostok core [*Boutron and Patterson*, 1986; *Boutron et al.*, 1987].

Later, the "Caltech know how" was transferred not only to the Laboratoire de Glaciologie in Grenoble but also to several other laboratories in Cambridge (Eric Wolff and his colleagues), Perth (Kevin Rosman and his colleagues), Moscow (Michael Bolshov and his colleagues), Venice (Carlo Barbante and his colleagues) and Seoul (Sungmin Hong and his colleagues).

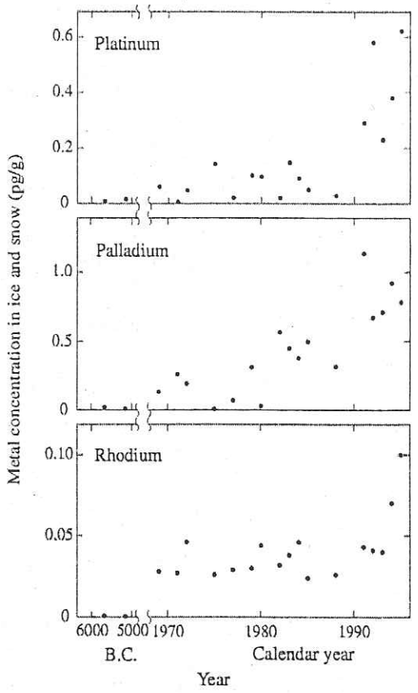

Fig 1: *Pt, Pd, Rh variation from Greenland snow and ice archives during the last decades* [*Barbante et al.*, 2001]. *The increase of these metals revealed a hemispheric pollution due to the emissions of vehicles equipped with catalytic converters.*

The joint efforts between these different laboratories allowed during the last 15 years to produce a considerable number of reliable data on heavy metals and other trace elements in snow and ice collected at various location in Greenland, Antarctica, the Alps and the Andes. Amongst the most spectacular results obtained so far are the evidence of an early pollution of the Northern Hemisphere for lead and copper two millennia ago at the peak of the Roman civilization [*Hong et al.*, 1994; *Hong et al.*, 1996a], the evidence of the large scale pollution for platinum, palladium and rhodium linked with the use of catalytic converters (see Fig. 1) [*Barbante et al.*, 2001], and the evidence of an early pollution of the Antarctic continent for lead [*Planchon et al.*, 2003; *Wolff and Suttie*, 1994].

1.1.3 Importance of further trace elements studies in ice cores

The study of heavy metals and other trace elements in deep Antarctic and Greenland ice cores spanning successive climatic cycles has the potential to provide with very interesting information on past natural cycles of these elements for different climatic conditions. Such information is especially needed to provide a firm understanding of natural background levels against which recent man induced changes can be evaluated. Also, it can provide with various information, which can be of high interest for climate specialists. In addition, deep ice cores can allow obtaining unique information on various geophysical parameters such as, for instance, the fallout of extraterrestrial material to Earth.

Despite this high interest, data on heavy metals and other trace elements in deep ice cores remain rather limited and pertain only to a few elements, mainly lead.

Just to give a few examples, there were almost no data on Ir and Pt in deep Antarctic ice when this work was initiated. Also, there were almost no data on lead isotopes, and no data at all on methylmercury.

The general aim of this work is to take advantage of several deep international ice cores (the 3029 m GRIP ice core drilled in Central Greenland [*Dansgaard et al.*, 1993]; the 3623 m Vostok ice core drilled in East Antarctica [*Petit et al.*, 1999] and the new 3190 m Dome C/EPICA ice core drilled in East Antarctica [*Epica community members*, 2004]) to obtain extensive data on the past variations of various trace elements during the last few climatic cycles, with special emphasis on iridium and platinum and to a lesser extent on other trace elements, lead isotopes and methylmercury. Our work benefited from the considerable advances made in analytical instrumentation during recent years, especially the availability of the highly sensitive inductively coupled plasma sector field mass spectrometry instruments.

1.2 Ir and Pt studies in snow and ice: state of the art

1.2.1 Ir as tracer of cosmic material

Platinum Group Elements (PGEs) are depleted in the upper terrestrial crust [*Wedepohl*, 1995] and enriched in the terrestrial mantle and in meteorites [*Anders and Grevesse*, 1989]. In particular, Ir average concentration in the Earth's crust is 0.05 ppb, while the corresponding value for chondritic meteorites is 481 ppb, about 10,000 times more.

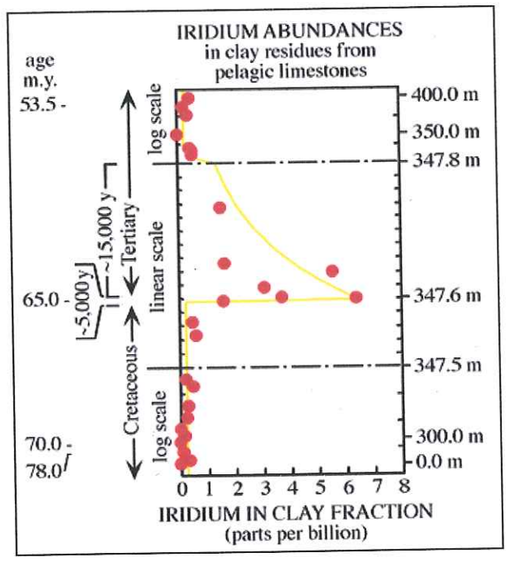

Fig. 2: *The Ir anomaly in the Cretaceous/Tertiary boundary clay layer suggesting the impact of a large extraterrestrial body against Earth about 65 millions years ago [Alvarez et al., 1980].*

Amongst the first attempts for measuring the extraterrestrial accretion rate, using PGEs as a proxy, was the determination of Ir in marine sediments [*Barker and Anders*, 1968]. The impetus in the field of PGEs studies came suddenly in 1980 when L. W. Alvarez and his co-workers determined Ir in geological deposits, trying to determine the sediment accumulation rate. He was using the comic flux of Ir, assumed to be constant over time, as a normalization factor for the determination of the accumulation rate of the sediments. He discovered incidentally an anomalous and large Ir enrichment in a boundary clay layer dated from the end of the Cretaceous and the beginning of the Tertiary period, about 65 millions years ago [*Alvarez et al.*, 1980]. This layer, nowadays widely know as the KT boundary, was surprisingly synchronous with a massive biological extinction. He proposed that a large extraterrestrial body hit the Earth at that time, both causing a large biological extinction and the global Ir enrichment recorded in the KT boundary clay layer.

This theory remained controversial for at least a decade but finally the discovery of the Chicxulub crater close to the Mexico coast [*Hildebrand and Boynton*, 1990] concurrently with several others cosmic impact's evidences, such as for instance the discovery of the occurrence of Ir micro-particles in terrigenous sediments [*Schuraytz et al.*, 1996], convinced most of the scientific community. It became therefore clear that Ir enrichment in sediments were potentially striking evidence of large extraterrestrial bodies impacts. It opened the way also to the search of these iridium anomalies in different environmental archives such deep polar ice cores.

1.2.2 Previous studies of Ir in polar snow and ice

From an historical point of view, the first attempt for measuring Ir in an ice core was reported in 1978 by Takahashi et al., who determined Ir in a single sample of Greenland ice, using Instrumental Neutron Activation Analysis (INAA). They found an Ir concentration of 0.37-3.4 ppb in particulates obtained from that sample [*Takahashi et al.*, 1978]. A major drawback of this study is that we do not know where the sample was collected and what was its age.

Early attempts by glaciologists for determining the signature of the impact of a large extraterrestrial bodies in polar snow and ice archives were focused on the historically well documented event which occurred at Tunguska in 1908, when a medium size extraterrestrial body exploded in the atmosphere above this remote area in Siberia. This region, covered essentially by conifers, experienced a strong heating in an area of several hundred square km. Two decades after the event, a scientific expedition exploring that region, discovered a devastated forest with remnants of a large forest fire.

In 1983, Ganapathy claimed that he had discovered the signature of the Tunguska explosion in the snow of the geographic South Pole: he found an Ir peak of ~150 10^6 atom cm^{-2} y^{-1} in snow dated from the time of the Tunguska event, by analysing particulate matter filtered from snow core samples [*Ganapathy*, 1983]. In 1990, Rocchia and his co-workers repeated the same test at the South Pole but did not detect any significant peak above an Ir flux background of about 5 10^6 atom cm^{-2} y^{-1} [*Rocchia et al.*, 1990]. In 1995, Rasmussen and his co-workers did not detect any Ir anomaly in Greenland ice core samples dated back at the beginning of the last century. They determined an Ir background flux of about ~1.5 10^{-15} g cm^{-2} y^{-1} [*Rasmussen et al.*, 1995] by measuring the Ir concentration in filtered particulate

matter. Concentrations in the analysed particulate matter ranged from ~100 and ~600 ppt, which corresponds to ~0,02 - 0,05 ppq concentrations, relative to the wet mass of ice.

In 2003, Karner and his co-workers measured Ir in dust obtained by filtering ice from a few sections of the GISP2 deep ice core drilled at Summit in Central Greenland about 30 km from the GRIP core. These sections were dated back from the Holocene and the last glacial period. They recorded a concentration of Ir in the dust ranging from ~50 and ~150 ppt, corresponding to a concentration of ~0,002 up to ~0,15 ppq relative to the wet mass of ice [*Karner et al.*, 2003]. These measurements were at least one order of magnitude lower than the Ir values previously reported by the other authors mentioned above. Therefore serious concerns were arisen by Karner and co-workers regarding the cleanliness of the analytical protocols adopted in the studies conducted before their own work.

It must be emphasized that all the different studies discussed above pertain only to Ir measurements in particulate matter of an equivalent diameter larger than 0.45 μm obtained by filtering the melted ice. The analyses were performed by INAA.

1.2.3 Previous determination of the total concentration of Ir

To our knowledge, the first attempt to determine the total concentration of Ir in polar ice without filtration is that reported very briefly by Takahashi in the paper mentioned in the previous section. He made a preliminary measurement of Ir by INAA, irradiating a single sample of (melted?) ice retrieved at Dome C (East Antarctica) whose depth and age are unknown [*Takahashi et al.*, 1978].

This attempt is very poorly documented. However, it looks like he found a total Ir concentration of 0.31± 0.12 ppq with a blank corresponding of ~75% of the analytical determination and possibly due to the HCl used as a reagent before the irradiation [*Takahashi et al.*, 1978]. This attempt is of particular interest only because it is the only one in which it was not implicitly assumed that Ir in polar ice was prevalently contained in large particles such as micrometeorites or even larger meteoric debris. This assumption drove in fact all the successive investigators to filter their ice and snow samples, so that they measured Ir concentrations in the filtered dust fraction only (larger than about 0.45 μm).

In the following years several analytical procedures were developed for measuring the total concentration of Ir in seawater [*Anbar et al.*, 1997; *Fresco et al.*, 1985; *Hodge et al.*, 1986]. The most recent estimation of Ir concentration in natural waters gives values ranging from 0.1–3 ppq [*Anbar et al.*, 1996]. Nevertheless, this procedure based on isotope dilution negative thermal ionization mass spectrometry was, until now, never applied to ice core studies.

1.2.4 Previous determinations of the total concentration of Pt in environmental samples

Hodge and co-workers developed also a method for measuring Pt in sea water [*Hodge et al.*, 1986]. At that time investigations about Pt were very few, compared with Ir, but the interest for this metal increased when it became clear that enrichment of PGEs other than Ir, were common in the KT boundary layer and that these could be potentially used for detecting the traces left in terrestrial archives by the fallout of debris produced by the impacts of large extraterrestrial bodies [*Evans et al.*, 1993]. Pt

mean concentration in the upper crust and in chondritic meteorites are 0.4 ppb and 990 ppb, respectively, i.e. a factor of about 2,000.

However, it was never used as proxy for extraterrestrial matter in ice and snow studies. In contrast, Pt was recently measured in shallow snow dated from the last few decades because of its recent dispersion as global pollutant due to the emissions from vehicles equipped with catalytic converters based on Pt as a catalyst [*Barbante et al.*, 2001]. To study this recent form of pollution, a procedure aimed at determining Pt, Pd and Rh by Inductively Coupled Plasma Sector Field Mass Spectrometry (ICP SFMS) was developed [*Barbante et al.*, 1999]. This was also the starting point for the development of the new procedure [*Gabrielli et al.*, 2004] for measuring Ir and Pt in polar ice that will be illustrated in chapter 2.1 of this thesis.

1.3 Cosmic matter studies in polar regions: scientific context and interest

1.3.1 A 100 kyr oscillation for climate and cosmic dust flux?

Since the middle of the Pleistocene, about one million of years ago, successive climatic oscillations with a period of ~100 kyr have taken place on Earth [*Imbrie et al.*, 1992; *Petit et al.*, 1999](see Fig. 3) but this periodicity in the Earth's climate record has not yet been explained satisfactorily [*Epica community members*, 2004].

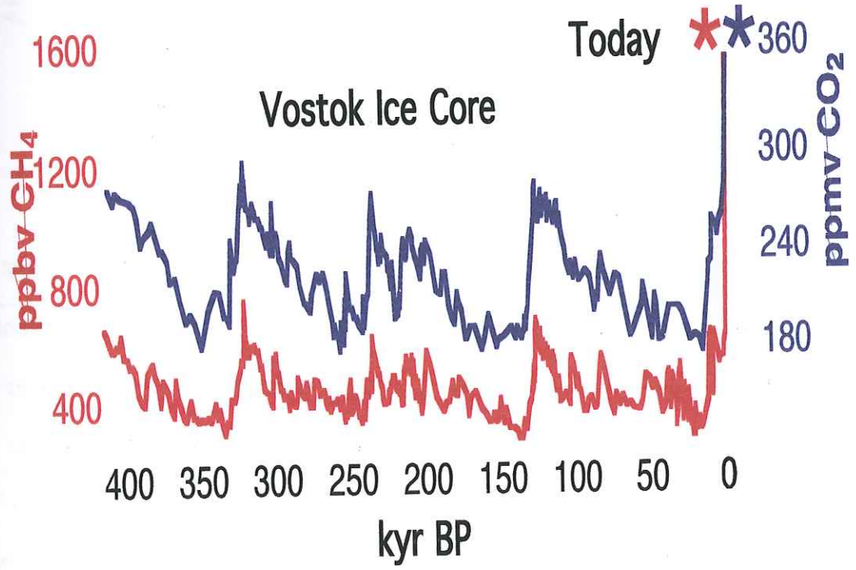

Fig. 3: *Greenhouse gases (CH_4 and CO_2) variations in the Vostok Antarctic ice core during the last 420 kyr [Petit et al., 1999]. These parameters are co-varying with T and evidence that climate has changed with a strong 100 kyr cycle during the late Quaternary, alternating long glacial ages with short interglacial periods.*

An apparent ~100 kyr periodical variation, by nearly a factor of 4, in the flux of extraterrestrial ^{3}He to the sea floor was recorded in 1995 [*Farley and Patterson*, 1995]. This suggests a periodic variation in the accretion of interplanetary dust particles (IDPs), roughly in phase with the climate periodicity. This observation supported the strongly disputed proposal that the ~100 kyr climate cycle is not caused by the Earth's orbit eccentricity variation, as suggested by the Milankovitch astronomical theory of climate [*Berger*, 1988], but by the ~100 kyr tilt variations of the Earth's orbital plane that would have induced this periodicity in the IDPs fallout flux to Earth [*Muller and MacDonald*, 1995].

1.3.2 Possible links between climate and IDPs flux variations

A variation in IDPs accretion rate could affect climate in two different ways: changes in stratospheric ozone and cosmic iron fertilization. Currently about 40 kt of IDPs enter the atmosphere every year. Most of these particles, with initial velocities of 12 – 72 km s^{-1}, heat up to temperature in excess of 2000 K and completely ablate into various metal atoms and ions [*Hunten et al.*, 1980] [*Love and Brownlee*, 1991]. This process is the source of the layers of metal atoms that occur globally between 80 and 110 km of altitude [*Kane and Gardner*, 1993]. Lower in the mesosphere these metals form compounds that agglomerate into particles [*Plane*, 2004]. These metallic particles appear to be the major source of condensation nuclei for sulphuric acid (Junge layer) aerosols [*Murphy et al.*, 1998], which is one of the precursors of polar stratospheric clouds [*Wayne*, 2000]. The chemistry, which is catalysed on the surfaces of these clouds, causes very efficient ozone depletion [*Wayne*, 2000]. In addition,

metallic particles are alkaline, and assist in the removal of nitric acid from the lower stratosphere, thereby enhancing ozone destruction [*Prather and Rodriguez*, 1988].

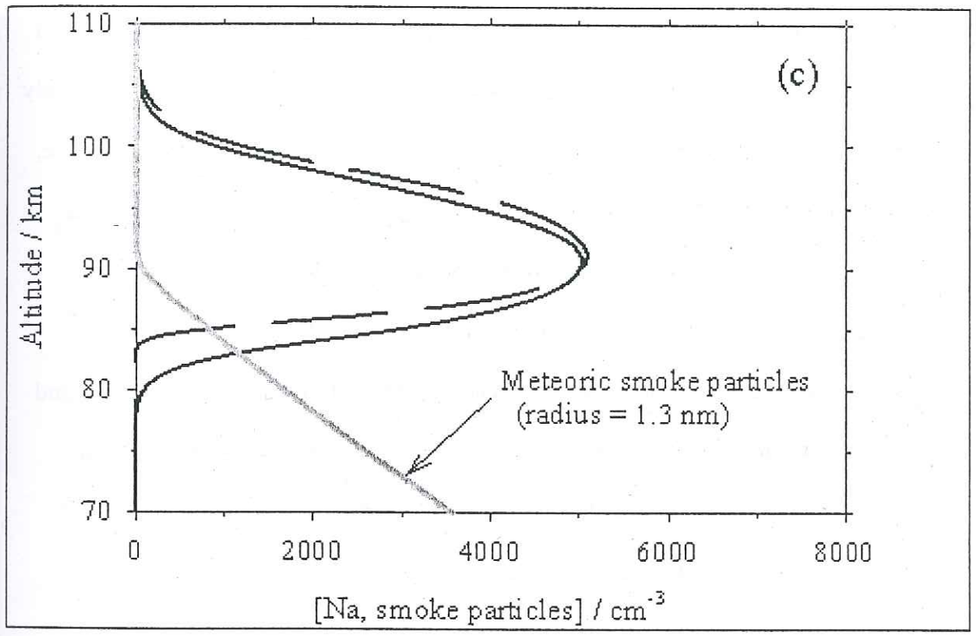

Fig. 4: *Cosmogenic Na layer originating from the meteoroids ablation in the high mesosphere/low thermosphere [Plane, 2004]. The continuous line shows experimental data, while the dotted line shows the variations predicted by a model. Meteoric smoke concentrations are indicated by the grey line; particles coagulate at about 90 km of altitude and then sediment in the lower mesosphere.*

The strong increase in atmospheric CO_2 during the last deglaciation [*Monnin et al*, 2001] has been suggested to be associated to a decrease in the aeolian bio available iron supply to the Southern Ocean [*Martin*, 1990]. Recent iron fertilization experiments have shown that the resulting increase in plankton population leads to a pronounced increase in CO_2 drawdown rate [*Watson et al.*, 2000]. There is also likely to be an increased production of dimethylsulfide, which evades into the atmosphere, where it is oxidised to sulphuric and methane sulphonic acids. These condensable gases provide condensation nuclei for marine stratus clouds, leading to increased albedo and lower surface temperatures [*Charlson et al.*, 1987]. Cosmic ablated material, probably consist of loosely bound polymers of iron (metal) hydroxides and carbonates [*Plane*, 2004]. These may be much more soluble once deposited in the ocean, compared with crustal dust transported from the continents, and thus could make a larger contribution to biological productivity.

1.3.3 Polar Regions and meteoric flux

Polar regions seem to be a key place to study the meteoric flux. Although the flux of meteoric material from ablated IDPs appears to be quite low, averaged over the whole Earth, the material could be transported from the mesosphere to lower altitudes in a non-uniform way. In particular, at the solstices there is a very strong meridional circulation in the mesosphere from the summer pole to the winter pole [*Rees and Bilitza*, 1990](see Fig. 5). It has been shown that a large fraction of air descending from the mesosphere into the stratosphere is concentrated in the winter polar areas [*Russel III et al.*, 1993]. Thus, an enhanced meteoric fallout to polar

regions could give the possibility to more easily detect in polar ice, cosmic proxies like platinum group elements (Pt, Pd, Rh, Ir, Ru, Os) that are strongly enriched in chondritic meteorites when compared with the terrestrial upper crust [*Anders and Grevesse*, 1989; *Wedepohl*, 1995].

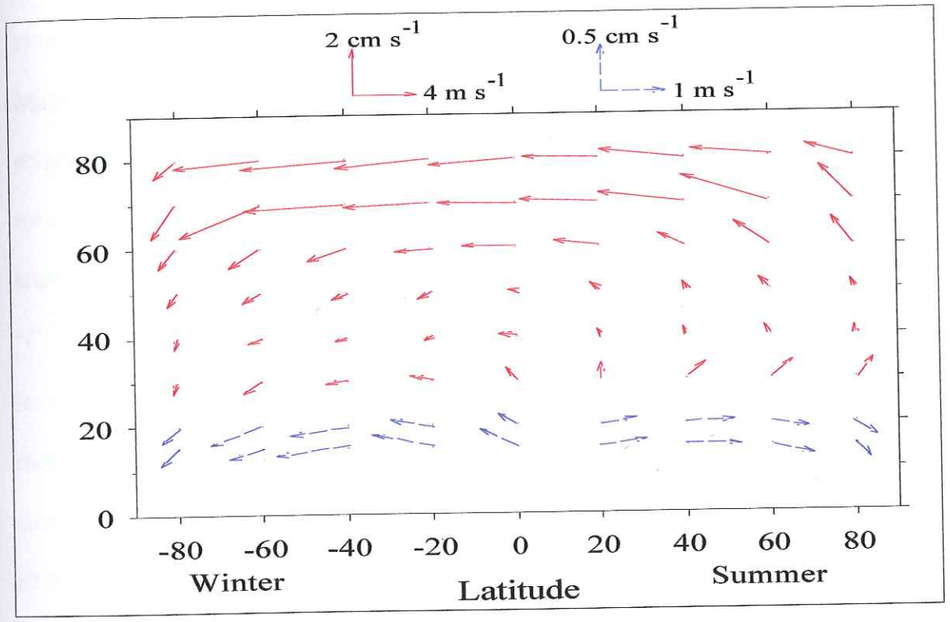

Fig. 5: *Atmospheric global circulation up to 90 km of altitude (from [Plane, 2003]). A feature of atmospheric circulation in the mesosphere is the strong meridional wind flow from the summer to the winter polar region. The velocity is typically 3-5 m s^{-1} between about 60 and 85 km, so that air from the entire global upper mesosphere is essentially funnelled down into the lower stratosphere within the winter polar vortex.*

These tracers can potentially help also to identify larger size extraterrestrial bodies that have impacted Earth in the past hundreds thousands of years. Even small impacts could have caused global catastrophic climate changes by totally destroying the ozone layer by halogen oxide catalysis (P. Crutzen, personal communication). Unfortunately, impact time intervals in the range of ~3300 years for bodies of a diameter of about 150 m up to 146,000 years for 1000 m diameter (J. Birks, personal communication to P. Crutzen) reduce very much the likelihood to capture a horizon due to a cosmic impact in the few discrete ice core sections used for this study.

1.4 Sampling sites and description of the samples

1.4.1 Dome C (Antarctica): the EPICA ice core

The European Project for Ice Coring in Antarctica (EPICA) is a consortium of laboratories and Antarctic logistics operators from ten European nations which aimed at retrieving two deep ice cores in Antarctica. The core currently drilled in Dronning Maud Land (Atlantic sector of Antarctica, Fig.6) is expected to produce a high-resolution record of the last climatic cycle, which could be related to the Greenland records obtained at the other extremity of the Atlantic ocean. The second core drilling site is Dome C (75° 06'S, 123°21'E, 3233 m a.s.l., mean annual temperature –54.5 °C, ice thickness 3309 ± 22 m, present snow accumulation rate of 2.5 g cm^{-2} y^{-1}), located on the East Antarctic plateau (see Fig. 6). Just to mention, the "Dome C" mentioned here is about 50 km away from the "old Dome C" where a 905 m deep core was successfully drilled in the late 70s [*Lorius et al.*, 1979]. The objective of the EPICA drilling at Dome C was to obtain a record of the longest time period possible. Only the EPICA/Dome C core was considered in this study.

The ice drilling of the EPICA/Dome C ice core started during the 1996-1997-field season. Unfortunately, the drill became stuck at the depth of 788 m. The corresponding 788 m is referred to as the "EDC96" core. After a new drill was built, a new drilling was started in 1999, giving the so-called "EDC99" core. Cores EDC96 and EDC99 were drilled 10 m apart. During the 2002/2003-field season drilling operations reached a depth of 3190 m providing the longest temporal ice record ever obtained (~740 kyr) [*Epica community members*, 2004]. In this study we have analysed 46 sections from the EDC96 core (depth from 32.5 m to 763.4 m, which corresponds to snow/ice dated from ~0.6 to 43 kyr BP), and 38 sections from the

EDC99 core (depth from 818.1 m to 2193.4 m, which corresponds to ice dated from ~47 to 217 kyr BP). Altogether they cover the Holocene, the last ice age, the last interglacial (Eemian) and the next to last ice age. In this international program, a given core section (typically 55 cm long) was cut longitudinally into several parts which were used for different kinds of measurements. Thus, only part of the cross section (about 30%) was available.

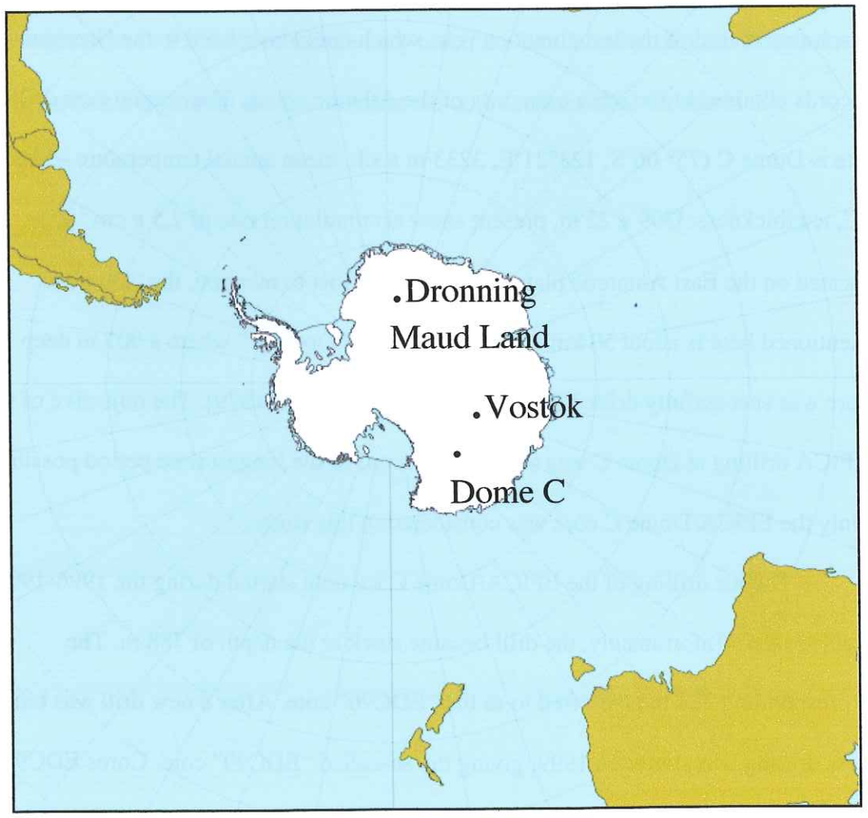

Fig. 6: *Map of Antarctica with the drilling sites illustrated in sections 4.1.1 and 4.1.2.*

1.4.2 Vostok (Antarctica): the Vostok ice core

The ice drilling project at Vostok station in East Antarctica (78°28'S, 106°48'E, 3480 m a.s.l. mean annual temperature –55 °C) (Fig.6) was undertaken in the framework of a long-term collaboration between Russia, France and the USA. This site is located on the East Antarctic plateau where the lowest temperature on Earth (-89 °C) was recorded. In January 1998 the ice core drilling reached a depth of 3623 m, providing the deepest ice core ever recovered [*Petit et al.*, 1999]. The drilling was voluntarily stopped 120 m above the top of the large Vostok subglacial lake [*Jouzel et al.*, 1999]. The Vostok ice core climatic record spans the last 420 kyrs [*Petit et al.*, 1999].

In this work we have analysed 37 core sections, whose depth ranged from 126.73 m (which corresponds to an estimated age of 4.6 kyr BP) to 3,285 m (which corresponds to an estimated age of ~410 kyr BP). Each section was 35-45 cm in length which corresponds to ~10 to 200 of snow accumulation, depending upon the depth. The depth of the sections to be analysed was chosen according to the deuterium isotopic curve in such as way that they represent different climatic conditions. Some sections were dated from the last four interglacial periods. Various other samples were dated from the last four ice ages, with sections corresponding to both very cold and less cold stages.

1.4.3 Summit (Greenland): the GRIP ice core

In the years 1990-1992 a deep ice core was drilled at Summit in Central Greenland (72° 58'N, 37° 64'W, 3238 m a.s.l. mean annual temperature –32 °C, present day mean snow accumulation rate of 23 g cm^{-2} y^{-1}) as part of the international European Greenland Ice Core Project (GRIP) [*Dansgaard et al.*, 1993].

Fig. 7: *Map of Greenland with the ice core-drilling site of Summit.*

An electromechanical drill allowed retrieving a 3029 m deep ice core, with the undisturbed part covering a time period of about 100 kyr. In this work we have analysed for Ir and Pt 36 ice sections whose depth range from 184.3 to 2843 m (estimated age from 0.7 kyr to ~100 kyr), which cover the Holocene and the full last glacial age. Each core section was 55 cm in length, integrating time intervals ranging from a few years for the shallow depths to about to several tens of years for the deep sections. These sections were decontaminated by Sungmin Hong as part of his PhD work [*Hong et al.*, 1994; *Hong et al.*, 1996b].

1.5 Analytical procedures

1.5.1 Decontamination of the core sections

The core sections available for this study are cylinders of ice (lengths of about 55 cm, initial diameter of about 10 cm), whose outside was heavily contaminated during drilling operations especially because of the wall-retaining fluid (a mixture of kerosene and freon or freon substituted). Each section was therefore decontaminated either at the Laboratoire de Glaciologie et Geophysique de l'Environnement (LGGE) in Grenoble or at the Korean Polar Research Institute (KOPRI) in Seoul, by chiselling successive veneer layers of ice in progression from the outside to the inner part of the core, using a procedure which was initially described by Candelone and co-workers [*Candelone et al.*, 1994]. Various improvements, were however, made compared with the initial procedure. Especially, one additional step was added at the beginning of the procedure to remove the highly contaminated ~5mm or so external ice before putting the ice section on the polyethylene lathe.

The procedural blanks for the decontamination procedures were estimated by processing an artificial ice core made by freezing ultra pure water from the Department of Applied Physics of Curtin University of Technology (CUT) in Perth whose composition was known beforehand.

1.5.2 Preparation of the samples for the analysis

Each veneer layer and inner cores so obtained, were melted separately in the clean laboratories of Grenoble [*Boutron*, 1990] [*Planchon et al.*, 2001] or Seoul [*Hong et al.*, 2000]. Various aliquots were prepared in ultra clean low density

polyethylene bottles for the different analyses in Grenoble, Venice, Perth, Antwerpen and Seoul. They were transported and kept frozen until analysis.

1.5.3 Analysis by Inductively Coupled Plasma Sector Field Mass Spectrometry (ICP-SFMS)

The samples were analysed for Li, Mg, V, Cr, Mn, Co, Cu, As, Rb, Sr, Cd, Ba, Ir, Pt, Hg, Bi and U by ICP-SFMS at the Department of Environmental Sciences of the University Ca' Foscari of Venice, using an Element2 instrument from Thermo-Finnigan. The procedure used to determine Li, Mg, V, Cr, Mn, Co, Cu, As, Rb, Sr, Cd, Ba, Bi and U has already been described (see for instance [*Planchon et al.*, 2001]). The procedures used to determine Ir, Pt and Hg were developed as part of this work [*Gabrielli et al.*, 2004; *Planchon et al.*, 2004], see chapters 2.1 and 5.1 of the thesis.

1.5.4 Analysis by Thermal Ionization Mass Spectrometry (TIMS)

Part of the samples were analysed for Pb, Pb isotopes and Ba by TIMS using a VG354 instrument from, Fisons Instruments, at the Department of Applied Physics of Curtin University of Technology (CUT) in Perth. The procedure has been described in detail elsewhere [*Vallelonga et al.*, 2002] [*Chisholm et al.*, 1995].

1.5.5 Analysis by Solid-phase Microextraction and Multicapillary Gas Chromatography Hyphenated to Inductively Coupled Plasma-Time-of-Flight-Mass Spectrometry

Part of the samples were analysed for Methyl-Hg and Hg^{2+} by Solid-phase Microextraction and Multicapillary Gas Chromatography Hyphenated to Inductively Coupled Plasma-Time-of-Flight-Mass Spectrometry at the Department of Chemistry at the University of Antwerpen, using a procedure which has been described elsewhere [*Jitaru and Adams*, 2004].

1.5.6 Analysis by Graphite Furnace Atomic Absorption Spectrometry (GFAAS)

Part of the samples were analysed for elements such as Al, Zn, Cd, Cu and Pb by GFAAS with or without pre-concentration [*Gorlach and Boutron*, 1990] either at the LGGE in Grenoble, or at the Korean Polar Research Institute (KOPRI) in Seoul, using Perkin Elmer Aanalyst 100 or 4110ZL instruments as described in detail elsewhere (see for instance [*Hong et al.*, 2000])

CHAPTER 2: PAST FALLOUT OF METEORIC SMOKE TO THE POLAR ICE CAPS

2.1 ARTICLE 1: Determination of Ir and Pt down to the sub-femtogram per gram level in polar ice by ICP-SFMS using preconcentration and a desolvation system

Paolo Gabrielli, Anita Varga, Carlo Barbante, Claude Boutron, Giulio Cozzi, Vania Gaspari, Frédéric Planchon, Warren Cairns, Sungmin Hong, Christophe Ferrari and Gabriele Capodaglio

Journal of Analytical Atomic Spectrometry, 19, 831-837, 2004

ARTICLE

JAAS
www.rsc.org/jaas

Determination of Ir and Pt down to the sub-femtogram per gram level in polar ice by ICP-SFMS using preconcentration and a desolvation system†

Paolo Gabrielli,[a,b] Anita Varga,[b] Carlo Barbante,*[b,c] Claude Boutron,[a,d] Giulio Cozzi,[b] Vania Gaspari,[b] Frédéric Planchon,[b] Warren Cairns,[c] Sungmin Hong,[e] Christophe Ferrari[a,f] and Gabriele Capodaglio[b,c]

[a]*Laboratoire de Glaciologie et Géophysique de l'Environnement du CNRS, 54 rue Molière, B.P. 96, 38402 St. Martin d'Heres cedex, France*
[b]*Department of Environmental Sciences, University of Venice, Ca' Foscari, I-30123 Venice, Italy. E-mail: barbante@unive.it; Fax: +39-041-2348549; Tel: +39-041-2348942*
[c]*Institute for the Dynamics of Environmental Processes-CNR, University of Venice, Ca' Foscari, I-30123 Venice, Italy*
[d]*Observatoire des Sciences de l'Univers et Unité de Formation et de Recherche de Physique (Institut Universitaire de France), Université Joseph Fourier, Domaine Universitaire, B.P. 68 38041 Grenoble, France*
[e]*Korea Polar Research Institute, Korea Ocean Research & Development Institute, Ansan, PO Box 29, Seoul 425-600, Korea*
[f]*École Polytechnique Universitaire de Grenoble (Institut Universitaire de France), Université Joseph Fourier, 28 avenue Benoît Frachon, B.P. 53 38041 Grenoble, France*

Received 12th December 2003, Accepted 24th February 2004
First published as an Advance Article on the web 5th May 2004

A new analytical methodology, based on inductively coupled plasma sector field mass spectrometry (ICP-SFMS) coupled with a micro-flow nebulizer and desolvation system, has been set up for the quantification of Ir and Pt down to the sub-ppq level (1 ppq = 1 fg g^{-1} = 10^{-15} g g^{-1}) in polar ice samples. Ultra-clean procedures were adopted during the pre-treatment phases in our laboratories in order to avoid possible contamination problems and a preconcentration step by evaporation at sub-boiling temperatures was necessary. A procedural detection limit of 0.02 ppq and 0.08 ppq for Ir and Pt, respectively, was obtained. The reproducibility of the analytical procedure at the ppq level was about 50% for Ir and 30% for Pt and the recoveries were 75% and 93% for Ir and Pt, respectively. Spectral interferences, which affect the determination of Ir and Pt, were reduced by using a desolvation system for sample introduction. The contribution of the interfering species was determined and subtracted. This new method allowed us to analyse Ir and Pt in remote uncontaminated ice samples from Antarctica and Greenland down to the sub-ppq level. The concentration ranges were from 0.1 up to 5 ppq for Ir and from 0.2 up to 7 ppq for Pt. These measurements represent the first data of Ir concentrations in unfiltered melted ice samples and the lowest concentrations ever recorded for Pt in environmental samples.

Introduction

The discovery of the anomalous enrichments of platinum-group elements (PGEs) in the globally extended clay layer signifying the Cretaceous–Tertiary (K–T) boundary provided the first evidence of a large extraterrestrial body impacting the Earth 65 million years ago.[1] This study produced an enormous increase in the interest of the geochemistry of PGEs, and many multidisciplinary studies were conducted in the following years.[2]

Successively dated snow and ice layers deposited in permanent glaciers in polar regions have proved to be valuable archives for reconstructing biogeochemical cycles of heavy metals on Earth.[3–7] Nevertheless, studies on PGEs in polar archives have not previously progressed very far because of the ultra-low concentrations (down to sub-ppq levels, 1 ppq = 1 fg g^{-1} = 10^{-15} g g^{-1}) of these elements in ice and the very low volume of ice available for study.

Only a few studies, assessing iridium levels in particulate matter trapped in polar ice, have been reported until now.[8–13] The analytical methods were, however, only suitable for determining the Ir concentrations in the filtered particles (>0.45 μm, except in the work by Koeberl,[10] which measured the decanted particulate fraction obtained after melting) by instrumental neutron activation analysis (INAA), missing the fine and soluble fractions. Total concentrations of iridium have only been determined in natural waters (river, ocean and estuarine water) by negative thermal ionisation mass spectrometry (NTIMS) for instance,[14,15] but no analytical procedure has ever been reported, until now, to determine the total concentration of Ir in ice.

Until recently there were no studies on Pt in ice and snow archives. However, thanks to the sensitivity of inductively coupled plasma sector field mass spectrometry (ICP-SFMS), and the use of strict contamination control throughout the analytical procedure, much progress has been made in the determination of Pt, Pd and Rh in polar and alpine archives from the beginning of the industrial period.[16–18] These studies have revealed a global contamination of these heavy metals originating mainly from the exhaust gases of vehicles fitted with catalytic converters.

† Presented at the 4th International Conference on High Resolution Sector Field ICP-MS, Venice, Italy, October 15–17, 2003.

DOI: 10.1039/b316283d

Nevertheless, where anthropogenic enrichment has not occurred, the determination of the total concentration of PGEs in uncontaminated polar ice samples remains an analytical challenge. Concentrations of Ir and Pt in remote ancient ice are extremely low (down in the sub-ppq range), and their concentrations in polar archives offer the fascinating possibility of studying the flux of cosmic material. Ir and Pt are relatively abundant in cosmic material (average concentrations in chondrites, the most common meteorites, are 481 ppb for Ir and 990 ppb for Pt)[19] but are rare in the terrestrial crust (average concentrations are 0.05 ppb for Ir and 0.4 ppb for Pt).[20] When inputs of terrestrial dust to polar ice were low, the cosmic fraction of Ir and Pt could be distinguishable from the terrestrial background. Thus, the concentrations of Ir and Pt in ancient polar ice could allow the reconstruction of the input of cosmic material entering the Earth's atmosphere during the last climatic cycles.

In this work we present the development of a method for the determination of the total concentrations of Ir and Pt at sub ppq levels using only about 60 ml of melted ice from Greenland and Antarctica. Samples have been measured after sub-boiling evaporation under ultra-clean condition by ICP-SFMS coupled with a micro-flow nebulisation/desolvation system.

Experimental

Clean conditions

The analytical procedures were performed at the Laboratory of Glaciology and Geophysics of the Environment (LGGE) in Grenoble and at the Department of Environmental Sciences (DES) in Venice. Both laboratories have developed special areas where ultra-clean procedures can be adopted to control contamination problems.[21–24] At the LGGE, the cleaning of the low density polyethylene (LDPE) bottles, Teflon (PFA) beakers (both from Nalgene Corporation, Rochester, USA) and the stainless steel items for the decontamination procedure were carried out in a class 100 clean bench located in a class 10000 clean room.[21]

The ultra pure water used was obtained from a mixed bed of ion-exchange resins (maximum flow rate was 2 l h^{-1}) from Maxy (La Garde, France).[21] Chloroform (Merck, Darmstadt, Germany) and Suprapur grade HNO_3 (65% Merck) were used for the initial steps of the cleaning procedure. Ultra pure double distilled HNO_3, supplied by the Department of Applied Physics of Curtin University of Technology (CUT) in Perth, Australia (Prof. K. Rosman), was used for the final steps of the cleaning procedure and for sample acidification and standard addition.

Sample treatment

To sample the deep ice layers in polar glaciers, electromechanical drills were used to obtain ice cores, with a diameter of about 10 cm. The ice cores were collected in Greenland at Summit (72°34′ N, 37°37′ W, 3238 m, mean annual temperature −32 °C) within the framework of the European Greenland Ice Core Project (GRIP) and in Antarctica at Dome C (75°06′ S, 123°21′ E, 3233 m, mean annual temperature −54 °C) within the framework of the European Project for Ice Coring in Antarctica (EPICA). In these international programmes, a given core section (typically 55 cm long) is cut longitudinally into several parts which are used for different kinds of measurements. Thus, only part of the cross section (about 30%), for both the GRIP and EPICA ice cores, was available.

A major problem is that the ice cores are always contaminated on their outside by several heavy metals. The contamination is from the wall retaining fluid, which is used to prevent the closing of the drilling hole at great depths in the glaciers. The possible contamination, derived from the drilling fluid and the core handling, was carefully evaluated. A special decontamination procedure[25] was performed in a cold laboratory (t = −15 °C) at the LGGE in a class 100 clean bench under laminar flow conditions. A preliminary removal of the outermost layer with a special stainless steel knife had to be performed outside the clean bench to prevent the heavily contaminated superficial layer of the ice core from entering the clean area. Then, at least three annular concentric layers were chiselled off inside the clean bench with acid cleaned stainless steel knifes before reaching and recovering the uncontaminated inner part of the core which was stored in an ultra-clean 1 l LDPE bottle. With regards to the GRIP samples a single core was recovered from each section, whereas two successive cores were obtained for each EPICA sample. The samples were then melted at room temperature in a class 100 clean bench and an aliquot of about 60 ml was transferred to a 60 ml ultra-clean LDPE bottle and kept frozen until the succeeding analytical step. The typical sample volume required (60 ml) is about 65 times smaller than that previously used for assessing total Ir concentrations in natural water (4 l).[15] This volume represents about 20% of the decontaminated part of the inner core.

Preconcentration[26] was performed by evaporation at sub-boiling temperatures in order to increase the concentration of Ir and Pt by a factor of approximately 60. A metal hot plate, covered by a Teflon film, was used to preconcentrate 1l samples and an ultra pure water aliquot as a reference. PFA ultra-clean beakers were used to contain the samples during evaporation. The beakers had been immersed in a heated 0.1% (v/v) HNO_3 solution in a class 100 clean bench, and were then carefully rinsed and preconditioned for 1 h on the hot plate with ultra-pure water before use. The samples had a typical initial volume of ~60 ml and were reduced to ~1 ml with an evaporation rate of approximately 10 ml h^{-1}. The preconcentrated solution was then spiked with HNO_3 up to a final HNO_3 concentration of 1% (v/v), by using a 10 µl precleaned tip (Eppendorf, Germany), before the subsequent transfer into an ultra clean 15 ml LDPE bottle. Preconcentrated samples were then kept frozen until analysis by ICP-SFMS.

Instrumentation and measurement parameters

The analytical measurements by ICP-SFMS (Element2, Thermo Finnigan MAT, Bremen, Germany) were carried out in a clean laboratory at DES under a class 100 clean bench adopted as a clean sample introduction area for the instrument. The instrumental conditions and measurement parameters are reported in Table 1.

Table 1 Instrumental conditions and measurement parameters for the ICP-SFMS and the desolvation unit

Forward power/W	1150
Gas flow rates	
Cool/l min^{-1}	11.00
Auxiliary/l min^{-1}	1.29
Sample/l min^{-1}	0.886
Sweep gas/l min^{-1}	3.59
Nitrogen flow rate/ml min^{-1}	15
Membrane temperature/°C	175
Spray chamber temperature/°C	95
Sample uptake/µl min^{-1}	100
Acquisition mode	E-scan: over small mass range
Selected isotopes	^{193}Ir, ^{195}Pt
Resolution adopted	Low ($m\,\Delta m^{-1}$) = 300
No. of scan	100
Dwell time per acquisition points/ms	10
No. of acquisition points per mass segment (sample per peak)	40
Acquisition window (%)	100
Search window (%)	100
Integration window (%)	50

The low resolution mode (LRM) with a resolution setting of $m/\Delta m$ = 300 was used to measure Ir and Pt in order to maximise ion transmission at low concentrations. The samples were melted in the sample introduction area of the instrument and were handled by operators wearing LDPE gloves and clean room clothing.

A micro-flow nebulisation/desolvation sample introduction system[27] (Aridus, Cetac Technologies, Omaha, NE, USA) was used to reduce the spectral interferences. The instrument consists of a micro-flow (<100 µl min^{-1}) PFA nebuliser, a heated PFA spray chamber and a heated microporous PTFE tubular membrane. The solvent vapour passes through the membrane and is removed by an exterior flow of Ar gas (sweep gas). In this way the solvent based interferences can be reduced while the signal to background ratio can be increased.

The gas flow rate was optimised daily to obtain the maximum signal intensity.[24] The maximum sensitivities at the optimum flow rate in LRM were 2–3 × 10^6 counts s^{-1} (cps) for 1 ppb of In, depending on the tuning conditions. The good signal stability meant that internal standards could be eliminated, avoiding the possible introduction of contamination into the samples.

Mass calibration using a 1 ppb multi-element standard solution was carried out weekly in LRM.

Results and discussion

Calibration

External calibration curves were used for the quantification of the analytes. Standards were prepared weekly from a 10 mg l^{-1} in 10% HCl, PGE multi-element ICP-MS stock solution (CPI International, The Netherlands) in 1% (v/v) HNO_3 acidified ultra-pure water. Standard solutions were stored at about 4 °C to minimise ion exchange with the walls of the LDPE bottle. The concentrations in the final standard solutions, used to quantify the preconcentrated samples, were 10, 20, 50 and 200 ppq. In this range, linear calibration curves were obtained for ^{193}Ir ($y = 2.379x + 3.7$; $R^2 = 0.9998$) as well as for ^{195}Pt ($y = 0.750x + 6.2$; $R^2 = 1$) (where y is expressed in cps and x in ppq). Calibration standard solutions were analysed at the beginning and at the end of the measurement session. Whenever differences in the slope of the calibration curves were higher than 10%, they were taken into account during the quantification.

Interference study

Because of the high purity of ancient ice samples from Antarctica and Greenland, they could be characterised as an ideal matrix for the determination of ultra trace elements. Nevertheless, the relatively high input of dust to polar regions, especially during glacial periods, and the adopted preconcentration step of the samples, could produce a relatively complex matrix possibly interfering with the determination of the analytes.

Table 2 shows a list of the most abundant isotopes[28] of Ir and Pt, together with the most important interfering species. ^{193}Ir and ^{195}Pt were chosen because they are the naturally most abundant and should have fewer interferences than other isotopes. The most important interferences for ^{193}Ir and ^{195}Pt are $^{177}Hf^{16}O$ and $^{179}Hf^{16}O$, with an abundance of 18.51% and 13.6 %, respectively. Hf is a trace element in the continental crust (4.9 ppm), but is much more abundant than Ir (0.05 ppb) and Pt (0.4 ppb).[20] Even very low concentrations of Hf (present at a sub-ppt level in our samples; 1 ppt = 1 pg g^{-1} = 10^{-12} g g^{-1}) could therefore interfere with the determination of Ir and Pt.

Working in LRM, the spectroscopic resolution of the interfering species from the analyte peaks is not feasible. Therefore, it was necessary to reduce the interfering species by using a desolvation system, and contemporaneously quantifying the residual interference of Hf and applying a mathematical correction.

Table 2 Potential spectral interferences that could affect the determination of ultra trace levels of Ir and Pt in polar ice

Analyte		Potential interference		
Isotope	Abundance (%)	Species	Abundance[a]	Resolution ($m/\Delta m$)
^{191}Ir	37.30	$^{175}Lu^{16}O$	97.17	7667
		$^{173}Y^{18}O$	0.03	8222
		$^{174}Y^{17}O$	0.01	8449
^{193}Ir	62.70	$^{177}Hf^{16}O$	18.51	7782
		$^{177}Lu^{16}O$	0.19	8389
^{194}Pt	32.90	$^{178}Hf^{16}O$	27.17	8100
		$^{177}Hf^{17}O$	0.007	9600
		$^{176}Hf^{18}O$	0.01	8800
		$^{176}Yb^{18}O$	0.02	9200
		$^{176}Lu^{18}O$	0.005	9200
^{195}Pt	33.80	$^{179}Hf^{16}O$	13.6	8200
		$^{178}Hf^{17}O$	0.01	6900
		$^{177}Hf^{18}O$	0.04	8800
^{196}Pt	25.20	$^{180}Hf^{16}O$	35.00	8348
		$^{180}W^{16}O$	0.13	8408
		$^{180}Ta^{16}O$	0.01	8692
		$^{178}Hf^{18}O$	0.05	8875
		$^{179}Hf^{17}O$	0.005	9803
		^{196}Hg	0.14	226 550

[a] For polyatomic species calculated as the product of the natural abundances of each isotope divided by 100.

The correction was calculated with the following eqns. ((1)–(2)):

$$I_{Ir} = I_{Ir,s} - (I_{(177)Hf,s} \times R_{(177)Hf(16)O,\,(177)Hf}) \quad (1)$$

$$I_{Pt} = I_{Pt,s} - (I_{(179)Hf,s} \times R_{(179)Hf(16)O,\,(179)Hf}) \quad (2)$$

where I_{Ir} and I_{Pt} are the corrected intensity of the element to be determined, $I_{Ir,s}$ and $I_{Pt,s}$ the apparent intensity of the interfered element in the sample, $I_{(177)Hf,s}$ and $I_{(179)Hf,s}$ the intensity of the interfering element in the sample and $R_{(177)Hf(16)O,\,(177)Hf}$ and $R_{(179)Hf(16)O,\,(179)Hf}$ the ratio between the interfering species and the interfering element.[29] $I_{(177)Hf,s}$ was quantified indirectly from the $I_{(180)Hf,s}$ signal because the former isotope could be affected by an interference caused by $^{40}Ar^{137}Ba$ (abundance 11.27%).

The ratios between the interfering species and the interfering elements were determined daily using four acidified (1% v/v HNO_3) ultra-pure water solutions spiked to 0, 1.7, 4.8 and 9.2 ppt of Hf, respectively. During the analysis the intensities of ^{193}Ir, ^{195}Pt, as well as ^{179}Hf and ^{180}Hf, were measured. From the experimental data in Table 3 it can be established that in both cases the effect of oxide formation exceeded the blank signal at Hf concentrations above ~5 ppt.

Applying eqns. (1) and (2), the contributions of $^{177}Hf^{16}O$ and $^{179}Hf^{16}O$ on the signal of ^{193}Ir and ^{195}Pt can be determined. For example, analysing Ir and Pt in a sample dated at 941 BP from

Table 3 Intensity values (cps) of blank solutions spiked with different amounts of Hf

		Concentration of Hf (ppt)[a]			
Isotope	Interference	0	1.7	4.8	9.2
^{177}Hf		7 (27)	538 (5)	1423 (6)	3137 (22)
^{193}Ir	$^{177}Hf^{16}O$	4 (56)	5 (29)	6 (28)	13 (25)
^{179}Hf		5 (45)	380 (9)	1060 (6)	2308 (21)
^{195}Pt	$^{179}Hf^{16}O$	7 (24)	8 (38)	9 (34)	15 (20)

[a] In parentheses,are relative standard deviation in % (RSD)

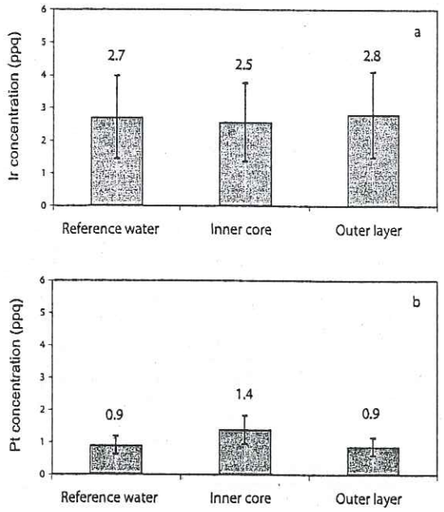

Fig. 1 Outer layer and inner core concentrations of Ir (a) and Pt (b) in an artificial ice core prepared at CUT (Curtin University of Technology, Perth) and a comparison with the reference water produced in the same laboratory and used to prepare the artificial ice core. Error bars refers to the reproducibility at 1 ppq level.

Summit (Greenland), using the conventional sample introduction system, the contributions of the interfering species were 93% of the Ir signal and 69% of the Pt signal. As the ratios of the interference signal to the corrected signal were very high in both cases, the determination was considered unacceptable.[30] These contributions were reduced to 3% for both Ir and Pt by using the desolvation system, making the application of mathematical correction to the determination of Ir and Pt concentrations in ancient ice samples feasible. However in many cases the correction was negligible, because the concentration of Hf in the samples was often below 5 ppt even after preconcentration.

Blanks

Considering the extremely low concentrations of Ir and Pt in the samples, special care was taken to evaluate the procedural blanks in each step of sample preparation and in particular during the decontamination and preconcentration procedures.

Blank of the decontamination procedure. In order to assess whether any Ir and Pt contamination occurs when chiselling the outer layer with stainless steel knives, an artificial ice core was prepared at CUT by freezing ultra-pure water[31] and was then processed at the LGGE using the ice core decontamination procedure.[25] Ir and Pt concentrations were determined in the external layer and compared with the inner core values as well as with an ultra-pure water aliquot used to prepare the artificial ice core. Figs. 1(a) and (b) show that the concentrations measured in the external layer, in the inner core and in the reference ultra-pure water, show negligible differences both for Ir and for Pt, indicating that there is no detectable contribution due to the decontamination procedure.

The outermost layer of real ice cores is heavily contaminated for several heavy metals because of the extensive use of drill fluid during the sampling operations in Greenland and Antarctica. Therefore it was necessary to check if contamination by Ir and Pt had occurred and to what extent. For this purpose, concentrations were determined in three successive outer layers and in the inner core of real ice core sections. A real example is the radial profile of Ir and Pt in an Antarctic ice core section drilled at Dome C at a depth of 1863.1 m, which is reported in Fig. 2. It can be observed that the concentration of Ir and Pt in the external layers and in the inner core shows only an insignificant variation, probably due more to the inhomogeneity of the test sample solutions and/or (as discussed later) to the measurement uncertainty than to a possible contamination originating from the external layer. In general, Ir and Pt concentrations are extremely low even in the outermost layers of both the GRIP and EPICA ice core sections. Therefore it can be stated that, thanks to the careful precautions taken, any additional Ir or Pt deriving from the drilling fluid does not affect the innermost parts of the core sections.

Blank of the preconcentration procedure. The blank of the preconcentration procedure was assessed by preconcentrating three aliquots of different volumes (30–100 ml) of ultrapure water to about 1 ml. These preconcentration factors (32, 62 and 99, respectively) covered the range of factors used for the real samples (typically about 60 but varying between 30 and 100). For every aliquot two repeat measurements of Ir and Pt concentrations were performed.

Plotting the calculated mass of Ir and Pt as a function of the initial mass of the ultra-pure water (Fig. 3(a) and (b)) we have calculated a regression line for which the intercept represents an interpolation of the mass of Ir and Pt eventually released (positive masses) or adsorbed (negative masses) by the walls of the Teflon beakers during preconcentration. The intercepts are close to zero for both Ir (-19 ± 32 fg) and Pt (3 ± 38 fg) (uncertainty is given with a confidence interval of 0.95), suggesting a small exchange for both metals with the beakers

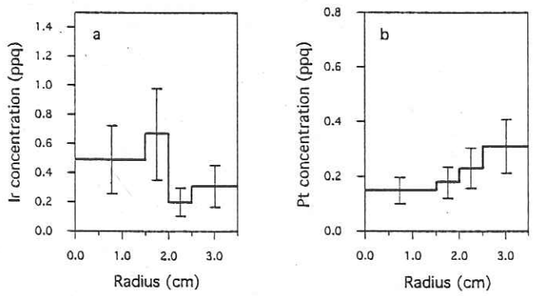

Fig. 2 Radial concentration profile of Ir (a) and Pt (b) for an Antarctic EPICA ice core section (Dome C, depth of 1863.1 m). Error bars refers to the reproducibility at 1 ppq level.

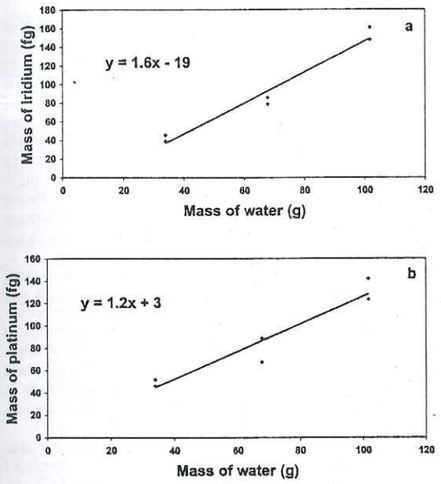

Fig. 3 Measurements of the mass (in fg) of Ir (a) and Pt (b) released/adsorbed by the walls of the beakers during the preconcentration procedure as the intercept of the regression line of the mass of Ir and Pt recovered *versus* different quantities of ultra-pure water preconcentrated.

during the sample preconcentration procedure. The contribution from acidification of the sample was also checked and was always found to be below the detection limit of the instrument.

Concentration of Ir and Pt in the ultra-pure water. The slope of the previously calculated regression line (Fig. 3(a) and (b)) represents an estimation of the concentration of Ir (1.6 ± 0.4 ppq) and Pt (1.2 ± 0.5 ppq) in the ultra-pure water. These concentration values could be directly related to the water production rate: a longer ion exchange of the tap water with the resin columns (corresponding to a low production rate of about 0.5 l h^{-1}) resulted in the concentration dropping down to 0.3 and 0.4 ppq for Ir and Pt, respectively. These results are consistently lower than the lowest concentrations found in the real preconcentrated samples (Ir = 5 ppq and Pt = 15 ppq; before application of the preconcentration factor). This means that any contribution from small ultra-pure water drops left on the instruments after rinsing is negligible when added to the much larger sample volume.

Detection limits

The instrumental limit of detection (LOD) was calculated as 3 times the standard deviation of the 1% v/v HNO_3 ultra-pure water response: the LODs were 1 and 5 ppq for Ir and Pt, respectively. Nevertheless, to know what is the minimum measurable Ir and Pt concentration, it is necessary to calculate the procedural detection limit because the preconcentration step can decrease it by a factor corresponding to the preconcentration factor. So, dividing the instrumental detection limit by the typical preconcentration factor (~60) we obtain procedural detection limits of 0.02 ppq for Ir and 0.08 ppq for Pt. These are 5 and 3 times less than the minimum concentrations detected in polar ice samples for Ir and Pt, respectively.

Reproducibility

An estimation of the instrumental repeatability of the data was obtained from 3 repeat analyses (on a 1.2 ml sample) of a polar preconcentrated ice sample (Greenland, Summit, depth 1394.3 m, age 8723 BP). The mean values and the relative standard deviations (in parentheses) were the following: 0.3 ppq (4%) for Ir and 0.5 ppq (3%) for Pt. A more realistic estimation of the repeatability of the measurements is given by taking into account the uncertainty produced by the preconcentration step so we can estimate the overall reproducibility. This was done by simultaneously preconcentrating 6 aliquots of ultra-pure water, thus obtaining the following mean values and the relative standard deviations (in parentheses): 0.5 ppq (47%) for Ir and 1.1 ppq (32%) for Pt. These high relative standard deviations are due to the extraordinarily low concentrations in the ultra-pure water samples (comparable with the lowest concentrations in our samples) and can be considered as an upper limit of the method reproducibility.

Recovery

Estimating the accuracy for ultra-trace determinations down to the sub-ppq level is very difficult due to the numerous sources of error and especially because of the lack of an adequate reference material. The most critical step affecting the procedural accuracy of the measurements is probably the preconcentration step, a delicate and not completely conservative analytical procedure that could produce analyte losses by evaporation.

To estimate the accuracy of the method, a recovery test, by preconcentrating a series of standards with Ir and Pt concentrations similar to the sample concentrations with the same initial volume (~60 ml) and with the same preconcentration factor (~60), was performed. The final concentrations of the standards were 0, 0.1, 0.5, 1.1, 2.1, 5.3 and 11.0 ppq. Fig. 4(a) and (b) show the found concentration as a function of the added concentration for Ir and Pt. The slope given by the linear regression represents the fraction of the analyte conserved in the final solution. The recovery for Ir was 75% while for Pt it was 93%. These values are in good agreement with other heavy metals treated in a similar manner (but with concentrations at least 3 orders of magnitude higher) published in previous work.[26] It is likely that the chemical form of Ir and Pt in the standards has different behaviour from the species present in real samples. For this reason the accuracy estimated with this recovery test can only be indicative and does not allow a systematic correction of analyte losses from real samples during preconcentration.

Ir and Pt concentrations in polar ice

The samples selected to test the developed method belong to unique ice archives covering past changes in atmospheric conditions. They cover the last and penultimate glacial and the last interglacial periods. The Greenland samples collected at Summit in Central Greenland were four deep ice core sections[7,32] dated 941, 8723, 27151 and 45358 years before present[33] that are part of 35 sections decontaminated for this project. The Antarctic samples collected at Dome C in East Antarctica were two ice core sections taken at a depth of 1753.1 m and 1863.1 m and dated, from an estimated chronology, in the proximity of the penultimate glacial–interglacial transition about 150 000 years before present. These two samples are part of 41 EPICA Dome C sections decontaminated for this project.

Concentrations of Ir and Pt in four ice core sections from central Greenland and the two from East Antarctica are reported in Table 4. The concentrations are within the sub-ppq and ppq levels, both in the samples from Greenland and Antarctica, ranging between 0.1 and 5 ppq for Ir and between 0.2 and 7 ppq for Pt. Among the four samples from Greenland, a large variation could be found: ice core sections from the Holocene (941 and 8723 years BP) show lower concentrations

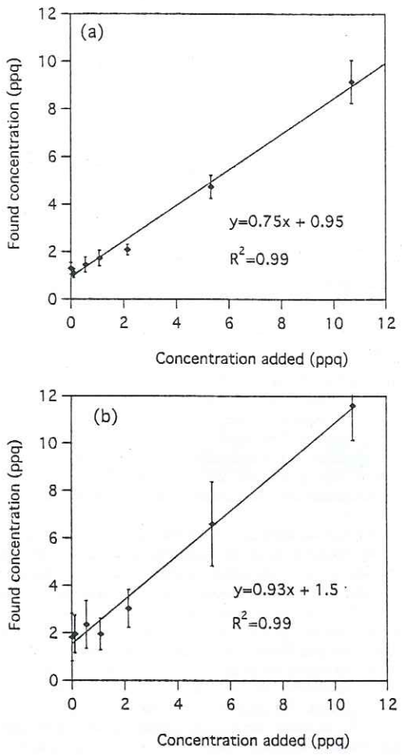

Fig. 4 Determination of the recovery of the preconcentration procedure for Ir (a) and Pt (b) using preconcentrated synthetic standards with ultra-low concentrations. Found concentration (ppq) refers to the measured concentration after evaporation divided by the preconcentration factor. Error bars as instrumental SD are also reported.

than from the last glacial age (27151 and 45358 years BP). The explanation, extensively discussed elsewhere,[34] for higher concentrations of Ir and Pt detected in Greenland during the last glacial age, could be mainly related to the extremely high input of continental dust at high latitudes, transferring a relatively large amount of terrestrial Ir and Pt into the ice and covering the much lower Ir and Pt signal of extraterrestrial origin. Conversely, the cosmic signature of Ir and Pt could be recognised in Holocene samples characterised by a much lower terrestrial dust content.

Table 4 Concentrations of Ir and Pt in four samples from central Greenland (Summit) and two samples from East Antarctica (Dome C)

Site	Depth/m	Age[a](years BP)	Ir (ppq)	Pt (ppq)
Greenland (Summit)	239.3	941	0.1	0.4
	1394.3	8723	0.3	0.5
	2054.3	27151	3.9	5
	2334.2	45358	5	7
Antarctica (Dome C)	1753.1	~130000	1.1	0.4
	1863.1	~150000	0.5	0.2

[a] Summit (GRIP), time scale is the ss09 sea, from ref. 33; Dome C (EPICA) time scale is extrapolated from the time scale of the Vostok ice core (see ref. 35).

Comparison with other studies

Few studies have attempted to estimate the concentrations of Ir in ice,[8–13] most using INAA almost exclusively to measure the particulate fraction (>0.45 μm) present, consequently missing the fine and the soluble fractions. The total concentration of Ir in ice has never been measured and therefore a comparison of these studies with our results is not possible.

Ir concentrations that are comparable with our values were measured by Negative Thermal Ionisation Mass Spectrometry (NTIMS) in natural water,[14,15] and total concentrations in the range of 0.1 and 3 ppq are reported. We report values in the ice with a similar range (between 0.1 and 5 ppq). The minimum concentration reported for the hydrosphere corresponds to the lowest value of Ir that we reported for the cryosphere.

Pt total concentration measurements in snow and ice were already attempted in samples from Greenland, Antarctica and the Alps but were mainly devoted to studying the anthropogenic contribution from the last few decades due to the emissions of vehicles fitted with catalytic converters.[16–18] Total concentration values from 8 ppq up to 830 ppq are reported in recent snow at Summit in Greenland and from 540 up to 640 ppq in recent shallow snow in Antarctica, exceeding our measurements by several orders of magnitude.

The only two values that could be comparable with our data are two ice core sections sampled at Summit in Greenland in the framework of the GRIP project, referring to 7260 and 7760 years BP, showing concentration values of 8 and 15 ppq, considerably higher, by a factor of 10, than the values that we report for the same ice core during the Holocene. It must be considered that these data were measured only to have an estimation of the natural background in order to assess the relatively high concentrations in the recent anthropogenically enriched samples and that there was not an accurate procedure developed for measuring Pt at the sub-ppq level.

Conclusions

We have developed an ultra-clean and simple method in order to measure the total concentration of ultra-low traces of Ir and Pt in polar ice down to the sub-ppq level. An ultra-clean procedure for decontaminating the ice core sections and a suitable ultra-clean preconcentration method by sub-boiling evaporation were fundamental sample preparation steps required to obtain negligible procedural blanks and to increase the concentration by a factor of 60. The volume used was about 65 times smaller than that used for assessing total Ir concentrations in natural water and the addition of reagents was limited to only a 1% (v/v) ultrapure HNO_3 addition to the 1 ml of preconcentrated solution. The extremely high sensitivity of the ICP-SFMS, the very low instrumental background, and the very low sample consumption with the reduction of spectral interferences by the desolvation system were the four most important factors that enabled us to obtain the first results of the total concentration of Ir in the cryosphere and the lowest concentrations ever recorded for Pt in environmental samples.

Acknowledgements

This work was supported in France by the Institut Universitaire de France, the Ministère de l'Environnement et de l'Amènagemont du Territoire, the Agence de l'Environnement et de la Maîtrise de l'Energie, the Institut National des Sciences de l'Univers and the Université Joseph Fourier of Grenoble. In Italy, it was supported by ENEA as part of the Antarctic National Research Program (under projects on Environmental Contamination and Glaciology) and the Alliance for Global Sustainability (project title: Platinum Group Elements from Automobile Emission to Global Distribution). This research has been also supported by Marie Curie Fellowships of the European Community programme (IHP) under contract number HPMF-CT-2000-00795 and HPMF-CT-2002-01772. Core samples were collected within the European programme GRIP and EPICA. This work is a contribution to the "European Project for Ice Coring in Antarctica" (EPICA), a joint ESF (European Science Foundation)/EC scientific programme, funded by the European Commission and by national contributions from Belgium, Denmark, France, Germany, Italy, the Netherlands, Norway, Sweden, Switzerland and the United Kingdom. This is EPICA publication no. 87. We would like to thank also all the personnel working in the field in Greenland and in Antarctica. Finally, we would like to thank Kevin Rosman for providing the ultra-pure HNO_3 and Paul Vallelonga for the artificial ice core preparation and laboratory assistance.

References

1 L. W. Alvarez, W. Alvarez, F. Asaro and H. V. Michel, *Science*, 1980, **208**, 1095–1108.
2 N. J. Evans and C. F. Chai, *Palaeogeography, Palaeoclimatology, Palaeoecology*, 1997, **132**, 373–390.
3 C. F. Boutron and C. C. Patterson, *Nature*, 1986, **323**, 222–225.
4 C. F. Boutron, C. C. Patterson, V. N. Petrov and N. I. Barkov, *Atmos. Environ.*, 1987, **21**, 1197–1202.
5 C. F. Boutron, C. C. Patterson and N. I. Barkov, *Earth Planet. Sci. Lett.*, 1990, **101**, 248–259.
6 C. F. Boutron, S. N. Rudniev, M. A. Bolshov, V. G. Koloshnikov, C. C. Patterson and N. I. Barkov, *Earth Planet. Sci. Lett.*, 1993, **117**, 431–441.
7 S. Hong, J. P. Candelone, C. Turetta and C. F. Boutron, *Earth Planet. Sci. Lett.*, 1996, **143**, 233–244.
8 H. Takahashi, Y. Yokoyoma, E. L. Fireman and C. Lorius, *Lunar Planet. Sci.*, 1978, **9**, 1131–1133.
9 R. Ganapathy, *Science*, 1983, **220**, 1158–1161.
10 C. Koeberl, *Earth Planet. Sci. Lett.*, 1989, **92**, 317–322.
11 R. Rocchia, P. Bonte, C. Jehanno, E. Robin, M. De Angelis and D. Boclet, *Geol. Soc. Am. Spec. Pap.*, 1990, **247**, 189–193.
12 K. Rasmussen, H. B. Clausen and G. W. Kallemeyn, *Meteoritics*, 1995, **30**, 634–638.
13 D. B. Kerner, J. Levine, R. A. Muller, F. Asaro, M. Ram and M. R. Stolz, *Geochim. Cosmochim. Acta*, 2003, **67**, 751–763.
14 A. D. Anbar, G. J. Wasserburg, D. A. Papanastassious and P. S. Andersson, *Science*, 1996, **273**, 1524–1528.
15 A. D. Anbar, D. A. Papanastassiou and G. J. Wasserburg, *Anal. Chem.*, 1997, **69**, 2444–2450.
16 C. Barbante, G. Cozzi, G. Capodaglio, K. Van de Velde, C. Ferrari, A. Veysseyre, C. F. Boutron, G. Scarponi and P. Cescon, *Anal. Chem.*, 1999, **71**, 4125–4133.
17 C. Barbante, A. Veysseyre, C. Ferrari, K. Van de Velde, C. Morel, G. Capodaglio, P. Cescon, G. Scarponi and C. F. Boutron, *Environ. Sci. Technol.*, 2001, **35**, 835–839.
18 K. Van de Velde, C. Barbante, G. Cozzi, I. Moret, T. Bellomi, C. Ferrari and C. F. Boutron, *Atmos. Environ.*, 2000, **34**, 3117–3127.
19 E. Anders and N. Grevesse, *Geochim. Cosmochim. Acta*, 1989, **53**, 197–214.
20 K. H. Wedepohl, *Geochim. Cosmochim. Acta*, 1995, **59**, 1217–1232.
21 C. F. Boutron, *Fresenius' J. Anal. Chem.*, 1990, **337**, 482–491.
22 C. P. Ferrari, A. I. Moreau and C. F. Boutron, *Fresenius' J. Anal. Chem.*, 2000, **366**, 433–437.
23 F. A. M. Planchon, C. F. Boutron, C. Barbante, E. W. Wolff, G. Cozzi, V. Gaspari, C. Ferrari and P. Cescon, *Anal. Chim. Acta*, 2001, **450**, 193–205.
24 C. Barbante, T. Bellomi, G. Mezzadri, P. Cescon, G. Scarponi, C. Morel, S. Jay, K. Van de Velde, C. Ferrari and C. F. Boutron, *J. Anal. At. Spectrom.*, 1997, **12**, 925–931.
25 J. P. Candelone, S. Hong and C. F. Boutron, *Anal. Chim. Acta*, 1994, **299**, 9–16.
26 U. Gorlach and C. F. Boutron, *Anal. Chim. Acta*, 1990, **236**, 391–398.
27 M. P. Field and R. M. Sherrel, *J. Anal. At. Spectrom.*, 2003, **18**, 254–259.
28 K. J. R. Rosman and P. D. P. Taylor, *Pure Appl. Chem.*, 1998, **70**, 217–235.
29 A. Varga, C. Barbante, G. Cozzi, I. Mantovan, G. Rampazzo and P. Cescon, *J. Phys. IV*, 2003, **107**, 1337–1340.
30 S. Rauch, M. Lu and G. M. Morrison, *Environ. Sci. Technol.*, 2001, **35**, 595–599.
31 P. Vallelonga, K. Van de Velde, J. P. Candelone, K. J. R. Rosman, C. F. Boutron, V. I. Morgan and D. J. Mackey, *Anal. Chim. Acta*, 2002, **453**, 1–12.
32 S. Hong, J. P. Candelone and C. F. Boutron, *Atmos. Environ.*, 1997, **31**, 2235–2242.
33 S. Johnsen, D. Dahl-Jensen, N. Gundestrup, J. P. Steffensen, H. B. Clausen, H. Miller, V. Masson-Delmotte, E. A. Sveinbjörnsdottir and J. White, *J. Quatern. Sci.*, 2001, **16**, 299–307.
34 P. Gabrielli, C. Barbante, J. Plane, A. Varga, S. Hong, G. Cozzi, V. Gaspari, F. A. M. Planchon, W. Cairns, P. Cescon, C. Ferrari and C. F. Boutron, in preparation.
35 J. R. Petit, J. Jouzel, D. Reynaud, N. I. Barkov, J. M. Barnola, I. Basile, M. Bender, J. Chapellaz, M. Davis, G. Delaygue, M. Delmotte, V. I. Kotlyakov, M. Legrand, V. Y. Lipenkov, C. Lorius, L. Pépin, C. Ritz, E. Saltzman and M. Stievenard, *Nature*, 1999, **399**, 429–436.

J. Anal. At. Spectrom., 2004, 19, 831–837

2.2 ARTICLE 2: **Meteoric smoke fallout over the Holocene revealed by iridium and platinum in Greenland ice**

Paolo Gabrielli, Carlo Barbante, John M.C. Plane, Anita Varga, Sungmin Hong, Giulio Cozzi, Vania Gaspari, Frédéric A.M. Planchon, Warren Cairns, Christophe Ferrari, Paul Crutzen, Paolo Cescon and Claude F. Boutron

Submitted to *Nature,* revised version, August 2004

Meteoric smoke fallout over the Holocene revealed by iridium and platinum in Greenland ice

Paolo Gabrielli*†, Carlo Barbante†‡, John M.C. Plane§, Anita Varga†, Sungmin Hong∫, Giulio Cozzi†, Vania Gaspari†, Frédéric A.M. Planchon†, Warren Cairns‡, Christophe Ferrari*#, Paul Crutzen⊆, Paolo Cescon†‡ and Claude F. Boutron*ξ

* *Laboratoire de Glaciologie et Géophysique de l'Environnement (UMR CNRS/ Université Joseph Fourier 5183) 54, rue Molière, B.P. 96, 38402 St Martin d'Heres cedex, France*

† *Department of Environmental Sciences, University of Venice, Ca' Foscari, 30123 Venice, Italy*

‡ *Institute for the Dynamics of Environmental Processes-CNR, University of Venice, Ca' Foscari, 30123 Venice, Italy*

§ *School of Environmental Sciences, University of East Anglia, Norwich , NR47TJ, U.K.*

∫ *Korea Polar Research Institute, Korea Ocean Research & Development Institute, Ansan, PO Box 29, Seoul 425-600, Korea*

Ècole Polytechnique Universitaire de Grenoble (Institut Universitaire de France), Université Joseph Fourier, 28 avenue Benoît Frachon, B.P. 53, 38041 Grenoble, France

⊆ *Max Planck Institute for Chemistry, Atmospheric Division, Joh.-J.-Becher-Weg 27, 55128 Mainz, Germany*

ξ *Unité de Formation et de Recherche de Physique et Observatoire des Sciences de l'Univers (Institut Universitaire de France) , Université Joseph Fourier, Domaine Universitaire, B.P. 68 38041 Grenoble, France*

The iridium anomaly in the Cretaceous/Tertiary boundary layer revealed that an extraterrestrial body impacted the Earth 65 million years BP[1]. Although for this event the carrier of iridium was likely to be a micrometric silicate-enclosed aggregate[2] and/or the nanophase material of the vaporized impactor[3], the fate of platinum group elements (PGEs), regularly entering the atmosphere via ablating meteoroids, remains largely unknown. Here we report the first record of iridium and platinum fluxes on a climatic cycle time scale, back to 128,000 years BP, from a Greenland ice core[4]. We find that a remarkably constant fallout of extraterrestrial matter to Greenland occurred during the Holocene, whereas a greatly enhanced input of terrestrial iridium and platinum masked the cosmic flux in the dust-laden atmosphere of the last glacial age. We suggest that nanometric meteoric smoke particles[5,6], formed from the recondensation of ablated meteoroids in the atmosphere above 70 km, are transported into the winter polar vortices by the mesospheric meridional circulation[7] and preferentially deposited in the polar ice caps. This implies an average global fallout of 14 ± 5 kt y^{-1} of meteoric smoke during the Holocene.

We determined Ir and Pt in 35 sections from the 3028.8 m European Greenland Ice-Core Project (GRIP) ice core, drilled at Summit (72°34'N, 37°37'W) in central Greenland[4] (see method section). Twenty-two sections, spanning from ~2 up to ~10 years, were selected from the period between ~700 and 11,500 years BP covering the Holocene (uncertainty in this period is ~1%)[8], and 13 sections, spanning from ~10 up to ~100 years, between ~13,000 and 128,000 years BP covering the Last Glacial Age (LGA) back to the last interglacial (uncertainty in the LGA is up to ~10%)[8]. There is a lack of data from ~4000-7000 years BP, due to poor ice core quality. Low and remarkably constant concentrations are recorded in the Holocene both for Ir and Pt (averages of 0.3 and 0.6 ppq, respectively), whereas higher and more variable values are observed during the LGA (averages of 2 and 3 ppq). Part of the glacial-interglacial difference in concentration is caused by changes in the snow accumulation rate[8]; this rate was therefore combined with the concentration to determine the flux. The average deposition fluxes of Ir and Pt during the Holocene (8 and 15 fg cm^{-2} y^{-1}, respectively) are clearly lower by a factor of 2–3 than those during the LGA (24 and 32 fg cm^{-2} y^{-1}), (Fig.1).

Two contrasting situations emerge from our data between the Holocene and the LGA. In the Holocene, Ir and Pt have high crustal enrichment factors (EF_c), with mean values of 70 and 17, respectively (where $EF_c=\{[Metal]_{ice}/[Al]_{ice}\}/\{[Metal]_{crust}/[Al]_{crust}\}$; $\{[Ir]_{crust}/[Al]_{crust}\}=6.5x10^{-10}$ and $\{[Pt]_{crust}/[Al]_{crust}\}=5.2x10^{-9}$ from ref.[9]; $[Al]_{ice}$ is taken from ref.[10] and references therein, and it is used as crustal reference), (Fig. 1). These high EF_c values show that the contribution to the fluxes of these metals from terrestrial dust is negligible during the Holocene, averaging only 2% (Ir) and 7% (Pt). Additional sources were therefore predominant during the present interglacial. Although Ir is enriched in volcanic emissions[11], the possibility that such a constant Ir input to Greenland ice originates from explosive volcanism can be ruled out, whereas a contribution from quiescent degassing to Central Greenland ice seems to be unlikely because Ir species, such as iridium hexafluoride, are thought to react rapidly with the available particulate and are deposited close to the source. In contrast, the average Ir:Pt ratio in the ice during the Holocene, 0.49 (±0.20), is essentially the chondritic ratio (0.49)[12]. This evidence, together with the high elemental correlation ($R_{Ir-Pt}=0.67$), and the lack of correlation with Al, strongly supports a common extraterrestrial origin for Ir and Pt.

Ir and Pt can therefore be considered as equivalent proxies of extraterrestrial matter, without making necessary, as in most of the previous studies, any assumptions about their cosmic origin, and can be used to calculate the cosmic fallout to the Earth. Hence, by using the Ir or Pt chondritic concentration[12], we obtain from Greenland ice an average global extraterrestrial input during the Holocene of 78±30 kt y^{-1}. The micrometeorite content measured in central Greenland[13], based on dust >0.45 μm in ice, shows that these particles constitute less than 1% of our estimate of the extraterrestrial mass accretion to the Greenland ice sheet. This lends strong support to the hypothesis that the fraction of cosmic input determined with our innovative methodology[14] in Greenland ice arises from the deposition of the nanometric meteoric smoke particles[5,6] formed from the recondensation of ablated meteoroids in the mesosphere (see method section). Note that if these smoke particles are less than 5 nm in radius (see below), then the number of meteoric smoke particles per gram of ice sample is more than $1x10^9$, providing excellent counting statistics.

The ablation input of 78±30 kt y^{-1} is in reasonable agreement with the meteoroid input measured with the Long Duration Exposure Facility[15], an orbital impact detector placed on a spacecraft for several years, that yielded an estimate of 40±20 kt y^{-1}. This supports the current understanding that a substantial fraction of meteoroids ablates completely on entering the Earth's atmosphere[16]. However our value is significantly higher than most of the recent estimates of the cosmic material influx (see Table 1 and Supplementary Fig. 2), in particular those based on incoherent scatter radar observations of meteors[17] and the input required to model the global atomic Na layer in the upper mesosphere[16].

An important point to consider is whether meteoric smoke is deposited uniformly over the Earth's surface, as assumed in the above estimate of the meteoric smoke input, or whether atmospheric circulation is likely to drive preferential deposition pathways. In order to examine the effects of meteoric smoke formation and atmospheric circulation on the distribution of meteoric smoke entering the troposphere, first consider the evolution of meteoric smoke in the mesosphere. A model describing condensation, coagulation and gravitational settling (see Fig. 2 for details) shows that smoke particles do not grow large enough (>2 nm in radius) to sediment rapidly, and thus take about 45 days to descend below 60 km. However, a dominant feature of mesospheric circulation is the seasonal wind flow from the summer to the winter pole. The velocity is typically 3–5 m s^{-1} between about 60 and 85 km[18], so that most of the smoke particles will be transported meridionally within the mesosphere to the winter polar vortex, before descending rapidly into the lower stratosphere. If most of the material then enters the troposphere and is deposited polewards of 55° latitude (which is about one-fifht of the global surface area), the measured input from the ice record must be divided by a factor of about 5 (since the meridional flow reverses every 6 months). This gives a global input of ablated meteoroids of 14±5 kt y^{-1}, which is in closer agreement to the estimates from conventional meteor radar measurements[19] and modelling of the Na layer[16] (Table 1).

The scenario is different when considering the origin of Ir and Pt during the LGA. Lower and rather constant EF_c for Ir and Pt (average values of 11 and 2, respectively), (Fig.1), and generally high elemental correlations even with Al ($R_{Al\text{-}Ir}$=0.67; $R_{Al\text{-}Pt}$=0.87; $R_{Ir\text{-}Pt}$=0.73) are evidence of a noticeable contribution of Ir and Pt from the terrestrial crust during the LGA (the sample outlier for Ir:Pt of ~97,000 years BP is excluded from this analysis). This period was in fact characterised by a high dust loading in the Earth's atmosphere because of enhanced dry and windy conditions and the concurrent exposure of larger areas of the

continental shelf because of lower sea levels. The rather significant EF_c(Ir) during the LGA could be due to an underestimate of the $[Ir]_{crust}$ value used for the calculation above, possibly arising from Ir spatial inhomogenity in the Earth's crust. Alternatively, the Ir enrichment in ice could be due to the aeolian transport of Ir enriched oxic sediments[20] eroded from the exposed continental shelf or to the frequent occurrence of clay minerals in the GRIP ice core during the LGA[21]. These small-sized mineral grains can in fact be produced by the weathering of rocks relatively rich in Ir (mafic and volcanic) and are abundant in aeolian dust because of the occurrence of gravitational settling during the tropospheric transport.

The dominant fallout of terrestrial Ir and Pt into Greenland ice during the LGA means that it is difficult to test the hypothesis that there is a glacial-interglacial variation in the input of interplanetary dust, which has been proposed to account for the 100 kyr climate periodicity[22]. Nevertheless, when a temporarily low input of dust occurred ~50,000 years BP during the LGA, as a result of the general instability of the climate at that time[4] (see the Al drop and the associated temperature variation in Fig. 1), the Ir and Pt flux returned to low holocenic values. Assuming an unchanged extraterrestrial accretion rate over the Holocene and the LGA and by correcting the Ir and Pt flux for the meteoric smoke contribution, the average glacial EF_c(Pt) becomes essentially 1 and the EF_c(Ir) the more likely value of 5, therefore making clearer the dominant contribution of terrestrial Ir and Pt over the cosmic fraction. Thus, it appears that there was no significant variation in the flux of extraterrestrial matter over the LGA. A definitive solution to this problem will likely be provided by measuring PGEs concentrations in Antarctic ice records such as those obtained at Dome C (EPICA) and Vostok, since these are relatively less affected by the input of terrestrial dust.

Method section

Polar ice cores have provided valuable historical records of changes in heavy metal fluxes in the Earth's atmosphere[23,24]. Until now the Ir occurrence in polar ice sheets was thought to be related mainly to the deposition of micrometeorites, extraterrestrial particles smaller than ~1 mm in diameter that do not ablate in the mesosphere. The few attempts to measure ultralow levels of Ir in ice cores have been restricted to particles larger than 0.45 μm, obtained from filtered samples[13]. Unfortunately it has been shown that the typically small volumes retrieved from ice cores caused a severe under-sampling of the micrometeorite input[25]. Statistically significant collections of micrometeorites have required large masses, of up to 8000 ton, of polar ice and firn to be investigated[26].

In contrast with the situation for micrometeorites, ice cores can be used to estimate the input of meteoroids that do not survive entry into the Earth's atmosphere (estimated to lie between 60 and nearly 100% of the total)[16]. Because of their very high entry velocities, meteoroids undergo rapid frictional heating by collision with atmospheric molecules. Their constituent minerals subsequently vaporize between an altitude of 80 and 120 km[5,6]. In the middle mesosphere (50-80 km) the resulting metallic compounds are believed to polymerize with silicon oxides to form metal-rich nano-particles known as meteoric smoke[5].

As a consequence, PGEs which are highly enriched in chondritic meteorites[12], are redistributed from individual sub-millimetric onto multiple nanometric particles before deposition at the Earth's surface. Thus, the concentration of PGEs in ice cores can be used to evaluate the ablated fraction of the meteoroid input. Furthermore, ice cores benefit from three relevant advantages with respect to other environmental archives for studying PGEs on a long time scale. Firstly, the properties of PGEs remain unaltered in a low interference matrix such

as ice; secondly, their deposition can be dated more precisely; and finally, their flux can be calculated via the better known past accumulation rate.

Traditional methods for determining Ir in micrometric particulate matter filtered from ice samples[13] fail to include the potentially significant contribution from the much smaller sized meteoric smoke. This can only be taken into account by measuring the total Ir concentration relative to the wet mass of the sample. Recently, on the basis of experience in measuring PGEs in ice cores by using inductively coupled plasma sector field mass spectrometry (ICP-SFMS)[27], we have developed a new method (see details in ref.[14]) for quantifying the total concentration of Ir and Pt in ice, down to the sub-ppq level (1 ppq=1 fg $g^{-1}=10^{-15}$ g g^{-1}). Ultra-clean procedures and a preconcentration step have enabled us to achieve negligible procedural blanks (see also Supplementary Method 1) and procedural detection limits of 0.02 and 0.08 ppq for Ir and Pt, respectively[14]. This method benefits from an ultra-clean chemical processing of the sample based on the simple addition of ultrapure HNO_3 to the melted and pre-concentrated ice samples. The complete ionization of the meteoric smoke in the plasma (at ~ 7000 K) of the ICP-SFMS, is assured by the already quasi-molecular size of these particles, without the need to add any supplemental chemical reagent.

Supplementary Information accompanies the paper on *Nature's* website (http://www.nature.com)

Acknowledgements This work was supported in France by the Institut Universitaire de France, the Ministère de l'Environnement et de l'Amènagement du Territoire, the Agence de l'Environnement et de la Maîtrise de l'Energie, the Intitut National des Sciences de l'Univers and the Universite Joseph Fourier of Grenoble. In Italy, it was supported by ENEA as part of the Antarctic National Research Programme, and in the UK, by the Natural Environment Research Council. This research has been also supported by two Marie Curie Fellowships of the European Community programme (IHP) and by the *Alliance for Global Sustainability* (project title: Platinum Group Elements from Automobile Emission to Global Distribution). This work is a contribution of GRIP organised by the European Science Foundation: we would like to thank all the personnel working in the field in Greenland.

Competing Interests statement The authors declare that they have no competing financial interests.

Correspondence and requests for materials should be addressed to C. Barbante (e-mail: barbante@unive.it).

1. Alvarez, L. W., Alvarez, W., Asaro, F. & Michel, H. V. Extraterrestrial cause for the Cretaceous/Tertiary Extinction. *Science* **208**, 1095-1108 (1980).
2. Schuraytz, B. C. et al. Iridium metal in Chicxulub impact melt: forensic chemistry on the K-T smoking gun. *Science* **271**, 1573-1576 (1996).
3. Wdowiak, T. J. et al. Presence of an iron-rich nanophase material in the upper layer of the Cretaceous-Tertiary boundary clay. *Meteorit. Planet. Sci.* **36**, 123-133 (2001).
4. Dansgaard, W. et al. Evidence for general instability of past climate from a 250- Kyr ice core record. *Nature* **364**, 218-220 (1993).
5. Hunten, D. M., Turco, R. P. & Toon, O. B. Smoke and dust particles of meteoric origin in the mesosphere and stratosphere. *J. Atmos. Sci.* **37**, 1342-1357 (1980).
6. Love, S. G. & Brownlee, D. E. Heating and thermal transformation of micrometeoroids entering the Earth's atmosphere. *Icarus* **89**, 26-43 (1991).
7. Prather, M. J. & Rodriguez, J. M. Antarctic ozone: meteoric control of HNO3. *Geophys. Res. Lett.* **15**, 1-4 (1988).
8. Johnsen, S. J. et al. Oxygen isotope and palaeotemperature records from six Greenland ice-core stations: Camp Century, Dye-3, GRIP, GISP2, Renland and NorthGRIP. *Quatern. Sci.* **16**, 299-307 (2001).
9. Wedepohl, K. H. The composition of the continental crust. *Geochim. Cosmochim. Acta* **59**, 1217-1232 (1995).
10. Hong, S., Candelone, J. P. & Boutron, C. F. Changes in zinc and cadmium concentrations in Greenland ice during the past 7760 years. *Atmos. Environ.* **31**, 2235-2242 (1997).
11. Zoller, W. H., Parrington, J. R. & Kotra, J. M. P. Iridium enrichment in airborne particles from Kilauea Volcano: January 1983. *Science* **222**, 1118-1121 (1983).
12. Anders, E. & Grevesse, N. Abundances of the elements: Meteoritic and solar. *Geochim. Cosmochim. Acta* **53**, 197-214 (1989).
13. Karner, D. B. et al. Extraterrestrial accretion from the GISP2 ice core. *Geochim. Cosmochim. Acta* **67**, 751-763 (2003).
14. Gabrielli, P. et al. Determination of Ir and Pt down to the sub-femtogram per gram level in polar ice by ICP-SFMS using preconcentration and a desolvation system. *J. Anal. At. Spectrom.* **19**, 831-837 (2004).
15. Love, S. G. & Brownlee, D. E. A direct measurement of the terrestrial mass accretion rate of cosmic dust. *Science* **262**, 550-553 (1993).
16. Plane, J. M. C. A new time-resolved model of the mesospheric Na layer: constraints on the meteor input function. *Atmos. Chem. Phys. Disc.* **4**, 39-69 (2004).
17. Mathews, J. D., Janches, D., Meisel, D. D. & Zhou, Q. H. The micrometeoroid mass flux into the upper atmosphere: Arecibo results and a comparison with prior estimates. *Geophys. Res. Lett.* **28**, 1929-1932 (2001).
18. Rees, D. & Bilitza, D. COSPAR International Reference Atmosphere: 1986, Part II: Middle atmosphere models. *Adv. Space Res.* **10** (1990).
19. Hughes, D. W. in *Cosmic dust* (ed. McDonnel, J. A. M.) 123-185 (Wiley, London, 1978).
20. Ravizza, G. & Pyle, D. PGE and Os isotopic analysis of single sample aliquots with NiS fire assay preconcentration. *Chem. Geol.* **141**, 251-268 (1997).

21. Svensson, A., Biscaye, P. E. & Grousset, F. E. Characterization of late glacial continental dust in the Greenland Ice Core Project ice core. *J. Geophys. Res.* **105**, 4637-4656 (2000).

22. Muller, R. A. & MacDonald, G. J. Glacial cycles and orbital inclination. *Nature* **377**, 107-108 (1995).

23. Boutron, C. F. & Patterson, C. C. Lead concentration changes in Antarctic ice during the Wisconsin/Holocene transition. *Nature* **323**, 222-225 (1986).

24. Hong, S. et al. Climate-related variations in lead concentrations and sources in Vostok Antarctic ice from 65,000 to 240,000 years BP. *Geophys. Res. Lett.* **30**, 2138-2142 (2003).

25. Peucker-Ehrenbrink, B. & Ravizza, G. The effects of sampling artifacts on cosmic dust flux estimates: A reevaluation of nonvolatile tracers (Os, Ir). *Geochim. Cosmochim. Acta* **64**, 1965-1970 (2000).

26. Taylor, S., Lever, J. H. & Harvey, R. Accretion rate of cosmic spherules measured at the South Pole. *Nature* **392**, 899-903 (1998).

27. Barbante, C. et al. Determination of Rh, Pd, and Pt in polar and alpine snow and ice by double-focusing ICPMS with microcentric nebulization. *Anal. Chem.* **71**, 4125-4133 (1999).

28. Brown, P., Spalding, R. E., ReVelle, D. O., Tagliaferri, E. & Worden, S. D. The flux of small near-Earth objects colliding with the Earth. *Nature* **420**, 294-296 (2002).

29. Maurette, M., Jehanno, C., Robin, E. & Hammer, C. U. Characteristics and mass distribution of extraterrestrial dust from the Greenland ice cap. *Nature* **328**, 699-702 (1987).

30. Jacobson, M. Z., Lu, R., Jensen, E. J. & Toon, O. B. Modelling coagulation among particles of different composition and size. *Atmos. Environ.* **28A**, 1327-1338 (1994).

Table 1 **Reported estimates of global extraterrestrial matter accretion rate**

Method	Proxy	Type of input measured	Accretion rate (kt y^{-1})
	Space		
Long Duration Exposure Facility[15]	Micro impact in space	Meteoroids	20 – 60
Defence satellite measurments[28]	Bolids detonations	Bolids	0.6[a]
	Atmosphere		
Conventional meteor radar[19]	Ablating meteoroids	Ablating meteoroids	16
Large aperture radars[17]	Ablating meteoroids	Ablating meteoroids	1.6 – 2.7
Modelling[16]	Na layer	Meteoric smoke[b]	3.7 - 11
	Glacial archives		
Collection from blue ice[29]	(direct measurement in Greenland ice)	Cosmic spherules	3.2
High ice volume melting[26]	(direct measurement in South Pole ice and firn)	Cosmic spherules	2.7
Instrumental neutron activation analysis[13]	Ir in Greenland dust	Micrometeorites	0.22 (0.17-6.25)[c]
ICP-SFMS (this paper)	Ir and Pt in Greenland ice	Meteoric smoke[b]	14[d] – 78[e]

[a] Obtained by integrating the particle flux with an infall frequency of more than once every 100 years

[b] This kind of input refers only to the ablated fraction of meteoroids, see text

[c] Corrected for the micrometeorite under-sampling in small ice cores volumes

[d] Corrected by dividing for the latitudinal and seasonal factor, see text

[e] Integrated over the entire Earth's surface (no correction).

FIGURE CAPTIONS

Figure 1 Change in Ir, Pt and Al depositional fluxes in central Greenland over the last climatic cycle. **a** ^{18}O, expressed in per mil δ units ($\delta^{18}O$), used as a proxy of temperature, with less negative values indicating higher temperatures during interglacial periods and more negative values showing cold climatic stages. Open circles refer to values measured in our samples. **b** Al flux (as a terrestrial dust proxy, used to calculate the crustal enrichment factor (EF_c) of Ir and Pt). **c** Ir flux and EF_c(Ir) (dotted line). **d** Pt flux and EF_c(Pt) (dotted line). Rather constant Ir and Pt fluxes are observed during the last ~11,500 years (Holocene) while higher and more variable values are observed during the last glacial age (LGA) with a fairly synchronous variation for $\delta^{18}O$, Al, Ir and Pt (see for instance the metals flux drop and the associated $\delta^{18}O$ variation at ~50,000 years BP evidenced by the vertical dotted line). Low Ir and Pt values in the deepest sample (~128,000 years BP) suggest low fluxes also during the last interglacial period (Eemian). High EF_c values are observed for Ir and Pt during the Holocene showing that contribution from crustal dust was negligible during that period and suggesting an alternative source that several cross evidences show to be cosmic (see text). Conversely much lower EF_c values are observed during the LGA indicating that Ir and Pt mainly derived from crustal dust during glacial times.

Figure 2 Vertical profiles of meteoric smoke particles of selected size. The 1-dimensional model, calculated for a mass influx of 18 kt y^{-1}, includes meteoric ablation, polymerization

of metal-containing molecules[16], growth by condensation and coagulation, and sedimentation[30]. The model shows that the meteoric smoke particles do not grow large enough (>2 nm) to sediment rapidly. It would take about 45 days for the meteoric smoke particles to sediment to below 60 km, long enough to be transported by mesospheric circulation into the Polar vortices.

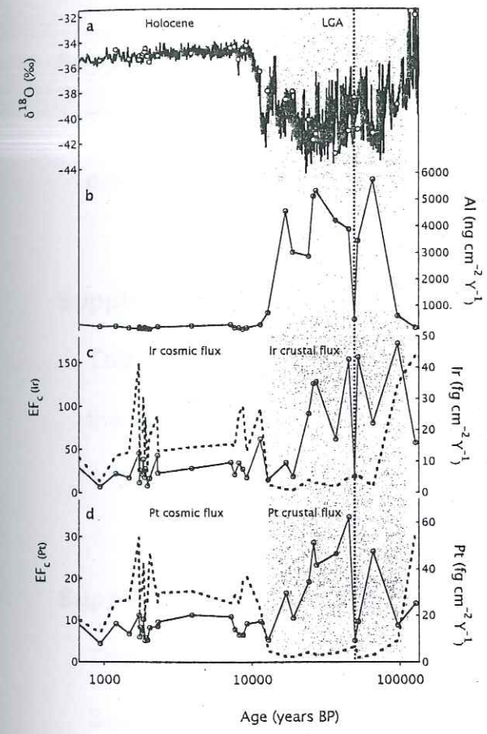

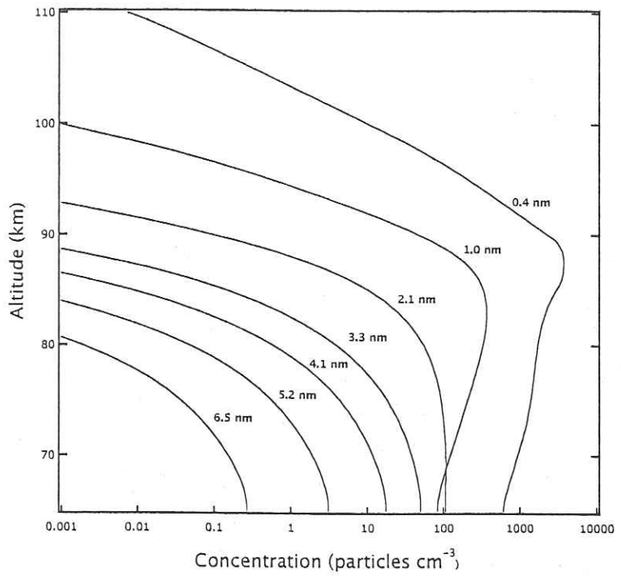

Supplementary Method 1

This section illustrates the quantification of the procedural blank related to the pre-concentration procedure of Greenland ice samples (Word, 36 kB).

Supplementary Table 1

This table shows the Ir and Pt concentrations measured in Greenland ice with the associated instrumental standard deviation from 100 acquisitions (Word, 108 kB).

Supplementary Figure 1

This figure shows how the procedural blank was determined in the section Supplementary Method 1. The mass (in fg) of Ir (a) and Pt (b) released/adsorbed to/from the solution during the pre-concentration procedure is the intercept of the regression line of the Ir and Pt masses measured *vs.* different initial masses of pre-concentrated ultra pure water. The error bars given are the instrumental standard deviations from 100 acquisitions (Word, 40 kB).

Supplementary Figure 2

This figure shows a comparison of different extraterrestrial accretion rate estimates as shown in Table 1. Our direct measurement estimate of 78 kt y^{-1} is slightly larger also than the commonly accepted value of around 40 kt y^{-1}

(ref. 15) whereas our estimation of the corrected average global fallout of 14 kt y^{-1} (see text) agrees well with other recent different estimates (Word, 72 kB).

Supplementary Method 1

Measuring Ir and Pt in polar ice down to the sub-ppq level (1 ppq = 1 fg/g = 10^{-15} g/g), is an unprecedented analytical result obtained thanks to the high sensitivity offered by inductively coupled plasma sector field mass spectrometry (ICP-SFMS), combined with careful control of contamination and the evaluation of the analytical blanks. A detailed description of our analytical methodology is reported in ref. 14 (http://www.rsc.org/CFmuscat/intermediate_abstract.cfm?FURL=/ej/JA/2004/b316283d.PDF). Here we report additional experiments that confirm the analytical methodology and in particular the quantitative determination of the procedural blanks.

To determine Ir and Pt in polar ice, a pre-concentration procedure was adopted using sub-boiling evaporation, to increase metal concentrations by almost two orders of magnitude. The procedural blank for the pre-concentration procedure was quantitatively assessed by pre-concentrating different volumes of ultra pure water (UPW) (2, 5, 8, 17, 54 and 108 ml; one aliquot of 1 ml was measured directly) to about 1 ml of solution in ultra acid clean PFA (polyfluoroalkoxy) beakers (Nalgene, Rochester, NY, USA) spiked with ultra pure HNO_3 to a final concentration of 1% v/v. The blank contribution of HNO_3 was evaluated separately and was found always to be under the instrumental detection limit. (see ref. 14 for details on materials and reagents).

Supplementary Figure 1 is a plot of the measured Ir and Pt masses *vs*. the initial mass of UPW. The intercepts of the regression lines on the *y* axis indicate the masses of Ir and Pt released (positive intercept) or adsorbed (negative intercept) by the PFA beaker during the pre-concentration. The intercepts in Supplementary Figure 1 for Ir and Pt are (-1 ± 13 fg) and (4 ± 4 fg), respectively (uncertainty is given at the 0.95 confidence level). This means that the blanks affecting the Greenland ice samples are -0.02 ppq and 0.07 ppq, respectively,

calculated as the mass given by the intercept divided by the typical initial Greenland sample ice mass of ~60 g. This is evidence of a negligible exchange for both metals, even at the sub-ppq level, when compared to our typical instrumental standard deviations (see Supplementary Table 1).

The slopes of the regression plots in Supplementary Figure 1 yield the concentrations of the metals in UPW: Ir = 3.5 ppq and Pt = 1.7 ppq. Measuring ultra trace levels in ancient ultra pure polar ice we are working at the limits of the conventional analytical chemistry; it is therefore not uncommon that the metal concentrations are comparable to concentrations found in UPW. However, significant contamination of the samples from UPW seems to be very unlikely because the initial sample volume (~60 ml) is much larger than the few UPW droplets (with a volume in the order of ~0.01 ml, ~6000 times smaller than our typical sample volume) that could remain adhered to the PFA beakers walls after the rinsing steps. This thesis is strongly reinforced by the fact that the Ir/Pt mass ratio in UPW was found clearly to be >1 in most of the tests performed, whereas the Ir/Pt mass ratio in the lowest Greenland holocenic samples, is consistently ~0.5, that is also the chondritic ratio[12].

To summarize, these additional tests confirm our previous conclusions reported in ref. 14, that no procedural blank need to be subtracted from the concentrations found in Greenland samples. The very high sensitivity of the ICP-SFMS thus enables Ir and Pt to be measured down to the sub-ppq per gram level in polar ice.

Supplementary Table 1. Ir and Pt concentrations measured in Greenland ice.

Depth (m)	Age (years BP)	Ir (ppq)	± SD (ppq) [a]	Pt (ppq)	± SD (ppq) [a]
184.3	680	0.35	0.03	0.7	0.1
239.3	941	0.1	0.1	0.4	0.1
294.3	1205	0.25	0.02	0.7	0.1
349.3	1478	0.20	0.02	0.5	0.1
399.3	1731	0.58	0.04	0.9	0.1
401.0	1740	0.1	0.1	0.5	0.1
404.3	1757	0.3	0.1	0.6	0.1
416.9	1823	0.2	0.1	0.5	0.1
422.4	1851	0.5	0.1	0.8	0.1
430.7	1893	0.20	0.02	0.40	0.04
435.1	1915	0.3	0.1	0.4	0.1
446.1	1972	0.10	0.01	0.44	0.05
459.3	2041	0.22	0.02	0.7	0.1
509.3	2308	0.5	0.1	0.7	0.1
511.0	2317	0.25	0.02	0.7	0.1
789.3	3926	0.3	0.1	0.8	0.1
1230.4	7182	0.38	0.04	0.78	0.04
1286.5	7674	0.2	0.1	0.6	0.1
1339.3	8179	0.40	0.03	0.5	0.1
1394.3	8723	0.3	0.1	0.5	0.1
1449.3	9291	0.19	0.02	0.7	0.1
1614.3	11417	0.79	0.04	0.8	0.1
1669.3	12843	0.25	0.02	0.6	0.1
1834.3	16960	0.7	0.1	2.2	0.3
1894.2	18949	0.5	0.1	1.8	0.4
1999.3	24280	2.4	0.3	3	1
2034.5	26127	4	1	6	1
2054.3	27151	3.9	0.2	5	1
2214.3	36924	2.3	0.3	6	1
2334.2	45358	5	1	7	2
2384.3	49433	0.34	0.04	0.6	0.1
2424.4	52437	4.0	0.3	1.6	0.2
2527.3	65417	2.5	0.3	5	1
2714.3	96521	3.2	0.1	1.1	0.1
2843.0	128157	0.6	0.2	0.9	0.3

[a] Instrumental standard deviation calculated from 100 acquisitions

Supplementary Figure 1

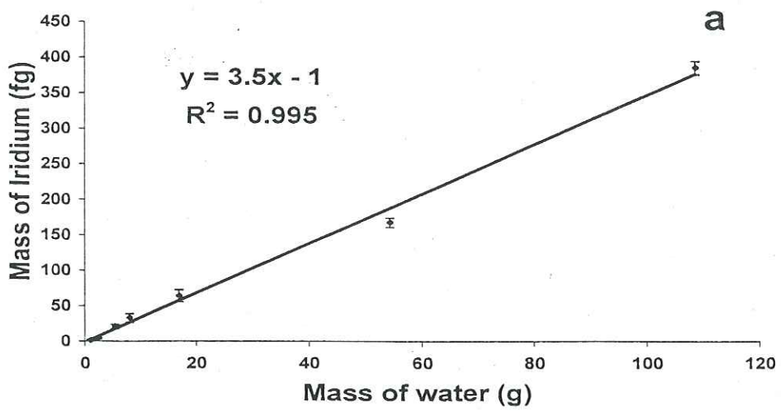

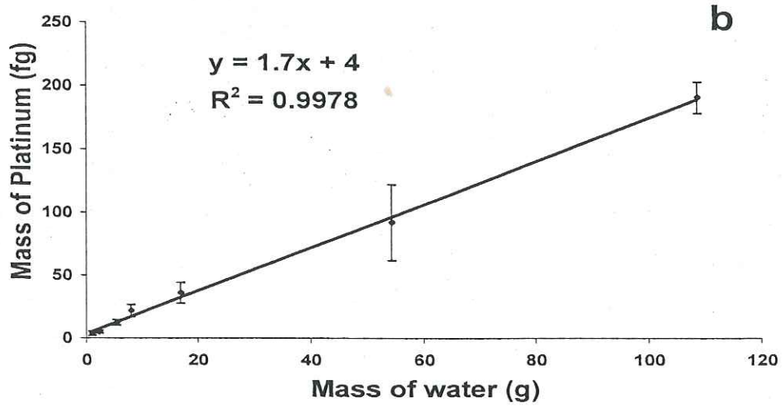

The mass (in fg) of Ir (a) and Pt (b) released/adsorbed to/from the solution during the pre-concentration procedure is the intercept of the regression line of the Ir and Pt masses measured *vs.* different initial masses of pre-concentrated ultra pure water (UPW). The error bars given are the instrumental standard deviations from 100 acquisitions.

Supplementary Figure 2

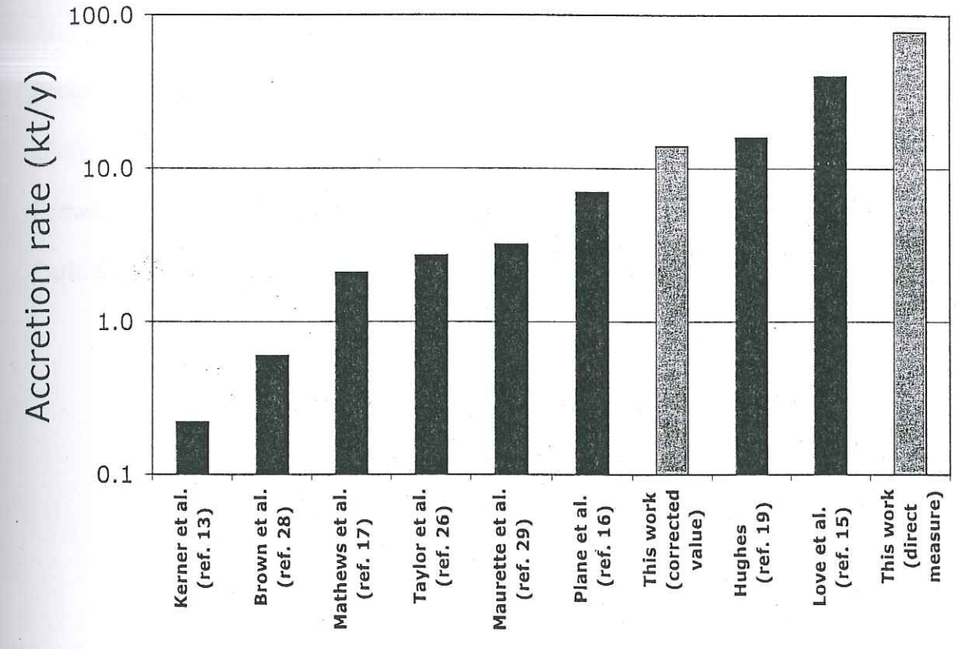

Comparison of different cosmic accretion rates. Our direct measurement estimate of 78 kt y^{-1} is slightly larger also than the commonly accepted value of around 40 kt y^{-1} (ref. 15) whereas our estimation of the corrected average global fallout of 14 kt y^{-1} (see text) agrees well with other recent different estimates.

2.3 ARTICLE 3: **Change in atmospheric circulation revealed by meteoric smoke fallout to Antarctica over glacial stages**

Paolo Gabrielli, John M.C. Plane, Claude F. Boutron, Anita Varga, Sungmin Hong, Giulio Cozzi, Vania Gaspari, Frédéric A.M. Planchon, Warren Cairns, Christophe Ferrari, Paul Crutzen Paolo Cescon, Jean Robert Petit, Vladimir Y. Lipenkov and Carlo Barbante

To be submitted to *Science*

Change in atmospheric circulation revealed by meteoric smoke fallout to Antarctica over glacial stages

Paolo Gabrielli[a,b], John M.C. Plane[c], Claude F. Boutron[a,d], Anita Varga[b], Sungmin Hong[e], Giulio Cozzi[b], Vania Gaspari[b], Frédéric A.M. Planchon[b], Warren Cairns[f], Christophe Ferrari[a,g], Paul Crutzen[h] Paolo Cescon[b,f], Jean Robert Petit[a], Vladimir Y. Lipenkov[i] and Carlo Barbante[b,f]

[a]*Laboratoire de Glaciologie et Géophysique de l'Environnement (UMR CNRS/ Université Joseph Fourier 5183) 54, rue Molière, B.P. 96, 38402 St Martin d'Heres cedex, France*

[b]*Department of Environmental Sciences, University of Venice, Ca' Foscari, 30123 Venice, Italy*

[c]*School of Environmental Sciences, University of East Anglia, Norwich , NR47TJ, U.K*

[d]*Unité de Formation et de Recherche de Physique et Observatoire des Sciences de l'Univers (Institut Universitaire de France) , Université Joseph Fourier, Domaine Universitaire, B.P. 68 38041 Grenoble, France*

[e]*Korea Polar Research Institute, Korea Ocean Research & Development Institute, Ansan, PO Box 29, Seoul 425-600, Korea*

[f]*Institute for the Dynamics of Environmental Processes-CNR, University of Venice, Ca' Foscari, 30123 Venice, Italy*

[g]*Polytech Grenoble (Institut Universitaire de France), Université Joseph Fourier, 28 avenue Benoît Frachon, B.P. 53, 38041 Grenoble, France*

h *Max Planck Institute for Chemistry, Atmospheric Division, Joh.-J.-Becher-Weg 27, 55128 Mainz, Germany*
i Arctic and Antarctic Research Institute, Beringa Street 38, 199397, St Petersburg, Russia

Meteoric smoke particles originate from meteoroid vaporization and re-condensation in the mesosphere. Recently, these particles have been detected from measurements of iridium and platinum in a glacial archive from Greenland. Here we report two new records of iridium and platinum from ice cores retrieved at Dome C and Vostok, Antarctica, extending back to ~240 kyr BP. The meteoric smoke fallout in these records is strongly correlated with low local temperatures which is evidence of an increased subsidence of cold air masses from the low stratosphere/upper troposphere of East Antarctica during coldest stages. Conversely, the higher input of Ir and Pt observed during warmer periods was probably caused by volcanogenic aerosol, which was transported polewards via a lower path within the troposphere and deposited onto the Antarctic plateau.

Meteoroids enter the Earth's atmosphere with initial velocities between 12 and 72 km s^{-1}, causing rapid frictional heating and the subsequent vaporization of their constituent minerals (*1, 2*). This process is the source of the layer of metal atoms and ions that occur globally at an altitude between 80 and 110 km (*3*). In particular, above Polar Regions, cosmogenic atoms such as Fe, can be completely removed by efficient up take onto the surface of ice particles in the polar mesospheric clouds (*4*). In general, lower down in the middle mesosphere, all around the globe, the metallic compounds, formed by oxidation reactions, polymerise together (probably also with the silicon oxides produced by meteoric ablation) to form metal-rich particles (*5*), known as meteoric smoke (*1*). These particles do not grow large enough (>2 nm) to sediment rapidly out of the mesosphere and therefore can be transported by the meridional mesospheric circulation into the polar vortex of the winter hemisphere, before descending into the lower stratosphere (*6*).

Polar regions seem therefore to be a key place to study meteoric smoke particles and their path of transport toward the surface. Recently, these particles have been detected in an ice core from Summit in Central Greenland (GRIP), from measurements of Ir and Pt, which are proxies of cosmic material fallout (*6*). The remarkably constant input of Ir and Pt over the Holocene strongly suggests that most of the extraterrestrial material accreted by the Earth ablates in the upper layers of the atmosphere and is then deposited as smoke particles onto the polar ice caps. This record provides an estimate of the meteoric smoke global fallout, but also contains evidence of a strong terrestrial component of Ir and Pt transported onto the Greenland ice cap concomitantly with the high aeolian dust flux during the last glacial period (*6*).

Here we report the first records of Ir and Pt from two deep Antarctic ice cores retrieved at Dome C (75°06' S; 123°21' E, 3,233 m, t=-54 °C), in the framework of the European Project for Ice Coring in Antarctica (EPICA) (*7*), and at Vostok (78°28′S, 106°48′E, 3,488 m, t=–55 °C), in the framework of a joint program between Russia, France and USA (*8*). These two sites are located on the East Antarctic plateau, about 550 km apart, and have provided the two longest ice records ever retrieved on Earth.

We have analysed 41 samples from the first 2193 m of the Dome C ice core (EDC), and 23 samples from the first 2751 m of the Vostok ice core (VK), covering an

approximately equivalent period of ~217 and ~237 kyr, respectively. That is, from the current interglacial (the Holocene) back to the next-to-last interglacial period. The measurement of ultra-low Ir and Pt concentrations in Antarctic ice, down to the sub-ppq level (1ppq=1 fg g^{-1}=10^{-15} g g^{-1}), required ultra-clean sample preparation and the adoption of a pre-concentration step, by sub-boiling evaporation, prior to the analysis. Analyses were conducted by Inductively Coupled Plasma Sector Field Mass Spectrometry (ICP SFMS). Procedural detection limits of 0.02 ppq for Ir and 0.08 ppq for Pt were achieved, with negligible procedural blanks. The method is described in detail elsewhere (*6, 9*).

Concentrations of Ir and Pt appear to be quite variable in EDC, and less so in VK (see Tables 1 and 2). Minimum concentrations of Ir and Pt are lower than 1 ppq at both sites, whereas the maxima are quite different: in EDC, maxima of 18 and 12 ppq for Ir and Pt were found at 1.2 and 21.9 kyr BP, respectively, whereas in VK 2.1 and 5.2 ppq of Ir and Pt were determined at 118.5 and 142.5 kyr BP, respectively. However, the median values at both sites are comparable (Ir=1.9 ppq, Pt=2.3 ppq in EDC; Ir=1.1 ppq, Pt=1.8 ppq in VK). The two records differ essentially because of the presence of few large spikes of Ir and Pt in the upper part of EDC.

The median concentrations found in GRIP (0.3 and 0.7 ppq for Ir and Pt respectively)(*6*) are lower than in EDC and VK. This could be due to the lower snow accumulation rate on the East Antarctic plateau, smaller by about one order of magnitude than in Central Greenland. When concentrations are combined with snow accumulation rates to calculate the fluxes, Ir and Pt fallouts to the East Antarctic plateau are clearly lower than to the Greenland ice cap (*6*) (median values of 2 and 4 fg cm^{-2} y^{-1} in EDC, 3 and 4 fg cm^{-2} y^{-1}in VK; 11 and 23 fg cm^{-2} y^{-} in GRIP for Ir and Pt respectively).

The Ir and Pt fluxes in GRIP were high during the last ice age, because of the greatly enhanced aeolian contribution, and clearly lower in the Holocene when the input was mostly due to the meteoric smoke fallout (*6*). In contrast, the Ir and Pt fluxes in East Antarctica seem to show a different response to climatic conditions: high fluxes occur during warm periods whereas, apart from few Pt measurements in VK, the cold stages are characterized by low fluxes (Fig. 1).

The crustal enrichment factor EF_c (where EF_c=$\{[Metal]_{ice}/[Mn]_{ice}\}/\{[Metal]_{crust}/[Mn]_{crust}\}$; $\{[Ir]_{crust}/[Mn]_{crust}\}$=$9.5\times10^{-8}$ and $\{[Pt]_{crust}/[Mn]_{crust}\}$=$7.6\times10^{-7}$ from ref. (*10*); $[Mn]_{ice}$ from ref. (*11, 12*)), where Mn is a useful indicator of the crustal source. The respective median EF_c values for Ir and Pt are 182 and 32 in EDC, and 121 and 27 in VK. Inspection of the individual EF_c values (Tables 1 and 2) shows that even during the strongest glacial dust fallout to the Antarctic plateau, the Ir and Pt fluxes are most often not explained by a crustal contribution. This indicates that non-crustal natural sources were dominant not only in interglacial but even in glacial periods. However, we cannot exclude a crustal contribution to Pt in VK during glacial periods when, although the EF_c is rather high, Pt and Mn show a good correlation between their respective highest glacial values. A possible continental contribution could therefore explain the occurrence of some higher values of the Pt flux recorded in VK during cold periods.

The Ir and Pt elemental ratio (Ir/Pt) can also help to identify the origin of these metals. When Ir/Pt is compared with δD (*7, 8*), taken as proxy of the past local temperature, it emerges clearly that these two parameters are strongly correlated both in EDC and in VK (Fig. 2). In particular, more negative δD values are associated with Ir/Pt

≈0.5 whereas less negative δD values are associated with Ir/Pt close or higher than 1, both in EDC and in VK. This means that Ir/Pt in East Antarctica is essentially chondritic ($[Ir/Pt_{chondr.}]$= 0.49 from ref. (*13*)) during glacial periods, whereas in warmer times it is neither chondritic nor crustal ($[Ir/Pt_{crust.}]$= 0.2 from ref. (*10*)), due to the relatively large Ir fluxes that most of the time exceed the Pt fluxes.

Interestingly, in the holocenic part of EDC the Ir/Pt ratios calculated from the few large Ir and Pt spikes agree well with the non-chondritic ratios from the other lower values during this period. Extremely high Ir and Pt fluxes of several tens of fg cm^{-2} y^{-1}, occurring mainly in the Holocene, cannot therefore be explained by rare large extraterrestrial impacts, but appear to be caused by fluctuations in a continuous terrestrial source. High elemental correlations between Ir and Pt in Dome C (0.96) and in Vostok (0.87), together with non-chondritic ratios during interglacial periods, suggest a common but non-crustal terrestrial origin of these two metals.

Platinum group elements (PGEs) are strongly depleted in the Earth's upper crust (*10*) but are highly enriched in the mantle, where they can exhibit also non-chondritic elemental ratios (*14*). The volcanic emission of PGEs, originating from the Earth's inner crust- mantle, have already been documented (*15*). However, the atmospheric lifetime of PGEs was thought to be rather short because of the likely fast oxidation and deposition of very reactive components such as Ir hexafluoride (*16*). As far as we are aware, the only volcanic Ir enrichment in ice was recorded by analysing large particles decanted after melting an Antarctic tephra ice layer sample, most likely originating from the eruption of a local volcano (*17*). Nevertheless, we have recently measured traces of Ir and Pt in Greenland snow layers that are clearly associated with the June 1991 Pinatubo eruption (Gabrielli et al., unpublished results). This is the first clear evidence that PGEs of volcanic origin can undergo long-range transport on a global scale. Moreover, a visible tephra layer was not observed in the Greenland snow, indicating that PGEs can be transported also within a much smaller volcanic particulate fraction. Therefore, we suggest that the persistent Ir and Pt non-chondritic fallout to the East Antarctic plateau that occurred during warm periods originates from volcanic activities, and is likely related to long-term quiescent emissions (*18*).

The analysis of trace elements (e.g., Cd and Bi) and Pb isotopes indicate that Dome C (*12, 19*) and Vostok, to a lesser extent (*11*), have been subjected to fairly frequent volcanic fallout. This volcanic influence could be due to Mt. Erebus (3,795 m) (*20*), a currently active volcano situated at Ross Island, about 1000 km from Dome C and 1100 km from Vostok. Comparing our Ir and Pt data recorded in Dome C during warm periods with the corresponding Vostok data, EDC shows a higher Ir and Pt non-chondritic fallout and a higher Ir/Pt ratio, consistent with a stronger signature of a nearby volcano at Dome C. Wherever these local volcanic sources are actually located, the persistent fallout at Dome C and Vostok implies a path within the troposphere during warm periods.

In contrast, during glacial periods the essentially chondritic Ir/Pt ratio, the significant Ir-Pt correlation coefficients (0.53 in EDC (excluding the high Pt value at ~22 kyr BP because of its large uncertainty) and 0.80 in VK), and generally high EF_c are evidence of fallout of meteoric smoke particles (*6*) occurring to the East Antarctic plateau. This last observation implies a concomitant descent of cold air masses from the upper layer of the troposphere/low stratosphere conveying the meteoric smoke particles

down to the surface of the East Antarctic plateau during cold periods. Due to the colder surface during glacial times, a stronger thermal anticyclone over the Antarctic plateau would have in fact increased the subsidence of cold air masses (*21*), containing meteoric smoke, onto the East Antarctic ice cap surface.

Our observations are in agreement with the proposal that the reduced dust size observed in EDC during the last glacial age was associated with an enhanced subsidence of cold air masses from the upper tropospheric levels (*22*). However, while subsidence may modulate the tropospheric advection of continental dust from one site to one other in East Antarctica (*22*), our data suggests an overall enhanced subsidence of cold air masses from the low stratosphere/upper troposphere over East Antarctica during cold periods.

The total accretion rate of meteoric smoke over the whole Earth's surface can be calculated from samples showing an approximate chondritic ratio (Ir/Pt $\leq$0.8) by scaling the Ir and Pt fluxes using the relative abundances of these metals in chondrites (*13*). This yields 24±11 and 21±8 kt y^{-1} in EDC and VK, respectively. These estimates, obtained from data during glacial periods, are in good accord, but are lower by a factor of 3 - 4 than a previous estimate (78±30 kt y^{-1}) obtained from GRIP in the Holocene (*6*).

Unfortunately, a synchronous comparison between the accretion rates to the Greenland and Antarctic ice caps is not possible. This is because in Greenland a strong continental input of terrestrial Ir and Pt masked the meteoric smoke signature during the last glacial age, whereas in East Antarctica the lower continental input allows the cosmic signature to be recognised in cold periods, but the probable volcanic fallout of Ir and Pt prevents this during warm times. Nevertheless, another estimate of the smoke accretion rate to Antarctica has been obtained from Ir and Pt concentrations measured in relatively recent snow layers (1837 - 1990) at Coatsland, an Antarctic site facing the Atlantic (Gabrielli et al., unpublished results). The rate of 120±59 kt y^{-1} is in good accord with the North hemispheric estimate of 78±30 kt y^{-1} during the Holocene (*6*).

However, the lower than expected fallout of meteoric smoke particles onto the East Antarctic plateau during cold periods, compared to these accretion rates over the Holocene, remains unexplained. One possibility is that there has been a roughly 3-fold increase in the interplanetary dust flux during interglacial periods, which was proposed to explain the accretion of ^{3}He in deep-sea sediments (*23*). The dust flux would then be positively correlated to the earth's orbital inclination relative to the invariable plane of the solar system.

A more likely explanation of the observed difference in meteoric smoke fallout fluxes to Central Greenland and East Antarctica, is suggested by the rapid uptake of metallic species on the ice particles in polar mesospheric clouds (*4*). This emerging physical property indicates that the meteoric smoke fallout could occur mostly by wet deposition. Thus, meteoric smoke could be preferentially deposited in areas characterized by a remarkable snow accumulation rate, thus explaining why the fallout to Central Greenland is higher than to the East Antarctic plateau. In Antarctica, meteoric smoke could be mostly deposited on coastal sites, which are generally characterized by a higher snow accumulation rate.

Acknowledgements

This work was supported in France by the Institut Universitaire de France, the Ministère de l'Environnement et de l'Amènagemont du Territoire, the Agence de

l'Environnement et de la Maîtrise de l'Energie, the Intitut National des Sciences de l'Univers and the Universite Joseph Fourier of Grenoble. In Italy, it was supported by ENEA as part of the Antarctic National Research Program (under projects on Environmental Contamination and Glaciology). This work is a contribution to the European Project for Ice Coring in Antarctica (EPICA), a joint European Science Foundation (ESF)/EC scientific programme, funded by the European Commission under the Environment and Climate Programme (1994-1998) contract ENV4-CT95-0074 and by the national contributions from Belgium, Denmark, France, Germany, Italy, The Netherlands, Norway, Sweden, Switzerland and U.K. This is EPICA publication No. X. The Vostok ice core was obtained as part of a joint program between Russia, France and USA. We thank the Russian Antarctic Expeditions, the Institut Polaire Paul Emile Victor and the Division of Polar Programs (NSF) for logistic support, and the drilling team from St. Petersburg Mining Institute for fieldwork. In Korea, grants from the Korea Ocean Research and Development Institute (PP02105) and a National Research Laboratory program from the Ministry of Science and Technology (PN43400) supported this research. Finally, we would like to thank all the scientific and logistic personnel working in Dome C and Vostok, Antarctica.

Table 1

Depth (m)	Age (years BP)	Ir (ppq)	(SD)	Pt (ppq)	(SD)	Ir flux (fg cm^{-2} y^{-1})	Pt flux (fg cm^{-2} y^{-1})	Ir/Pt	Mn (ppt)	EF_c Ir	EF_c Pt
32.5	569	3.3	0.2	3.1	0.3	8.9	8.4	1.1	7	5100	601
59.1	1227	19	1	9	1	58.4	26.8	2.2	9	21827	1254
86.6	2006	2.7	0.2	3.2	0.2	7.2	8.3	0.9	12	2314	337
152.1	4156	2.3	0.1	1.5	0.2	5.9	4.0	1.5	8	2919	246
229.1	6938	5	1	2.7	0.3	14.8	7.8	1.9	14.5	3756	248
316.0	10270	3.3	0.2	2.3	0.2	11.6	7.8	1.5	12	2832	239
379.2	12809	2.3	0.1	2.3	0.5	5.0	5.0	1.0	14	1737	214
405.6	14204	3.0	0.3	2.3	0.2	6.3	4.8	1.3	39	823	79
419.4	14910	10.0	0.5	5.5	0.3	27.7	15.2	1.8	20	5346	367
432.6	15611	3.7	0.2	2.1	0.2	9.4	5.4	1.7	40	967	69
461.2	17380	2.3	0.1	2.3	0.3	4.0	4.0	1.0	170	140	18
471.1	18133	1.0	0.1	2.8	0.3	1.6	4.3	0.4	341	32	11
488.7	19627	3.1	0.1	3.8	0.4	4.5	5.6	0.8	529	61	10
515.6	21944	2	1	12	6	3.3	17.0	0.2	760	32	21
573.9	27009	1.5	0.2	5.1	0.2	2.1	7.2	0.3	394	39	17
598.1	29094	3.7	0.2	2.7	0.3	6.0	4.3	1.4	319	123	11
653.1	33661	1.3	0.1	2.3	0.2	2.1	3.6	0.6	176	80	17
653.7	33706	0.42	0.04	1.4	0.2	0.6	2.1	0.3	236	19	8
680.9	35967	1.6	0.1	1.8	0.3	2.5	2.7	0.9	201	84	12
708.7	38135	1.7	0.2	1.7	0.2	3.0	3.1	1.0	103	176	22
735.6	40375	2.2	0.2	3.5	0.4	3.2	5.2	0.6	229	99	20
763.1	42801	6.1	0.3	4.5	0.4	10.0	7.4	1.4	127	505	47
818.1	47175	1.8	0.2	2.3	0.2	2.7	3.6	0.8	163	114	19
900.6	53830	1.3	0.1	1.7	0.2	2.2	2.9	0.8	223	59	10
983.1	60647	1.0	0.1	2.5	0.4	1.6	3.7	0.4	340	32	10
1010.6	63425	0.8	0.1	2.6	0.3	1.2	3.8	0.3	396	23	9
1093.1	71637	1.7	0.2	2.0	0.2	3.1	3.7	0.8	40	453	68
1148.1	76576	2.5	0.2	2.3	0.4	4.2	3.9	1.1	96	276	32
1203.1	81050	0.7	0.1	1.3	0.2	1.5	2.8	0.5	50	148	34
1258.1	86002	1.3	0.1	1.8	0.2	2.3	3.2	0.7	107	130	22
1313.1	91429	1.5	0.2	2.2	0.2	2.8	4.2	0.7	27	566	106
1423.1	102253	1.6	0.1	2.2	0.3	2.9	4.1	0.7	59	281	50
1533.1	114119	2.7	0.2	2.2	0.4	7.1	5.8	1.2	11	2463	254
1643.1	122810	2.7	0.5	2.1	0.1	8.4	6.7	1.3	21	1356	135
1753.1	131856	1.1	0.1	0.4	0.1	2.4	0.8	3.3	64	189	7
1863.1	152184	0.5	0.0	0.1	0.0	0.7	0.2	3.3	480	11	0.4
1973.1	174430	0.6	0.1	2.0	0.1	1.0	3.1	0.3	296	23	9
2050.1	191286	0.8	0.1	1.5	0.2	1.4	2.4	0.6	174	51	11
2094.1	198898	4.1	0.2	1.9	0.2	10.0	4.6	2.2	12	3667	212
2138.1	207177	1.9	0.1	2.0	0.2	4.7	4.9	1.0	16	1246	162
2193.1	216992	1.3	0.2	1.9	0.2	2.7	4.0	0.7	76	182	33

Table 2

Depth (m)	Age (years BP)	Ir (ppq)	(SD)	Pt (ppq)	(SD)	Ir flux (fg cm^{-2} y^{-1})	Pt flux (fg cm^{-2} y^{-1})	Ir/Pt	Mn (ppt)	EF_c Ir	EF_c Pt
126.7	4640	1.2	0.2	1.1	0.1	2.59	2.36	1.1	14	952	108
150.5	5750	2.0	0.2	2.0	0.1	4.23	4.18	1.0	18	1191	147
193.9	7845	2.0	0.4	2.2	0.1	3.97	4.55	0.9	28	734	105
513.0	30200	0.9	0.1	1.6	0.1	1.28	2.24	0.6	250	39	9
938.1	65080	1.1	0.1	4.2	0.3	1.49	5.75	0.3	552	21	10
948.0	66045	1.6	0.1	4.2	0.2	2.18	5.63	0.4	883	19	6
1050.0	75065	0.7	0.1	1.1	0.1	1.22	1.74	0.7	77	101	18
1205.7	86500	1.5	0.1	2.5	0.2	2.74	4.50	0.6	57	282	58
1353.5	97145	1.0	0.1	1.2	0.1	1.80	2.21	0.8	42	250	38
1514.5	108400	0.3	0.2	0.7	0.2	0.41	1.12	0.4	201	14	5
1651.4	118500	2.1	0.2	2.1	0.2	4.94	5.05	1.0	17	1283	164
1815.5	127800	1.1	0.1	1.6	0.1	3.34	4.99	0.7	37	312	58
1879.8	131200	0.8	0.1	1.4	0.1	2.22	3.61	0.6	14	656	133
1917.5	133950	0.6	0.1	1.3	0.1	1.20	2.43	0.5	116	57	14
1999.0	142500	1.9	0.2	5.2	0.4	2.80	7.63	0.4	638	31	11
2199.4	165150	1.6	0.1	4.1	0.1	2.46	6.35	0.4	387	44	14
2252.4	171520	0.6	0.1	1.5	0.1	1.13	2.74	0.4	407	16	5
2378.4	187770	0.8	0.1	3.0	0.1	1.37	4.93	0.3	294	29	13
2504.5	203100	1.0	0.1	1.8	0.2	2.48	4.41	0.6	30	368	82
2534.0	206630	1.2	0.1	2.2	0.2	2.55	4.55	0.6	95	137	31
2616.0	216400	0.8	0.1	1.8	0.1	2.00	4.48	0.4	63	136	38
2682.4	226250	1.4	0.1	2.1	0.1	2.70	4.15	0.6	119	121	23
2751.0	237280	0.5	0.2	1.2	0.2	1.39	3.60	0.4	60	82	27

Figure caption

Fig. 1. Fluxes of Ir (full circles) and Pt (open circles) in the Epica Dome C ice core (EDC) (A) and in the Vostok ice core (VK) (B) during the last two climatic cycles. Climate changes are indicated by variation in the δD ‰, taken as a proxy of local temperature. Ir and Pt fluxes seem related to climate variations, with generally higher fluxes during warm periods. The only clear exceptions are some high values of Pt in the Vostok ice core during cold phases, possibly caused by crustal contributions. Note that the large spikes of Ir and Pt in EDC during the Holocene are not present in VK.

Fig. 2. Ratios (full circles) of Ir and Pt in the Epica Dome C ice core (A) and in the Vostok ice core (B) during the last two climatic cycles. Climate changes are indicated by variation in δD ‰, taken as a proxy of local temperature. Open circles indicate the δD ‰ measured at the same depth as the samples analysed in this study. The Ir/Pt ratio correlates strongly with temperature; chondritic values (about 0.5) are seen during cold periods, and non-chondritic values, close or higher than 1, during warm periods. This indicates a fallout of meteoric smoke to the East Antarctic plateau during cold stages, and a probable terrestrial contribution from volcanic emissions during warm periods. Such different sources for Ir and Pt are evidence of a significant subsidence of cold air masses, carrying the meteoric smoke from the upper layers of the atmosphere during cold periods, and indicate a possible more pronounced transport via a lower path within the troposphere during warm phases. Outliers ratios from Dome C samples dated at ~132 kyr and ~152 kyr are omitted from the figure.

Figure 1

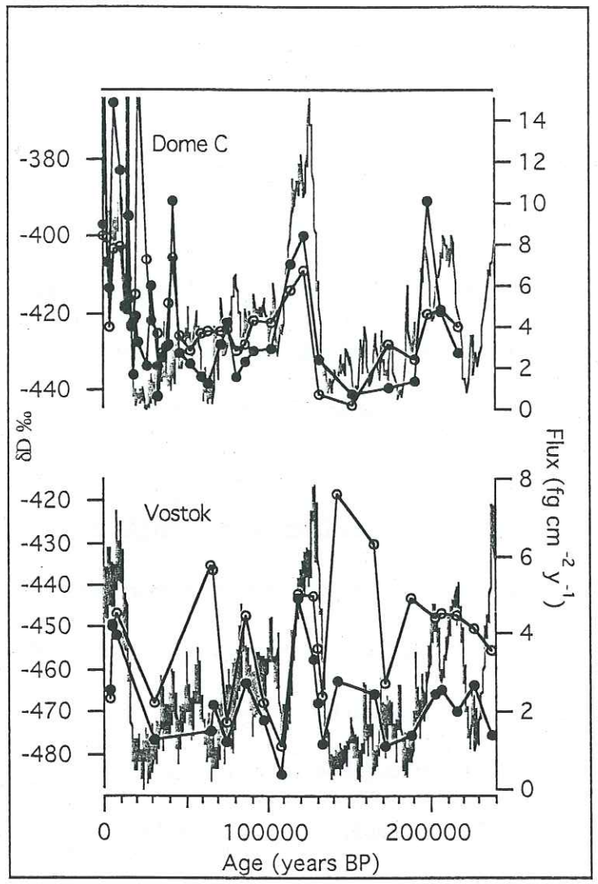

Figure 2

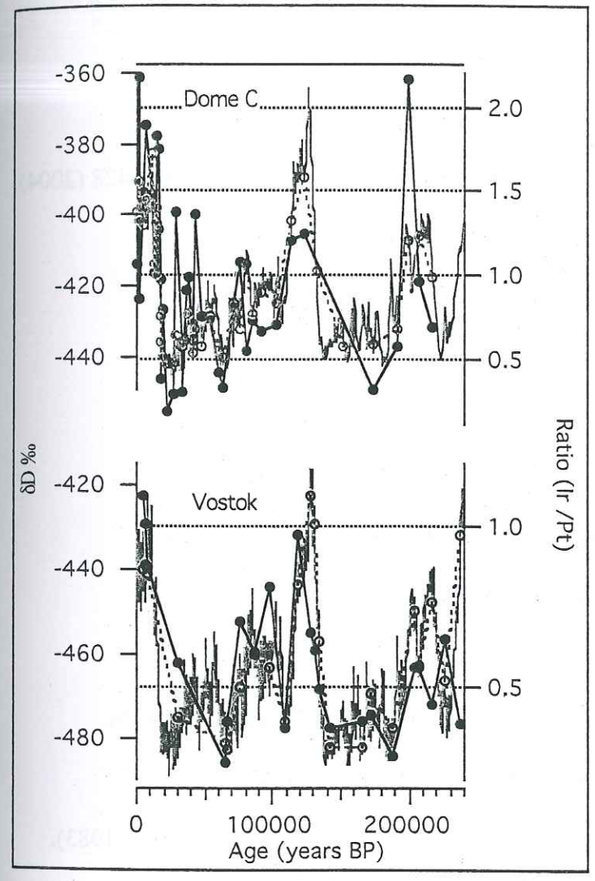

References

1. D. M. Hunten, R. P. Turco, O. B. Toon, *J. Atmos. Sci.* **37**, 1342-1357 (1980).
2. S. G. Love, D. E. Brownlee, *Icarus* **89**, 26-43 (1991).
3. T. J. Kane, C. S. Gardner, *Science* **259**, 1297-1300 (1993).
4. J. M. C. Plane, B. J. Murray, X. Chu, C. S. Gardner, *Science* **304**, 426-428 (2004).
5. J. M. C. Plane, *Atmos. Chem. Phys. Disc.* **4**, 39-69 (2004).
6. P. Gabrielli *et al.*, *Submitted to Nature* (2004).
7. Epica community members, *Nature* **429**, 623-628 (2004).
8. J. R. Petit *et al.*, *Nature* **399**, 429-436 (1999).
9. P. Gabrielli *et al.*, *J. Anal. At. Spectrom.* **19**, 831-837 (2004).
10. K. H. Wedepohl, *Geochim. Cosmochim. Acta* **59**, 1217-1232 (1995).
11. P. Gabrielli *et al.*, *Submitted to Earth Planet. Sci. Lett.* (2004).
12. P. Gabrielli *et al.*, *To be submitted to Atmos. Environ.*
13. E. Anders, N. Grevesse, *Geochim. Cosmochim. Acta* **53**, 197-214 (1989).
14. L. Pattou, J. P. Lorand, M. Gros, *Nature* **379**, 712-715 (1996).
15. W. H. Zoller, J. R. Parrington, J. M. P. Kotra, *Science* **222**, 1118-1121 (1983).
16. F. T. Kyte, J. T. Wasson, *Science* **232**, 1225-1229 (1986).
17. C. Koeberl, *Earth Planet. Sci. Lett.* **92**, 317-322 (1989).
18. A. Matsumoto, T. K. Hinkley, *Earth Planet. Sci. Lett.* **186**, 33-43 (2001).
19. P. Vallelonga, P. Gabrielli, K. Rosman, C. Barbante, C. F. Boutron, *Submitted to Geophys. Res. Lett.* (2004).
20. G. Zreda-Gostynska, P. R. Kyle, *J. Geophys. Res.* **102**, 15039-15055 (1997).
21. I. N. James, *Antarctic Science* **1**, 279-290 (1989).
22. B. Delmonte *et al.*, *Clim. Dyn.* **23**, 427-438 (2004).
23. R. A. Muller, G. J. MacDonald, *Nature* **377**, 107-108 (1995).

CHAPTER 3: TRACE ELEMENTS VARIATION IN EAST ANTARCTICA OVER THE LATE QUATERNARY

3.1 ARTICLE 4: **Trace elements in Vostok Antarctic ice during the last four climatic cycles**

Paolo Gabrielli, Frédéric A. M. Planchon, Sungmin Hong, Yeadong Kim, Jae-Kyung Oh, Claude F. Boutron, Carlo Barbante, Christophe P. Ferrari, Jean Robert Petit, Vladimir Y. Lipenkov, Paolo Cescon

Submitted to *Earth and Planetary Science Letter*, September 2004

Trace elements in Vostok Antarctic ice during the last four climatic cycles

Paolo Gabrielli[1,2], Frédéric A. M. Planchon[3], Sungmin Hong[4], Khang Hyun Lee[4], Carlo Barbante[2,3*], Christophe P. Ferrari[1,5], Jean Robert Petit[1], Vladimir Y. Lipenkov[6], Paolo Cescon[2,3], Claude F. Boutron[1,7]

1. Laboratoire de Glaciologie et Géophysique de l'Environnement (UMR CNRS/UJF 5183), B.P. 96, 38402 Saint Martin d'Hères, Cedex, France
2. Department of Environmental Sciences, University of Venice, Ca' Foscari, 30123 Venice, Italy
3. Institute for the Dynamics of Environmental Processes - CNR, University of Venice, Ca' Foscari, 30123 Venice, Italy
4. Korea Polar Research Institute, KORDI, Ansan, PO Box 29, Seoul 426-744, Korea
5. Polytech Grenoble, Université Joseph Fourier de Grenoble (Institut Universitaire de France), 28 avenue Benoît Frachon, B.P. 53, 38041 Grenoble, France
6. Arctic and Antarctic Research Institute, Beringa Street 38, 199397, St Petersburg, Russia
7. Unité de Formation et de Recherche de Physique et Observatoire des Sciences de l'Univers, Université Joseph Fourier de Grenoble (Institut Universitaire de France), B.P. 68, 38041 Grenoble, France

Submitted to: *Earth and Planetary Science Letters* on September 23rd 2004

* *Corresponding author. Phone : +39-041-2348942 ; Fax : +39-041-2348549; e-mail : barbante@unive.it*

Abstract:

Li, V, Cr, Mn, Co, As, Rb, Sr, Ba, Bi and U were determined by inductively coupled plasma sector field mass spectrometry (ICP-SFMS) in various sections of the 3623 m Vostok deep Antarctic ice core dated from 4,600 to 410,000 years BP, which corresponds to the last four climatic cycles back to isotopic stage 11.3. Concentrations of all elements were found to be highly variable with low values during interglacial periods and warm interstadials and much higher values during the coldest periods of the last four ice ages. Crustal enrichment factors suggest various sources for the different elements. Rock and soil dust is the dominant source of V, Mn, Rb, Ba and U whatever the period, and of Li, Cr, Co, Sr and As during cold periods. Sea salt aerosol, together with aeolian dust, also contributes significantly to Sr whereas volcanic emissions could provide a significant input for As and Bi especially during warm periods.

1. Introduction

Deep Antarctic ice cores have the potential to give unique information on past natural changes in the biogeochemical cycles of trace elements. Deciphering these frozen archives for trace elements has however proved to be exceedingly difficult because of the very high purity of Antarctic snow and ice, which makes it a challenge to obtain fully reliable data from the analysis of ice cores whose outside is heavily contaminated during drilling operations. The impetus in the field came from the pioneering work of Clair Patterson and his colleagues at the California Institute of Technology. They indeed developed original ultra-clean procedures to efficiently decontaminate deep polar ice cores by mechanically chiseling successive veneers of ice in progression from the contaminated outside to the center, in order to obtain the uncontaminated inner part of the core [1].

Until now these methods were only used to analyze ice cores of intermediate depths (less than 1 km), because such cores can be obtained from drill holes not filled with a wall retaining fluid, which strongly reduces contamination brought to the outside of the core [2]. The drawback is that such cores cover only rather short time periods (~ 40,000 years. for the 905 m core drilled at Dome C in 1978, for instance [3]).

Until recently these methods were however never used for comprehensive analysis of very deep Antarctic ice cores covering several climatic cycles such as the 3,623 m Vostok core [4] or the newly drilled 3,190 m EPICA Dome C core [5]. The huge pressure encountered at great depths makes it indeed mandatory to fill the drilling hole with a wall retaining fluid, resulting in an enormous contamination of the outside of the core sections. The few attempts which were made to analyze such very deep cores for

heavy metals were largely unsuccessful: even the most central parts of the cores were found to be contaminated, probably because a significant fraction of outside contamination was transferred toward the center during the decontamination of the sections [6-8].

Extremely time consuming analytical efforts are recompensed by the fact that trace elements studies in deep ice cores provide remarkable information about changes in different biogeochemical cycles during the last climatic cycles. Heavy metals can in fact help to distinguish between the different natural sources from which the particles and the aerosol transported over Polar Regions have originated. Rock and soil dust, marine aerosol and volcanic emissions are the three main contributors of the overall heavy metals input in Polar Regions during the pre-industrialized period. They constitute important components interacting with atmospheric processes that could produce positive and/or negative feed back mechanisms influencing climate.

We present here comprehensive data on past changes in the occurrence of various trace elements (Li, V, Cr, Mn, Co, As, Rb, Sr, Ba, Bi and U) in Antarctic ice during the last four climatic cycles (the past ~ 410,000 years). They were obtained by analyzing various sections of the upper 3,285 m of the 3,623 m Vostok ice core, using improved decontamination procedures and highly sensitive inductively coupled plasma sector field mass spectrometry (ICP-SFMS).

2. Experimental Procedures

2.1. Core Sections

The 3,623 m Vostok ice core was drilled from a fluid filled hole at the Russian Vostok Station (78°28′S, 106°48′E, elevation 3,488 m, mean annual temperature –55 °C) in East Antarctica. 37 sections (length 35-45 cm, diameter 10 cm) were selected from the part of the core, which corresponds to the last four climatic cycles (last ~410,000 years). The detailed deuterium profile previously published by Petit et al. [9], Figure 1a, allowed us to select sections dated from the successive climatic stages [10]. Parts of the sections were chosen from the Holocene, the last interglacial period (Marine Isotopic Stage (MIS) 5.5), the next to last interglacial (MIS 7.5), the third from last interglacial (MIS 9.3) and the fourth from last interglacial (MIS 11.3). The other sections were chosen from the last four ice ages. The depth of the sections ranged from 126.73 m (which corresponds to an estimated age of 4,640 years) to 3,285 m, corresponding to an estimated age of 409,000 years. Further information are given in Table 1.

2.2. Core Decontamination

Each core section was decontaminated using the method described by Candelone et al. [11], in which the core section is held in a polyethylene lathe and mechanically chiselled using acid cleaned stainless steel knives. Various improvements were however made compared with the original procedure: up to seven concentric layers were removed successively prior to collection of the inner part of the core and improved cleaning procedures were used for the preparation of the equipment used during the whole operation.

2.3. ICP-SFMS determinations

Each concentric layer and inner core were analysed separately in special clean laboratories. Li, V, Cr, Mn, Co, As, Rb, Sr, Ba, Bi and U were determined by ICP-SFMS using an Element*2* instrument from Thermo Electron Corporation (Bremen, Germany) using a micro-flow (< 100 μl min^{-1}) PFA nebulisation system that let us to analyse only a few ml of the melted samples [12]. Thanks to the possibility of working at three different resolution modes (m/Δm=400, low resolution mode, LR; m/Δm=4,000, medium resolution mode, MR; m/Δm=10,000, high resolution mode, HR), most of the analytes peaks could be physically resolved from spectroscopic interferences that potentially hamper their accurate determination [12]. During the present work the LR mode was used for the analysis of Li, Rb, Sr, Ba, Bi and U, while the MR mode was preferred during the analysis of V, Cr, Mn and Co. Arsenic was analysed by taking advantage of the highest resolution (HR, m/Δm = 10,000) of the sector field mass spectrometer to resolve the interference of $^{40}Ar^{35}Cl$ on ^{75}As.

2.4. Blanks, precision and detection limits

Experimental blanks for the whole analytical procedure were determined by processing an artificial ice core prepared by freezing ultra-clean water [13]. Blanks were found to be negligible for all the metals except Cr, for which a slight contamination, due to the Cr rich stainless steel knives, was observed at the picogram per gram level. Therefore Cr concentrations at the few pg/g level must be considered as an upper limit of the genuine concentration. However high Cr glacial concentrations are probably only negligibly affected from this slight contamination that was found to be in the range of the instrumental standard deviation. The overall precision of the data was found to range from 2% for Sr to 15% for As at the lowest level of sample concentrations during interglacial periods. Detection limits expressed in pg/g were as follows: Li (1), V (0.4), Cr (1), Mn (0.3), Co (0.5), As (1), Rb (0.5), Sr (5), Ba (2), Bi (0.02) and U (0.01).

2.5. Reliability of the data

We established radial profiles of variations of concentration for the different metals from the outside to the inside of the cores, to make sure that the concentrations measured in the inner part were obtained after the decontamination was completed, and therefore represented the original concentration in the ice free from any contamination.

As an example, typical profiles obtained for U, Co, As and Mn for the 1879.78 m section (age of 131,200 yr. BP, which corresponds to interglacial stage 5.5 characterised by extremely low concentration in the ice) are shown in Fig. 2. The profiles shown in the figure however do not include the data for the most contaminated outside layer, which was not analysed because such high concentrations would have contaminated the sample introduction system of the ICP-SFMS instrument. It can be seen that concentration values level reach well established plateau values in all four cases, despite

the fact that the 1879.78 m section corresponds to interglacial ice with extremely low concentration values. It indicates that the concentrations measured in the inner core represent pristine metal concentration in the ice.

3. Results and discussion

3.1. Changes in concentrations and fluxes during the last four climatic cycles

Concentrations measured in the innermost part of the 37 sections are given in Table 1. They are the first data ever published on past variations of these different elements in Antarctic ice during the last four climatic cycles. Concentrations range from 0.03 pg/g for Bi in the 3284.95 m section to 1.3 ng/g for Mn in the 2870.0 m section.

Pronounced variations in concentrations are observed for all the elements over the ~410,000 years time period covered by our samples. For instance the highest concentrations measured for V (121 pg/g) is about 80 times higher than the lowest (1.5 pg/g). The variations appear to be strongly linked with climatic conditions. Their maximum amplitudes however, vary strongly from one element to another. The highest amplitude is for Li (max/min = 102), the lowest is for Cr (max/min = 20). Concentrations of most elements were very low during warm periods, characterised by less negative δD values (Figure 1). Conversely, much higher trace element concentrations are observed during cold periods, characterised by more negative $\delta^{18}D$ values (Figure 1). As an illustration, Figure 1 shows the variations observed for Li, Co, Rb and U.

Fallout fluxes were calculated for each element by combining the concentrations measured in the ice with the yearly ice accumulation rate at each depth [9, 14]. The ice accumulation rate at Vostok has varied by a factor of ~2 during the last two climatic cycles, with lowest values during the cold climatic stages when concentrations of the elements considered in our work are at a maximum. Taking that into account, changes in fallout fluxes closely parallel changes in concentrations, but with a smaller amplitude.

3.2. Crustal Enrichment Factors (EF_c)

Rock and soil dust is a major source of trace elements in the atmosphere [15]. In order to assess the importance of rock and soil dust contribution in Vostok ice during the last two climatic cycles, we calculated crustal enrichment factors (EF_c) for each element and depth. EF_c is defined as the concentration ratio of a given element to that of

Al (which is a good proxy for rock and soil dust; Al concentrations were determined in each section by graphite furnace atomic absorption spectrometry [16]) in the ice, normalised to the same concentration ratio characteristic of the upper continental crust. For example, the EF_c for Co is thus:

$$EF_c = \frac{[Co]_{ice}/[Al]_{ice}}{[Co]_{crust}/[Al]_{crust}}$$

We have used here the data for the upper continental crust given by Wedepohl [17]. It should however be emphasised that the choice of other crustal compositions, for instance that given by Rudnick and Fountain [18], would not make any significant differences in the interpretation. Despite the fact that the composition of rock and soil dust reaching Antarctica might significantly differ from the composition of the mean upper crust, EF_c values close to unity (up to ~5) will indicate that the corresponding elements mainly originate from rock and soil dust. Conversely, values significantly larger than unity will most likely indicate a significant contribution from other natural sources.

EF_c values calculated for the 37 sections are given in Table 2. When looking at the values obtained for the different elements and their variations during the last four climatic cycles, the elements considered in our study can be separated into several groups.

The first group consists of V, Mn, Rb, Ba and U; these are elements for which the EF_c values are close to the unity, whatever the period, Table 2. This is illustrated in Figure 3 for Mn. These EF_c values show that the atmospheric cycle of these five elements in the remote polar area of the Southern Hemisphere was dominated by crustal dust, both during glacial and interglacial periods. They also indicate that V, Mn, Rb, Ba and U could eventually substitute Al as a crustal reference element in Antarctic ice during the preceding climatic cycles.

A second group of elements is made of Li, Cr, Co and Sr. For these elements, low EF_c values are observed in some of the sections, while moderately elevated values are observed in other sections, Table 2. As illustrated in Figure 3 by Sr, the lowest values are generally observed during the coldest periods, while the higher values occurred during interglacial periods. The atmospheric cycles of Li, Co and Sr were dominated by crustal dust during the coldest stages, while the influence of additional sources was probably important during warmer periods. Some of the observed changes may however also be linked with changes in rock and soil dust source areas, soil physical conditions (variations in humidity), or transport processes (settling) between glacial and interglacial periods [19, 20].

Arsenic and Bi are special cases. EF_c values close to unity are indeed rarely

observed for these elements, Table 2. The lowest values are observed during the coldest climatic stages, while the higher values are observed during the warm stages, Figure 3. The moderate values during the coldest stages indicate that inputs from sources other than dust were probably significant even during these periods. Alternatively, they could be linked with changes in the composition of crustal dust reaching Antarctica, with an enrichment in As and Bi in rock and soil from Patagonia, which is a dominant source area for dust during the coldest climatic stages [4, 21, 22]. The rather high values recorded during the warm periods show that in all likelihood the atmospheric cycles of As and Bi in the remote polar area of the Southern Hemisphere were dominated by sources other than rock and soil dust during these periods.

3.3. Contributions from sea salt and volcanoes

Besides rock and soil dust, other important sources of atmospheric trace elements are sea salt spray, volcanic emissions and continental and marine biogenic emissions [15].

The contribution from sea salt spray was evaluated from Na concentrations measured in the ice [16] (after correction for the Na contribution from rock and soil dust) and the elemental ratios in ocean water. These ratios were not combined with possible enrichments found in sea-derived aerosols relative to seawater, when marine aerosol is formed by bubble bursting through the sea surface micro layer, because recent studies have cast some doubt on the values of these possible enrichments [25].

The contribution from sea salt is found to be important for Sr, especially during interglacial periods (about 40%) and to a lesser extent during cold periods (about 20%). The contribution from sea salt is negligible for all the other elements, whatever the period.

A rough estimate of the contribution from volcanoes was made from the concentration of non-sea-salt sulfate (nss-SO_4) in the ice [16], by assuming that ~10-15% of nss-SO_4 originates from volcanoes [2]. This was combined with the most recent estimates available of element/S ratios in volcanic emissions [26]. It must however be emphasized that such estimates are rather crude, especially because of the large variations in published elements/S ratios in volcanic emissions. Just to give an example, the As/S mass ratio (3.8×10^{-4}) given for worldwide volcanic emissions by Nriagu [15] is one order of magnitude higher than the same ratio (0.3×10^{-4}) for these emissions given by Hinkley and his co-workers [26]. Also estimates of element/S ratios in volcanic emissions are not available for several of the elements considered in this work. The calculation shows that volcanic emissions were possibly a significant source for As and

Bi during warm periods. However, such a contribution cannot entirely explain the high EF_c values observed for As during warm climatic stages. In contrast, the volcanic contribution calculated for Bi would imply concentrations in the order 1 pg/g, whereas concentrations found in Vostok ice are in general much lower. However this calculation suggests a possible strong volcanic contribution for Bi.

A possible local source within Antarctica could be Mount Erebus, a volcano that is located ~1100 km from Vostok. Zreda-Gostynska and co-workers [27] have indeed shown that Erebus is a significant source of various trace elements to the Antarctic atmosphere. They made a rough estimate of the potential contribution of Mt. Erebus to the trace elements content of East Antarctic snow assuming homogeneous fallout over the whole continent. When compared with the concentrations we find in Vostok ice, it appears that Mt. Erebus could be a significant contributor to the fallout of several heavy metals, especially during warm periods. It must however be kept in mind that the data by Zreda-Gostynska and co-workers derive only from short sampling periods between 1986 and 1991. It might not then be applicable to the ~410,000 years period covered by our samples. In addition, it is likely that fallout from Erebus volcano is not evenly deposited over the Antarctic continent. It thus makes it difficult to perform any quantitative estimate of the possible contribution from Mt. Erebus (or other Antarctic volcanoes).

Finally, our data do not allow any estimate of the contributions from continental marine biogenic activity to be made. Such contributions cannot however be neglected, as illustrated for instance by recent studies of the production of methylated metals by polar marine bacteria [28, 29].

3.4. Trace elements vs climate relationship

Concentrations of trace elements in Vostok ice remain very low for δD values between – 420 and – 470‰, but show a sharp increase when δD values fall below – 470‰. This is illustrated in Figure 4 for Co and As. This observation suggests that there is a critical point in the climate mechanism beyond which the fallout of trace elements to the Antarctic plateau is activated and the deposition is enhanced. The main inputs of trace elements to the Antarctic ice cap could have been driven by large changes in wind strength, which occurred when a critical temperature gradient between low and high latitudes was reached, allowing larger amounts of trace metals to be carried by dust to Antarctica. A transport activation could be also related to fast changes in local conditions of the source areas from which the trace elements originated [20]. For instance, a variation in the humidity of dust source areas such as Patagonia [19] could

have resulted in a different amount of dust suspended and transported by wind circulation to the Antarctic plateau, therefore enhancing the fallout of trace elements.

4. Conclusion

Our work has documented large natural changes in the occurrence of various trace elements in Antarctic ice over the last four climatic cycles, highlighting important changes in the atmospheric cycles of trace elements in the remote polar areas of the Southern Hemisphere in parallel with climate.

It will now be important to extend this study to the preceding climatic cycles within the new EPICA Dome C ice core, and to include other trace elements such as Hg and Se, which could be valuable tracers of marine biogenic emissions, or Ir and Pt, which are good indicators of fallout of cosmic material.

Acknowledgements

The Vostok ice cores were obtained as part of a joint program between Russia, France and the USA. We thank the Russian Antarctic Expeditions, the Institut Polaire Paul Emile Victor and the Division of Polar Programs (NSF) for logistical support, and the drilling team from St. Petersburg Mining Institute for fieldwork. In Italy this study was performed within the framework of Projects on "Environmental Contamination" and "Glaciology and Paleoclimatology" of the Italian *Programma Nazionale di Ricerche in Antartide* and financially supported by ENEA through co-operation agreements with the Universities of Venice and Milan, respectively. In Korea, grants from the Korea Ocean Research and Development Institute (PP04105) and a National Research Laboratory program from the Ministry of Science and Technology (PN51200) supported this research. It was also supported in France by the Institut Universitaire de France, the Ministère de l'Environnement et de l'Aménagement du Territoire, the Agence de l'Environnement et de la Maîtrise de l'Energie, the Institut National des Sciences de l'Univers and the University Joseph Fourier of Grenoble. Finally we would like to thank Giulio Cozzi and Vania Gaspari for laboratory assistance, and Paul Vallelonga for the preparation of the artificial ice core.

References

[1] A. Ng and C.C. Patterson, Natural concentrations of lead in ancient Arctic and Antarctic ice, Geochim. Cosmochim. Acta 45 (1981) 2109-2121.

[2] C.F. Boutron and C.C. Patterson, Lead concentration changes in Antarctic ice during the Wisconsin/Holocene transition, Nature 323 (1986) 222-225.

[3] C. Lorius, L. Merlivat, J. Jouzel and M. Pourchet, A 30,000 yr isotope climatic record from Antarctic ice, Nature 280 (1979) 644-648.

[4] J.R. Petit, J. Jouzel, D. Reynaud, N.I. Barkov, J.M. Barnola, I. Basile, M. Bender, J. Chapellaz, M. Davis, G. Delaygue, M. Delmotte, V.I. Kotlyakov, M. Legrand, V.Y. Lipenkov, C. Lorius, L. Pépin, C. Ritz, E. Saltzman and M. Stievenard, Climate and atmospheric history of the past 420,000 years from the Vostok ice core, Antarctica, Nature 399 (1999) 429-436.

[5] EPICA, eight glacial cycles from an Antarctic ice core, Nature, 429 (2004) 623-628.

[6] C.F. Boutron, C.C. Patterson, V.N. Petrov and N.I. Barkov, Preliminary data on changes of lead concentrations in Antarctic ice from 155,000 to 26,000 years BP, Atmos. Environ. 21 (1987) 1197-1202.

[7] C.F. Boutron, C.C. Patterson and N.I. Barkov, The occurrence of zinc in Antarctic ancient ice and recent snow, Earth & Planet. Sci. Lett. 101 (1990) 248-259.

[8] C.F. Boutron, S.N. Rudniev, M.A. Bolshov, V.G. Koloshnikov, C.C. Patterson and N.I. Barkov, Changes in cadmium concentrations in Antarctic ice and snow during the past 155,000 years, Earth Planet. Sci. Lett. 117 (1993) 431-444.

[9] J.R. Petit, I. Basile, A. Leruyuet, D. Reynaud, C. Lorius, J. Jouzel, M. Stievenard, V.Y. Lipenkov, N.I. Barkov, B.B. Kudryashov, M. Davis, E. Saltzman and V. Kotlyakov, Four climate cycles in Vostok ice core, Nature 387 (1997) 359-360.

[10] F.C. Bassinot, L. Labeyrie, E. Vincent, X. Quidelleur, N.J. Shackleton and Y. Lancelot, The astronomical theory of climat and the age of the Brunhes-Matuyama magnetic reversal, Earth & Planet. Sci. Lett. 126 (1994) 91-108.

[11] J.P. Candelone, S. Hong and C.F. Boutron, An improved method for decontaminating polar snow and ice cores for heavy metals analysis, Anal. Chim. Acta 299 (1994) 9-16.

[12] F.A.M. Planchon, C.F. Boutron, C. Barbante, E.W. Wolff, G. Cozzi, V. Gaspari, C.P. Ferrari and P. Cescon, Ultrasensitive determination of heavy metals at the sub-picogram per gram level in ultraclean Antarctic snow samples by inductively coupled plasma sector field mass spectrometry, Anal. Chim. Acta 450 (2001) 193-205.

[13] P. Vallelonga, K. Van de Velde, J.P. Candelone, C. Ly, K.J.R. Rosman, C.F. Boutron, V.I. Morgan and D.J. Mackey, Recent advances in measurement of Pb isotopes in polar ice and snow at sub-picogram per gram concentrations using thermal ionisation mass spectrometry, Anal. Chim. Acta 453 (2002) 1-12.

[14] F. Parrenin, J. Jouzel, C. Waelbroeck, C. Ritz and J.-M. Barnola, Dating the Vostok ice core by an inverse method, J. Geophys. Res. 106, 31837-31851, 2001.

[15] J.O. Nriagu, A global assessment of natural sources of atmospheric trace metals, Nature 338 (1989) 47-49.

[16] S. Hong, Y. Kim, C.F. Boutron, C. Ferrari, J.R. Petit, C. Barbante, K. Rosman and V.Y. Lipenkov, Climate related variations in lead concentration and sources in Vostok Antarctic ice from 65,000 to 240,000 years BP, Geophys. Res. Lett. 30 (2003) doi:10.1029/2003GL018411.

[17] K.H. Wedepohl, The composition of the continental crust, Geochim. Cosmochim.Acta 59 (1995) 1217-1232.

[18] R.L. Rudnick and D.M. Fountain, Nature and composition of continental crust:

A lower crustal perspective, Rev. Geophys. 33 (1995) 267-309.

[19] R. Rothlisberger, R. Mulvaney, E. Wolff, M. Hutterli, M. Biegler, S. Sommer and J. Jouzel, Dust and sea salt variability in central East Antarctica (Dome C) over the last 45 kyrs and its implications for southern high latitude climate, Geophys. Res. Lett. 29 (2002) 1963-1966.

[20] B. Delmonte, J.R. Petit and V. Maggi, Glacial to Holocene implications of the new 27000-year dust record from the EPICA Dome C (East Antarctica) ice core, Clim. Dyn. 18 (2002) 647-660.

[21] I. Basile, F.E. Grousset, M. Revel, J.R. Petit, P.E. Biscaye and N.I. Barkov, Patagonian origin of glacial dust deposited in East Antarctica (Vostok and Dome C) during glacial stages 2,4 and 6, Earth & Planet. Sci. Lett. 146 (1997) 573-589.

[22] J. Smith, D. Vance, R.A. Kemp, C. Archer, P. Toms, M. King and M. Zarate, Isotopic constraints on the source of Argentinian loess with implication for atmospheri circulation and the provenance of Antarctic dust during recent glacial maxima, Earth and Planet. Sci. Lett. 212 (2003) 181-196.

[23] J.R. Donat and K.W. Bruland, Trace element in the Oceans, in: Trace Elements in Natural Waters, B. Salbu and E. Steines, eds., pp. 247-280, CRC Press, Boca Raton, 1995.

[24] AGU, Natural abundance of Trace Elemnts in Sea 2004, AGU, 2004.

[25] K.A. Hunter, Chemistry of the sea-surface microlayer, in: P.S. Liss and R.A. Duce, (Eds.), The sea surface and global chang, Cambridge University Press, 1997. pp. 287-319.

[26] T. Hinkley, P.J. Lamothe, S.A. Wilson, D.L. Finnegan and T.M. Gerlach, Metal emission from Kilauea, and a suggested revision of the estimated worldwide metal output by quiescent degassing of volcanoes, Earth & Planet. Sci. Lett. 170 (1999) 315-325.

[27] G. Zreda-Gostynska, P.R. Kyle, B. Finnegan and K.M. Prestbo, Volcanic gas emissions from Mount Erebus and their impact on the Antarctic environment, J. Geophys Res. 102 (1997) 15,039-15,055.

[28] K.G. Heumann, Determination of inorganic and organic traces in the clean room compartment of Antarctica, Anal. Chim. Acta 283 (1993) 230-245.

[29] K. Heumann, Biomethylation in the Southern Ocean and its contribution to the geochemical cycle of trace elements in Antarctica., in: S. Caroli, P. Cescon and D. Walton, (Eds.), Environmental Contamination in Antarctica: A Challenge to Analytical Chemistry, Elsevier, Amsterdam, 2001, pp. 181-218.

Table 1. Trace element concentrations (in pg/g) measured in 37 sections of the 3,623 m Vostok ice core, Antarctica

Depth[a] (m)	Estimated age (yr BP)	Trace element concentrations (pg/g)										
		Li	V	Cr	Mn	Co	As	Rb	Sr	Ba	Bi	U
126.73	4640	4	2	<3.1	14	1.6	3	3.2	63	11	-	0.15
150.45	5750	9	3	<4.1	18	1.1	4	4	81	12	0.08	0.1
193.90	7845	10	3	11	28	1	2	6	88	15	0.31	0.5
513.00	30200	45	22	14	250	4.5	7	53	467	183	0.54	2
938.10	65080	96	82	30	552	11	16	115	740	429	0.8	3.1
948.00	66045	68	72	30	883	19	32	63	510	318	0.63	2.4
1050.00	75065	11	8	6	77	2.5	1	11	136	33	0.10	0.3
1205.68	86500	12	3	7.1	57	2.2	2	7	108	24	0.17	0.5
1353.50	97145	5	2	<4	42	1.0	3	6.3	115	17	0.08	0.10
1514.45	108400	29	9	11	201	1.9	8	24	188	70	0.36	0.7
1651.40	118500	4	1.5	<2	17	0.5	2	3.6	60	10	0.07	0.06
1815.45	127800	1	4	<4	37	2.3	5	3	43	16	-	0.4
1879.78	131200	<1	3	<5	14	1.1	<1	1.5	35	4.5	0.04	0.10
1917.45	133950	16	15	17	116	2	7	16	216	55	0.27	0.4
1999.00	142500	102	80	29	638	14	20	107	926	466	0.9	4
2078.60	151300	46	29	15	255	6	13	48	378	200	0.47	1.2
2199.40	165150	68	41	27	387	8	16	72	625	314	1.0	1.9
2252.40	171520	40	36	22	407	8	17	38	363	157	0.40	1.3
2378.40	187770	60	53	23	294	5.2	12	52	403	229	0.8	1.3
2504.50	203100	3	3	6	30	2.2	4	5	61	15	-	0.1
2534.00	206630	21	9	14	95	1.9	3	11	121	34	0.27	0.3
2616.00	216400	4	6	7	63	2.3	4	7	79	23	-	0.11
2682.40	226250	17	13	21	119	1.9	3	14	158	45	0.3	0.2
2751.00	237280	5	6	9	60	2.5	4	8	70	30	-	0.2
2770.40	239500	1	2.0	<2	32	0.6	2	4.2	80	13	0.08	0.1
2816.36	248450	26	31	19	455	8	11	28	387	147	0.21	1.0
2848.68	255400	41	63	28	598	12	15	46	319	186	0.30	1.2
2870.00	260800	97	121	53	1297	26	34	105	622	475	0.9	3
2886.00	265055	52	40	25	773	13	17	40	352	226	-	-
2984.00	289270	16	9	7	172	3.0	8	12	151	68	0.99	0.27
3059.00	309650	4	2	2.6	31	0.8	2	2.8	68	17	0.08	0.07
3107.01	321785	2.6	2	2.7	24	0.6	1	2.0	19	15	0.03	0.06
3149.01	335100	49	61	29	890	16	1	48	384	239	0.25	1.2
3184.92	353275	53	-	-	-	-	-	-	481	279	0.35	1.5
3223.99	374480	14	14	8	159	3.3	7	13	132	56	0.10	0.32
3263.00	397255	3.4	2.5	<3	30	1.0	1	2.7	67	17	0.05	0.06
3284.95	408990	2.3	2	<2	17	0.6	1	2	39	10.9	0.03	0.05

a Depth of the bottom of the core section.

Table 2. Crustal Enrichment Factors in 37 sections of the 3,623 m Vostok ice core, Antarctica

Depth[a] (m)	Estimated age (yr BP)	Crustal Enrichment Factor										
		Li	V	Cr	Mn	Co	As	Rb	Sr	Ba	Bi	U
126.73	4640	9	1.4	3.8	1.1	5.8	70	1.2	9	0.7	-	2.5
150.45	5750	9	1.0	2.4	0.7	1.9	37	0.8	5	0.4	13	1.2
193.90	7845	6	0.7	4.4	0.7	1.3	16	0.7	4	0.3	34	2.7
513.00	30200	4	0.8	0.8	0.9	0.7	7	0.9	3	0.5	8	1.4
938.10	65080	3	1.0	0.5	0.7	0.6	5	0.7	2	0.4	4	0.8
948.00	66045	2	0.7	0.5	0.9	0.9	8	0.3	1	0.3	3	0.5
1050.00	75065	3	1.1	1.2	1.0	1.5	3	0.7	3	0.3	6	0.8
1205.68	86500	9	0.9	3.1	1.7	3.0	15	1.0	5	0.6	22	3.2
1353.50	97145	2	0.5	1.4	0.9	1.0	17	0.7	4	0.3	8	0.5
1514.45	108400	3	0.3	0.6	0.7	0.3	8	0.4	1	0.2	6	0.5
1651.40	118500	4	0.5	1.1	0.6	0.9	17	0.6	4	0.3	11	0.4
1815.45	127800	0.4	0.8	1.3	0.8	2.2	26	0.3	2	0.3	-	1.6
1879.78	131200	-	2.0	5.8	1.0	3.5	-	0.5	4	0.3	13	1.6
1917.45	133950	3	1.3	2.2	1.0	0.9	16	0.7	3	0.4	10	0.8
1999.00	142500	3	0.8	0.5	0.7	0.6	6	0.5	2	0.4	4	0.9
2078.60	151300	3	0.8	0.6	0.7	0.7	9	0.6	2	0.4	5	0.7
2199.40	165150	3	0.8	0.8	0.7	0.7	8	0.7	2	0.5	8	0.8
2252.40	171520	2	0.9	0.8	1.0	0.9	11	0.5	2	0.3	4	0.7
2378.40	187770	4	1.3	0.9	0.7	0.6	8	0.6	2	0.4	8	0.7
2504.50	203100	2	1.0	3.4	1.1	3.7	35	0.9	4	0.4	-	1.0
2534.00	206630	11	1.9	4.3	2.0	1.8	16	1.1	4	0.6	25	1.2
2616.00	216400	3	1.6	3.3	1.8	3.1	31	1.0	4	0.5	-	0.7
2682.40	226250	7	2.1	5.0	1.9	1.4	11	1.1	4	0.6	22	0.7
2751.00	237280	3	1.4	3.4	1.5	2.8	28	0.9	3	0.6	-	1.0
2770.40	239500	1	0.6	1.2	1.0	0.9	15	0.6	4	0.3	10	0.8
2816.36	248450	2	0.9	0.9	1.4	1.2	9	0.4	2	0.4	3	0.6
2848.68	255400	2	1.2	0.8	1.1	1.0	7	0.4	1	0.3	2	0.5
2870.00	260800	2	0.9	0.6	1.0	0.9	7	0.4	1	0.3	3	0.6
2886.00	265055	2	0.7	0.7	1.4	1.1	8	0.4	1	0.3	-	-
2984.00	289270	3	0.7	0.9	1.4	1.1	18	0.5	2	0.4	36	0.5
3059.00	309650	3	0.6	1.2	1.0	1.2	16	0.4	4	0.4	11	0.5
3107.01	321785	2	0.6	1.5	0.9	0.9	12	0.4	1	0.4	5	0.5
3149.01	335100	2	0.9	0.6	1.3	1.0	0.2	0.3	1	0.3	1	0.4
3184.92	353275	2	-	-	-	-	-	-	1	0.3	2	0.4
3223.99	374480	3	1.2	1.1	1.4	1.4	16	0.6	2	0.4	4	0.6
3263.00	397255	3	0.8	1.5	0.9	1.4	7	0.4	3	0.4	6	0.4
3284.95	408990	4	1.3	2.4	1.2	1.9	20	0.5	4	0.6	8	0.7

a Depth of the bottom of the core section.

Figure caption

Figure 1. Vostok Antarctic ice core: changes in Li, Co, Rb and U concentrations as a function of the age of the ice during the last four climatic cycles (the past ~410,000 years). Also shown at the top of the figure is the deuterium profile from Petit et al.[9], with Marine Isotope Stage (MIS) numbers from Bassinot et al.[10]. D, expressed in per mil δ units (δD), is used as a proxy of temperature, with less negative values indicating higher temperatures during interglacial periods and more negative values showing cold climatic stages

Figure 2. Changes in U, Co, As and Mn concentrations as a function of radius in the 1879.78 m ice core section (131,200 yr. BP).

Figure 3. Vostok Antarctic ice core: changes in crustal enrichment factors (EF_c) for Mn, As and Sr as a function of the age of the ice during the last four climatic cycles (the past 410,000 years). Also shown at the top of the figure is the deuterium profile from Petit et al.[9], with MIS numbers from Bassinot et al.[10].

Figure 4. Vostok Antarctic ice core: changes in concentrations of Co and As a function of the deuterium content of the ice (expressed in per mill δ units).

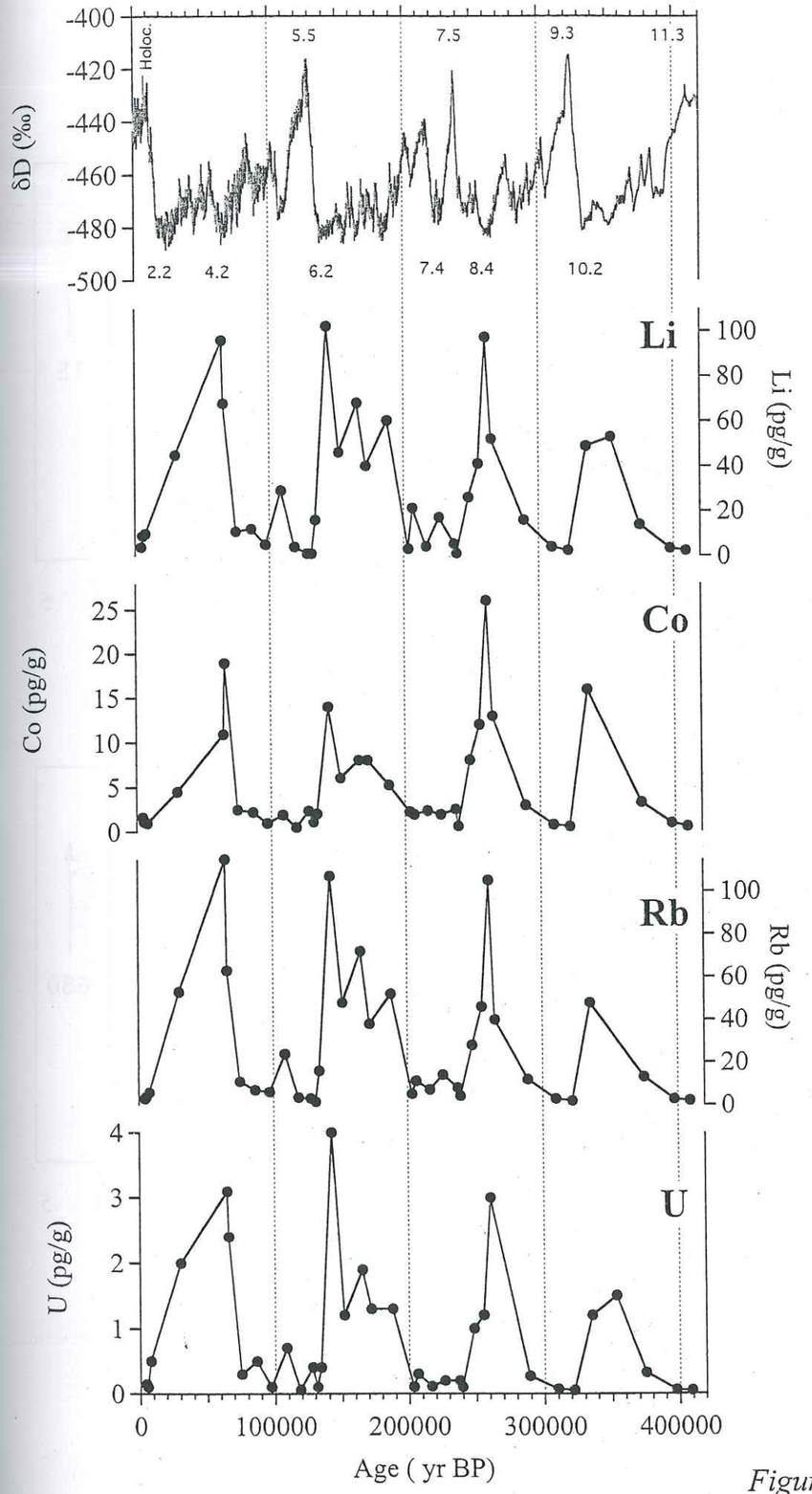

Figure 1

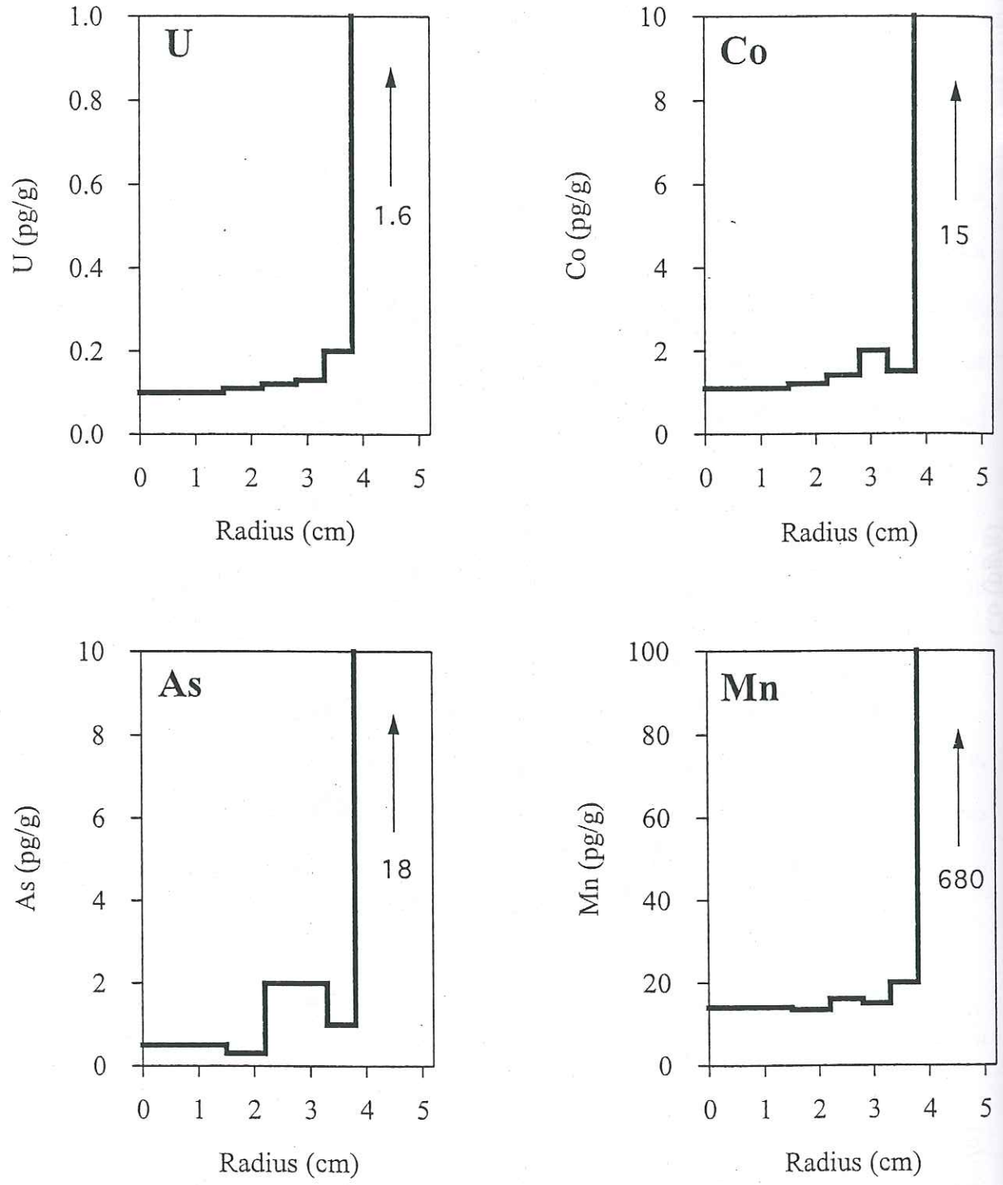

Figure 2

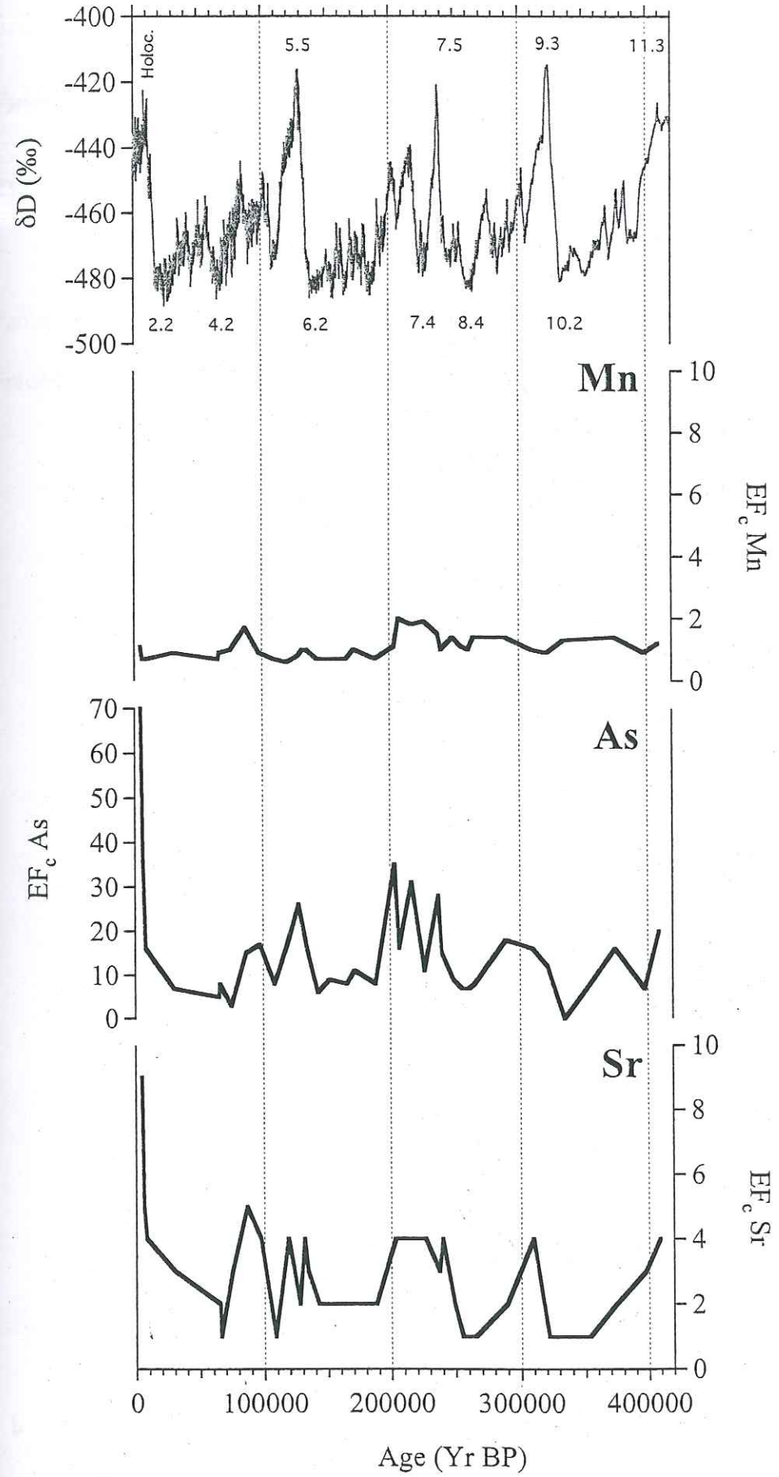

Figure 3

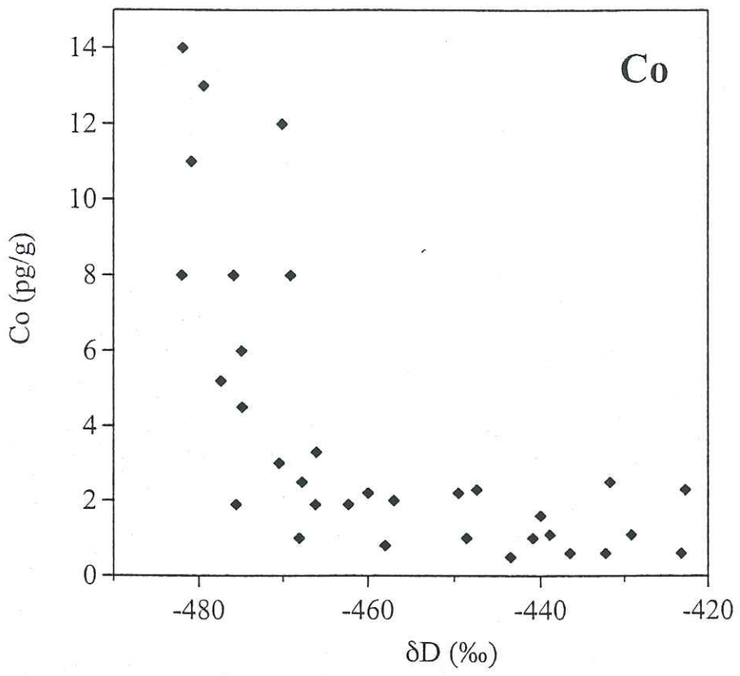

Figure 4

3.2 ARTICLE 5: **Variations in atmospheric trace elements in Dome C (East Antarctica) ice over the last two climatic cycles**

Paolo Gabrielli, Carlo Barbante, Claude Boutron, Giulio Cozzi, Vania Gaspari, Frédéric Planchon, Christophe Ferrari and Paolo Cescon

To be submitted to *Atmospheric Environment*

Variations in atmospheric trace elements in Dome C (East Antarctica) ice over the last two climatic cycles

Paolo GABRIELLI[a,b], Carlo BARBANTE[b,c*], Claude BOUTRON[a,d], Giulio COZZI[b], Vania GASPARI[b], Frédéric PLANCHON[b], Christophe FERRARI[a,e] and Paolo CESCON[b,c]

[a] *Laboratoire de Glaciologie et Géophysique de l'Environnement du CNRS 54, rue Molière, B.P. 96, 38402 St Martin d'Heres cedex, France*

[b] *Department of Environmental Sciences, University of Venice, Ca' Foscari, I-30123 Venice, Italy*

[c] *Institute for the Dynamics of Environmental Processes-CNR, University of Venice, Ca' Foscari, I-30123 Venice, Italy*

[d] *Observatoire des Sciences de l'Univers et Unité de Formation et de Recherche de Physique (Institut Universitaire de France) , Université Joseph Fourier, Domaine Universitaire, B.P. 68 38041 Grenoble, France*

[e] *Polytechnique Grenoble (Institut Universitaire de France), Université Joseph Fourier, 28 avenue Benoît Frachon, B.P. 53, 38041 Grenoble, France*

*Corresponding author. Phone: +39-041-2348942; Fax: +39-041-2348549; E-mail: barbante@unive.it

Abstract Concentrations of Li, Mg, Cr, Mn, Co, Cu, As, Rb, Cd, Ba and Bi have been determined by inductively coupled plasma sector field mass spectrometry (ICP-SFMS) in

various sections of the new Dome C/EPICA Antarctic ice core, down to the depth of 2193 m, covering a time period of two climatic cycles. The time resolution of these records is at least twice as good as previously published ultra trace elements profiles obtained from the Vostok ice core. During the ~217 kyr period spanned by this record, a high variability in concentrations is observed for most elements, with low values during warm periods and high values during cold periods. The highest concentrations are recorded at the times of the last two glacial maxima (~20 and ~140 kyr BP). The timing and the amplitude of the main concentration peaks match remarkably well the insoluble dust concentration profile previously obtained by Delmonte and co-workers. It confirms that dust was the main carrier of atmospheric trace elements to East Antarctica during the cold periods. For Ba, Co, Cu and Rb the crustal origin remained unchanged between warm and cold periods. For other elements the situation is more complex during interglacial periods, when other sources such as volcanic quiescent emissions, became probably significant for several trace elements such as Cd and Bi. Peculiarly high concentration values are observed for Cd and Bi at a short depth interval dated at ~18 kyr BP. It is the same depth interval in which elevated F^- values were observed previously. These very high concentrations are attributed to fallout from major local volcanic emissions at that time.

1 Introduction

Polar ice cores studies have well documented large changes in the content of atmospheric constituents such as ionic species [*Legrand et al.*, 1988], dust [*Delmonte et al.*, 2004a; *Epica community members*, 2004] and trace elements [*Hong et al.*, 2004; *Hong et al.*, 2003] during the late quaternary. The large increase in dust fallout to the East Antarctic plateau during glacial periods has been shown to be largely responsible for the variation of heavy metals recorded in the deep Antarctic Vostok ice core [*Hong et al.*, 2004; *Hong et al.*, 2003]. This phenomenon, occurring during the coldest stages of the last glacial age, was produced essentially by three concomitant factors. First, the reduction of seawater evaporation reduced the strength of the hydrological cycle, consequently decreasing the scavenging process of particles from the atmosphere and increasing the aridity of the soils. Second, an increased storage of water in the form of ice in the polar ice caps caused a lowering of the sea level, exposing a larger portion of the continental shelf to the wind erosion. Finally the enhanced thermometric and barometric gradient between low and high latitudes strengthened poleward atmospheric circulation and dust transport. The combination of these factors augmented the number of dust particles mobilised from the terrestrial surface, caused a longer atmospheric residence time, and elongated the dust trajectories therefore enhancing the global transport and fallout of dust and trace elements to the polar ice caps [*Delmonte et al.*, 2004a; *Krinner and Genthon*, 2003; *Petit et al.*, 1981; *Petit et al.*, 1999; *Smith et al.*, 2003].

However, scenarios describing aerosol transport and the general atmospheric circulation of trace elements in past climates are far from being well understood. A major problem concerns, for instance, the relative importance of the volcanic and crustal contribution to the fallout of trace elements to the Antarctic continent [*Hong et al.*, 2003; *Marino et al.*, 2004; *Matsumoto and Hinkley*, 2001]. Another major question regards the localisation of the areas where dust particles recovered in Antarctic ice were mobilised from during cold and especially warm periods [*Delmonte et al.*, 2004a; *Vallelonga et al.*, 2004]. Finally, zonal and meridional bi-dimensional past trajectories followed by aerosols that reached the Antarctic plateau were not well understood and only recently a more likely three-dimensional approach, involving vertical transport of the air masses, has been proposed [*Delmonte et al.*, 2004b].

Trace elements studies in ice cores can potentially contribute to improved explanations of issues concerning aerosol origin, transport and deposition. Thanks to multi-elemental analysis techniques, many different variables of the environmental system can now be taken into account [*Planchon et al.*, 2002]. Trace elements as proxies of crustal, volcanic, oceanic and cosmic material can be used to evaluate the contributions from different sources, which leads to hypotheses regarding the localisation of the source areas and therefore the transport processes prior to deposition. Here we present a new trace elements record covering the last two climatic cycles from the new Dome C/EPICA ice core, recently retrieved from the East Antarctic plateau.

2 Experimental

2.1 Description of the ice samples

The 84 samples, considered in this study, derive from 43 core sections from the upper 2193 m of the new deep ice core recently drilled at Dome C (75°06' S; 123°21' E, 3233 m, mean annual temperature - 54 °C) on the East Antarctic plateau within the framework of the European Project for Ice Coring in Antarctica (EPICA) [*Epica community members*, 2004]. This deep ice core was electromechanically drilled during several field seasons between the years 1996 and 2003. A first attempt conducted during the seasons 1996-1999 reached the depth of 788 m when the drill became stuck. This first ice core is named EDC96. A second parallel ice core, named EDC99, was successfully retrieved during the following field seasons down to the depth of 3190 m [*Epica community members*, 2004].

The depth of the 84 samples ranged from 32.5 m to 2193.4 m (Table 1). Since the close off depth at Dome C is ~95 m, the samples above that depth were firn, while the samples below that depth were ice. The upper first 46 samples, down to the depth of 763 m, were taken from the EDC96 core, while the remaining 38 samples (between 818 m and 2193 m) were taken from the EDC99 core. Age dating of the ice [*Epica community members*, 2004] shows that the ice at 2193.4 m is dated at ~217 kyr BP, which correspond to marine isotopic stage 7.4 [*Bassinot et al.*, 1994], while the firn at 32.5 m is dated at ~630 years BP. Our samples thus cover a ~217 kyr time period from the beginning of the penultimate ice age to the late Holocene.

2.2 Decontamination of the core sections

In the EPICA program, a given core section (typically 55 cm long, radius ~5 cm) is cut longitudinally into several parts which are used for different kinds of measurement. For this specific project, only ~ 30% of the cross section was available. Due to the extensive use of wall-retaining fluid that fills the borehole below the close off depth, the external part of ice sections is heavily contaminated for most trace elements. Each core section was therefore decontaminated at the Laboratory of Glaciology and Geophysics of the Environment (LGGE) using a procedure that has been extensively described elsewhere [*Boutron*, 1990; *Candelone et al.*, 1994; *Gabrielli et al.*, 2004]. Several annular concentric layers of ice were chiselled off before reaching the uncontaminated inner part of the core. Most of the inner cores obtained this way were then divided in two parts (top and bottom), which were analysed separately giving the 84 samples mentioned above. All samples were melted at room temperature in a special clean laboratory [*Boutron et al.*, 1990; *Planchon et al.*, 2001]. A 5 ml aliquot was then transferred into a 15 ml ultra clean LDPE bottle, and kept frozen until analysis.

2.3 Analysis by ICP-SFMS, blanks and precision

Li, Mg, Cr, Mn, Co, Cu, As, Rb, Cd, Ba and Bi were measured by inductively coupled plasma sector field mass spectrometry (ICP-SFMS) using an Element2 instrument from Thermo Electron Corporation (Bremen, Germany) using a micro-flow (< 100 µl min^{-1}) PFA nebulization system [*Planchon et al.*, 2001]. Thanks to the possibility of working at three different resolution modes (m/Δm=400, low resolution mode, LR; m/Δm=4,000, medium resolution mode, MR; m/Δm=10,000, high resolution mode, HR), most of the analytes peaks can be physically resolved from spectroscopic interferences that potentially hamper their accurate determination. For this work the LR mode was used for the analysis of Li, Rb, Cd, Ba and Bi, while the MR mode was adopted for the analysis of Mg, Cr, Mn, Co and Cu. Arsenic was analysed in the high resolution mode in order to resolve the interference of $^{40}Ar^{35}Cl$ on ^{75}As.

The overall procedural blanks were determined by processing an artificial ice core, made by freezing ultra-pure water in which the concentrations of the different trace elements was known beforehand [*Vallelonga et al.*, 2002]. The blanks were found to be negligible for all elements except Cr. For this last metal, a slight contamination at the ppt level (1 ppt = 1 pg g^{-1} = $1x10^{-12}$ g g^{-1}) was observed. It most likely originated from the stainless steel chisels that are used during the decontamination procedure. As a consequence, all Cr values at the ppt level are given as upper limits only.

The overall precision of the data was found to range between 5% for Mg and 20% for As, at the lowest levels of sample concentrations. Detection limits expressed in ppt were as follows: Li (1), Mg (10), Cr (1), Mn (0.3), Co (1), Cu (2), As (2), Rb (0.5), Cd (0.1), Ba (2), Bi (0.05).

2.4 Outside to inside concentration profiles

It was of utmost importance to make sure that the inner cores, obtained after the decontamination procedure was completed, were free from any contamination. To ensure this changes in concentrations of the different elements from the outside to the centre of the sections were then monitored. In most cases concentrations were found to level off at to a well defined plateau in the inner part of the sections, showing that the values measured in these inner parts did indeed represent the original concentrations in the ice. As an example, internal external profiles of Cu, Cd and Ba from an interglacial ice section are showed in Fig. 1. Contamination problems have been encountered for some trace elements only in a few ice sections (see for instance, Cr and Li profiles in Fig. 2) and in few firn sections located in the upper part of EDC96 above the ice close off depth, where porous channels allowed contaminants to reach the innermost part of the core. In these cases concentrations were found not to be to level off to a plateau in the inner part of the sections. Therefore, in these particular sections, the concentration values of some trace elements, which are probably affected by contamination, are reported only as upper limits of the values of the pristine concentration in snow (Table 1).

3 Results and discussion

3.1 Changes in trace elements concentrations and fallout fluxes as a function of climate

Trace elements concentrations measured in the 84 depth intervals are listed in Table 1. Fig. 3 shows that there is a very high variability in concentrations over the last two

climatic cycles, with generally high values during cold periods and low values during warm periods. However, the maximum amplitude of the variations markedly differs from one trace element to another, Table 2, shows the highest maximum/minimum concentration ratio is for Ba (~300) whilst the lowest ones are for Co and As (~15).

For most trace elements (namely Li, Mg, Cr, Mn, Co, Cu, As, Rb, Ba and Bi), three main sharp maxima are observed around ~20, 60 and 150 kyr BP i.e. at the time of particularly cold periods characterized by very low δD values, Fig. 3. They correspond to marine isotopic stages 2.2 (Last Glacial Maximum, LGM), 4.2 and 6.2 respectively, Fig. 3. Conversely, shows that very low concentrations are observed during warmer periods, characterized by less negative δD values. These variations closely follow the variations of insoluble dust previously documented in the same core by Delmonte and co-workers [*Delmonte et al.*, 2004a]. This is illustrated in Fig. 4, which compares the variations of Mn and Ba with those of insoluble dust. The situation is less clear for Cd, Fig. 3 because the observed variations are different for this metal.

As illustrated in Fig. 5, for Li, Mg and Ba, the concentrations of most trace elements remains very low for δD values larger than ~ -430 ‰. Conversely, a sharp increase in concentrations is observed for δD values below ~ -430 ‰. The only exception is Cd. For this element concentrations are found to increase progressively as function of the decrease of δD, as illustrated in Fig. 5.

Trace element fallout fluxes were calculated by combining concentrations measured in the ice at each depth with the estimated ice accumulation rate at that depth (Table 2). The snow accumulation rate has varied by nearly a factor of 2 at Dome C between the coldest climatic stages (~1.3 g H_2O cm^{-2} yr^{-1}) and warm interglacials (~2.7 g H_2O cm^{-2} yr^{-1}). For most elements, changes in fallout fluxes match changes in the corresponding concentrations very well, meaning that the variation in snow accumulation rate does not play an essential role in explaining the overall variability. The ratio between the highest and the lowest fluxes is in general about half of the corresponding maximum/minimum concentration ratio, since the accumulation rate in warm stages, when concentrations are at a minimum, is about the half that during cold stages, when concentrations are at a maximum. Cd appears once more to be a special case, with limited variations in fallout flux for this metal, which might be largely linked with changes in snow accumulation rate.

3.2 Crustal enrichment factors

Continental dust is one of the main sources of atmospheric trace elements [*Nriagu*, 1989]. In order to evaluate the importance of continental dust in Dome C/EPICA ice over the last two climatic cycles, we have calculated crustal enrichment factors (EF_c) for each element and depth. EF_c is defined as the concentration ratio of a given element to that of Mn (which is a good proxy of continental dust) in the ice, normalised to the same concentration ratio characteristic of the upper continental crust. For instance, the EF_c for Cu is thus: $EF_c=\{[Cu]_{ice}/[Mn]_{ice}\}/\{[Cu]_{crust}/[Mn]_{crust}\}$.

We have used here the data for the upper continental crust given by Wedepohl [*Wedepohl*, 1995]. It should however be emphasised that the choice of other crustal compositions, for instance that given by Rudnick and Fountain [*Rudnick and Fountain*, 1995], would not make any significant differences in the interpretation. Given the fact that the composition of continental dust reaching Dome C might significantly differ from the composition of the mean upper crust, EF_c values close to unity (up to ~5) will indicate that the corresponding element mainly originated from continental dust. Conversely, values significantly larger than unity will indicate a significant contribution from other natural sources.

Table 3 shows the mean EFc values obtained for the different elements both during warm/temperate periods with low dust input to Antarctica and much colder periods with higher continental dust input [*Delmonte et al.*, 2004a]. When considering the Dome C/EPICA δD variation profiles [*Epica community members*, 2004], we have assumed that the coldest periods correspond to ice with δD values larger than about –430 ‰ while warm/temperate periods correspond to ice with lower δD values. This 430 ‰ value corresponds to the value below which the concentrations of most trace elements considered in our work are found to strongly increase, as discussed previously (Fig. 5).

For Ba, Rb and possibly Co and Cu EF_c values, are found to be consistently always close to unity. Moreover the R^2 value calculated between Co, Mn, Rb and Ba is often higher than 0.95 indicating a contemporaneous arrival at Dome C. These observations are evidence that continental dust was the main source of these elements at Dome C whatever the climate conditions during the last ~217 kyr. To a lesser extent Li, EF_c values are close to unity only during the last and the penultimate glacial ages. This shows that the high input of continental dust during glacial periods was the main contributor for this trace element. This is independently confirmed by the high similarity of their concentration profiles with the insoluble dust concentration variation in the EPICA Dome C ice core [*Delmonte et al.*, 2004a].

When EF_c values are significantly higher than unity, it suggests additional inputs from one or several other natural sources and/or significant changes in the characteristics of continental dust arriving at Dome C, such as source area or transport parameters. EF_c values significantly larger than unity are observed for Mg, Bi, As and especially Cd whatever the period, and for Li during interglacial periods.

For Li, there are recent indications that the higher EF_c values observed during the Holocene could be linked to a different dust-material that was introduced to the air mass over Dome C after the glacial interglacial transition [*Siggaard-Andersen et al.*, 2004]. In fact, a distinct change in the geo-physical/chemical properties of this element was shown to occur between the Last Glacial Age and the Holocene with a prevalently insoluble component observed during the Last Glacial Age and an enhanced soluble fraction being deposited during the Holocene.

3.3 Contributions from natural sources other than continental dust

The main possible natural sources other than continental dust are sea salt spray, volcanic emissions and marine biogenic activity [*Nriagu*, 1989].

The contribution from sea salt spray was evaluated from Na^+ concentrations measured in the ice [*Bigler et al.*, 2004] and the elemental ratios in ocean water (www.agu.org/eos_elec/97025e-refs.html). These ratios were not combined with possible enrichments in ocean-derived aerosols relative to bulk seawater, when marine aerosol is formed by bubble bursting through the ocean surface micro layer, since some studies have put doubt on such possible enrichments [*Hunter*, 1997].

Sea salt spray contribution is found to be important for Mg whatever the period, with a mean contribution comprising about 60% of the total concentration of Mg in warm periods and 25% in cold periods. As suggested from high correlation with crustal elements such as Mn (R^2=0.87) and Ba (R^2=0.82) values, the remaining fraction is from continental dust at least during cold periods. The contribution from sea salt is negligible for all the other elements, whatever the period.

A rough estimate of the contribution from volcanic emissions was calculated from the concentration of non-sea-salt sulfate (nss-SO_4) in the ice [*Udisti et al.*, 2004] by assuming that ~15% of nss-SO_4 originates from volcanoes [*Boutron and Patterson*, 1986]. It was combined with recent estimates of element/S ratios in volcanic emissions [*Hinkley et*

al., 1999]. It must however be kept in mind that such estimates are rather uncertain, because of the large variations in published elements/S ratios in volcanic emissions. Also, there are no data for several of the elements analysed in our work. Volcanic emissions are found to be possibly a significant source for As during warm periods and for Cd and Bi whatever the period. Nevertheless, the rather high R^2 value calculated for Bi with crustal elements such as Mn (0.53) and Ba (0.53) strongly suggests an important crustal contribution for this element at least during cold periods.

A possible local volcanic source within the Antarctic continent could be Mount Erebus, which is located ~1000 km from Dome C. Zreda-Gostynska and co-workers [*Zreda-Gostynska and Kyle*, 1997] have suggested that Mount Erebus could be a significant source of various trace elements to the Antarctic atmosphere and to Antarctic snow.

Finally, our data do not allow any estimate of the contribution from continental marine biogenic activity to be made. Such contribution might be significant, since recent studies have documented production of methylated metals by polar marine bacteria [*Heumann*, 2001; *Pongratz and Heumann*, 1999].

3.4 Cd and Bi concentrations spike ~18 Kyrs BP

An interesting event has been recorded in the ice at a depth of 471.4 m (dated ~18 kyrs BP). In that sample, elevated concentrations of Cd and Bi have been observed ([Cd]=20 ppt; [Bi]=2.7 ppt). These concentrations are much higher than the concentrations observed for these elements in the nearby samples, Table 1. The corresponding EF_c values are 411 and 47. Interestingly, a particular high radiogenic value of 1.26 has been also observed for the $^{206}Pb/^{207}Pb$ isotopic ratio, but only in that particular sample [*Vallelonga et al.*, 2004] indicating a dominant volcanic contribution for Pb in that sample ([Pb]=~29 ppt).

Preliminary F analysis of the EDC1 core [*Schwander et al.*, 2001] confirms this indication by revealing an elevated fluoride concentration at a depth interval (471.3-472.8 m) which corresponds to a ~10 cm section of the length of our inner core sample (~471.2-471.4 m). This F^- enrichment was synchronously and also more strongly recorded in a West Antarctic ice core drilled at Byrd station, in which Cl^- and acidity levels were also found to be abnormally high [*Hammer et al.*, 1997]. It was concluded that high values of acidity recorded in the Byrd ice core were due to a dramatic and massive volcanic event that fluctuated and lasted for ~170 years.

There are several arguments that point to a local (Antarctic) volcanic eruption for explaining the origin of this event. The first concerns the less pronounced acid signal found in EDC1 in comparison with the Byrd ice core. Moreover, elevated sulphate concentrations were neither observed in that particular EDC1 ice section [*Castellano et al.*, 2004] nor in the corresponding Byrd samples [*Hammer et al.*, 1997]. An evident volcanic horizon in the ice without a clear sulphate peak can be most likely produced by the rapid fallout of volcanic aerosol in which SO_2 has not had enough time to be oxidized. These observations are consistent with the hypothesis of local volcanic fallouts onto West and East Antarctica at about 18 kyr.

The arguments reported above therefore show that the extremely high values observed for Cd and Bi in the ice section dated at 18 kyr are linked with the fallout from these local volcanic emissions. The Bi/Cd concentration ratio in that sample is 0.14. Interestingly, the Bi/Cd ratio observed in Dome C ice during interglacial periods, when the crustal contribution for Cd and Bi is negligible, falls very close to that value. For instance the mean Bi/Cd ratio during the Holocene is 0.19. It further supports the suggestion made in section 3.3 that the volcanic contribution is important for these two elements during

warm periods. Furthermore, the lack of large variations in Cd fallout flux together with the elevated EF_c values during the glacial periods, suggest a dominant volcanic origin for Cd whatever the period. In contrast, for Bi, the strong dust contribution during the coldest periods does not allow us to clearly distinguish the volcanic input actually present at that time. However if the importance of the volcanic contribution in interglacial periods for these elements is correct, it seems reasonable that this contribution mainly originates from quiescent volcanic emissions [*Hinkley et al.*, 1999; *Matsumoto and Hinkley*, 2001].

Conclusions

Analyses of various sections of the new EPICA/Dome C ice core, back to about 220 kyr BP, have documented strong variations in the trace element fallout to the East Antarctic plateau.

Elevated fluxes are generally recorded during glacial periods corresponding to marine isotopic stages 2.2, 4.2 and 6.2. The enhanced fallout of trace elements is caused essentially by the higher dust flux.

Much lower fluxes occurred during warmer periods when the dust flux shut down dramatically. During these periods the contribution from volcanoes was probably important.

It will be interesting in the future to extend this work to the part of the EPICA/Dome C ice core, which has not been considered here. The drilling has very recently reached a depth of 3190 m [*Epica community members*, 2004], which corresponds to ~ 800,000 kyr, back to the time of the last reversal of the magnetic field of the Earth. It would allow us to determine the variations in trace elements fallout to the East Antarctic plateau over eight glacial cycles.

Acknowledgements

This work was supported in France by the Institut Universitaire de France, the Ministère de l'Environnement et de l'Amènagemont du Territoire, the Agence de l'Environnement et de la Maîtrise de l'Energie, the Intitut National des Sciences de l'Univers and the Universite Joseph Fourier of Grenoble. In Italy, it was supported by ENEA as part of the Antarctic National Research Program (under projects on Environmental Contamination and Glaciology). This is EPICA publication No. X. This work is a contribution to the European Project for Ice Coring in Antarctica (EPICA), a joint European Science Foundation (ESF)/EC scientific programme, funded by the European Commission under the Environment and Climate Programme (1994-1998) contract ENV4-CT95-0074 and by the national contributions from Belgium, Denmark, France, Germany, Italy, The Netherlands, Norway, Sweden, Switzerland and U.K. We would like to thank all the scientific and logistic personnel working in Dome C, Antarctica. Finally we would like to thank Kevin Rosman for providing the ultra-pure HNO_3 and Paul Vallelonga for the artificial ice core preparation and laboratory assistance.

		Concentration (ppt)										
Age (years BP)*	Depth (m)	Li	Mg *	Cr	Mn	Co	Cr	As	Rb	Cd	Ba	Bi
569	32.5	<16	5	<5	7	1.0	<6	<2	5.1	0.6	5.0	<0.16
1,227	59.1	7	10	<2.2	9	1.0	<2	2	4.0	1.0	7	0.10
1,234	59.4	7	8	<2.1	20	2	6	3	3.2	0.7	7	0.10
2,006	86.6	6	9	<2.2	12	<1	<2	<2	4.3	0.5	8	0.10
2,015	86.9	10	14	7	48	2.1	5	2	4.8	0.5	15	0.10
4,156	152.1	13	5	<2	8	1.1	<2	2	5	1.0	3.6	0.23
4,166	152.4	13	5	<1.5	5	<1	<2	2	6	1.0	3.3	0.12
6,938	229.1	3	8	<2.5	15	1.0	<2	2	3.4	0.3	10	0.08
6,949	229.4	5	6	<2.2	12	1.4	<2	<2	8	0.5	9	0.06
7,353	239.5	2	4	<2	8	<1	<2	2	1.2	0.5	2	0.13
7,364	239.8	2	1	<1.0	9	<1	<2	2	2	0.5	<2	0.13
10,270	316.0	<1	1	<2.3	12	1.0	3	2	9	0.2	6	0.06
10,280	316.3	3	1	<4	10	1.5	<2	<2	4.8	0.3	6	0.06
11,247	341.8	3	1	<1.4	14	1.2	<2	<2	4.8	0.9	2.7	0.19
11,258	342.1	<1	1	<1.1	8	<1	<2	<2	4.9	0.7	3.0	0.08
12,809	379.2	8	11	<2.5	14	<1	<2	3	5	0.6	15	0.13
12,823	379.5	6	9	<2.2	8	<1	<2	2	3.4	0.4	8	0.07
14,204	405.6	6	16	<3.2	39	1.3	2.0	<2	4.4	0.7	17	0.12
14,219	405.9	6	16	<4	38	1.1	2.0	2	5	0.6	18	0.13
14,910	419.4	16	9	<2	20	1.3	<2	3	12	0.5	19	0.10
14,924	419.7	7	13	7	66	2.2	3.4	<2	4.1	0.4	15	0.07
15,611	432.6	10	13	<3	40	1.2	3.2	2	6	0.6	21	0.10
15,626	432.9	9	15	<4	52	1.6	9	2	7	0.9	26	0.15
17,380	461.2	24	30	13	170	3.4	12	8	21	1.5	80	0.33
17,400	461.5	30	38	10	215	3.3	8	9	25	1.4	117	0.33
18,133	471.1	54	61	13	341	6	14	15	51	2.7	236	0.9
18,155	471.4	43	51	11	248	4.5	13	24	47	20	180	2.7
19,627	488.7	76	71	23	529	10	22	20	93	1.2	440	0.9
19,651	489.0	95	71	20	624	11	28	16	99	1.2	543	1.0
21,944	515.6	131	75	29	760	15	31	25	124	0.9	657	1.0
21,967	515.9	73	69	22	506	9	21	14	82	0.9	478	1.0
27,009	573.9	60	71	15	394	7	107	18	54	1.2	287	0.59
27,033	574.2	72	68	16	480	8	22	16	76	1.8	358	1.2
29,094	598.1	49	59	21	319	6	13	11	51	0.8	195	0.40
29,117	598.4	65	60	17	484	8	19	10	78	1.0	305	0.8
33,661	653.1	32	46	9	176	3.0	8	8	27	0.6	116	0.28
33,682	653.4	37	43	9	200	3.3	30	14	33	0.7	132	0.37
33,706	653.7	36	46	9	236	5	12	11	38	0.9	171	0.53
33,729	654.0	44	53	10	260	5	13	13	51	1.0	185	0.43
35,967	680.9	33	41	8	201	2.9	9	12	30	1.0	133	0.84
38,135	708.7	11	29	6	103	1.5	3.2	4	13	1.3	52	0.20
38,155	709.0	9	30	6	74	1.5	2.6	5	11	1.4	41	0.20
40,375	735.6	35	46	10	229	4.0	9.3	7	28	0.7	158	0.36
40,401	735.9	40	58	13	318	5.3	15	9	45	0.7	224	0.46
42,801	763.1	23	38	8	127	2.3	5	5	20	0.4	79	0.24
42,825	763.4	24	39	12	159	2.9	11	7	18	0.8	83	0.23
47,175	818.1	30	46	8	163	2.8	8	8	24	0.5	113	0.29
47,198	818.4	41	44	8	189	3	13	12	32	0.5	131	0.31
53,830	900.6	34	39	11	223	3.9	12	6	35	0.9	-	0.44
53,853	900.9	25	25	16	247	2.6	7	6	19	0.7	-	0.3
60,647	983.1	45	52	13	340	5.1	12	11	53	1.1	219	0.48
60,674	983.4	44	53	14	272	6	16	9	44	1.3	200	0.63
63,425	1010.6	57	57	15	396	7	17	16	62	1.1	281	0.60
63,453	1010.9	69	63	22	513	9	23	17	78	1.1	392	0.8
71,637	1093.1	13	24	<4	40	1.5	3.0	3	7	1.0	27	0.17
71,660	1093.4	14	20	<4	55	1.7	2.5	5	9	1.0	32	0.21
76,576	1148.1	15	17	<5	96	2.8	4	6	14	0.5	55	0.13
76,601	1148.4	9	20	<6	129	3.1	4.7	4	12	1.2	51	-
81,050	1203.1	10	13	<4	50	1.6	4.2	2	8	1.5	23	0.18
81,071	1203.4	6	13	<2.8	25	1.0	<2	3	5.4	1.1	16	0.14
86,002	1258.1	8	28	<5	107	2	9	8	11	0.5	50	-
86,028	1258.4	8	26	<5	112	3.0	7	7	11	1.0	53	-
91,429	1313.1	10	16	<3.0	27	1.6	2.7	2	6	0.6	16	0.12
91,456	1313.4	6	20	<2.6	31	1.1	2.1	4	5.3	0.5	22	0.13
102,253	1423.1	9	14	<4	59	1.7	3	5	8	0.8	34	0.12
102,283	1423.4	6	15	8	140	3	5	5	11	0.9	45	-
114,119	1533.1	6	9	<3	11	<1	<2	2	3.2	0.6	9	0.09
114,142	1533.4	12	7	<3	10	1.1	<2	2	8.7	0.8	12	-
122,810	1643.1	1	5	<3.3	21	1.2	2	3	1.3	0.2	10	0.05
122,832	1643.4	1	5	<3.1	26	1.3	<2	2	2	0.4	11	0.04
131,856	1753.1	12	19	<6	64	2.8	2.6	4	9	1.1	30	0.16
131,892	1753.4	9	25	<4	74	1.7	3	4	7.4	1.0	31	0.13
152,184	1863.1	69	63	17	480	8	18	13	71	2.4	336	1.2
152,239	1863.4	88	67	19	574	10	23	14	91	1.5	446	1.1
174,430	1973.1	50	45	10	296	4.7	12	9	39	0.9	208	0.37
174,491	1973.4	40	45	9	242	4	9	11	31	1.2	156	0.64
191,286	2050.1	9	18	10	174	2.4	4.5	5	11	0.4	61	-
191,345	2050.4	8	22	7	142	2.8	4	4	11	0.6	48	-
198,898	2094.1	9	9	<2.5	12	1.7	<2	<2	2.5	0.6	8	0.06
198,944	2094.4	10	8	<3	13	1.3	<2	<2	9	0.5	12	-
207,177	2138.1	9	11	<5	16	1.3	<2	<2	9	0.7	13	-
207,225	2138.4	9	12	<2.6	19	1.0	2.4	<2	4	0.7	10	0.08
216,992	2193.1	9	17	<5	76	1.8	4	3	10	0.6	35	0.09
217,051	2193.4	14	18	6	95	2.3	4	4	9	0.6	30	-

*Mg is expressed in ppb
** Age from ref. (Epica community members, 2004)

Table 1

		Flux (pg cm^{-2} y^{-1})										
Age (years BP)*	Depth (m)	Li	Mg**	Cr	Mn	Co	Cu	As	Rb	Cd	Ba	Bi
569	32.5	>50	16	>16	21	3	7	>6	16	2	16	>0.5
1,227	59.1	23	30	>7	28	3	>6	6	12	3	22	0.3
1,234	59.4	21	25	>6	61	5	18	9	10	2	21	0.3
2,006	86.6	16	24	>6	31	>3	>5	>5	11	1	21	0.3
2,015	86.9	27	36	18	126	6	13	6	13	1	39	0.3
4,156	152.1	33	14	>5	21	3	>5	5	13	3	9	0.6
4,166	152.4	33	13	>4	13	>3	>5	5	15	3	8	0.3
6,938	229.1	9	22	>7	41	3	>6	5	10	1	29	0.2
6,949	229.4	13	16	>6	34	4	>6	>6	22	1	27	0.2
7,353	239.5	6	12	>5	21	>3	>5	5	3	1	6	0.3
7,364	239.8	5	4	>3	25	>3	>5	5	6	1	>5	0.4
10,270	316.0	>3	5	>8	43	3	10	5	30	1	19	0.2
10,280	316.3	9	5	>14	35	5	>7	>7	17	1	21	0.2
11,247	341.8	8	4	>4	41	4	>6	>6	15	3	8	0.6
11,258	342.1	>3	2	>3	23	>3	>6	>6	15	2	9	0.3
12,809	379.2	18	24	>5	30	>2	>4	6	11	1	32	0.3
12,823	379.5	12	19	>5	18	>2	>4	3	7	1	17	0.1
14,204	405.6	13	33	>7	81	3	4	>4	9	1	36	0.2
14,219	405.9	12	33	>8	80	2	4	3	11	1	38	0.3
14,910	419.4	44	24	>6	55	4	>6	7	32	1	53	0.3
14,924	419.7	18	33	18	172	6	9	>5	11	1	40	0.2
15,611	432.6	24	31	>7	92	3	7	4	15	1	48	0.2
15,626	432.9	22	37	>10	132	4	24	4	17	2	66	0.4
17,380	461.2	42	53	23	298	6	22	13	37	3	140	0.6
17,400	461.5	50	62	17	358	5	13	14	42	2	194	0.6
18,133	471.1	84	95	20	531	9	22	23	79	4	369	1.4
18,155	471.4	66	80	17	387	7	20	37	73	31	281	4.3
19,627	488.7	112	103	34	772	14	32	29	135	2	643	1.3
19,651	489.0	139	104	29	911	17	41	24	144	2	793	1.5
21,944	515.6	185	107	41	1079	21	43	35	177	1	934	1.4
21,967	515.9	104	98	31	719	13	30	19	117	1	678	1.4
27,009	573.9	85	100	21	560	10	151	26	77	2	408	0.8
27,033	574.2	102	97	23	682	12	31	23	108	3	508	1.7
29,094	598.1	79	95	34	514	10	20	17	81	1	314	0.6
29,117	598.4	105	97	27	779	13	30	17	126	2	491	1.3
33,661	653.1	50	72	14	276	5	12	13	42	1	183	0.4
33,682	653.4	58	68	14	314	5	46	21	52	1	207	0.6
33,706	653.7	56	70	14	363	8	18	17	59	1	264	0.8
33,729	654.0	68	82	15	401	7	20	20	79	2	286	0.7
35,967	680.9	52	65	13	315	5	14	18	47	2	208	1.3
38,135	708.7	20	51	11	183	3	6	6	23	2	92	0.4
38,155	709.0	16	52	11	131	3	5	9	19	3	73	0.3
40,375	735.6	51	67	15	339	6	14	10	42	1	234	0.5
40,401	735.9	60	86	19	471	8	22	14	67	1	331	0.7
42,801	763.1	38	63	13	209	4	9	8	33	1	130	0.4
42,825	763.4	40	64	20	263	5	19	12	29	1	137	0.4
47,175	818.1	46	70	12	251	4	12	12	38	1	174	0.4
47,198	818.4	62	68	12	290	5	20	18	50	1	201	0.5
53,830	900.6	59	69	19	388	7	21	11	61	2	-	0.8
53,853	900.9	44	43	28	430	4	12	10	33	1	-	0.5
60,647	983.1	67	79	20	509	8	17	16	80	2	329	0.7
60,674	983.4	65	79	20	408	9	23	13	66	2	299	0.9
63,425	1010.6	84	83	22	578	10	25	23	91	2	411	0.9
63,453	1010.9	100	93	32	749	13	34	25	113	2	572	1.2
71,637	1093.1	24	44	>7	73	3	5	6	13	2	49	0.3
71,660	1093.4	25	36	>7	101	3	5	9	16	2	58	0.4
76,576	1148.1	25	28	>8	159	5	7	10	23	1	92	0.2
76,601	1148.4	14	33	>10	212	5	8	7	19	2	83	-
81,050	1203.1	23	28	>9	111	4	9	4	18	3	49	0.4
81,071	1203.4	14	29	>6	54	2	>4	7	12	2	36	0.3
86,002	1258.1	14	49	>9	189	4	16	14	20	1	88	-
86,028	1258.4	15	46	>9	199	5	13	12	20	2	94	-
91,429	1313.1	19	31	>6	53	3	5	4	12	1	30	0.2
91,456	1313.4	11	40	>5	60	2	4	7	10	1	42	0.2
102,253	1423.1	17	27	>7	110	3	6	9	16	2	63	0.2
102,283	1423.4	12	28	15	261	5	9	10	21	2	84	-
114,119	1533.1	16	24	>8	30	>3	>5	4	9	2	24	0.2
114,142	1533.4	32	19	>8	27	3	>5	5	23	2	33	-
122,810	1643.1	4	15	>10	65	4	5	11	4	1	31	0.1
122,832	1643.4	4	16	>10	83	4	>6	8	7	1	34	0.1
131,856	1753.1	25	41	>13	137	6	5	9	19	2	63	0.3
131,892	1753.4	20	54	>9	157	4	6	9	16	2	66	0.3
152,184	1863.1	105	97	26	734	13	27	20	109	4	514	1.9
152,239	1863.4	134	103	29	878	16	36	21	139	2	683	1.7
174,430	1973.1	77	70	16	459	7	19	14	61	1	323	0.6
174,491	1973.4	63	70	14	375	7	14	18	48	2	242	1.0
191,286	2050.1	15	30	17	287	4	8	9	18	1	101	-
191,345	2050.4	13	36	12	235	5	7	6	17	1	80	-
198,898	2094.1	23	23	>6	29	4	>5	>5	6	1	19	0.2
198,944	2094.4	24	20	>7	30	3	>5	>5	22	1	30	-
207,177	2138.1	23	28	>12	40	3	>5	>5	22	2	32	-
207,225	2138.4	22	30	>6	46	3	6	>5	9	2	24	0.2
216,992	2193.1	20	36	>10	158	4	7	6	21	1	73	0.2
217,051	2193.4	29	37	12	198	5	8	9	18	1	63	-

* Age from ref. (Epica community members, 2004)
**Mg flux is expressed in (ng cm^{-2} y^{-1})

Table 2

Mean EFc in warm and cold periods										
	Li	**Mg**	**Cr**	**Co**	**Cu**	**As**	**Rb**	**Cd**	**Ba**	**Bi**
Mean EFc in cold periods	4	7	0.7	0.8	2.0	11	0.7	31	0.5	9
Standard deviation	1	2	0.2	0.1	1.6	4	0.1	68	0.1	8
Mean EFc in warm periods	9	17	-	3	3.3	28	1	185	0.5	26
Standard deviation	11	10	-	2	2.8	21	1	190	0.2	25

Table 3

Figure caption

Fig.1. Exterior to interior profiles of Cu (a), Cd (b) and Ba (c) for an interglacial EPICA section at 1753.4 m of depth. High concentration levels are mainly present only in the first external layer, whereas concentrations drop sharply in the second layer removed. The good plateaus obtained are evidence that concentrations in the innermost part of the core represent the original levels in ancient ice, even at very low interglacial concentrations.

Fig.2. Exterior to interior profiles of Li (a) Cr (b) in an interglacial EPICA section at 1753.4 m. The concentration profiles do not show a clear drop and the concentration levels decrease towards the inner core but do not reach a plateau. This is evidence that contamination reached the inner core. Therefore these concentrations must be taken only as an upper limit of the pristine concentration in ice.

Fig. 3. Concentrations, of Li, Mg, Cr, Mn, Co, Cu, As, Rb, Cd, Ba, Pb and Bi in the EPICA Dome C ice core down to the depth of 2193 m. δD ‰ profile is a proxy of past local temperature.

Fig. 4. Concentrations of Mn and Ba are compared with the insoluble dust concentration profiles obtained by Delmonte and co-workers [*Delmonte et al.*, 2004a].

Fig. 5. EPICA Dome C ice core. Li (a), Mg (b), Cd (c) and Ba (d) concentrations versus δD ‰. An abrupt increase in concentrations is observed for Li, Ba and to a lesser extent for Mg at –530 ‰ whereas a slower increase in concentration is observed for Cd when δD ‰ is decreasing.

Figure 1 (a)

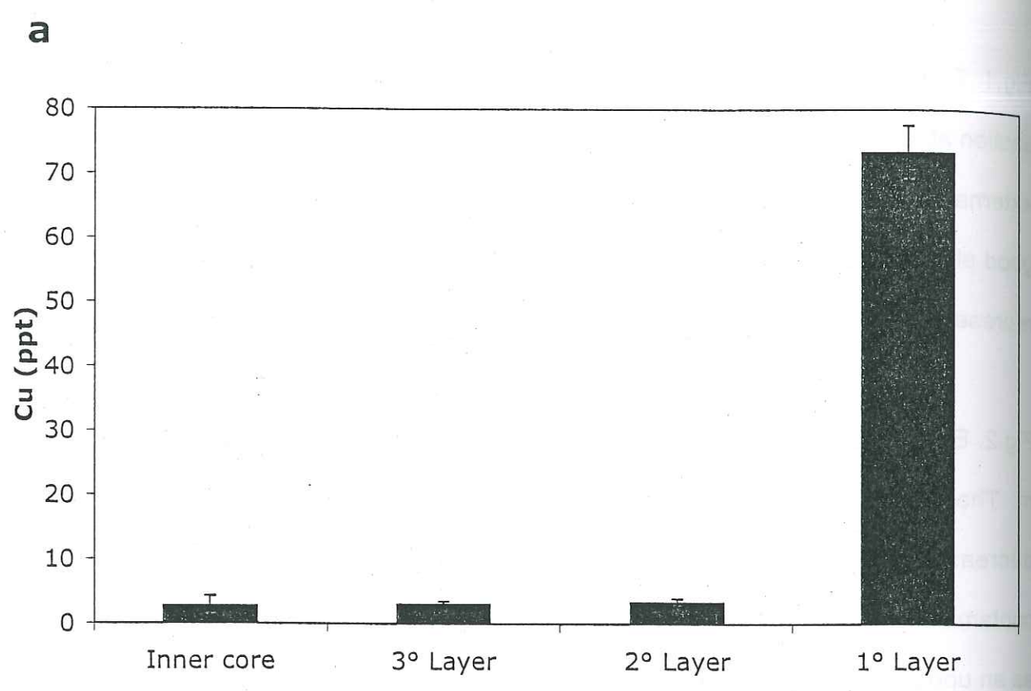

Figure 1 (b)

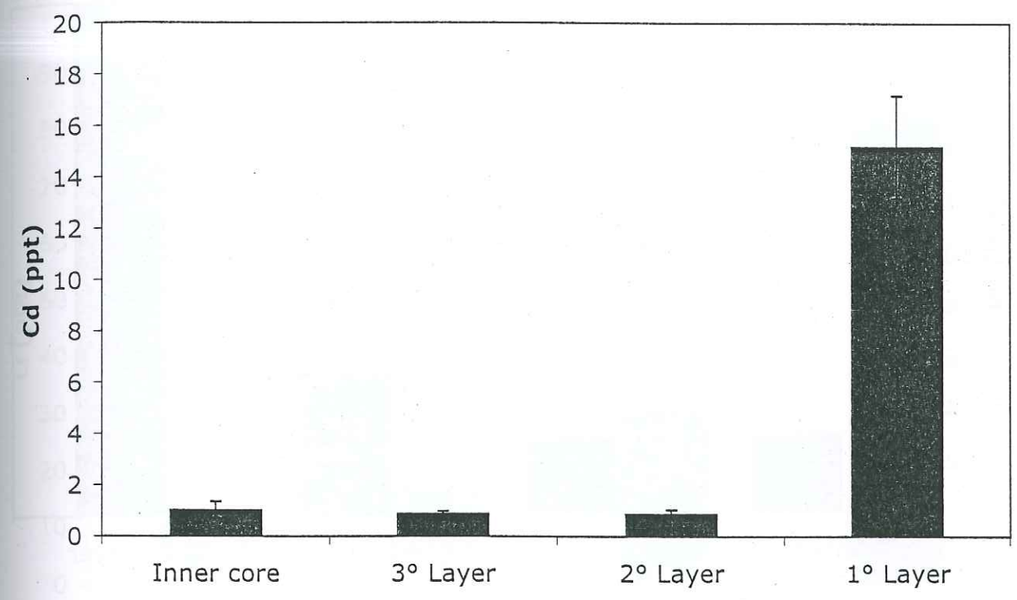

Figure 1 (c)

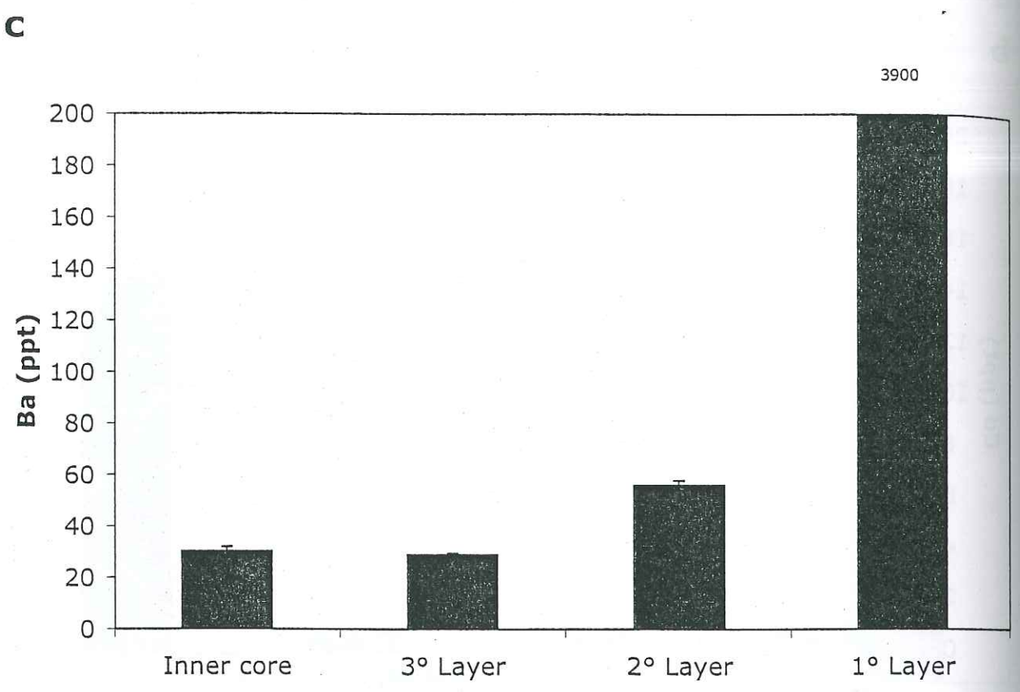

Figure 2 (a)

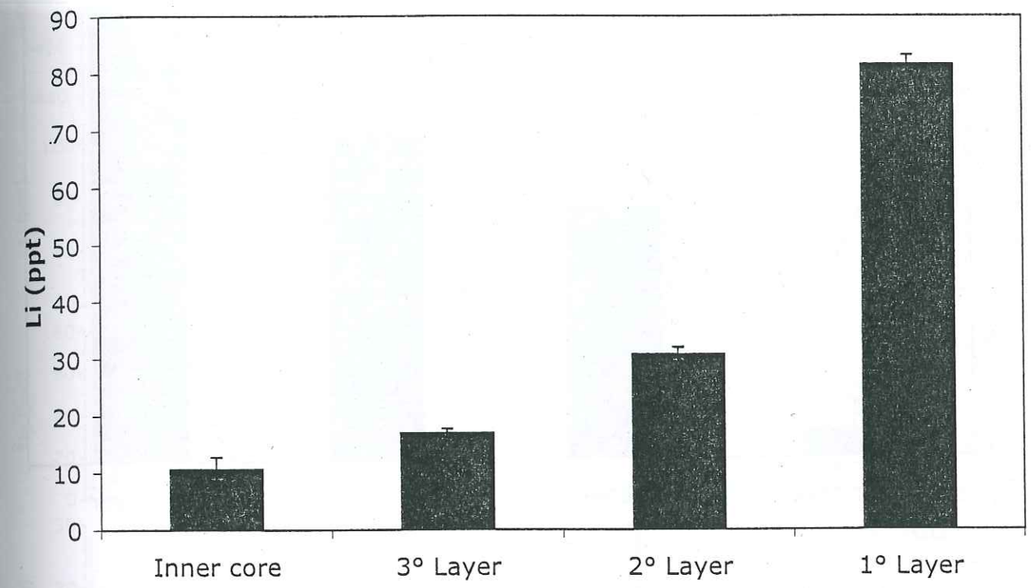

Figure 2 (b)

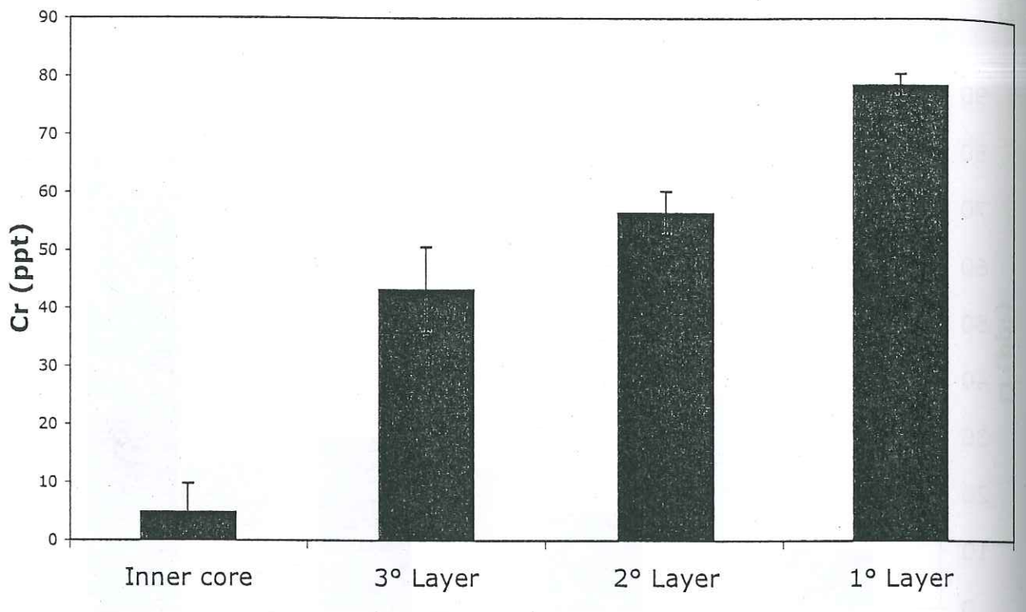

Figure 3

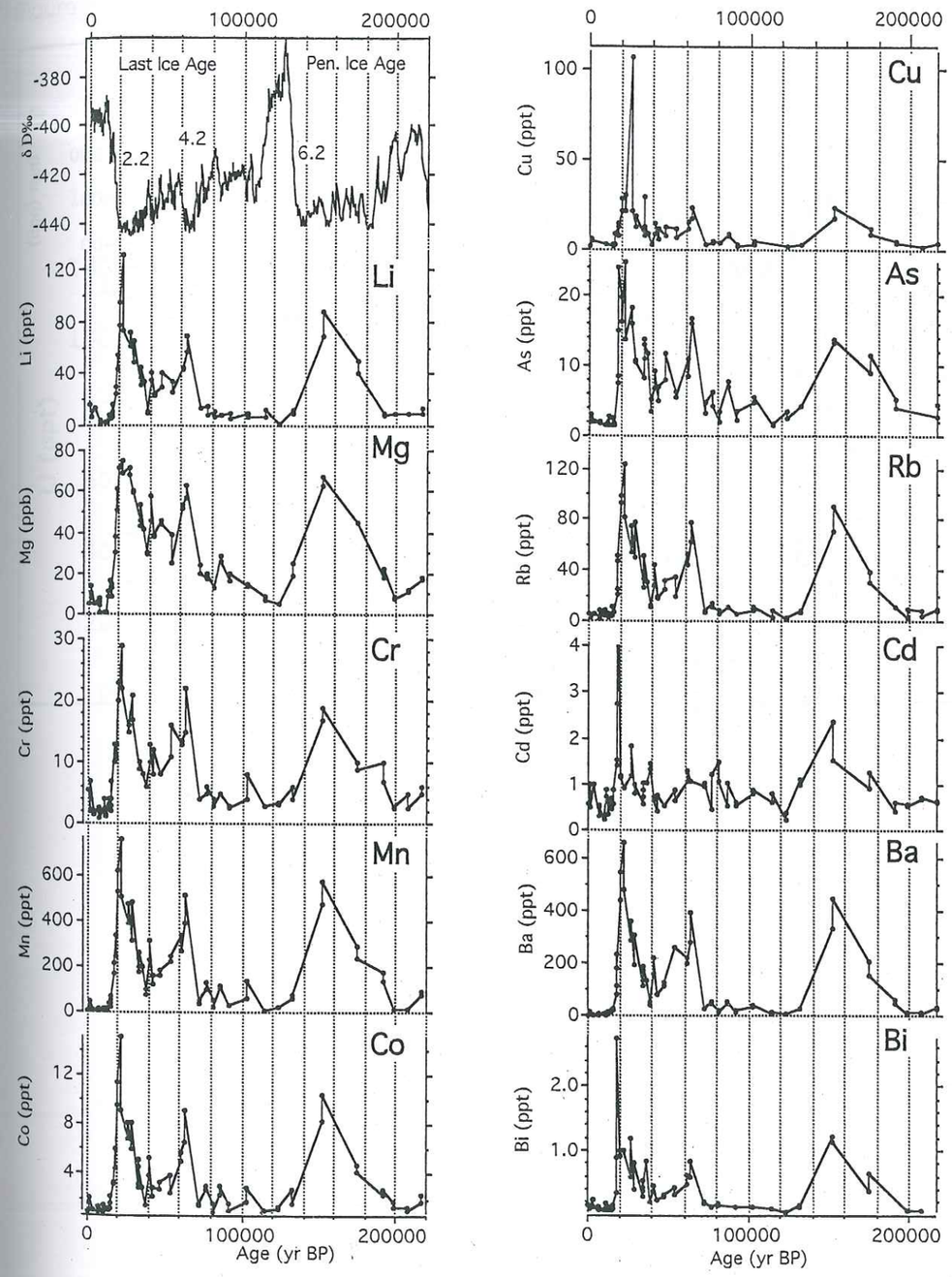

Figure 4

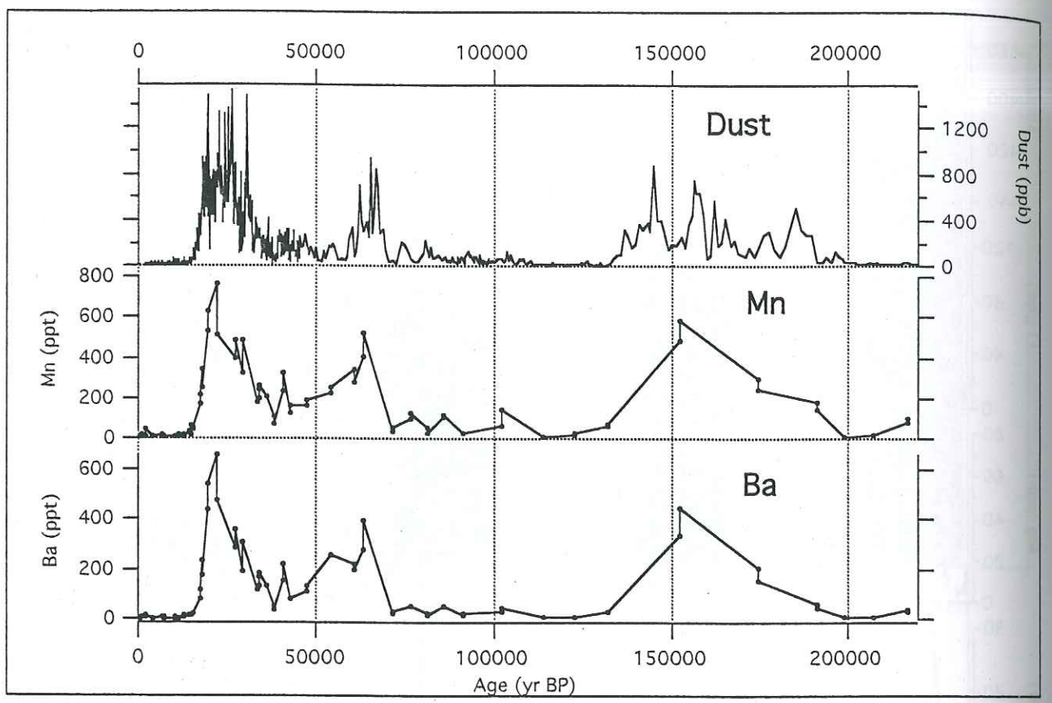

Figure 5 (a)

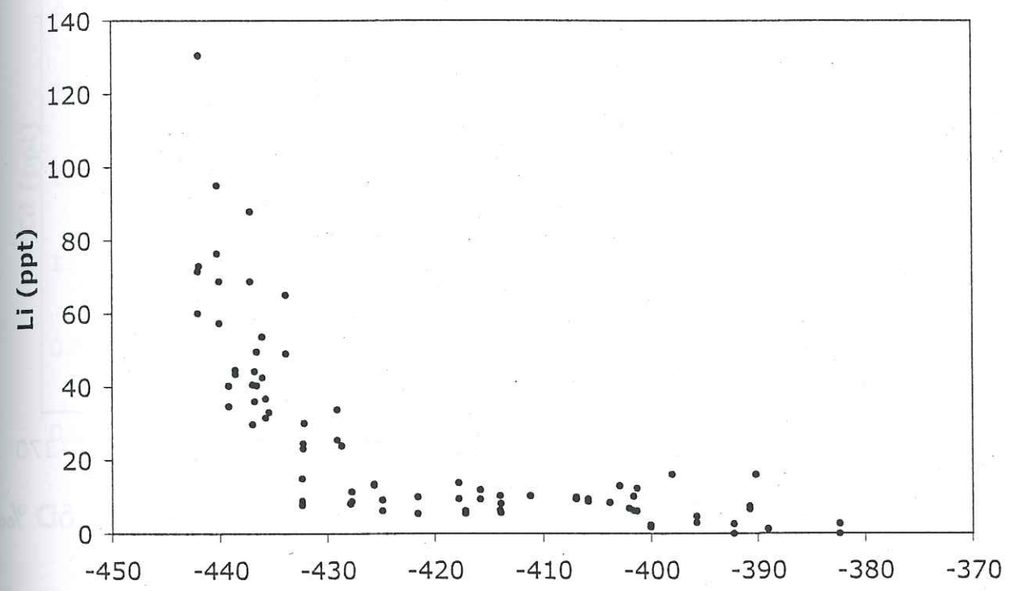

Figure 5 (b)

b

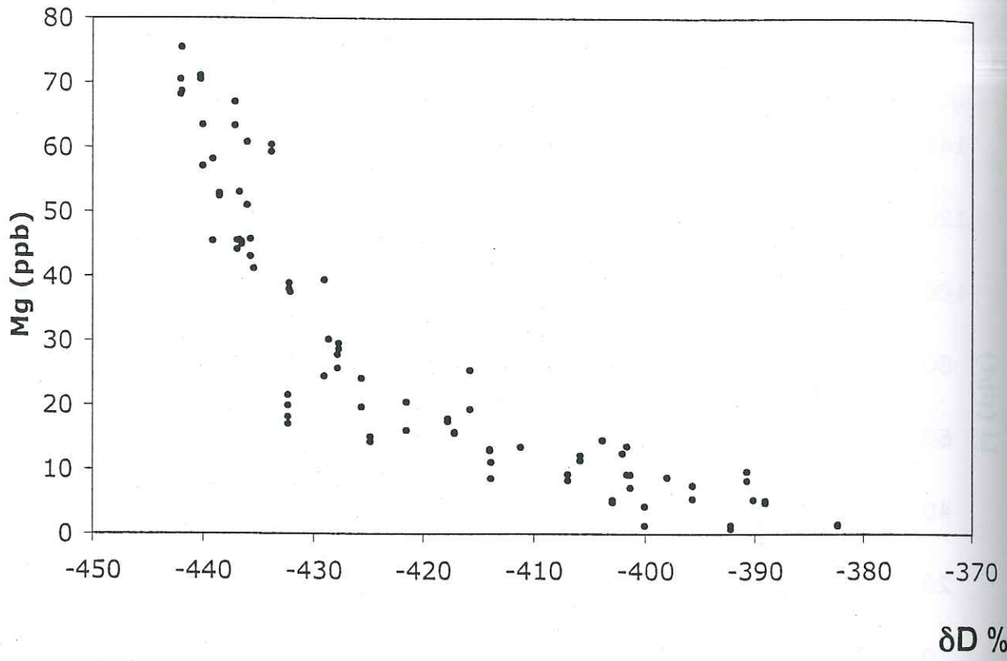

Figure 5 (c)

c

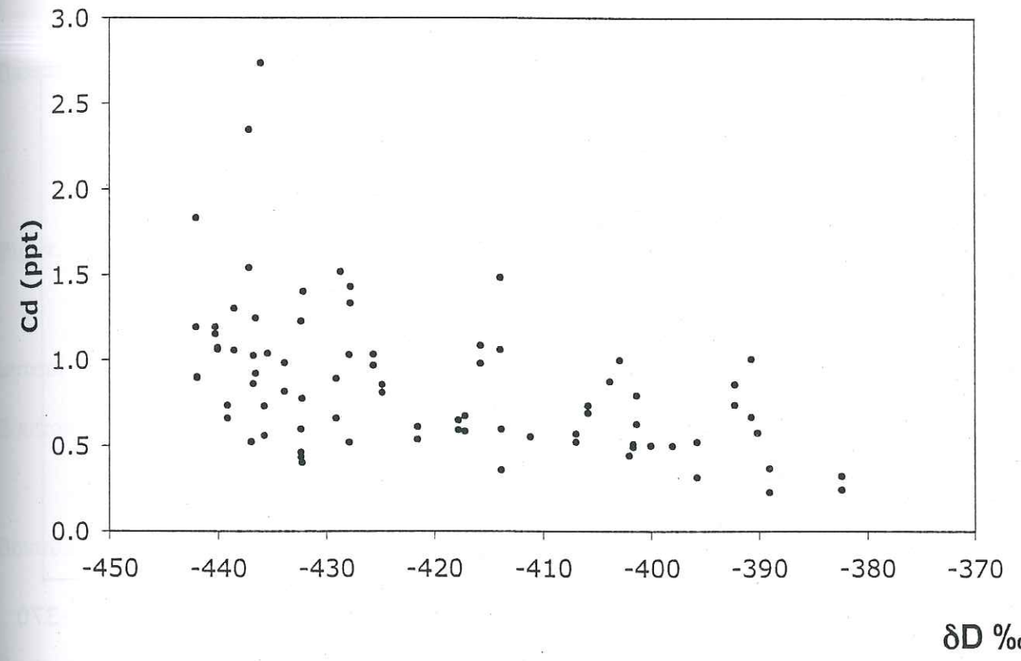

Figure 5 (d)

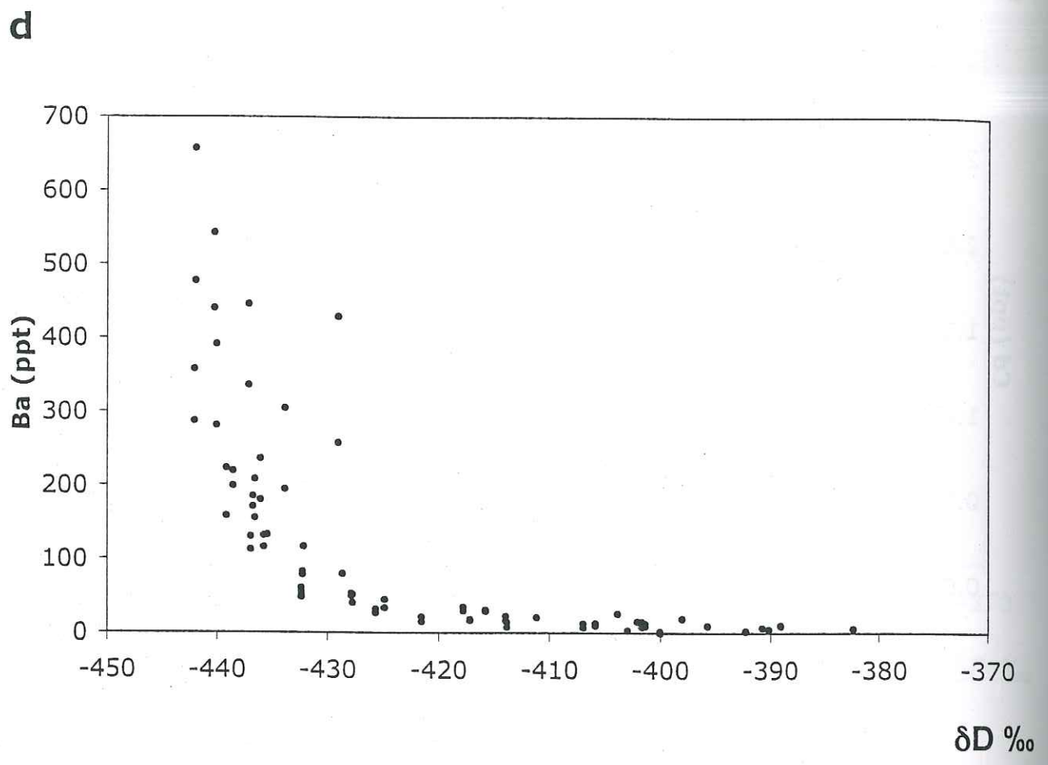

References

Bassinot, F. C., L. D. Labeyrie, E. Vincent, X. Quidelleur, N. J. Shackleton, and Y. Lancelot, The astronomical theory of climate and the age of the Brunhes-Matuyama magnetic reversal, *Earth Planet. Sci. Lett., 126*, 91-108, 1994.

Bigler, M., R. Rothlisberger, F. Lambert, T. Stocker, G. C. Littot, E. W. Wolff, and D. Wagenbach, The continental contribution to the water-soluble

aerosol deposited on the East Antarctic plateau (EPICA Dome C), *In preparation*, 2004.

Boutron, C. F., A clean laboratory for ultralow concentration heavy metal analysis, *Fresenius J. Anal. Chem., 337*, 482-491, 1990.

Boutron, C. F., and C. C. Patterson, Lead concentration changes in Antarctic ice during the Wisconsin/Holocene transition, *Nature, 323*(6085), 222-225, 1986.

Boutron, C. F., C. C. Patterson, and N. I. Barkov, The occurrence of zinc in Antarctic ancient ice and recent snow, *Earth Planet. Sci. Lett., 101*, 248-259, 1990.

Candelone, J. P., S. Hong, and C. F. Boutron, An improved method for decontaminating polar snow and ice cores for heavy metals analysis, *Anal. Chim. Acta, 299*, 9-16, 1994.

Castellano, E., S. Becagli, J. Jouzel, A. Migliori, M. Severi, J. P. Steffensen, R. Traversi, and R. Udisti, Volcanic eruption frequency over the last 45 ky as recorded in Epica-Dome c ice core (East Antarctica) and its relationship with climatic changes, *Glob. Planet. Change, 42*, 195-205, 2004.

Delmonte, B., I. Basile-Doelsch, J. R. Petit, V. Maggi, M. Revel-Rolland, A. Michard, E. Jagoutz, and F. E. Grousset, Comparing the Epica and Vostok dust records during the last 220,000 years: stratigraphical correlation and provenance in glacial periods, *Earth-Sci. Rev., 66*, 63-87, 2004a.

Delmonte, B., J. R. Petit, K. K. Andersen, I. Basile-Doelsch, V. Maggi, and V. Y. Lipenkov, Dust size evidence for opposite regional atmospheric circulation changes over east Antarctica during the last climatic transition, *Clim. Dyn., 23*, 427-438, 2004b.

Epica community members, Eight glacial cycles from an Antarctic ice core, *Nature, 429*, 623-628, 2004.

Gabrielli, P., A. Varga, C. Barbante, C. F. Boutron, G. Cozzi, V. Gaspari, F. Planchon, W. Cairns, S. Hong, C. Ferrari, and G. Capodaglio, Determination of Ir and Pt down to the sub-femtogram per gram level in polar ice by ICP-SFMS using preconcentration and a desolvation system, *J. Anal. At. Spectrom., 19*, 831-837, 2004.

Hammer, C. U., H. B. Clausen, and C. C. J. Langway, 50,000 years of recorded global volcanism, *Climatic Change, 35*, 1-15, 1997.

Heumann, K. G., Biomethylation in the Southern Ocean and its contribution to the geochemical cycle of trace elements in Antarctica, in *Environmental Contamination in Antarctica: A Challenge to Analytical Chemistry*, edited by S. Caroli, P. Cescon and D. Walton, Elsevier, Amsterdam, 2001.

Hinkley, T. K., P. J. Lamothe, S. A. Wilson, D. L. Finnegan, and T. M. Gerlach, Metal emissions from Kilauea, and a suggested revision of the estimated worldwide metal output by quiescent degassing of volcanoes, *Earth Planet. Sci. Lett., 170*, 315-325, 1999.

Hong, S., C. F. Boutron, P. Gabrielli, C. Barbante, C. Ferrari, J. R. Petit, K. Lee, and V. Y. Lipenkov, Past natural changes in Cu, Zn and Cd in Vostok Antarctic ice dated back to the beginning of the next to last ice age, *Submitted to Geophys. Res. Lett.*, 2004.

Hong, S., Y. Kim, C. F. Boutron, C. Ferrari, J. R. Petit, C. Barbante, K. Rosman, and V. Y. Lipenkov, Climate-related variations in lead concentrations and sources in Vostok Antarctic ice from 65,000 to 240,000 years BP, *Geophys. Res. Lett., 30*(22), 2138-2142, 2003.

Hunter, K. A., Chemistry of the sea-surface microlayer, in *The Sea Surface and Global Change*, edited by P. S. Liss and R. A. Duce, pp. 287-319, Cambridge University Press, 1997.

Krinnen, G., and C. Genthon, Tropospheric transport of continental tracers towards Antarctica under varyng climatic conditions, *Tellus, 55B*, 54-70, 2003.

Legrand, M., C. Lorius, N. I. Barkov, and V. N. Petrov, Vostok (Antarctic ice core): atmospheric chemistry changes over the last climatic cycle (160,000 years), *Atmos. Environ., 22*, 317-331, 1988.

Marino, F., V. Maggi, B. Delmonte, G. Ghermandi, and J. R. Petit, Elemental Composition (Si, Fe, Ti) of Atmospheric Dust Over the Last 220 kyrs from the EPICA ice core (Dome C, Antarctica), *Ann. Glaciol.*, 2004.

Matsumoto, A., and T. K. Hinkley, Trace metal suites in Antarctic pre-industrial ice are consistent with emissions from quiescent degassing of volcanoes worldwide, *Earth Planet. Sci. Lett., 186*, 33-43, 2001.

Nriagu, J. O., A global assesment of natural sources of atmospheric trace metals, *Nature, 338*, 47-49, 1989.

Petit, J. R., M. Briat, and A. Royer, Ice Age aerosol content from East Antarctic ice core samples and past wind strenght, *Nature, 293*, 391-394, 1981.

Petit, J. R., J. Jouzel, D. Raynaud, N. I. Barkov, J. M. Barnola, I. Basile-Doelsch, M. Bender, J. Chappellaz, M. Davis, G. Delaygue, M. Delmotte, V. M. Kotlyakov, M. Legrand, V. Y. Lipenkov, C. Lorius, L. Pépin, C. Ritz, E. Saltzman, and M. Stievenard, Climate and atmospheric history of the past 420,000 years from the Vostok ice core, Antarctica, *Nature, 399*, 429-436, 1999.

Planchon, F., C. F. Boutron, C. Barbante, G. Cozzi, V. Gaspari, E. W. Wolff, C. Ferrari, and P. Cescon, Changes in heavy metals in Antarctic snow from Coats Land since the mid-19th to the late-20th century, *Earth Planet. Sci. Lett., 200*, 207-222, 2002.

Planchon, F., C. F. Boutron, C. Barbante, E. W. Wolff, G. Cozzi, V. Gaspari, C. Ferrari, and P. Cescon, Ultrasensitive determination of heavy metals at the sub-picogram per gram level in

ultraclean Antarctic snow samples by inductively coupled plasma sector field mass spectrometry, *Anal. Chim. Acta, 450*, 193-205, 2001.

Pongratz, P., and K. G. Heumann, Production of methyled mercury, lead and cadmium by marine bacteria as significant source for atmsopheric heavy metals in polar regions, *Chemosphere, 39*, 89-102, 1999.

Rudnick, R. L., and D. M. Fountain, Nature and composition of continental crust: A lower crustal perspective, *Rev. Geophys., 33*, 267-309, 1995.

Schwander, J., J. Jouzel, C. U. Hammer, J. R. Petit, R. Udisti, and E. W. Wolff, A tentative chronology for the EPICA Dome Concordia ice core, *Geophys. Res. Lett., 28*(22), 4243-4246, 2001.

Siggaard-Andersen, M. L., P. Gabrielli, J. P. Steffensen, T. Stromfeldt, C. Barbante, C. F. Boutron, H. Fisher, and H. Miller, Soluble and insoluble chemistry of lithium in the EPICA Dome C ice core, in *EGU*, Nice, 2004.

Smith, J., D. Vance, A. Kemp, C. Archer, P. Toms, and M. King, Isotopic constraints on the source of Argentinian loess - with implications for atmsopheric circulation and the provenance of Antarctic dust during recent glacial maxima, *Earth Planet. Sci. Lett., 212*, 181-196, 2003.

Udisti, R., S. Becagli, S. Benassi, M. de Angelis, M. E. Hansson, J. Jouzel, J. Shwander, J. P. Steffensen, R. Traversi, and E. W. Wolff, Sensitivity of chemical species to climatic changes in the last 45 kyrs as revealed by high resolution Dome C (Antarctica) ice core analysis, *Ann. Glaciol. in press*, 2004.

Vallelonga, P., P. Gabrielli, K. Rosman, C. Barbante, and C. F. Boutron, A 220 kyr record of Pb isotopes from the EPICA Dome C Antarctic ice core, *Submitted to Geophys. Res. Lett.*, 2004.

Vallelonga, P., K. Van de Velde, J. P. Candelone, C. Ly, K. Rosman, C. F. Boutron, V. I. Morgan, and D. J. Mackey, Recent advances in measurment of Pb isotopes in polar ice and snow at sub-picogram per gram concentrations using thermal ionisation mass spectrometry, *Anal. Chim. Acta, 453*, 1-12, 2002.

Wedepohl, K. H., The composition of the continental crust, *Geochim. Cosmochim. Acta, 59*, 1217-1232, 1995.

Zreda-Gostynska, G., and P. R. Kyle, Volcanic emissions from Mount Erebus and their impact on the Antarctic environment, *J. Geophys. Res., 102*(B7), 15039-15055, 1997.

CHAPTER 4: LEAD ISOTOPES DETERMINATION IN EAST ANTARCTICA OVER THE LAST TWO CLIMATIC CYCLES

4.1 ARTICLE 6: A 220 ky record of Pb isotopes at Dome C Antarctica from analyses of the EPICA ice core

Paul Vallelonga, Paolo Gabrielli, Kevin Rosman, Carlo Barbante and Claude F. Boutron

Submitted to *Geophysical Research Letters*, September 2004

A 220 ky record of Pb isotopes at Dome C Antarctica from analyses of the EPICA ice core

P. Vallelonga[1], P. Gabrielli[2,3], K.J.R. Rosman[1], C. Barbante[3,4] and C.F. Boutron[2].

1. Department of Applied Physics, Curtin University of Technology, GPO Box U 1987, Perth 6845, Australia. Email: p.vallelonga@curtin.edu.au, Fax: +618 9266 2377.

2. Laboratoire de Glaciologie et Géophysique de l'Environnement du CNRS, 54 rue Molière, Domaine Universitaire, BP 96, 38402 St Martin d'Hères Cedex, France.

3. Department of Environmental Sciences, University of Venice, Ca' Foscari, Dorsoduro 2137, 30123 Venice, Italy.

4. Institute for the Dynamics of Environmental Processes - CNR, Dorsoduro 2137, 30123 Venice, Italy.

Keywords: Lead isotope, ice core, Antarctica, Dome C, EPICA, glacial cycle

Abstract

Pb isotopic compositions and Pb and Ba concentrations are reported in EPICA Dome C ice core samples extending back to 220 ky BP, providing conclusive evidence that Pb isotopic compositions in Antarctic ice vary with changing climate. $^{206}Pb/^{207}Pb$ ratios decrease during glacial periods, with the lowest values occurring during colder climatic periods (stages 2, 4 and 6) and the Holocene. Pb and Ba concentrations are low, <1 pg/g, during the Holocene and Eemian (climate stage 5.5) interglacials and higher, >10 pg/g, during cold climatic periods with crustal Pb sources usually accounting for ~70% of total Pb. Pb isotopic compositions at Dome C are similar to those reported in pre-industrial ice from other Antarctic locations, resulting from the mixing of crustal and volcanic Pb emissions in the Southern Hemisphere. This record, covering the past two glacial cycles, is the longest time series of Pb isotope data reported from an ice core.

1. Introduction

The deep ice cores from East Antarctica have provided an insight into climatic conditions and aerosol fluxes and provenance during the Holocene and previous glacial and interglacial periods [*EPICA community members*, 2004]. High Pb concentrations observed during cold climate stages 2, 4 and 6 in the Vostok [*Petit et al.*, 1999] and "old" (1978) Dome C [*Lorius et al.*, 1979] ice cores have been attributed to increased dust levels [*Boutron et al.*, 1988; *Hong et al.*, 2003] while analyses of Sr and Nd isotopes [*Delmonte et al.*, 2004] have shown that the southern South American regions of Patagonia and the Pampas are the most likely origins of this dust. *Rosman et al.* [1999], reporting Pb isotopic compositions in the earlier Dome C ice core, noted that Pb isotopic compositions were less radiogenic during the last glacial maximum (LGM) compared to the Holocene.

Recent analyses of Pb isotopes at coastal locations in Antarctica have determined pre-industrial Holocene Pb isotopic signatures [*Matsumoto and Hinkley*, 2001; *Planchon et al.*, 2003; *Vallelonga et al.*, 2002b] and revealed that different proportions of crustal and volcanic Pb are observed across the Antarctic ice sheet. Typical Holocene Pb isotopic compositions are similar across Antarctica, but the provenance of crustal Pb is still restricted by a dearth of Pb isotope data for emission sources such as the loess-covered areas of Patagonia, the Pampas, New Zealand and the Antarctic Dry Valleys.

We present the first Pb isotopic compositions from the EPICA Dome C ice core and the longest Pb isotopic record available from an ice core. These data (Table 1) allow variations in Pb deposition to be evaluated, as well as variations in crustal and volcanic Pb emissions over the past two glacial cycles.

2. Methods

2.1 Samples

Thirty samples were obtained from 26 sections of the EPICA ice cores drilled at Dome C (75°06'S, 123°21'E; 3233 m; mean annual temperature –54°C, figure 1) between 1996 and 2003. From the surface to 763 m depth, samples were from the EDC96 core drilled between 1996 and 1999, while samples below 763 m depth were from another EPICA Dome C core drilled between 2000 and 2003. The sections obtained were in the depth range 229 m to 2193 m, which corresponds to the time period 6.9 to 217 ky BP using the EDC2 timescale [*EPICA community members*, 2004]. In the EPICA program, a given core section (typical length 55 cm and radius 5 cm) was cut longitudinally into several parts which were then used for various analyses. For Pb isotope analyses a radial part corresponding to about 30% of the core cross-section was available for decontamination, from which two samples were usually produced.

2.2 Sample preparation and mass spectrometry

Samples were prepared (decontaminated) from ice core sections at the Laboratory of Glaciology and Geophysics of the Environment (LGGE) in Grenoble, France, in a clean bench supplied with High Efficiency Particulate Air (HEPA) filtered air and located within a cold room (temperature –15°C). The decontamination procedure [*Candelone et al.*, 1994; *Gabrielli et al.*, 2004] involved the chiselling of concentric layers of an ice core to remove any external contamination that may have been introduced during drilling, transport and/or storage. Decontaminated samples were melted at room temperature in a class 100 laboratory and aliquotted into LDPE bottles that were then frozen. These frozen samples were sent to Curtin University in Perth, Australia, for Pb and Ba analysis.

Samples were prepared for analysis of Pb and Ba by Thermal Ionisation Mass Spectrometry (TIMS) according to the procedures described by *Vallelonga et al.* [2002a]. Samples were melted and approximately 5 g was transferred to a Teflon beaker. HNO_3, HF, H_3PO_4 and an enriched tracer solution were added to the sample before the solution was evaporated to dryness. The evaporated sample was transferred in 4 µl of silica gel to a zone-refined rhenium filament and again evaporated to dryness by passing a current through the filament. Samples were then loaded into the mass spectrometer.

All samples were measured using an isotope ratio thermal ionisation mass spectrometer (model VG354, Fisons Instruments), according to the procedures described by *Chisholm et al.* [1995]. All Pb isotopes (^{204}Pb, ^{205}Pb, ^{206}Pb, ^{207}Pb and ^{208}Pb) were measured using the Daly detector, with 50 to 80 isotope ratios collected per sample. The enriched tracer solution enabled the determination of Pb and Ba concentrations (by isotope dilution) and Pb isotopic compositions in one analysis. The accuracy of the concentrations is estimated to be ±15% (95% confidence interval), due to the accuracy of dispensing the spike into the sample. The accuracy of the isotope ratio measurements was monitored by routine analysis of a 200 pg sample of Standard Reference Material 981 (NIST, Gaithersburg, USA). A correction for isotopic fractionation correction of 0.24±0.06 % per mass unit was applied to the measured ratios.

3. Preliminary Results

3.1 Pb and Ba concentrations

Pb and Ba concentrations have varied greatly over the past 220 ky with the highest concentrations constrained to particular cold climatic periods (Figure 2), in agreement with the findings of *Hong et al.* [2003] and *Boutron et al.* [1988]. Low Pb and Ba concentrations were observed during the Holocene and the Eemian (climate stage 5.5) interglacials, while higher Pb and Ba concentrations occurred during climate stages 2 (LGM), 4 (~65 ky BP) and 6 (the penultimate glacial maximum). During the Holocene, average Dome C Pb and Ba concentrations are ~0.4 pg Pb/g and ~11 pg Ba/g, similar to Pb concentrations reported for Coats Land [*Planchon et al.*, 2003] and Law Dome [*Vallelonga et al.*, 2002b] but lower than those reported for Taylor Dome [*Matsumoto and Hinkley*, 2001].

Average Pb/Ba ratios were ~0.05, similar to reported values for the upper continental crust (~0.03, [*McLennan*, 2001]). Using Ba concentrations to estimate crustal Pb inputs [*Patterson and Settle*, 1987; *Vallelonga et al.*, 2002b], a Pb/Ba ratio of 0.05 indicates a crustal Pb input of ~70%. While crustal Pb inputs averaged 70%, inputs of non-crustal Pb occasionally contributed up to 65% of total Pb in samples. More-radiogenic Pb isotopic compositions were observed in samples with high Pb/Ba ratios, suggesting that these samples contain greater proportions of volcanic Pb. An LGM sample (471.4 m) with exceptionally high Pb/Ba and $^{206}Pb/^{207}Pb$ values displayed the lowest proportion of crustal Pb (~20%), indicating that a substantial input of volcanic Pb occurred at that time.

3.2 Pb isotopes

Pb isotope ratios have varied with the climate changes of the past 220 ky (Figure 2). The data indicate that $^{206}Pb/^{207}Pb$ ratios decreased during the penultimate glacial period, from ~1.21 to ~1.19, and also during the last glacial period, changing steadily from ~1.23 to ~1.20 by the end of the LGM. Higher $^{206}Pb/^{207}Pb$ ratios are seen during the glacial-interglacial transition stages 2 and 6, while lower $^{206}Pb/^{207}Pb$ ratios can be seen clearly during the cold climate stage 4 (~63 ky BP).

Increases in $^{206}Pb/^{207}Pb$ ratios occur at glacial-interglacial transitions, most clearly seen in climate stage 2, indicating an increasing proportion of volcanic Pb in Antarctic aerosols. Just prior to and during the Antarctic Cold Reversal (ACR), $^{206}Pb/^{207}Pb$ ratios were substantially higher (1.22-1.23) than those during the LGM and Holocene (~1.19). High $^{206}Pb/^{207}Pb$ ratios were also observed ~18 ky BP, near the end of stage 2, and ~13 ky BP, the coldest part of the ACR. Similarly, the $^{206}Pb/^{207}Pb$ ratio at the end of climate stage 6, at the onset of the Eemian interglacial (~132 ky BP), is greater than those preceding and following it. These variations appear to be climate related but the relationship between the $^{206}Pb/^{207}Pb$ ratio and temperature (δD) is not a simple linear one.

Isotopic ratios of Pb at Dome C ice are within the range $^{206}Pb/^{207}Pb$ = 1.19-1.26 and $^{208}Pb/^{207}Pb$ = 2.46 – 2.51 (Figure 3). Most of the EPICA Dome C samples display less-radiogenic (lower $^{206}Pb/^{207}Pb$ and $^{208}Pb/^{207}Pb$ ratios) Pb isotopic compositions that those observed at Taylor Dome and Law Dome. At the latter locations, where the proportion of crustal Pb in ice is consistently less than 30%, more radiogenic Pb isotopic compositions are observed, similar to those reported for volcanic Pb emission sources such as Antarctic Peninsula basalts [*Hole et al.*, 1993], Ross Island basanitoids [*Sun and Hanson*, 1975] and Marie Byrd Land volcanics [*Hart et al.*, 1997]. The less-radiogenic EPICA Dome C samples display Pb isotopic compositions that are more like those representing crustal Pb emission sources such as South Atlantic Ocean pelagic sediments [*Chow and Patterson*, 1962] and South Sandwich Islands sediments [*Sun*, 1980].

Pb isotopic compositions corresponding to the colder climate stages 2, 4 and 6 are similar, supporting the findings of *Delmonte et al.* [2004] that dust deposited during these three cold periods originated from the same source(s), probably from South America and/or the Argentinean continental shelf which was then exposed to air. Pb isotopic compositions are not yet available for Patagonian or Pampas loess, so we have used sediments from the South Atlantic Ocean and South Sandwich Islands to represent this dust source. Pb isotopic compositions of pre-industrial Holocene ice from Dome C [this study, *Rosman et al.*, 1994; *Rosman et al.*, 1999], Law Dome [*Vallelonga et al.*, 2002b] and Coats Land [*Planchon et al.*, 2003] are generally similar, suggesting that Pb deposited in Antarctica during the Holocene also originates from similar source(s).

4. Discussion

These preliminary results support and extend existing data showing that Pb isotopic compositions [*Rosman et al.*, 1999] and concentrations [*Boutron et al.*, 1988; *Hong et al.*, 2003] in Antarctic ice vary with changing climate. High Pb concentrations were observed during colder climatic periods due to increased dust inputs. Over the past 220 ky, $^{206}Pb/^{207}Pb$ ratios steadily decrease during the glacial periods, with brief increases during glacial-interglacial transitions.

Interglacial (Holocene and Eemian) Pb concentrations were found to be constantly low at Dome C; in contrast to the findings of *Matsumoto and Hinkley* [2001] who reported higher and more variable Pb concentrations at Taylor Dome during the Holocene. At Dome C the Pb concentrations were ~0.4 pg/g during the Holocene (7 – 15 ky BP) and ~0.5 pg/g

during the Eemian (114 – 123 ky BP), while *Matsumoto and Hinkley* [2001] reported Pb concentrations ~5 pg/g between 2.2 and 10 ky BP and ~10 pg/g between 10.4 and 27.2 ky BP. They concluded that variations in dust and salt concentrations at Taylor Dome reflect changing atmospheric conditions since the LGM, and that global volcanic emissions of Pb are sufficient to account for the majority of Pb deposited in Antarctica. The Dome C results differ from those of Taylor Dome in two respects: firstly, stable and particularly low Pb and Ba concentrations are observed during the Holocene; secondly, interglacial Pb/Ba ratios (average ~0.04) indicate that ~80% of Pb deposited at Dome C during the interglacials originated from crustal Pb sources. These differences might be accounted for by the addition of continental dust to a background of Antarctic aerosols containing a relatively high proportion of radiogenic Pb of volcanic origin, with the proportion of volcanic Pb at Taylor Dome being greater than at Dome C.

The deeper sections of the EPICA Dome C core must be analysed to confirm the cyclical patterns observed for the past 220 ky. Pb isotopic compositions in Antarctic ice vary with changes in climate, but in a complex manner: such variations can occur over glacial periods of ~100 ky, but also within short periods (<1 ky) such as during the Antarctic Cold Reversal. It is also important that Pb isotopic compositions are reported for loess deposits in New Zealand, Patagonia, the Pampas and the Antarctic Dry Valleys, to further constrain the potential sources of dust particles deposited in central East Antarctica. Finally, reliable records of Pb and Ba concentrations over the Holocene-LGM transition are required from other Antarctic locations to better explain the differences that exist between element and isotopic records at Taylor Dome and Dome C.

Acknowledgements

This research was supported in Australia by grants from the Australian Research Council (A39938047) and the Antarctic Science Advisory Committee (Nos. 1092, 2334) in the Glaciology Section of the Australian Antarctic Division; in France by the Institut Universitaire de France, the Ministère de l'Environnement et de l'Amènagemont du Territoire, the Agence de l'Environnement et de la Maîtrise de l'Energie, the Intitut National des Sciences de l'Univers and the Universite Joseph Fourier of Grenoble; and in Italy by ENEA as part of the Antarctic National Research Program (under projects on Environmental Contamination and Glaciology). This work is a contribution to the "European Project for Ice Coring in Antarctica" (EPICA), a joint ESF (European Science Foundation)/EC scientific programme, funded by the European Commission and by national contributions from Belgium, Denmark, France, Germany, Italy, the Netherlands, Norway, Sweden, Switzerland and the United Kingdom. This is EPICA publication no. XX. We also thank all the personnel working in the field in Antarctica, Frédéric Planchon, G. Burton and L. Burn for laboratory support, and colleagues and students of the John de Laeter Centre of Mass Spectrometry – TIMS Laboratory for helpful discussion.

Reference list

Boutron, C.F., C.C. Patterson, C. Lorius, V.N. Petrov, and N.I. Barkov (1988), Atmospheric lead in Antarctic ice during the last climatic cycle, *Ann. Glaciol.*, *10*, 5-9.

Candelone, J.-P., S. Hong, and C.F. Boutron (1994), An improved method for decontaminating polar snow or ice cores for heavy metal analysis, *Anal. Chim. Acta*, *299*, 9 - 16.

Chisholm, W., K.J.R. Rosman, C.F. Boutron, J.-P. Candelone, and S. Hong (1995), Determination of lead isotopic ratios in Greenland and Antarctic snow and ice at picogram per gram concentrations, *Anal. Chim. Acta*, *311*, 141-151.

Chow, T.J., and C.C. Patterson (1962), The occurrence and significance of lead isotopes in pelagic sediments, *Geochim. Cosmochim. Acta*, *26*, 263-308.

Delmonte, B., I. Basile-Doelsch, J.-R. Petit, V. Maggi, M. Revel-Rolland, A. Michard, E. Jagoutz, and F.E. Grousset (2004), Comparing the Epica and Vostok dust records during the last 220,000 years: stratigraphical correlation and provenance in glacial periods, *Earth-Sci. Rev.*, *66*, 63-87.

EPICA community members (2004), Eight glacial cycles from an Antarctic ice core, *Nature*, *429*, 623-628.

Gabrielli, P., et al. (2004), Determination of Ir and Pt down to the sub-femtogram per gram level in polar ice by ICP-SFMS using preconcentration and a desolvation system, *J. Anal. At. Spectrom.*, *19*, 831-837, doi:10.1039/b316283d.

Hart, S.R., J. Blusztajn, W.E. LeMasurier, and D.C. Rex (1997), Hobbs Coast Cenozoic volcanism: Implications for the West Antarctic rift system, *Chem. Geol.*, *139*, 223-248.

Hole, M.J., P.D. Kempton, and I.L. Millar (1993), Trace-element and isotopic characteristics of small-degree melts of the asthenosphere: Evidence from the alkalic basalts of the Antarctic Peninsula, *Chem. Geol.*, *109*, 51-68.

Hong, S., Y. Kim, C.F. Boutron, C.P. Ferrari, J.R. Petit, C. Barbante, K.J.R. Rosman, and V.Y. Lipenkov (2003), Climate-related variations in lead concentrations and sources in Vostok Antarctic ice from 65,000 to 240,000 years BP, *Geophys. Res. Lett.*, *30*(22), 2138, doi:10.1029/2003GL018411.

Lorius, C., L. Merlivat, J. Jouzel, and M. Pourchet (1979), A 30,000-yr isotope climatic record from Antarctic ice, *Nature*, *280*, 644-648.

Matsumoto, A., and T.K. Hinkley (2001), Trace metal suites in Antarctic pre-industrial ice are consistent with emissions from quiescent degassing of volcanoes worldwide, *Earth Planet. Sci. Lett.*, *186*, 33-43.

McLennan, S.M. (2001), Relationships between the trace element composition of sedimentary rocks and upper continental crust, *Geochem. Geophys. Geosyst.*, *2*, doi:10.1029/2000GC000109.

Patterson, C.C., and D.M. Settle (1987), Review of data on eolian fluxes of industrial and natural lead to the lands and seas in remote regions on a global scale, *Mar. Chem.*, *22*, 137-162.

Petit, J.-R., et al. (1999), Climate and atmospheric history of the past 420,000 years from the Vostok ice core, Antarctica, *Nature*, *399*, 429-436.

Planchon, F.A.M., K. Van de Velde, K.J.R. Rosman, E.W. Wolff, C.P. Ferrari, and C.F. Boutron (2003), One hundred fifty-year record of lead isotopes in Antarctic snow from Coats Land, *Geochim. Cosmochim. Acta*, *67*, 693-708.

Rosman, K.J.R., W. Chisholm, C.F. Boutron, J.-P. Candelone, and C.C. Patterson (1994), Anthropogenic lead isotopes in Antarctica, *Geophys. Res. Lett.*, *21*(24), 2669-2672, doi:10.1029/94GL02603.

Rosman, K.J.R., W. Chisholm, C.F. Boutron, and J.-P. Candelone (1999), Lead isotopes as tracers of pollution in snow and ice, *Korean J. Polar Res.*, *10*, 53-58.

Sun, S.S., and G.H. Hanson (1975), Origin of Ross Island Basanitoids and Limitations upon the Heterogeneity of Mantle Sources for Alkali Basalts and Naphelinites, *Contrib. Mineral. Petrol.*, *52*, 77-106.

Sun, S.S. (1980), Lead isotopic study of young volcanic rocks from mid-ocean ridges, ocean islands and island arcs, *Philos. Trans. R. Soc. London, Ser. A*, *297*, 409-445.

Vallelonga, P., K. Van de Velde, J.-P. Candelone, C. Ly, K.J.R. Rosman, C.F. Boutron, V.I. Morgan, and D.J. Mackey (2002a), Recent advances in measurement of Pb isotopes in Polar ice and snow at sub-picogram per gram concentrations using Thermal Ionisation Mass Spectrometry, *Anal. Chim. Acta*, *453*, 1-12.

Vallelonga, P., K. Van de Velde, J.-P. Candelone, V.I. Morgan, C.F. Boutron, and K.J.R. Rosman (2002b), The lead pollution history of Law Dome, Antarctica, from isotopic measurements on ice cores: 1500 AD to 1989 AD, *Earth Planet. Sci. Lett.*, *204*, 291-306.

Table 1. Lead and Ba concentrations and Pb isotopic compositions in Antarctic Dome C ice.

Sample depth m	Sample age years BP	_deuterium ‰	$^{206}Pb/^{207}Pb$	±[a]	$^{208}Pb/^{207}Pb$	±[a]	$^{206}Pb/^{204}Pb$	±[a]	Pb conc.[b] pg/g	Ba conc.[b] pg/g	Pb/Ba by weight
229.1	6938	-398.96	1.190	0.016	2.471	0.020	19.2	1.2	0.19	7.4	0.026
229.4	6949	-398.96	1.195	0.022	2.467	0.032	19.0	1.7	0.22	6.3	0.035
316.3	10280	-389.14	1.194	0.024	2.460	0.026	19.0	1.7	0.19	6.7	0.028
379.2	12809	-409.31	1.220	0.009	2.486	0.011	19.7	0.8	0.70	13.2	0.053
405.9	14219	-414.96	1.217	0.009	2.481	0.011	19.3	0.5	0.82	16.5	0.050
432.6	15611	-410.93	1.193	0.013	2.483	0.012	18.7	1.4	0.52	16.1	0.032
461.5	17400	-433.73	1.226	0.002	2.488	0.009	19.0	0.4	6.06	107	0.057
471.4	18155	-438.79	1.257	0.004	2.507	0.008	19.8	0.6	29.49	176	0.168
489.0	19651	-442.46	1.190	0.011	2.493	0.065	18.3	0.8	14.98	460	0.033
515.6	21944	-441.83	1.199	0.014	2.465	0.019	18.5	0.3	14.33	467	0.031
574.2	27033	-444.24	1.207	0.008	2.465	0.014	17.7	0.4	16.14	362	0.045
598.1	29094	-437.46	1.203	0.017	2.468	0.057	18.4	1.5	8.63	219	0.039
654.0	33729	-438.4	1.205	0.003	2.477	0.013	18.7	0.3	8.16	185	0.044
709.0	38155	-427.01	1.226	0.007	2.470	0.019	17.6	1.6	2.65	36.7	0.072
818.1	47175	-434.26	1.206	0.004	2.467	0.008	18.6	0.3	5.43	127	0.043
983.4	60674	-437.01	1.214	0.006	2.484	0.004	18.3	0.6	9.84	225	0.044
1010.9	63453	-438.62	1.196	0.003	2.464	0.006	18.5	0.4	13.9	360	0.039
1093.1	71637	-422.76	1.227	0.013	2.504	0.024	18.1	2.2	1.44	19.4	0.074
1258.4	86028	-424.3	1.222	0.006	2.477	0.007	19.0	0.5	3.52	60.5	0.058
1423.4	102283	-419.54	1.225	0.003	2.477	0.010	18.9	0.5	3.17	42.8	0.074
1533.1	114119	-400.69	1.229	0.010	2.487	0.009	19.3	0.3	0.36	11.2	0.033
1643.1	122810	-386.62	1.216	0.014	2.497	0.023	18.9	1.0	0.73	15.9	0.046
1643.4	122832	-386.62	1.208	0.010	2.475	0.018	19.2	0.7	0.52	14.2	0.037
1753.4	131892	-411.61	1.237	0.006	2.488	0.010	18.6	1.2	2.61	30.4	0.086
1863.1	152184	-437.71	1.204	0.003	2.468	0.006	18.6	0.2	18.31	370	0.049
1863.4	152239	-437.71	1.193	0.003	2.459	0.009	18.6	1.0	18.90	447	0.042
1973.1	174430	-439.17	1.200	0.004	2.470	0.009	18.7	0.3	7.32	192	0.038
1973.4	174491	-439.17	1.192	0.005	2.462	0.009	18.6	0.2	9.73	150	0.065
2094.4	198944	-406.02	1.199	0.018	2.489	0.025	19.4	1.5	0.27	9.5	0.029
2193.4	217051	-420.45	1.214	0.009	2.476	0.006	19.4	1.0	1.98	32.3	0.061

[a] Uncertainties in the isotope ratios are 95% confidence intervals.
[b] Concentrations are accurate to ±15% (95% confidence interval).

Figure Captions

Figure 1. Map of Antarctica indicating the relative locations of Dome C and other sites for which Pb isotope data have been reported: Law Dome (LD; 66°46'S, 112°48'E), Taylor Dome (TD; 77°48'S, 158°43'E) and Coats Land (CL; 77°34'S, 25°22'W).

Figure 2. 220 ky record of _ deuterium and Pb concentration (A), Ba concentration (B) and $^{206}Pb/^{207}Pb$ (C) from the EPICA Dome C ice core. Marine isotope stage numbers [*Delmonte et al.*, 2004] are also shown in (A). _ deuterium data were reported by *EPICA community members* [2004].

Figure 3. Pb isotopic compositions in ice from Dome C and other Antarctic sites. Also included are Pb isotopic compositions of South Atlantic Ocean pelagic sediments [*Chow and Patterson*, 1962], South Sandwich Islands sediments [*Sun*, 1980], Antarctic Peninsula basalts [*Hole et al.*, 1993], Ross Island basanitoids [*Sun and Hanson*, 1975] and Marie Byrd Land volcanics [*Hart et al.*, 1997].

Figure 1

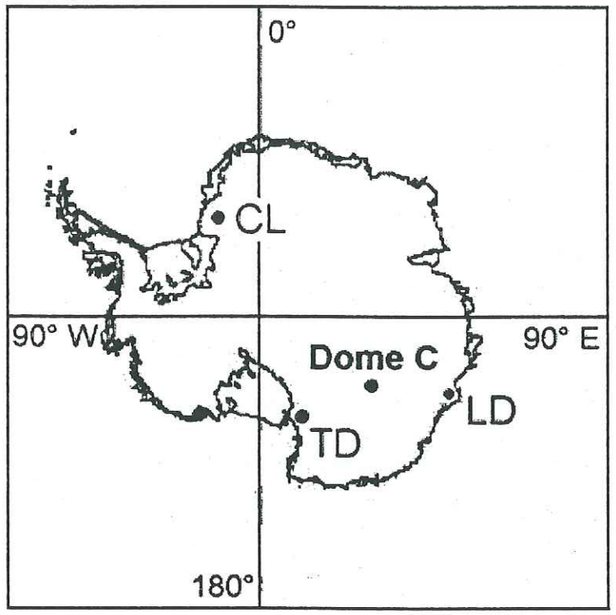

Figure 2

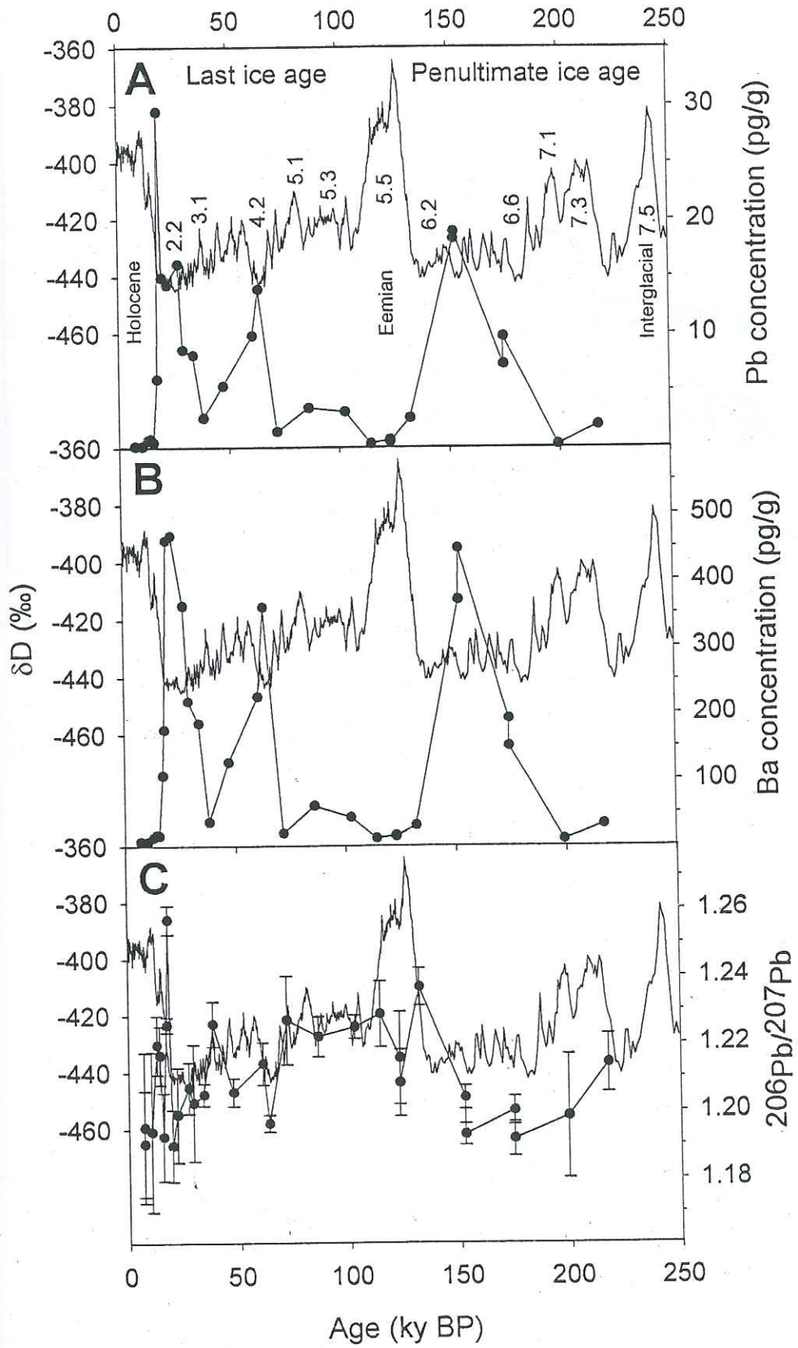

Figure 3

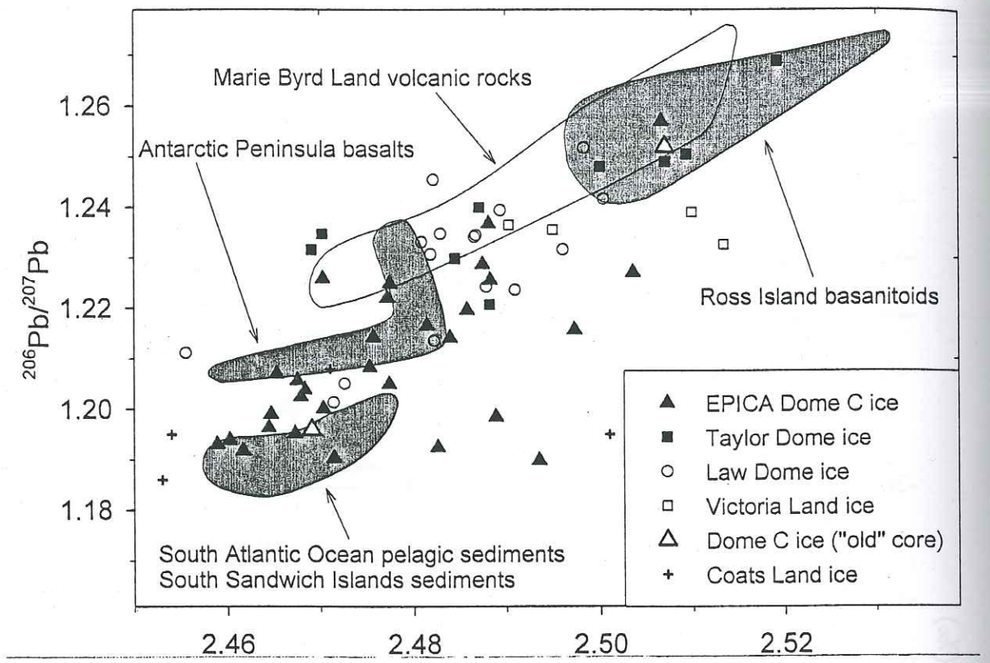
Marie Byrd Land volcanic rocks
Antarctic Peninsula basalts
Ross Island basanitoids
South Atlantic Ocean pelagic sediments
South Sandwich Islands sediments
EPICA Dome C ice
Taylor Dome ice
Law Dome ice
Victoria Land ice
Dome C ice ("old" core)
Coats Land ice
$^{206}Pb/^{207}Pb$
1.26
1.24
1.22
1.20
1.18
2.46
2.48
2.50
2.52

CHAPTER 5: DETERMINATION OF TOTAL MERCURY AND MERCURY SPECIES IN EAST ANTARCTICA OVER THE LAST TWO CLIMATIC CYCLES

5.1 ARTICLE 7: **Direct determination of mercury at the sub-picogram per gram levels in polar snow and ice by ICP-SFMS**

Frédéric Planchon, Paolo Gabrielli, Pierre Alexis Gauchard, Aurelien Dommergue, Carlo Barbante, Warren Cairns, Giulio Cozzi, Sonia Nagorski, Chiristophe Ferrari, Claude Boutron, Gabriele Capodaglio, Paolo Cescon, Anita Varga and Eric Wolff

Journal of Analytical Atomic Spectrometry, 19, 823-830, 2004

ARTICLE

JAAS
www.rsc.org/jaas

Direct determination of mercury at the sub-picogram per gram level in polar snow and ice by ICP-SFMS†

F. A. M. Planchon,[a] P. Gabrielli,[b,c] P. A. Gauchard,[b] A. Dommergue,[b] C. Barbante,*[a,c] W. R. L. Cairns,[a] G. Cozzi,[c] S. A. Nagorski,[b] C. P. Ferrari,[b,d] C. F. Boutron,[b,e] G. Capodaglio,[c] P. Cescon,[a,c] A. Varga[c] and E. W. Wolff[f]

[a]*Institute for the Dynamics of Environmental Processes-CNR, University of Venice, Ca'Foscari, Dorsoduro 2137, 30123 Venice, Italy. E-mail: barbante@unive.it; Fax: 39-041-2578549; Tel: +39-041-2348942*
[b]*Laboratoire de Glaciologie et Géophysique de l'Environnement du C.N.R.S., 54, rue Molière, Boîte Postale 96, 38402 Saint Martin d'Hères, France*
[c]*Department of Environmental Sciences, University of Venice, Ca'Foscari, Dorsoduro 2137, 30123 Venice, Italy*
[d]*Polytech Grenoble, Université Joseph Fourier de Grenoble (Institut Universitaire de France), 28 Avenue Benoît Frachon, B. P. 53, 38041 Grenoble, France*
[e]*Unité de Formation et de Recherche de Physique et Observatoire des Sciences de l'Univers, Université Joseph Fourier de Grenoble (Institut Universitaire de France), Boîte Postale 68, 38041 Grenoble, France*
[f]*British Antarctic Survey, High Cross, Madingley Road, Cambridge, United Kingdom CB3 0ET*

Received 23rd February 2004, Accepted 20th May 2004
First published as an Advance Article on the web 22nd June 2004

An analytical method for the direct determination of mercury (Hg) in polar snow and ice cores and surface snow based on inductively coupled plasma sector field mass spectrometry (ICP-SFMS) has been developed. Various Hg isotopes, such as ^{199}Hg, ^{200}Hg, ^{201}Hg and ^{202}Hg, appear to be free of polyatomic interferences in such matrices and allow the measurements to be made in low resolution mode, leading to high sensitivity. Ultra-low concentration Hg standards (from 1.5 to 20 pg g^{-1}) were used for the calibration of the Thermo Finnigan MAT Element2, and a detection limit as low as 0.18 pg g^{-1} was achieved using ^{202}Hg. Ultra-clean procedures used from field sampling to final laboratory analysis show no significant blank contributions and appear suitable for the reliable determination of Hg at ultra-low concentrations. Precision of the Hg measurements was estimated to be 15% in terms of relative standard deviation on five replicates and accuracy was checked with an analytical reference material (102% recovery). Hg concentrations in surface snow samples from the Northern Hemisphere collected in the Canadian Arctic and in Svalbard (Norway) show high variability (1.2–32.0 pg g^{-1}). In Antarctica, Hg was determined in different ice core sections from Dome C, spanning the last 18 000 years BP (range from 0.7 to 3.2 pg g^{-1}), and in snow samples from Coats Land covering the last 150 years (range from 0.2 to 16.1 pg g^{-1}).

Introduction

Due to its pronounced toxicity and possible adverse effects on ecosystems and human health, mercury (Hg) is widely considered to be among the highest priority environmental pollutants of continuing global concern.[1–3] Unlike other trace metals that are associated with aerosols, Hg occurs in the atmosphere predominantly as a long-lived gaseous specie that can be subjected to long-range transport and to inter-hemispheric mixing.[4–6] A subject of continuous debate is how anthropogenic sources contribute to the global atmospheric Hg burden and are responsible of a large atmospheric pollution.

Environmental atmospheric archives and especially the Hg record within well-preserved snow and ice layers from the Antarctic and Greenland ice caps may provide answers to such questions as well as some important information on the polar chemistry of Hg. However, few reliable data presently exist on the occurrence of Hg in snow and ice from the polar regions over the last few centuries, mainly because most studies on the topic were substantially plagued by contamination problems during field sampling and/or laboratory analysis. For Greenland, only one reliable time series covering a forty year record from 1949 to 1989 is available.[7] For Antarctica, the only existing data consist of a comparison between surface snow samples dated from 1982 to 1984 with ice dated from the Holocene and the Last Glacial Maximum (LGM),[8,9] and snow pit samples up to 4.6 m in depth collected in the late 1980s.[10,11] Though these results cannot be used to assess a temporal evolution of Hg deposition since the beginning of the industrial era, they have clearly demonstrated that stringent ultra-clean procedures, such as the one developed for lead determination by Boutron and Patterson,[12] in 1986, need to be applied for the reliable determination of Hg at the picogram per gram level in polar snow and ice. Ultra-clean procedures aim to avoid and control all the contamination sources along the entire analytical protocol, from field sampling to laboratory analysis.[13–15] Also necessary is the use of ultra-sensitive analytical techniques to detect such low concentration levels.

The determination of Hg at ultra-low levels in ice and snow from polar and high altitude regions is commonly carried out using cold vapour generation coupled with ultra-sensitive detectors such as atomic fluorescence spectrometry (CV-AFS),[16,17] atomic absorption spectrometry (CV-AAS)[15] and,

† Presented at the 4th International Conference on High Resolution Sector Field ICP-MS, Venice, Italy, October 15–17, 2003.

DOI: 10.1039/b402711f

more recently, with inductively coupled plasma mass spectrometry (CV-ICP-MS).[18] Using these methods, elemental Hg vapour is detected following the reduction of the various Hg species. These techniques allow the mercury vapour to be easily separated from the sample matrix because of its low vapour pressure, and detection limits at the sub-picogram per gram level can be achieved using preconcentration systems such as double two-stage gold amalgamation.[16,17,19]

However, cold vapour generation has some general disadvantages. Sample preparation is time-consuming as it includes dissociation of stable Hg associations using bromine chloride (BrCl), neutralisation of free halogens with hydroxylamine (NH_2OH) and reduction with stannous chloride ($SnCl_2$), and large sample volumes are required for a single analysis. Moreover, for ultra-low concentration levels, complex blank determinations are required in order to get reliable data. Finally, the sample preparation does not allow a multi-elemental determination of other trace metals.

Over the past few years, new analytical methods, especially those based on ICP-MS, have been developed for the determination of mercury. It has been shown that direct analysis of Hg is possible in several environmental matrices, such as drinking water, solid samples and biological fluids, and by choosing interference free isotopes such as ^{202}Hg, detection limits in the range of sub-ng g^{-1} levels could be achieved with a quadrupole mass spectrometer.[20,21] Developments using ICP-MS instruments have also been made in terms of Hg speciation analysis. By coupling multi-capillary gas chromatography with ICP-time-of-flight mass spectrometry (MCGC-ICP-TOFMS),[22] ultra-trace determination of Hg^{2+} and methylated mercury compounds at the sub-pg g^{-1} and at the fg g^{-1} levels, respectively, has been made possible in several environmental matrices, especially in ice and snow from polar regions.[23] However, this technique requires complex sample preparation based on the derivatization of mercury species with tetraethyl borate, and has similar drawbacks as those for cold vapour techniques.[22]

Inductively coupled plasma sector field mass spectrometers (ICP-SFMS) have proved to be among the most sensitive detectors commercially available, allowing detection limits down to pg g^{-1} and even to fg g^{-1} concentration levels for numerous trace metals. For ice and snow samples, ICP-SFMS has been successfully applied to the multi-elemental determination of numerous trace elements[14,24] but not yet to the direct determination of total concentrations of Hg.

Analysis of snow and ice from the polar regions is one of the most straightforward applications of ICP-SFMS, mainly because the matrix is one of the purest present on the Earth. Because dust, organic matter and ions occur at very low levels, matrix interferences are minimal, and Hg in snow and ice samples can be analysed directly in the same way as other trace elements without any complex pre-treatment. Moreover, Hg isotopes occur in the high mass range from 196 to 204 without any major interferences. This allows the measurements to be done using low mass resolution settings, with the highest ion transmission to the detector.

In this study, we present recent analytical developments in the direct determination of Hg in polar snow and ice at ultra-low concentration levels down to sub-pg g^{-1}. We describe the ultra-clean procedures required, instrumental parameters and optimisation of the instrument, calibration, and quality control for the analysis. Finally, we present some results obtained in different snow and ice samples from Antarctica, Svalbard (Norway) and the Canadian Arctic.

Experimental

Samples description

For the Northern Hemisphere, Hg was determined in snow samples from two sampling sites. The first one is located in Ny-Alesund (Svalbard, Norway). Twenty-eight samples were available for this study, including 25 surface snow samples collected daily from mid-April 2003 to mid-May 2003 and 3 snow pit samples collected from the surface to 45 cm depth. The second sampling site is located in Kuujjuarapik (Canada), from where 6 snow pit samples collected in April 2002 from the surface to 60 cm depth were analysed. Descriptions of the sampling procedures can be found elsewhere.[24,25]

For the Southern Hemisphere, the samples come from two sampling sites. The first one is located in Coats Land (Antarctica). The samples were collected as snow blocks (~40 × 30 × 33 cm) from the wall of a clean, hand dug pit from the surface to 8.3 m depth and as snow core sections drilled from the base of the pit (8.3 m depth) to 16.3 m depth. A detailed description of the clean field sampling operations can be found elsewhere.[14] In this study, we determined Hg concentrations in 160 samples from Coats Land covering the years 1834–1991. The second sampling site is situated in central East Antarctica at the French–Italian base of Dome C. Seven ice core sections retrieved by deep drilling operations in the framework of the international program EPICA from 152 m to 594 m depth covering the period from 3500 to 18 000 years BP were analysed.

Ultra-clean procedures

Because many previous studies have been plagued by major contamination problems, rigorous ultra-clean protocols have to be applied for state of the art ultra-low determinations of Hg and other trace metals in polar snow and ice. From field sampling to laboratory analysis, any sources of contamination must be avoided and controlled to reduce the blank contribution as much as possible.

For such investigations, clean room working conditions are required. Preparation of sampling equipment, production of ultra-pure water, cleaning of labware, aliquoting and acidification of samples were done in a class 10000 clean room equipped with class 100 laminar flow clean benches in the Laboratory of Glaciology and Geophysics of the Environment (LGGE) in Grenoble (France). Detailed descriptions of the clean laboratory facility in LGGE can be found elsewhere.[13–15]

The meticulous cleaning procedure is especially important for materials that come into direct contact with snow and ice samples, and the precautions necessary for Hg are the same as those required for other trace elements. Field sampling equipment, decontamination material and low density polyethylene (LDPE) storage bottles followed a strict acid cleaning procedure. It consisted of a five-step protocol over three weeks, in which after an initial degreasing with chloroform, the materials were soaked successively in three hot acid baths (t = 40 °C) of decreasing acidity (from 10% to 0.1% HNO_3) and of increasing purity in terms of trace metals from commercially available Merck Suprapur nitric acid to double distilled ultra-pure nitric acid. The ultra-pure double distilled nitric acid was obtained from the Department of Applied Physics of Curtin University of Technology in Perth, Australia (Professor K. Rosman). Between each acid bath, all materials were extensively rinsed with ultra pure water (Maxy, Inc., La Garde, Var, France). Finally, the different bottles were filled with a storage solution of 0.1% double distilled HNO_3 until their use.

Also of major importance is obtaining clean snow and ice samples. Procedures vary depending on the types of samples. For surface snow and shallow pits, it is possible to directly collect clean samples. Field collection is conducted by operators wearing full clean room clothes and polyethylene gloves with acid cleaned equipment.

For deeper samples, such as snow blocks and snow and ice cores that are retrieved from polar ice caps and high altitude glaciers, clean procedures become difficult to comply with for technical reasons. Pit sampling, drilling operations, handling and storage can greatly contaminate the outer part of the samples, as has been shown for Pb,[12] V, Cu and Ba[14] for example. To obtain reliable data, it is necessary to conduct a decontamination procedure which consists of the mechanical removal of the external contaminated layers before sub-sampling the most internal part of the snow block and snow and ice core sections. A detailed description of the procedures carried out in a cold room (t = −15 °C), under a laminar flow clean bench for snow blocks and snow and ice core sections, can be found elsewhere.[14,26]

Once the field collection and/or mechanical decontamination were completed, samples were brought back to the laboratory in double acid clean LDPE bags and kept frozen. The aliquotation was done after melting at room temperature, inside a class 100 laminar flow clean bench. For the analysis of mercury by ICP-SFMS, aliquots were transferred into 15 ml LDPE ultra-clean bottles, acidified to 1% with ultra-pure double distilled nitric acid and kept frozen until the analysis.

Instrumentation

A Thermo Finnigan MAT Element2 (Thermo Finnigan MAT Instrument, Bremen, Germany) ICP-SFMS was used for the analytical determination at the Department of Environmental Science (DES) of the University Ca'Foscari of Venice. The instrument has the capability to work in three different resolution settings. However, in the analysis of Hg, only low resolution mode (LRM) with $m/\Delta m$ (10% valley definition) of ~300, was used.

The sample introduction area of the instrument is located inside a class 100 laminar flow clean bench in order to prevent any contamination during the analysis. The sample is transferred from a 15 ml ultra clean LDPE bottle with a polyfluoroethylene (PFE) Teflon capillary tube connected to a 100 µl min^{-1} polyfluoroacetate (PFA) microflow nebuliser (Elemental Scientific, Inc., Omaha, NE, USA). The sample is nebulised in self-aspirating mode into an acid cleaned double-pass PFA spray chamber maintained at room temperature before entering the plasma torch.

Of utmost importance for the reliable determination of Hg at the sub-pg g^{-1} levels is the cleanliness of the sample introduction system. This is accomplished using a 5% ultra pure nitric acid solution prepared with ultra-pure ELGA water (Purelab Ultra, Elga, High Wycombe, UK) produced at the DES. To ensure the good cleanliness of the introduction system, ^{202}Hg is monitored in continuous acquisition mode and the cleaning solution is nebulised until the background Hg levels are stabilised at minimal values around 800 counts per second (cps).

The instrumental conditions and measurement parameters, used in this study, are reported in Table 1. Mass calibration was carried out weekly with a 1.0 ng g^{-1} multi-element solution (Li, B, Na, Sc, Fe, Co, Ga, Y, In, Rh, Ba, Lu, Tl, U) in the three resolution modes. For LRM, no mass drift was observed during the measurement session.

Optimisation of the sensitivity was carried out daily using a 1.0 ng g^{-1} solution of indium (In) prepared from a 1000 µg ml^{-1} mono-elemental solution (certified standard from CPI International, USA) with ultra-pure ELGA water and acidified at 0.5% with ultra-pure nitric acid. We adjusted the tuning parameters such as the torch position and the gas flow rates, essentially the sample gas and the additional gas, to obtain maximum signal response and short/long term signal stability. By working with a nebuliser in self-aspirating mode, the additional gas improves aerosol transport to the plasma torch and greatly improves the sensitivity. Typically, the average intensity range obtained for a 1 ng g^{-1} In solution was from 0.9×10^6 up to 1.2×10^6 cps. During the measurements, sensitivity variations were checked after 10 samples (each hour) and were shown to be less than ± 10%.

Table 1 Instrumental conditions and measurement parameters for the Thermo Finnigan Element II used for the determination of Hg

Forward power	1160 W
Gas flow rates	
Cool	11.1 l min^{-1}
Auxiliary	0.9–1.0 l min^{-1}
Sample	Optimised to obtain maximum signal intensity
Additional	Optimised to obtain maximum signal intensity
Sample uptake rate	100 µl min^{-1}
Washing time	3 min
Take up time	30 s
Internal standards	$^{40}Ar^{40}Ar$ signal was continuously monitored
Ion sampling depth	Optimised to obtain maximum signal intensity
Ion lens settings	Optimised to obtain maximum signal intensity
Acquisition mode	E-scan; electric scanning over small mass range
Resolution achieved	Low ($m/\Delta m \approx 300$)
Doubly charged ion formation	$Ba^{2+}/Ba^{+} = 0.03$
Selected isotopes	LRM: ^{182}W, ^{199}Hg, ^{200}Hg, ^{201}Hg, ^{202}Hg
Settling time	300 ms
Dwell time per acquisition point	10 ms
Total acquisition time	0.5 s per mass segment and scan
No. of acquisition points per mass segment (sample per peak)	50
Run and passes	LRM: 8–8
Acquisition window (%)	80–100
Search window (%)	LRM: 100
Integration window (%)	LRM: 40

Results and discussion

Selection of isotopes

Hg has seven stable isotopes with nominal masses ranging from 196 to 204; we have chosen the four most abundant isotopes (^{199}Hg, ^{200}Hg, ^{201}Hg and ^{202}Hg). The different isotopic abundances are reported in Table 2. For such high masses, no major spectral interferences exist so it is theoretically possible to acquire Hg isotopes in LRM. However, matrix interferences need to be carefully checked to ensure the accurate determination of mercury. Polar snow and ice are perhaps one of the purest matrices that can be found on Earth. More than 99.99% of their composition is water, and the major

Table 2 Abundances of Hg isotopes analysed in this study and potential polyatomic interferences that could affect the determination of Hg

Analyte		Potential interference		Required resolution
Isotope	Abundance (%)	Species	Abundance[a] (%)	$m/\Delta m$
^{199}Hg	16.87	$^{183}W^{16}O$	14.25	8609
		$^{181}Ta^{18}O$	0.20	9431
		$^{182}W^{17}O$	0.01	9513
^{200}Hg	23.10	$^{184}W^{16}O$	30.57	8907
		$^{182}W^{18}O$	0.05	9559
		$^{184}Os^{16}O$	0.02	9573
		$^{183}W^{17}O$	0.01	10 557
^{201}Hg	13.18	$^{185}Re^{16}O$	36.98	8970
		$^{184}W^{17}O$	0.03	9620
		$^{183}W^{18}O$	0.01	9944
^{202}Hg	29.86	$^{186}Os^{16}O$	1.64	9236
		$^{186}W^{16}O$	28.57	9463
		$^{184}W^{18}O$	0.06	9842
		$^{185}Re^{17}O$	0.01	10 902

[a] For polyatomic species calculated as the product of the natural abundance of each isotope divided by 100.

species that occur at the ng g^{-1} levels are derived mainly from sea salt aerosols, oceanic biogenic activity and wind blown dust particles. Polyatomic interferences by compounds such as Ta, Re and W oxides (Table 2) that could affect measurements of Hg are unlikely to occur. Considering the crust as the major source for these metals (Me), theoretical estimations of expected concentrations (based on Me/Al mass ratios found in the mean continental crust[27]) to be found in snow and ice indicate extremely low abundances. Moreover, oxide formation is proved to be very low (less than 0.1% with the introduction system used), and hence these interferences can safely be discounted. To fully verify these findings, we have analysed one tungsten isotope (^{182}W) at the same time as the Hg isotopes and it appears that average intensities of W are at least one order of magnitude lower than Hg. Therefore W interferences can be neglected.

Calibration of the instrument, detection limits, precision and accuracy

Considering the relatively simple matrix of the samples, the possible contamination introduced from using internal standard additions and the rather low sample volume available (<5 ml), an external calibration method of the ICP-SFMS was applied for Hg quantification. Ultra-low concentration Hg standards were prepared from serial dilutions of a mono-elemental Hg solution at 1000 μg ml^{-1} (CPI International, Santa Rosa, CA, USA) under ultra-clean conditions. The standards, with a final concentration range from 1.5 to 20 pg g^{-1}, were acidified at 1% with ultra-pure double distilled nitric acid. Linear calibration curves were obtained for ^{202}Hg ($y = 111x + 780$; $r^2 = 0.998$), ^{201}Hg ($y = 48x + 341$; $r^2 = 0.999$), ^{200}Hg ($y = 87x + 603$; $r^2 = 0.999$) and ^{199}Hg ($y = 60x + 457$; $r^2 = 0.998$) (where y is expressed in cps and x in pg g^{-1}). During the calibration of the instrument and between each standard, measurement of the background level was performed with ultra-pure water acidified at 1% (ultra-pure double distilled nitric acid) to check the memory effect of the introduction system. It was found that a three minute washing time was necessary after running a 20 pg g^{-1} Hg standard to retrieve the original background.

Fig. 1 presents an example of the temporal evolution of a 20 pg g^{-1} Hg standard prepared in ultra-clean LDPE bottles. It can be seen that ultra-low Hg standards are unstable and that half of the concentration can be lost within 6 hours. This situation has been observed in different ultra-low standards within a few hours after their preparation. The features observed in Fig. 1 reflect strong Hg adsorption onto the walls of the ultra clean LDPE bottles. To prevent this Hg loss, which can significantly alter the sample quantification, ultra-low Hg standards as well as the Hg mother solutions at 1 ng g^{-1} and 100 ng g^{-1} were freshly prepared each day. The final dilutions from the 1 ng g^{-1} Hg solution were performed inside the clean sample introduction area of the instrument just before the analysis. The stability of Hg concentrations in the samples is discussed separately in a following section.

Detection limits of Hg were calculated using each isotope as three times the standard deviation of the blank,[28] and are 0.18 pg g^{-1}, 0.51 pg g^{-1}, 0.22 pg g^{-1} and 0.33 pg g^{-1} when using ^{202}Hg, ^{201}Hg, ^{200}Hg and ^{199}Hg, respectively.

The precision of the measurements was estimated from the results obtained from five replicates of several snow and ice samples. Although the instrumental relative standard deviation (RSD) is low (range from 1 to 5%), the uncertainty associated with the samples depended on the measured concentration levels. For samples with a concentration above 1.5 pg g^{-1}, the RSD was around 15%, but for lower concentrations, close to the detection limit, the RSD increased to values around 50%.

As an accuracy check, we analysed an analytical reference material with a Hg content of 170.4 ± 38.4 pg g^{-1} (National Water Research Institute, Environment Canada) stabilised with 0.05% potassium dichromate and acidified at 1% with sulfuric acid. The analyses of NWRI reference material performed by ICP-SFMS show excellent recoveries with a measured concentration of 174 ± 12 pg g^{-1} for 3 replicates.

Procedural blanks and cleanliness of the samples

To obtain reliable data on Hg in ice and snow samples, it is of primary importance to evaluate the procedural blanks associated with the sample preparation procedure. This evaluation is done in a variety of ways depending on the types of samples being considered.

For surface snow samples, the overall blank contribution was evaluated using an artificial sample. For this purpose, an acid cleaned LDPE bottle was filled with ultra-pure water and then followed the same procedural steps (handling, transport, storage, melting and acidification) as a true sample. The comparison between the artificial sample and the reference water gives the total blank contribution. Analysis of the reference ultra-pure water (produced in LGGE) used to make the artificial sample showed an Hg concentration of 1.3 ± 0.5 pg g^{-1} and no significant difference is observed when compared to the artificial sample (1.4 ± 0.4 pg g^{-1}). This indicates that procedural blanks for the surface snow samples can be neglected and hence no blank subtraction was applied.

For other samples that needed to be decontaminated using the chiselling technique, we used an artificial ice core to evaluate the procedural blanks. The artificial ice core was produced by freezing ultra-pure water in an ultra-clean Teflon tube which was then processed using exactly the same procedure as for other ice or snow cores.[26] Fig. 2 shows Hg concentrations measured in an artificial ice core produced with ultra-pure water produced and decontaminated at the LGGE (Grenoble, France). It can be seen that the concentrations

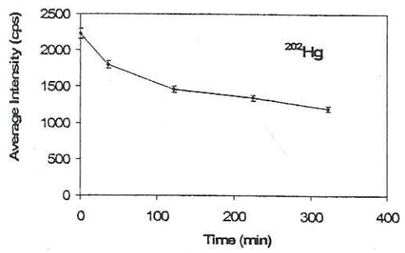

Fig. 1 Temporal evolution of the measured average intensity (cps) for a 20 pg.g^{-1} Hg standard solution.

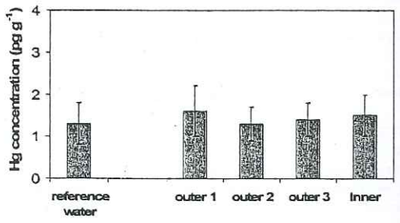

Fig. 2 Measured Hg concentrations in an artificial ice core and in the reference water (ref water). Outer 1–3 refer to the three successive veneer layers taken from the outside (outer 1) toward the centre of the core; inner refers to the remaining cylindrical part of the ice core.

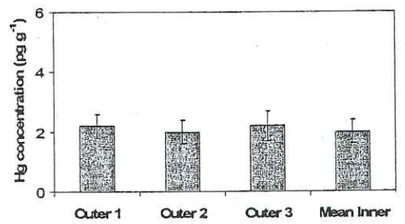

Fig. 3 Measured Hg concentrations from the exterior (outer 1) towards the central part of a snow block (dated from 1942–1944) collected in Coats Land (Antarctica) from the wall of an ultra-clean hand-dug pit. Mean inner refers to the mean of six individual sub-samples taken from the innermost part of the block.

measured in the artificial ice core are close to the reference water and surprisingly even the most external part (outer 1) that was subjected to handling and to direct contact with an LDPE acid cleaned bag did not exhibit any Hg contamination. Considering the uncertainties associated with Hg measurements, no significant blank is observed for the decontamination procedure. As for surface snow samples, no blank subtraction was applied for ice and firn core samples.

Even though the sample preparation did not introduce a significant Hg contribution, it was also important to check the effectiveness of the decontamination procedure carried out on real ice and snow samples. Fig. 3 shows an example of a concentration profile obtained from the exterior towards the centre of a snow block (dated from 1942–1944), collected from the wall of an ultra-clean hand-dug pit in Coats Land (Antarctica). It is evident that no significant contamination was present on the outside of the snow block; moreover, the trimming of successive outer layers and the sub-sampling of the internal part using ultra-clean protocols did not contaminate the Antarctic snow. This suggests that the measured Hg concentrations represent the genuine Hg levels in Antarctic snow. Such results have also been observed in snow and ice cores processed using the same procedure. Even ice core sections retrieved by deep drilling operations do not show heavy contamination on the outer most part.

For snow blocks, a detailed sub-sampling procedure on a centimetric scale was carried out to examine short term variations (inter/intra annual). To ensure the cleanliness of this procedure, we compared Hg concentrations measured in different pairs of parallel sub-samples taken in the same depth interval. Table 3 gives the results obtained for a snow block from Coats Land (Antarctica) for the depth interval of 42–62 cm depth below the surface, corresponding to the years 1982–1984. There is a good agreement between samples taken separately side by side.

Table 3 Hg concentrations in snow block collected from a clean hand dug pit in Coats Land, Antarctica: comparative measurements in parallel sub-samples retrieved from the same depth intervals

	Measured Hg concentration/pg g^{-1}			
	P1[b]		P2[b]	
Depth[a]/cm	Concentration	SD[c]	Concentration	SD[c]
42–47	3.9	0.5	5.8	0.5
47–50	4.3	0.8	3.0	0.5
50–54	7.6	1.1	8.3	1.0
54–58	4.2	0.3	4.1	0.5
58–62	3.6	0.4	3.9	0.4

[a] From the surface. [b] P1 and P2 refer to the two parallel series of subsamples. [c] Standard deviation.

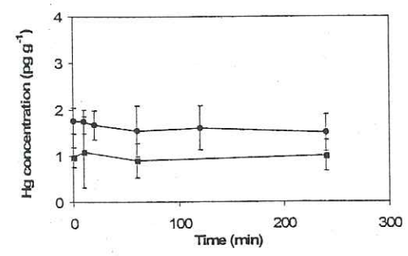

Fig. 4 Temporal evolution of the measured Hg concentrations for two sub-samples taken from the interior of a snow block (Coats Land, Antarctica) at two different depths: snow kept as frozen and melted just before the analysis. Circles (•) and squares (■) correspond to depth intervals 141–142 cm and 145–146 cm from the surface, respectively.

Stability of Hg concentrations in the samples

As we have shown that ultra-low Hg standards prepared in ultra-pure water were not stable, and were subjected to adsorption phenomena on LDPE, we studied the stability of Hg concentrations in various samples from Coats Land (Antarctica) and kept the snow frozen without any melting step until analysis. Samples were melted and acidified inside the clean sample introduction area of the ICP-SFMS just before analysis. Fig. 4 shows the evolution of Hg concentrations measured in two sub-samples. It is clear that Hg concentrations remained stable over the 240 min considered. This demonstrates that the melting procedure used to make the aliquots does not lead to significant losses of Hg. The different behaviour of Hg in real samples and in ultra-low standards within LDPE bottles might be due to matrix differences. In real snow samples, there are numerous other cations present in excess compared to the Hg concentration that can contribute to the saturation of the LDPE surface; this is not the case for Hg standards prepared with ultra pure water.

Comparison with flow injection mercury system (FIMS)

Fig. 5 presents Hg concentrations determined by ICP-SFMS and FIMS (FIMS 100, PerkinElmer) CV-AAS analyzer coupled to an amalgamation preconcentration unit, in 25 surface snow samples collected in Svalbard (Norway) between mid-April and early May, 2003. Comparison of the results reveals that for a large majority of the samples evaluated (22 of the 25 samples), the ICP-SFMS yielded higher Hg concentrations. There are only 3 cases in which FIMS concentrations were higher, and 2 of the values were the lowest concentrations measured by ICP-SFMS with high associated uncertainties.

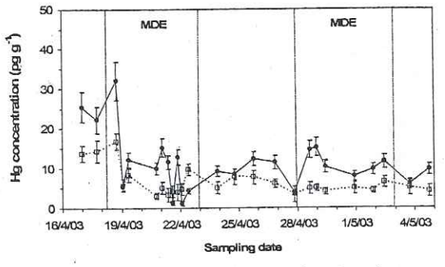

Fig. 5 Temporal evolution of Hg concentrations in surface snow samples collected in Svalbard (Norway) from the 16th of April 2003 to the 5th of May 2003: comparative determination of Hg by ICP-SFMS (•) and FIMS (□).

Table 4 Shallow pit snow samples collected in Kuujjuarapik (Canada) during the Arctic springtime 2002: comparative determination of Hg by ICP-SFMS, MC-GC-ICP-TOF-MS and FIMS

	Measured Hg concentration/pg g^{-1}		
Depth[a] /cm	ICP-SFMS	MC-GC-ICP-TOF-MS[b]	FIMS
Pit#1			
20	16.5 ± 2.5	15.4 ± 0.9	12.5 ± 1.5
40	17.7 ± 2.0	13.1 ± 1.7	16.2 ± 1.5
60	5.9 ± 0.7	3.8 ± 0.08	5.8 ± 1.0
Pit#2			
20	3.4 ± 0.5	1.5 ± 0.25	5.5 ± 1.0
40	24.5 ± 2.9	3.6 ± 0.05	9.9 ± 1.3
60	4.8 ± 0.5	4.4 ± 0.03	4.7 ± 0.8

[a] From the surface. [b] From Dommergue *et al*, 2003.[23]

While the temporal trends of the Hg concentrations in the snow are roughly similar according to the two methods (Fig. 5), there is no statistically valid correlative relationship (r^2 = 0.454, slope 0.52) between the ICP-SFMS and the FIMS measurements.

These results suggest that ICP-SFMS is better at determining total Hg concentrations. The lower Hg concentrations obtained by FIMS indicate that not all chemical forms of Hg in the snow samples are measurable according to that method. While the cold vapour analytical method should analyze all BrCl-oxidizable Hg forms (including Hg(II) and Hg(0), strongly organo-complexed Hg(II) compounds, adsorbed particulate Hg, and several covalently bound organomercurials,[19]) it is probably not able to adequately measure Hg bound within the cells of microorganisms[19] and perhaps Hg bound in other, unidentified organic or inorganic complexes. It has been previously suggested that samples be treated with UV irradiation or ultra-sonic shocking to recover non-reactive mercury species;[19,29] however, this step is unnecessary when using the ICP-SFMS, due its action of fully decomposing the sample material in the plasma.

The differing results based on the ICP-SFMS and FIMS indicate that some past measurements of Hg in snow using standard, cold-vapour methods may have resulted in underestimations of total Hg concentrations. Additionally, our results open the opportunity to explore the complex and poorly understood nature of Hg speciation and complexation in snow. We recommend that studies be carried out to account for the Hg that is not measurable by FIMS and to test our hypothesis that this Hg is somehow not oxidizable by BrCl due to its complexation with hydrophobic, organic ligands, with certain types of particulate matter, and/or its incorporation in the cellular structure of micro-organisms.

Comparison with multi-capillary gas chromatography coupled with inductively coupled plasma time of flight mass spectrometry (MC-GC-ICP-TOF-MS) and FIMS

Table 4 compares the Hg concentrations obtained using ICP-SFMS, MC-GC-ICP-TOF-MS and FIMS for 6 snow samples collected from the walls of two shallow pits in Kuujjuarapik (Canada) during Spring 2002 using ultra-clean procedures.[23] Good agreement is observed for most of the samples. However, for one sample (pit#2, 40 cm depth), ICP-MS and FIMS measurements reveal much higher concentrations. In this sample, plant debris and large dust particles were observed. Thus, the discrepancies in the Hg concentrations obtained by the three analytical methods may have been due to the heterogeneity of the sample, which was unfiltered and undigested. In future work, digestion, filtration or an ultracentrifugation step should be carried out to get rid of these inhomogeneities in these kinds of samples.

The overall good agreement among the three analytical techniques indicates that the snow pit samples from Canada were not as chemically heterogeneous and/or as biologically complex as the surface snow samples from Svalbard (previous section). Because the three forms of analysis yielded similar concentrations and the ICP-SFMS truly measures the total Hg concentration, it can be assumed that most or all of the Hg in the snow pit samples was adequately reactive for measurement by the FIMS and GC-ICP-TOF-MS techniques.

Examples of measured concentrations in snow and ice from polar regions

Table 5 shows Hg concentration ranges measured in this study by ICP-SFMS for different polar and sub-polar locations. For the Northern Hemisphere, Hg concentrations measured in surface snow and in shallow pit samples are highly variable, ranging from 1.2 to 32.0 pg g^{-1}. These concentrations are in good agreement with previously published data obtained using another analytical technique (CV-AFS).[30,31] The observed short-term variations of Hg in surface snow samples from the Northern Hemisphere (Svalbard and Canada) illustrate the complex atmospheric chemistry of mercury in polar regions. The Hg deposition velocity can be enhanced during mercury depletion events (MDE) which generally occur in the springtime after the polar sunrise.[32] Oxidation of elemental gaseous mercury and the transformation into more reactive species such as particulate Hg and divalent gaseous Hg lead to higher deposition fluxes and then to higher mercury concentrations in the snow.[23,30,31]

Table 5 also reports the concentration ranges found in snow and ice from Antarctica. As in the Northern Hemisphere, Hg concentrations are highly variable, ranging from 0.7 to 3.2 pg g^{-1} for ice core sections dated from 3500 years BP to 18 000 years BP, and from 0.2 to 16.1 pg g^{-1} for snow dated from 1834 to 1991. Comparison with published data for deep ice shows a good agreement with our Hg determinations. However, it appears that the ICP-SFMS yielded concentrations up to twice those measured using double stage gold amalgamation CV-AFS on the Dome C samples.[8] This phenomenon may be due to differences between the two analytical techniques. The ICP-MS with its high energy source probably atomises and ionises within the plasma all the Hg species present in the sample, including dust bound Hg, giving a total Hg determination. Analysis by CV-AFS yields a value only for all reducible Hg species available in solution. Alternatively, the observed differences can also be due to natural variations of Hg during the last 18 000 years at the sampling site Dome C, because the comparison has not been made on samples corresponding to the same depth intervals.

Table 5 also shows a comparison between concentration ranges found for different Antarctic sites (Coats Land, a traverse between Dome C and Adelie Land, South Victoria Land) for the 1980s. It can be seen that the Coats Land measurements for the period 1982–1984 are significantly higher than data from other sites. The same hypotheses regarding the differences in the analytical determination of Hg as discussed above can be made because the few previously published results were obtained using a CV-AFS[9] and a photoacoustic Hg analyser.[11] Moreover, in the latter study, analytical blanks represented more than 80% of the measured concentrations. The significantly higher concentrations found in Coats Land snow can also be due to different sampling site characteristics (accumulation rate, source contributions, distance from the sea).

Table 5 Measured Hg concentrations by HR-ICP-SFMS in various types of snow and ice samples from polar regions and comparison with previous published data

Location	Age of the sample	References	Analytical method	n^a	Hg concentration[b]/ pg g^{-1}
Northern Hemisphere					
Ny-Alesund (Svalbard)	Seasonal snow cover 2003	This study	ICP-SFMS	28	1.2–32.0[c]
Ny-Alesund (Svalbard)	Seasonal snow cover 2000–2001	Berg *et al.*, 2003[30]	CV-AFS	18	2–30[d]
Kuujjuarapik (Canada)	Seasonal snow cover 2002	This study	ICP-SFMS	6	3.4–24.5[e]
Canadian Arctic	Seasonal snow cover 1997	Lu *et al.*, 2001[31]	CV-AFS	50	2.0–160[f]
Antarctica					
Coats Land	1834–1986	This study	ICP-SFMS	160	0.2–16.1[g]
Coats Land	1982–1984	This study	ICP-SFMS	10	3.0–8.3[g]
Adelie Land–Dome C	1983–1984	Vandal *et al.*, 1995[9]	CV-AFS	4	0.1–0.5[h]
Victoria Land	Not determined	Sheppard *et al.*, 1991[11]	Photoacoustic Hg analyser	14	0.1–1.5[i]
Dome C (EPICA)	3500–18 000 years BP	This study	ICP-SFMS	7	0.7–3.2[j]
Dome C	3850–33 700 years BP	Vandal *et al.*, 1993[8]	CV-AFS	14	0.2–2.2[k]

[a] Number of analysed samples. [b] Concentration range. [c] Surface snow samples collected daily during the Arctic Spring from April to May 2003. [d] Surface snow samples collected weekly during the years 2000–2001. [e] Surface snow and shallow pit samples (<1 m depth) collected during the Arctic spring in April 2002. [f] Surface snow samples collected in 1997. [g] Snow and firn samples collected during the austral summer 1986–1987 from the surface to 16.3 m depth. [h] Surface snow blocks collected during the austral summer 1983–1984 along a traverse from Dome C to Adelie Land. [i] Snow samples collected during the austral summer 1988–1989 from the surface to 4.6 m depth. [j] Ice core sections from 152 m to 594 m depth. [k] Ice core section from 172 m to 796 m depth.

Conclusions

In this work we have demonstrated that by combining ultra-clean procedures and simple sample preparation it is possible to accurately determine Hg concentrations in snow and ice from polar regions by direct analysis with ICP-SFMS. This constitutes a major improvement for this kind of sample because with low sample volumes (less than 1 ml) without any preconcentration steps, detection limits as low as sub-pg g^{-1} levels can be achieved, with a methodology compatible with the simultaneous multi-elemental determination of other trace elements. It also offers the first opportunity to compare Hg results obtained using ICP-SFMS with other analytical methods, such as cold vapour or hydride generation techniques, in order to deduce the efficiency of their sample preparation protocols, such as the oxidation and reduction steps. Mercury concentrations obtained by ICP-SFMS are generally in good agreement with data produced using other methods on similar samples. However, in several cases, results with the ICP-SFMS yielded higher Hg concentrations than those obtained by use of other techniques. These results indicate that the ICP-SFMS is superior to the other methods in recovering total Hg concentrations, especially in samples with a significant portion of Hg bonded to organic complexes or in other poorly-reducible forms. The changing pattern of Hg deposition in polar ice caps over the last centuries and the last climatic cycles will be presented in forthcoming papers.

Acknowledgements

This work was supported in Italy by a Marie Curie Fellowship of the European Community (contract HPMF-CT-2002-01772) and by ENEA as part of the Antarctic National Research Program (under projects on Environmental Contamination and Glaciology). In France, it was supported by the Institut Paul-Emile Victor for the field sampling campaigns in the Canadian Arctic and in Svalbard, the Institut Universitaire de France, the Ministère de l'Environnement et de l'Aménagement du Territoire, the Agence de l'Environnement et de la Maîtrise de l'Energie, the Institut National des Sciences de l'Univers, the University Joseph Fourier of Grenoble and the French consulate in Quebec. In the UK, it was supported by the British Antarctic Survey and the Natural Environmental Research Council. This work is a contribution to the "European Project for Ice Coring in Antarctica" (EPICA), a joint ESF (European Science Foundation)/EC scientific programme, funded by the European Commission and by national contributions from Belgium, Denmark, France, Germany, Italy, the Netherlands, Norway, Sweden, Switzerland and the United Kingdom. This is EPICA publication no. 103. We thank Ash Morton who assisted with the sampling in Antarctica, Kevin Rosman for providing the ultrapure double distilled HNO_3, and Professor C. Lorius for the financial support.

References

1 S. E. Lindberg, *Atmos. Environ.*, 1998, **32**, 807–808.
2 W. F. Fitzgerald, D. R. Engstrom, R. P. Mason and E. A. Nater, *Environ. Sci. Technol.*, 1998, **32**, 1–7.
3 L. Poissant, A. Dommergue and C. P. Ferrari, *From the Impact of Human Activities on our Climate and Environment to the Mysteries of Titan*, ed. C. F. Boutron, EDP Science, 2002, ch. 12, pp.143–160.
4 F. Slemr, G. Schuster and W. Seiler, *J. Atmos. Chem.*, 1985, **3**, 407–434.
5 W. H. Schroeder and R. A. Jackson, *Chemosphere*, 1987, **16**, 183–199.
6 C. H. Lamborg, W. Fitzgerald, J. O'Donnell and T. Torgersen, *Geochim. Cosmochim. Acta*, 2002, **66**, 1105–1118.
7 C. F. Boutron, G. M. Vandal, W. F. Fitzgerald and C. P. Ferrari, *Geophys. Res. Lett.*, 1998, **25**, 3315–3318.
8 G. M. Vandal, W. F. Fitzgerald, C. F. Boutron and J. P. Candelone, *Nature*, 1993, **362**, 621–623.
9 G. M. Vandal, W. F. Fitzgerald, C. F. Boutron and J. P. Candelone, *Ice Core Studies of Global Biogeochemical Cycles*, ed. R. J. Delmas, Springer-Verlag, 1995, vol. 30, pp. 401–415.
10 A. L. Dick, D. S. Sheppard and J. E. Patterson, *Atmos. Environ.*, 1990, **24A**, 973–978.
11 D. S. Sheppard, J. E. Patterson and M. K. McAdam, *Atmos. Environ.*, 1991, **25A**, 1657–1660.
12 C. F. Boutron and C. C. Patterson, *Nature*, 1986, **323**, 222–225.
13 C. F. Boutron, *Fresenius' Z. Anal. Chem.*, 1990, **337**, 482–491.
14 F. A. M. Planchon, C. F. Boutron, C. Barbante, E. W. Wolff, G. Cozzi, V. Gaspari, C. P. Ferrari and P. Cescon, *Anal. Chim. Acta*, 2001, **450**, 193–205.
15 C. P. Ferrari, A. L. Moreau and C. F. Boutron, *Fresenius' Z. Anal. Chem.*, 2000, **366**, 433–437.
16 N. Bloom and W. F. Fitzgerald, *Anal. Chim. Acta*, 1988, **208**, 151–161.
17 G. A. Gill and W. F. Fitzgerald, *Mar. Chem.*, 1987, **20**, 227–243.
18 S. Eyrikh, M. Schwikowski, H. W. Gaggeler, L. Tobler and T. Papina, *J. Phys.*, 2003, **107**, 431–434.
19 US-EPA Method 1631, Revision C, U.S. Environmental Protection Agency, Office of Water, Office of Science and Technology, Engineering and Analysis Division (4303), Washington, DC, March, 2001.
20 B. Passariello, M. Barbaro, S. Quaresima, A. Casciello and A. Marabini, *Microchem. J.*, 1996, **54**, 348–354.
21 J. Allibone, E. Fatemian and P. J. Walker, *J. Anal. At. Spectrom.*, 1999, **14**, 235–239.
22 P. Jitaru, H. Goenaga Infante and F. C. Adams, *Anal. Chim. Acta*, 2003, **489**, 45–57.
23 A. Dommergue, C. P. Ferrari, P. A. Gauchard, C. F. Boutron,

L. Poissant, M. Pilote, P. Jitaru and F. Adams, *Geophys. Res. Lett.*, 2003, **30**, 1621–1624.
24 C. Barbante, T. Bellomi, G. Mezzadri, P. Cescon, G. Scarponi, C. Morel, S. Jay, K. Van de Velde, C. Ferrari and C. F. Boutron, *J. Anal. At. Spectros.*, 1997, **12**, 925–931.
25 C. P. Ferrari, A. Dommergue, A. Veysseyre, F. Planchon and C. F. Boutron, *Sci. Tot. Environ.*, 2002, **287**, 61–69.
26 J. P. Candelone, S. Hong and C. F. Boutron, *Anal. Chim. Acta*, 1994, **299**, 9–16.
27 K. H. Wedepohl, *Geochim. Cosmochim. Acta*, 1995, **59**, 1217–1232.
28 G. L. Long and J. D. Winefordner, *Anal. Chem.*, 1983, **55**, 712A–724A.
29 O. Lindqvist and H. Winefordner, *Tellus*, 1985, **37B**, 136–159.
30 T. Berg, S. Sekkesaeter, E. Steinnes, A. K. Valdal and G. Wibetoe, *Sci. Tot. Environ.*, 2003, **304**, 43–51.
31 J. Y. Lu, W. H. Schroeder, L. A. Barrie, A. Steffen, H. Welch, K. Martin, L. Lochard, R. V. Hunt, G. Boila and A. Richter, *Geophys. Res. Lett.*, 2001, **28**, 3219–3222.
32 W. H. Schroeder, K. G. Anlauf, L. A. Barrie, J. Y. Lu, A. Steffen, D. R. Schneeberger and T. Berg, *Nature*, 1998, **394**, 331–332.

J. Anal. At. Spectrom., 2004, 19, 823–830

5.2 ARTICLE 8: **High deposition of mercury species onto the Antarctic plateau during coldest climatic stages of the last 210,000 years**

Petru Jitaru, Paolo Gabrielli, Sonia Nagorski, Fréderic A. M. Planchon, Carlo Barbante, , Christophe P. Ferrari, Claude F. Boutron, and Freddy C. Adams

To be submitted to *Nature*

HIGH DEPOSITION OF MERCURY SPECIES ONTO THE ANTARCTIC PLATEAU DURING COLDEST CLIMATIC STAGES OF THE LAST 210,000 YEARS

Petru Jitaru[*], Paolo Gabrielli[†,‡], Sonia Nagorski[†], Fréderic A. M. Planchon[‡], Carlo Barbante[‡,§], Christophe P. Ferrari[†,**], Claude F. Boutron[†,††] and Freddy C. Adams[*]

Mercury is of current environmental concern because of its high toxicity and large scale pollution[1]. Polar ice archives are of prime importance to assess the natural mercury emissions to the global environment[2-4]. To date, a single study provides reliable information on mercury from an Antarctic ice core spanning ~34 kyr[3]. Here we report the records of total mercury (Hg_T), methylmercury (MeHg) and inorganic mercury (Hg^{2+}) from a new deep Antarctic ice record covering ~210 kyr. Mercury levels during the last glacial age are higher than concentrations previously obtained by nearly an order of magnitude. High mercury deposition occurs with the highest dust fallout fluxes and can be explained by atmospheric oxidation processes that are enhanced during cold conditions. These processes could convert gaseous elemental mercury (Hg^0) to Hg^{2+}, resulting in the transfer of Hg onto dust particle surfaces over cold conditions[5]. Moreover, the first determination of clearly detectable levels of MeHg could suggest the **important contribution of the Southern Ocean with mercury to Antarctica, especially during cold periods.**

---

[*] University of Antwerp, Department of Chemistry, Campus Drie Eiken, Universiteitsplein 1, B-2610 Wilrijk, Belgium

[†] Laboratoire de Glaciologie et Géophysique de l'Environnement du CNRS 54, rue Molière, B.P. 96, 38402 St Martin d'Heres cedex, France

[‡] Department of Environmental Sciences, University of Venice, Ca' Foscari, I-30123 Venice, Italy

[§] Institute for the Dynamics of Environmental Processes-CNR, University of Venice, Ca' Foscari, I-30123 Venice, Italy

[**] Polytech Grenoble (Institut Universitaire de France), Université Joseph Fourier, 28 avenue Benoît Frachon, B.P. 53, 38041 Grenoble, France

[††] Observatoire des Sciences de l'Univers et Unité de Formation et de Recherche de Physique (Institut Universitaire de France), Université Joseph Fourier, Domaine Universitaire, B.P. 68 38041 Grenoble, France

Understanding the global biogeochemical cycle of mercury and in particular its transport and deposition to polar areas is important because toxic mercury species accumulate in these regions[2]. The Antarctic and Arctic ice sheets are valuable archives that provide important information regarding recent and ancient mercury depositions. Nevertheless, information concerning mercury levels in polar snow and ice and most of all the speciation of mercury is lacking. This is essentially because mercury in such environments is difficult to ascertain and quantify owing to problems with sample contamination[6] as well as preservation and stabilization of species in samples, particularly during long-term storage[7]. Additionally, given that concentrations of mercury reported earlier in Antarctic ice[3] and snow[8] are generally a the picogram per gram level (1 pg g^{-1}= 1 10^{-12} g g^{-1}) and that its species such as methylmercury (MeHg) determined in polar snow[9] can be lower than fractions of pg g^{-1}, it is clearly necessary to use highly sensitive, reliable and ultra-clean analytical approaches for the quantification of mercury and mercury species in polar regions.

To date, there is only a single record of mercury from an ancient polar ice core[3]. The mercury determined by Vandal and co-workers, corresponding to the fraction involved in easily reducible complexes by $SnCl_2$, is essentially equivalent to the inorganic mercury (Hg^{2+}) measured in our work. Complexes such as $HgCl_2$ and $Hg(OH)_2$ and HgC_2O_4, that are easily reducible by $SnCl_2$ are also the species reactive with $NaBEt_4$ (used as a reagent in our method) quantified by the speciation analysis procedure. Vandal and co-workers measured Hg^{2+} in 14 sections of the first ice core[10] retrieved from Dome C (East Antarctic plateau), covering a time period back to ~34 kyr BP. They suggested that oceanic emissions of gaseous elemental mercury (Hg^0), was the principal source of Hg to Antarctica during pre-industrial times.

Here we report the first determination of total mercury (Hg_T) and MeHg concentrations and new measurements of Hg^{2+} in a new deep Antarctic ice core drilled at Dome C (East Antarctica, 75°06'S; 123°21E; 3233 m a.s.l.) as part of the European Project for Ice Coring in Antarctica (EPICA)[11]. This ice core was drilled ~50 km away from the location where the previous ice core was retrieved. Thirty-six ice sections were analysed for this study. Their depths range between 86.9 and 2138.4 m, covering a period from the late Holocene (~2 kyr BP) back to the penultimate glacial age, ~210 kyr BP.

Determination of Hg_T was carried using inductively coupled plasma-sector field-mass spectrometry (ICP-SFMS). The method detection limit for Hg_T determination is 0.18 pg g^{-1}; and the precision is ~ 15%, based on the relative standard deviation of analytical replicates[12]. Simultaneous determination of MeHg and Hg^{2+} was carried out using pre-concentration by solid-phase microextraction in combination with separation by multicapillary gas chromatography and detection using inductively coupled plasma-time of flight-mass spectrometry (ICP TOMS)[13]. The method detection limits are 0.027 pg g^{-1} (as metal) for MeHg and 0.27 pg g^{-1} for Hg^{2+}. The precision for both species in terms of relative standard deviation of analytical replicates was <4%. These new analytical procedures developed for the determination of Hg_T and simultaneous speciation analysis of MeHg and Hg^{2+} are extensively reported elsewhere[12,13].

The concentration of Hg_T, Hg^{2+} and MeHg are reported in Table 1. Concentrations of Hg_T and Hg^{2+} are at the pg g^{-1} whereas MeHg concentrations are about one order of magnitude lower. It can be observed that concentration values varied considerably during the last two climatic cycles (Fig. 1).

Hg_T concentrations were low during interglacial and warm stages, when Hg_T values were around ~3-4 pg g^{-1} and were higher during the coldest periods of the last two glacial ages, ranging from ~6 pg g^{-1} up to ~16 pg g^{-1}. Concentrations were particularly high during marine isotopic stage (MIS)[14] 2.2 and 4.2 and into a lesser extent during the next to last glacial age. Hg_T concentrations recorded during cold periods were higher by up to a factor of 5 than concentrations recorded in warm periods. These variations cannot be explained only

with variations in snow accumulation rate, varying in Dome C by only a factor of 2 between glacial and interglacial periods.

In order to assess the origin of Hg_T it must be considered that the main possible natural sources of atmospheric mercury are the oceans, continental rock/soil dust and volcanoes[15]. The contribution from rock and soil dust was evaluated using Mn concentrations determined in the same ice sections[16] to calculate the crustal enrichment factor (EF_c) defined as the Hg_T/Mn ratio determined in ice divided by the average Hg_T/Mn ratio relative to the upper continental crust[17]. The very high EF_c obtained, ranging from values higher than 100 during cold periods up to above 1000 during interglacial periods, is clear evidence of a negligible input of mercury from rocks and soil dust. A confirmation of this result, can be obtained using the concentrations of insoluble dust measured in the same ice core[18]. Based on the average concentration of mercury content in the crustal dust (0.056 $\mu g\ g^{-1}$)[17], the predicted Hg_T level corresponding to the maximum dust concentration value (1,5 ng g^{-1}, ~25 kyr BP) is ~0.085 pg g^{-1}. This level is ~200 times lower than maximum Hg_T level obtained in our study, which confirms that rock and soil dust contribution to the mercury budget in Antarctica is insignificant.

The contribution to Hg_T from volcanoes can be tentatively assessed using the estimated Hg/S ratios in volcanic emissions (~10^{-6})[15] and assuming that ~10-15% of the sulphur (in sulphate form) of non marine origin (nss.SO4) measured in the ice (from ref.[19] and unpublished results) is contributed by volcanoes[3]. Though the values for nss.SO_4 calculated in this study comprised over 90% of the total sulphate, the volcanic contribution to the Hg budget appears to be negligible.

Given that the Hg_T/Na ratio (Na values from ref. [19] and unpublished results) obtained in our study is on average ~10^{-5}, whereas the reported Hg/Na concentration ratio in the open ocean water is ~10^{-12}, the direct sea-spray contribution to the Antarctic mercury budget is also insignificant.

It is generally assumed that ~80% of the total nss.SO_4 is generated by the oxidation of DMS[20]. The biogenic oceanic contribution of mercury to Antarctica is estimated assuming a Hg/S mass ratio of 4.4 x 10^{-5} in the nss.SO_4 of oceanic origin (from DMS)[3]. Except for the samples of ~54 kyr BP, for which the predicted mercury oceanic mercury so calculated was ~120% of the corresponding level of Hg_T measured in the ice (by ICP-SFMS), for the other samples the calculated fraction of marine origin mercury accounted for 20-80% of Hg_T. On average, the biogenic oceanic contribution explains nearly half of the Hg_T determined in the ice.

The determination of the single Hg species such as Hg^{2+} and MeHg could be useful to better evaluate the contribution of the various natural sources to the budget of Hg_T. During the Holocene the levels of Hg^{2+} were found to be generally below 1.5 pg g^{-1}. Hg^{2+} levels below the detection limit were measured especially during the last glacial-interglacial transition and the last interglacial, the Eemian. Highest concentrations for this species were measured during the late stages of the last glacial age (LGA), when its levels reached ~15 pg g^{-1} (~36 kyr BP) and during the Last Glacial Maximum (LGM) (~9 pg g^{-1}, ~22 kyr BP).

The only published data on mercury determination in ancient Antarctic ice to which our Hg concentrations can be compared, at least for a limited time period, are those concerning Hg^{2+} reported by Vandal and co-workers[3]. It should be noted that the maximum level of Hg^{2+} obtained in our study during the LGM (~9 pg g^{-1} ,22 kyr BP) is significantly higher than their maximum Hg^{2+} concentration obtained at approximately the same time (~2 pg g^{-1}, 21 kyr BP). However, except this extreme value, the results from the two datasets are generally in good agreement, taking into account that, on one hand the ice samples compared

were not part of the same ice sections and on the other hand that different analytical approaches were used for the quantification.

It is worth noting that low levels of Hg_T are remarkably higher than low levels of Hg^{2+}. This significant difference (see Table 1 and Fig. 1) suggests that mercury may also be present in the ice in insoluble forms such as HgS or other strong bound Hg(II) complexes. This is in agreement with a recent study[21] that estimated levels of Hg_T (thus including HgS and strong bound Hg(II) complexes) in snow from the Alps as ~100 times higher than Hg^{2+}. The origin of such insoluble mercury species in snow and ice cannot be entirely explained. Conversely, high concentration levels of Hg_T and Hg^{2+} in the EPICA/Dome C ice core are in reasonable good agreement, indicating that the largest fraction of Hg_T is represented by Hg^{2+}.

In spite of the negligible contribution of rock and soil dust to the mercury budget, it is noticeable that Hg_T and to a lesser extent Hg^{2+}, follow variations in the insoluble concentration dust profile obtained in the EPICA/Dome C ice core remarkably well (see Fig. 1). In particular Hg_T, Hg^{2+} and insoluble dust are peaking roughly in phase and with comparable intensity and amplitude. This means that, although of different origins, Hg_T and Hg^{2+} were deposited contemporaneously with continental dust onto the East Antarctic plateau.

Recently it has been observed that Hg^0 can be rapidly transformed in Arctic and Antarctic coastal atmosphere during so-called Atmospheric Mercury Depletion Events (AMDEs)[22-24]. This rapid transformation, driven by ozone and halogen chemistry[25], converts Hg^0 to gaseous Hg^{2+} and could take place at the surface of dust particles[5]. Hg^{2+} can be rapidly adsorbed onto atmospheric particles and then deposited onto snow. Another key parameter leading AMDEs is the strongly negative atmospheric temperature: free halogen radicals oxidizing Hg^0 are in fact produced only in such cold conditions[5].

Over coldest glacial periods, the Antarctic atmosphere was characterized by a strong enhancement in dustiness[18], an increased advection of sea salt aerosols[26] (containing salt of halogens). We therefore propose that the finer-grained and more abundant quantity of dust particles[27] available in the Antarctic atmosphere during the coldest climatic stages, which were characterized by higher inputs of salt halogens and more negative temperatures, was linked to a strong process of oxidation of atmospheric Hg^0 to Hg(II) compounds. This in turn lead to the dry fallout of Hg(II) compounds together with dust to the East Antarctic plateau.

The time profile of MeHg concentration matches to a lesser extent the one of Hg_T, Hg^{2+} and dust (see Fig. 1). Apart from two extreme values, MeHg measured in the ice samples was generally below 0.5 pg g^{-1}. Levels below the detection limit were found during the last glacial-interglacial transition (~16 kyr BP) and at the onset of the Holocene (~10 kyr BP). Maximum levels were obtained during the LGA (~1.4 pg g^{-1}, ~40 kyr BP).

The origin of MeHg measured in polar environments is still a matter of debate, as it is not clear whether MeHg is transported onto the polar snow or it is produced on site[28]. Although Lindberg and co-workers[25] measured for the first time a so-called 'bioavailable' Hg^{2+} in the Arctic snow (that means available to genetically modified bacteria, which produce light when Hg^{2+} enters their cells), evidence that MeHg can be formed in the snow by biomethylation of Hg^{2+} has not been reported so far. Given the extremely low temperatures of the East Antarctic ice (about -50 °C close to the surface), this process seems to be highly unlikely in central East Antarctic locations such as Dome C.

The determination of clearly detectable levels of MeHg in Antarctic ice could rather be an indication of the Southern Ocean's contribution of mercury to Antarctica. A recent study has shown the role of macro algae and bacteria in producing MeHg and dimethylmercury (Me_2Hg) by methylation of Hg^{2+} in the Southern Ocean[29]. This study showed that Me_2Hg is the organic mercury species preferentially transferred from the ocean into the atmosphere, where it is decomposed to MeHg and ultimately to Hg^0. Due to its high volatility and very low solubility in water, Me_2Hg is the ideal species to 'escape' the 'water

barrier' and consequently be available for long-range transport. Although MeHg has a considerable higher water solubility and lower volatility compared to Me_2Hg, its enrichment in boundary layers of the ocean/air system makes it available for transport over land as sea-spray or sea-ice aerosols[30].

The time needed for the sea salt to reach Central Antarctica from the coast, is estimated to be 1-2 days[31]. Given that the residence time of MeHg and Me_2Hg in normal (actual) atmospheric conditions is on the order of a few days[30], we suggest that the gaseous Me_2Hg is the methylated mercury species predominantly transported from the Southern Ocean to Antarctica. Before deposition however, Me_2Hg should partially convert to MeHg and ultimately to Hg^0 (from ref.[30]). Hence the production of Me_2Hg and MeHg in the Southern Ocean, most likely contributes significantly to Hg^0 and possibly the total mercury budget deposited in Antarctica.

Acknowledgements. This work is a contribution to the European Project for Ice Coring in Antarctica (EPICA), a joint European Science Foundation/European Commission (EC) scientific programme, funded by the EC and by national contributors from Belgium, Denmark, France, Germany, Italy, The Netherlands, Norway, Sweden, Switzerland and UK. In Belgium the financial support was ensured by Flemish Fund for Scientific Research (FWO), Brussels, Belgium. The study was supported in France by the Institut Universitaire de France, the Ministère de l'Environnement et de l'Aménagement du Territoire, the Agence de l'Environnement et de la Maîtrise de l'Energie, the Institut National des Sciences de l'Univers, the French Polar institute (IPEV) and the Université Joseph Fourier of Grenoble. In Italy, it was supported by ENEA as part of the Antarctic National Research Programme and the Alliance for Global Sustainability. This research has been also supported by a Marie Curie Fellowships of the European Community programme (IHP). Finally we would like to thank all the personnel working in the field at Dome C.

Correspondence and request for materials should be addressed to barbante@unive.it

Table 1

Age (years BP)	Depth (m)	Concentrations					
		Hg_T (pg g^{-1})	SD	Hg^{2+} (pg g^{-1})	SD	MeHg (pg g^{-1})	SD
2015	86.9	5	1	1.5	0.5	0.32	0.03
6949	229.4	3.0	0.5	0.8	-	0.14	0.01
10280	316.3	8	1	0.5	0.2	<0.027	-
14204	405.6	6	1	<0.27	-	1.1	0.1
14910	419.4	4	1	<0.27	-	0.13	0.01
15626	432.9	5	1	<0.27	-	<0.027	-
17400	461.5	8	1	0.9	0.1	0.41	0.03
18133	471.1	8	1	2.1	0.1	0.19	0.01
19627	488.7	11	2	3.6	0.3	0.26	0.01
21967	515.9	14	2	9	1	0.17	0.01
27033	574.2	11	2	1.3	0.1	0.5	0.1
29117	598.4	8	1	0.9	0.1	0.24	0.04
33661	653.1	9	1	1.3	0.3	0.7	0.1
33729	654.0	16	2	9	1	0.1	0.1
35967	680.9	10	1	15	1	0.48	0.003
38135	708.7	9	1	<0.27	-	0.06	0.004
40375	735.6	8	1	2.7	0.1	1.4	0.1
42801	763.1	6	1	0.6	0.1	0.5	0.1
47175	818.1	5	1	0.4	-	0.4	0.1
53853	900.9	2.6	0.4	<0.27	-	0.3	0.1
60674	983.4	9	1	6.6	0.5	0.12	0.003
63453	1010.9	10	1	2.5	0.3	0.3	0.1
71637	1093.1	7	1	<0.27	-	0.6	0.1
76576	1148.4	7	1	5	1	1.1	0.2
81050	1203.1	5	1	<0.27	-	0.07	0.002
86002	1258.4	5	1	1.3	0.4	0.20	0.003
91456	1313.4	8	1	3.5	0.5	0.4	0.1
102283	1423.4	4	1	<0.27	-	0.24	0.04
114142	1533.4	3	1	0.7	0.2	0.22	0.03
122832	1643.4	4	1	<0.27	-	0.1	0.1
131892	1753.4	4	1	<0.27	-	0.4	0.1
152184	1863.1	8	1	0.56	0.03	0.15	0.03
174491	1973.4	5	1	1.4	0.1	0.8	0.1
191286	2050.1	7	1	0.83	-	0.4	0.1
198944	2094.4	5	1	0.3	0.1	0.2	0.1
207225	2138.4	3.3	0.5	<0.27	-	0.65	0.02

Figure caption

Fig. 1: Concentrations of total mercury (Hg_T) and inorganic mercury (Hg^{2+}) and methylmercury (MeHg) in the Epica/Dome C ice core during the last two climatic cycles. Climate changes are indicated by variation in the δD ‰, taken as a proxy of local temperature. Concentrations of Hg_T are compared with the insoluble dust concentration profile[18].

Figure 1

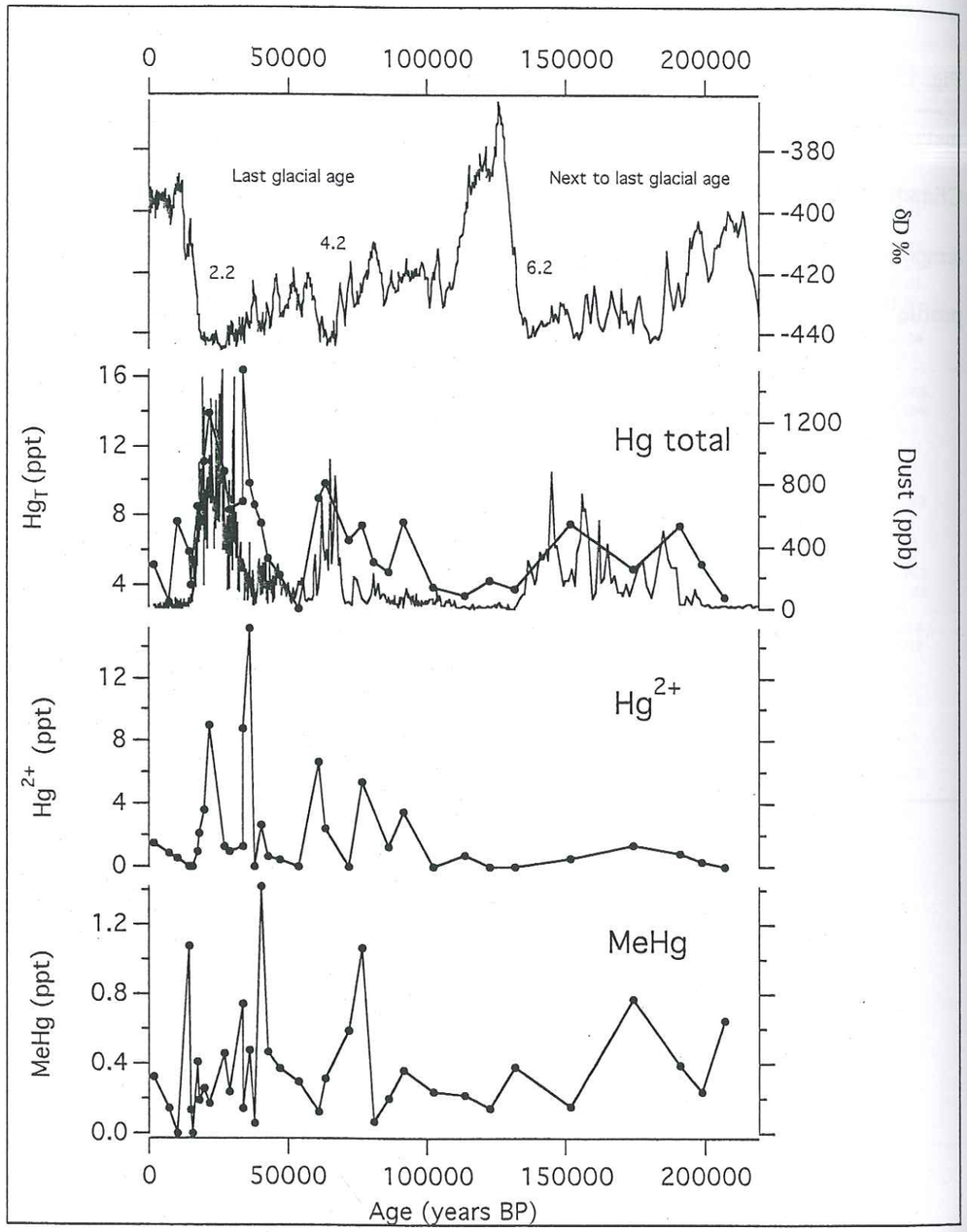

References

1. Morel, F. M. M., Krapiel, A. M. L. & Amyot, M. The chemical cycle and bioaccumulation of mercury. *Ann. Rev. Ecol. Syst.* **29**, 543-566 (1998).
2. Fitzgerald, W. F., R., E. D., P., M. R. & Nater, E. A. The Case of Atmospheric Mercury Contamination in Remote Areas. *Environ. Sci. Technol.* **32**, 1-7 (1998).
3. Vandal, G. M., Fitzgerald, W. F., Boutron, C. F. & Candelone, J. P. Variations in mercury deposition to antarctica over the past 34,000 years. *Nature* **362**, 621-623 (1993).
4. Boutron, C. F., Vandal, G. M., Fitzgerald, W. F. & Ferrari, C. A forty year record of mercury in central Greenland snow. *Geophys. Res. Lett.* **25**, 3315-3318 (1998).
5. Gauchard, P. A. et al. An international study of Mercury, Ny-Ålesund spring 2003: Characterizing atmospheric mercury depletion events. *To be submitted to Atmos. Environ.* (2004).
6. Ferrari, C., Moreau, A. L. & Boutron, C. F. Clean conditions for the determination of ultra-low levels of mercury in ice and snow samples. *Fresenius J. Anal. Chem.* **366**, 433-437 (2000).
7. Ping, L. & Yan, X. Factors affecting the stability of inorganic and methylmercury during sample storage. *Trends Anal. Chem.* **22**, 245-253 (2003).
8. Capelli, R., Mingianti, V., Chiarini, C. & De Pellegrini, R. Mercury in snow layers from Antarctica. *Int. J. Environ. Anal. Chem.* **7**, 245-253 (1998).
9. Ferrari, C., Dommergue, A., Boutron, C. F., Jitaru, P. & Adams, F. C. Profiles of Mercury in the snow pack at Station Nord, Greenland shortly after polar sunrise. *Geophys. Res. Lett.* **31** (2004).

10. Lorius, C., Merlivat, L., Jouzel, J. & Pourchet, M. A 30,000 yr isotope climatic record from Antarctic ice. *Nature* **280**, 644-648 (1979).

11. Epica community members. Eight glacial cycles from an Antarctic ice core. *Nature* **429**, 623-628 (2004).

12. Planchon, F. et al. Direct determination of mercury at the sub-picogram per gram levels in polar snow and ice by ICP-SFMS. *J. Anal. At. Spectrom.* **19**, 823-830 (2004).

13. Jitaru, P. & Adams, F. C. Solid-phase Microextraction and Multicapillary Gas Chromatography Hyphenated to Inductively Coupled Plasma-Time-of-Flight-Mass Spectrometry. *In press J. Chromatography A.* (2004).

14. Bassinot, F. C. et al. The astronomical theory of climate and the age of the Brunhes-Matuyama magnetic reversal. *Earth Planet. Sci. Lett.* **126**, 91-108 (1994).

15. Nriagu, J. O. A global assesment of natural sources of atmospheric trace metals. *Nature* **338**, 47-49 (1989).

16. Gabrielli, P. et al. Variations in atmospheric trace elements in Dome C (East Antarctica) ice over the last two climatic cycles. *To be submitted to Atmos. Environ.* (2004).

17. Wedepohl, K. H. The composition of the continental crust. *Geochim. Cosmochim. Acta* **59**, 1217-1232 (1995).

18. Delmonte, B. et al. Comparing the Epica and Vostok dust records during the last 220,000 years: stratigraphical correlation and provenance in glacial periods. *Earth-Sci. Rev.* **66**, 63-87 (2004).

19. Udisti, R. et al. Sensitivity of chemical species to climatic changes in the last 45 kyrs as revealed by high resolution Dome C (Antarctica) ice core analysis. *Ann. Glaciol. in press* (2004).

20. Prospero, J. M., Savoie, D. L., Saltzman, E. S. & Larsen, R. Impact of oceanic sources of biogenic sulphur on sulphate aerosol concentrations at Mawson, Antarctica. *Nature* **350**, 221-223 (1991).

21. Ferrari, C., Dommergue, A., Veysseyre, A., Planchon, F. & Boutron, C. F. Mercury speciation in the French seasonal cover. *Sci. Total Environ.* **287**, 61-69 (2002).

22. Schroeder, J. P. et al. Measurements of atmospheric mercury species at a coastal site in the Antarctic and over the south Atlantic ocean during polar summer. *Nature* **394**, 331-332 (1998).

23. Ebinghaus, R. et al. Antarctic springtime depletion of atmospheric mercury. *Environ. Sci. Technol.* **36**, 1238-1244 (2002).

24. Temme, C., Einax, J. W., Ebinghaus, R. & Schroeder, J. P. Measurements of Atmospheric Mercury Species at a Coastal Site in the Antarctic and over the South Atlantic Ocean during Polar Summer, Environmental Science and Technology. *Environ. Sci. Technol.* **37**, 22-31 (2003).

25. Lindberg, S. E. et al. Dynamic Oxidation of Gaseous Mercury in the Arctic Troposphere at Polar Sunrise. *Environ. Sci. Technol.* **36**, 1245-1256 (2002).

26. De Angelis, M., Barkov, N. I. & Petrov, V. N. Aerosol concentrations over the last climatic cycle (160 kyr) from an Antarctic ice core. *Nature* **325**, 318-321 (1987).

27. Delmonte, B., Petit, J. R. & Maggi, V. Glacial to Holocene implications of the new 27000-year dust record from the EPICA Dome C (East Antarctica) ice core. *Clim. Dyn.* **18**, 647-660 (2002).

28. Loseto, L. L., Lean, D. R. S. & Siciliano, S. D. Snowmelt Sources of Methylmercury to High Arctic Ecosystems. *Environ. Sci. Technol.* **38**, 3004-3010 (2004).

29. Pongratz, P. & Heumann, K. G. Production of methyled mercury, lead and cadmium by marine bacteria as significant source for atmsopheric heavy metals in polar regions. *Chemosphere* **39**, 89-102 (1999).

30. Heumann, K. G. in *Environmental Contamination in Antarctica: A Challenge to Analytical Chemistry* (eds. Caroli, S., Cescon, P. & Walton, D.) (Elsevier, Amsterdam, 2001).

31. Bodhaine, B. A., Deluisi, J. J., Harris, J. M., Houmere, P. & Bauman, S. Aerosol measurements at the South Pole. *Tellus* **38B**, 223-235 (1986).

CHAPTER 6: CONCLUSIONS AND PERSPECTIVES

This work allowed the investigation of trace elements variation in polar ice during the last few climatic cycles, taking advantage of ultra clean samples preparation procedures and the high sensitivity of mass spectrometry techniques. Special emphasis was given to Ir and Pt, which are valuable tracers of cosmic material fallout. These were measured by ICP-SFMS in various sections from deep ice cores retrieved in Greenland (GRIP) and Antarctica (EPICA/Dome C and Vostok).

Considerable attention was also given to various other trace elements such as Li, Mg, V, Cr, Mn, Co, Cu, As, Rb, Sr, Cd, Ba, Hg, Bi and U, which were measured by ICP SFMS in ancient Antarctic ice (EPICA/Dome C and Vostok ice cores) as such, interesting indicators of different terrestrial sources of aerosols such as the upper crust, volcanoes and the oceans. Other innovative parameters such as Pb isotopes, determined by TIMS, and Hg species (Hg^{2+} and MeHg), measured by ICP-TOFMS, have also been investigated in the EPICA/Dome C ice core.

In what follows the most innovative scientific knowledge produced by this work is summarised together with the most promising perspectives for future investigations, with special attention to further analytical work that need to be performed for the determination of ultra low concentrations of Ir and Pt in polar ice.

6.1 Conclusions

6.1.1 Ir and Pt in polar ice cores

A new method was developed to determine the total concentration of Ir and Pt in ancient polar ice down to the sub-ppq level by ICP-SFMS. This procedure takes advantage of a new ultra clean procedure for the pre-concentration of the samples by sub-boiling evaporation and a desolvation system for sample introduction [*Gabrielli et al.*, 2004]. The most innovative aspect of this method is the possibility to determine for the first time the total content of Ir in the melted samples whereas, all the attempts reported in the past were limited to the determination of Ir exclusively in particulate matter, larger than ~0.45 μm, obtained by filtering molten ice.

This new procedure allowed a clear detection through determination of Ir and Pt of the signature (chondritic ratio) of the fallout of nanometric particles, called "meteoric smoke", onto the Greenland and Antarctic polar ice caps. These particles, originate from meteoroids vaporization and re-condensation in the high mesosphere/low thermosphere [*Hunten et al.*, 1980] and are currently detected in the high atmosphere from the Earth surface mostly by using remote sensing techniques (for example LIDAR) [*Kane and Gardner*, 1993; *Plane et al.*, 2004]. It is the first time that the meteoric smoke signature is detected in a terrestrial archive. The measurements of Ir and Pt have provided new estimates of the input of comic material ablated when entering the Earth's atmosphere.

The influx of meteoric smoke, averaged on the Earth's surface, was calculated from Greenland ice (Summit, Central Greenland) during the Holocene and from Antarctic ice (Dome C and Vostok, East Antarctica) during the cold stages of the last two glacial periods. The Greenland estimate of the meteoric smoke input over

the Holocene (~78 kt y^{-1}), differs from current estimates of the interplanetary dust particles (IDPs) influx (~1-10 kt y^{-1}) by at least an order of magnitude. Nevertheless, estimates obtained from the EPICA/Dome C and Vostok Antarctic ice cores indicate a lower input of about 20 kt y^{-1} during glacial times. This remains, however, higher than most of the currently accepted estimates for the IDPs flux.

Unfortunately, synchronous estimates from the Greenland ice core of Summit and the Antarctic ice cores of EPICA/Dome C and Vostok were not possible. This was due to the occurrence of a strong contribution of terrestrial Ir and Pt inputs, linked with the high crustal dust fallout to Central Greenland during the Last Glacial Age and from the fallout to Dome C and Vostok of aerosol enriched in non-chondritic Ir and Pt, likely originating from volcanic emissions, during interglacial periods and warm stadials and interstadials.

The high meteoric smoke influx estimates obtained from Greenland ice during the Holocene and in East Antarctica over cold periods confirm new ideas concerning the transport of these particles throughout the atmosphere. A characteristic of the meteoric smoke particles is that they have a remarkable long residence time in the mesosphere, thus can be widely transported but the fallout to the Earth's surface is not homogeneous.

Thanks to a mathematical model developed by John Plane and his co-workers, we have shown that meteoric smoke, transported through the mesosphere by the meridional circulation, cannot sediment in the lower layers of the atmosphere before reaching the polar areas. It has been suggested that these particles are funnelled down into the polar vortices, sedimenting preferentially onto the polar ice caps. By assuming that all the meteoric smoke deposition occur seasonally only at latitudes larger than 65°, the Greenland estimate of the average meteoric smoke fallout to the

Earth's surface has been reconciled with most of other recent IDPs influx estimates suggested by other techniques. A corrected value of ~14 kt y^{-1} is obtained for the cosmic accretion rate.

In East Antarctic ice (EPICA/Dome C and Vostok ice cores), Ir and Pt were characterized by an unknown but persistent non-chondritic ratio emerging exclusively during interglacial and warm periods. As a consequence of this observation, it has been suggested that quiescent local volcanic sources were likely to be responsible of strong and rather continuous fallout of Ir and Pt to the East Antarctic plateau. This last observation suggests that East Antarctica is essentially subject to an atmospheric circulation with low paths within the troposphere during warm periods. In contrast, an Ir-Pt chondritic ratio strictly associated to cold climatic periods on the East Antarctic plateau indicates an enhanced subsidence of cold air masses transporting the meteoric smoke particles from the high troposphere/low stratosphere down to the surface of the East Antarctic plateau.

The mesospheric meridional circulation, occurring seasonally from the summer pole to the winter pole and the subsidence of cold air masses from the high levels of the troposphere, are processes that favour the deposition of the meteoric smoke particles onto the polar ice caps. Even slight differences in the circulations regimes or in snow accumulation rate (in case of wet deposition) from one region to another could account for substantially different fallouts of the meteoric smoke particles to the polar ice caps. It is therefore not surprising to observe an excellent agreement between the two meteoric smoke input estimates provided for cold stages by the EPICA/Dome C and Vostok cores (the distance between these two Antarctic sites is only ca 550 km), while there is a difference by a factor of nearly 4 with the Greenland estimates obtained for the Holocene.

6.1.2 Other trace elements in the EPICA/Dome C and Vostok ice cores

Besides Ir and Pt, various other trace elements such as Li, Mg, V, Cr, Mn, Co, Cu, As, Rb, Sr, Cd, Ba, Bi and U (Pb and Hg are discussed in sections 6.1.3 and 6.1.4) have been extensively measured in the EPICA/Dome C and Vostok samples. in In most cases fallout fluxes show large variations, with very low values during warm periods and much higher values during the cold periods. The advection of trace elements to the East Antarctic plateau is found to occur when a well-defined critical value of local temperature is reached.

A major result from our work is that crustal dust is the main carrier of atmospheric trace elements to East Antarctica during cold periods. With the exception of Cd, crustal dust is largely influencing the budget of all the trace elements during cold periods. The crustal component is also predominant for Li, V, Mn, Co, Cu, Rb, Ba and U during warm periods. The situation is more complex for several other elements with possible contributions from other natural sources such as volcanic emissions during the warm periods.

6.1.3 Pb isotopes in the EPICA/Dome C ice core

Pb and Ba concentration and Pb isotopes abundances have been investigated in the Dome C/EPICA ice core back to ~220 kyr. The observed changes in Pb and Ba concentrations as a function of climate are similar to those summarized in the previous section for the other trace elements, with very low values during warm periods and much higher values during the cold periods.

Interestingly, the 206/207 Pb ratios vary significantly in Dome C ice during the last two climatic cycles, with especially a decreasing trend during the last climatic cycle. Possible explanations for the observed variations are discussed. Pb isotopes ratios appear in fact to decrease slowly during the last two glacial ages, rapidly increasing during the last two glacial interglacial transitions and returning to low values during interglacial periods. The link of Pb isotopes with climate conditions appears therefore to be rather complex and further studies in the EPICA and in the Vostok ice core could contribute to clarify this relation.

Pb isotopes seem already to confirm that dust recovered in Dome C ice during cold periods is most likely originating from one particular source/area. Moreover, Pb isotopes radiogenic ratios suggest a possible significant quiescent volcanogenic component in the aerosol fallout to Dome C.

6.1.4 Hg in the EPICA/Dome C ice core

A new method has been developed for the direct determination of the concentration of total Hg in polar snow and ice down to the sub-ppt level by ICP-SFMS, chapter 5.1. In addition, an innovative analytical method has been developed by our colleagues at the Department of Chemistry of the University of Antwerpen (Belgium) for the determination of Hg^{2+} and MeHg [*Jitaru and Adams*, 2004], as part of our collaboration on polar snow and ice.

It allowed for the first time to measure total mercury (Hg_T), methylmercury (MeHg) and inorganic mercury (Hg^{2+}) in polar ice and snow. The results obtained from the analysis of the different sections of the EPICA/Dome C ice core considered in our work are the first obtained for mercury speciation in ancient ice. Levels of mercury higher by nearly an order of magnitude than concentrations previously obtained by Vandal and co-workers from the analysis of the 905 m "old Dome C" core [*Vandal et al.*, 1993] are observed during the cold periods. The high mercury deposition observed during the cold periods in our work can tentatively be explained by an enhanced oxidation of gaseous elemental mercury occurring onto the aeolian dust particles surface. The presence of MeHg in part of the samples is a further indication of the contribution of emissions from the Southern Ocean to Hg in the Antarctic atmosphere especially during cold periods.

6.2 Perspectives

6.2.1 Perspectives for Ir and Pt future studies in polar ice

There are several key questions regarding Ir and Pt fluxes that remain still open. The first is about the possible seasonal character of the meteoric smoke deposition onto the Greenland and Antarctic ice caps, discussed in chapter 2. When compared to the summer snow layers, winter layers could prove to be enriched in meteoric smoke particles. This suggestion could be verified by sampling a snow pit in polar sites characterized by suitable elevated snow accumulation rates such as the Summit site in Greenland. This verification is feasible if significant anthropogenic fallouts of Ir and Pt did not become largely predominant during the last decades. Anthropogenic fallout of Ir and Pt to the polar ice caps would make it impossible to detect of the meteoric smoke signature. This is the case for instance for Pt fallout in Central Greenland which is now dominated by anthropogenic Pt originating especially from automobile catalytic converters [*Barbante et al.*, 2001]. In Antarctica, a possible site for such study could be the geographic South Pole, which is a site with a medium snow accumulation rate and well-preserved annual layers, providing that there was no significant local contamination originating from the station itself.

A second open question is about the intensity of the meteoric smoke fallout to Greenland and Antarctica. In principle, when compared to the Northern Hemisphere, the much stronger polar vortex in the Southern Hemisphere should be responsible for larger fallout of the meteoric smoke to the Antarctic ice cap. Nevertheless, the results presented in chapter 2.3 seem to contradict this hypothesis although a synchronous comparison between the fallout to Central Greenland and to East Antarctica was not

possible. This hypothesis could be verified by analysing ice cores samples from an Antarctic site less influenced by volcanic fallout than Dome C and Vostok during warm periods. A possible candidate for such study could be the core, which is currently drilled as part of the EPICA programme in Dronning Maud Land in the part of Antarctica facing the Atlantic Ocean.

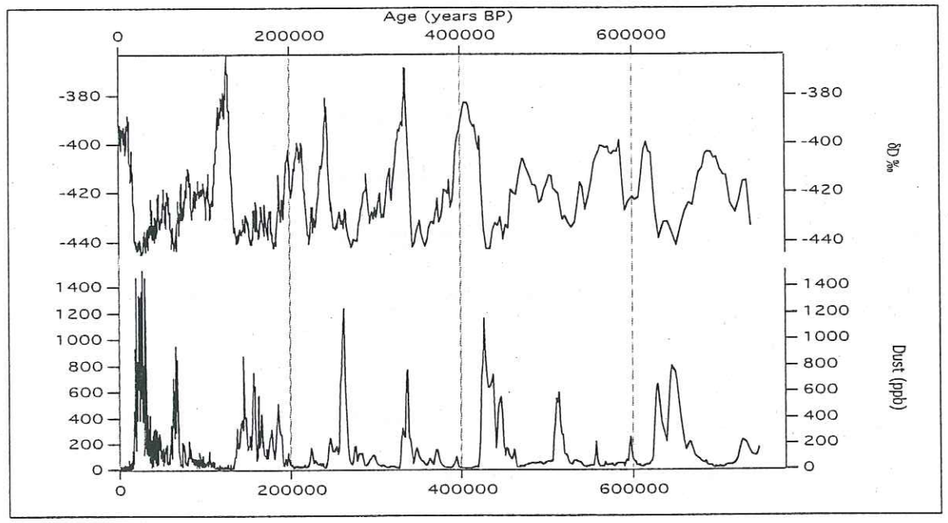

Fig. 8: *Deuterium content expressed in δ per mil units (δD ‰), used as a proxy of past local temperature, and insoluble dust concentration variation in the deep EPICA/Dome C Antarctic ice core during the last 740 kyr [Epica community members, 2004]. This PhD work has investigated the first 220 kyr of this ice record. Further studies will extend the measurements to the previous climatic cycles.*

Of course it will be of great interest to study the meteoric smoke fallout also in the deepest layers of the EPICA/Dome C and the Vostok ice cores, possibly back to almost about 1 million years (see Fig. 8). In the upper part of these ice cores, the non-chondritic fallout mentioned above occurring during interglacials and warm interstadials did not allow to clearly verifying if a glacial/interglacial variations in the cosmic flux occurred at the time of the glacial terminations [*Muller and MacDonald*, 1995]. The deepest part of Epica/Dome C and the Vostok ice core could give a completely different answer.

In addition, an interesting change in the "cosmic flux mode" could have occurred in the deepest part of these ice cores. The enhanced ice thinning occurring at great depths of these ice cores "compresses the time" spanned by each core section (from typically ~50 years m^{-1} about 20 kyr ago up to ~1000 years m^{-1} in the deepest part of the EPICA/Dome C ice core about 740 kyr ago). This fact could strongly enhance the probability to capture horizons enriched in Ir and Pt because of the fallout of debris produced by rare impacts of large extraterrestrial bodies striking Earth. This could allow a direct record of the frequency of the occurrence of such rare events that nowadays is largely uncertain.

6.2.2 Analytical further work for Ir and Pt determination in polar ice

As shown in Chapter 2.1, an exceptional sensitivity has been reached for the determination of Ir and Pt concentrations down to the sub-ppq level in polar ice. This innovative method has allowed for the first time to measure the total concentration of these two metals in deep polar ice cores, giving access to the detection of new and

fascinating scientific objects such as the meteoric smoke particles. In the future it will be, however, necessary to further address various analytical issues, which were only partially dealt with in this study because of lack of time. In what follows we give some ideas for future work.

6.2.2.1 Cleanliness of laboratories and ultra pure water

The major issues are not linked with the final analysis with the sensitivities and instrumental detection limits of the Element 2 ICP-SFMS instrument, but rather with the preparation of the ice samples and contamination (blank issues) before the analysis with the Element 2. The ultra clean preparation methods, which were initially developed by Clair Patterson and Claude Boutron at Caltech were optimized for the determination of a single metal, namely lead, down to the ppt level. It happened that these methods also proved to be suitable for various other metals. However, it does not mean that they will be the best for the determination of all trace elements, especially when dealing with extremely low concentrations at the ppq level as in the case of Ir and Pt.

It remains to be demonstrated that conventional class 10,000 clean laboratories and class 100 laminar flow clean benches, are sufficient for a satisfying control of air contamination when dealing with Ir and Pt at the sub-ppq level. The assumption that significant Ir and Pt episodes of contamination are unlikely to occur, because of the depletion of these elements in airborne dust, might not be justified at the sub-ppq level. New research is needed to investigate that airborne Ir and Pt contamination is not a problem in the clean laboratories, such as the tests performed for lead in the clean laboratory of the Department of Applied Physics of Curtin University of Technology (CUT) [*Vallelonga et al.*, 2002].

The major concern regards the relatively high concentration level of Ir and Pt detected in the ultra pure water (about 1 ppq) when compared with the lowest Ir and Pt concentrations found in polar ice (about 0.2 ppq). Ultra pure water is produced both in Grenoble and in Venice by using ion exchange resins ("Maxy" system in Grenoble [*Boutron*, 1990] and "Elga" system in Venice). We have shown during our work that the relatively high concentrations levels of Ir and Pt in such water cannot have significantly affected the concentrations determined in polar ice samples (See Chapter 2.2). However, it would be wise in the future to modify the system used for the production of the ultra pure water in order to lower the Ir and Pt concentration. A possibility could be to combine ion exchange resins and distillation, although the ultra pure water produced at the CUT using such a combination [*Chisholm et al.*, 1995] proved to have higher Ir and Pt concentrations (~2 ppq) than the Grenoble and Venice ultra pure water. In that respect, it is interesting to mention that Anbar and co-workers claimed that Ir concentration in the ultra pure water which they produced by triple successive distillation was as low as ~ 0.01 ppq [*Anbar et al.*, 1997]. Of course, the technique used to produce this water is certainly not the only parameter to be considered. Equally important are for instance the problem of the possible contamination during the transfer of the ultra pure water to the storage containers and during storage itself.

6.2.2.2 Decontamination procedure

The chiselling technique used in this work for the decontamination of the core sections provided highly reliable data for various trace elements in deep ice cores. It has however several limitations.

One limitation is that the method is very time consuming. This means that it does not allow the analysis of a large number of samples. As a consequence, it does not allow to study rare and interesting discrete events such as the impact of large extraterrestrial bodies or the detailed study of important paleo-climatic problems, such as the glacial-interglacial transitions. During the last few years, new methods have been developed with the aim of obtaining continuous variation profiles of trace elements in Alpine and Greenland ice cores [*Knusel et al.*, 2003; *McConnell et al.*, 2002]. It would be interesting to determine if the cleanliness of such methods can be improved sufficiently to allow for the reliable determinations of trace elements at the ppt or sub-ppt level in deep Antarctic ice. Especially, it will be necessary to be able to clearly determine the procedural blanks of these methods.

Another limitation of the chiselling procedure used in our work is the fact that stainless steel chisels are used. The choice of the exact kind of stainless steel was initially made by Clair Patterson at Caltech. He systematically analysed many different kinds of stainless steels (an other kinds of metals) for lead but not for Ir and Pt and selected the one with the lowest lead concentration. In that respect, it is interesting to mention that Rocchia and co-workers [*Rocchia et al.*, 1990] have shown that stainless steel filters, with an Ir content of the order of ~200 ppb, did contaminate their filtered ice samples. During a preliminary test conducted during this work by pre-concentrating ultra pure acidified (0.1 % ultra pure HNO_3) water, that was taken from a cleaning bath where stainless steel knives were immersed for several months,

Ir and Pt concentration of about 10 ppq and 100 ppq, respectively, have been determined. These relatively high values might be evidence of a slight release of Ir and Pt after a long immersion of our stainless steel knives in diluted HNO_3. This case is certainly extreme and far from the normal operation procedure performed during a typical decontamination when stainless steel knives are in contact only briefly with the solid ice sample.

By decontaminating an artificial ice core, it was demonstrated that in most cases the Ir and Pt contamination originating from the stainless steel knives is negligible. However, we cannot exclude that, very occasionally, stainless steel particles could contaminate the ice samples, hampering Ir and Pt determinations. It would be, therefore, of interest to test other materials, such as for instance ceramics [*Tao et al.*, 2001] or titanium, to eventually replace the stainless steel if these other materials proved to be better.

6.2.2.3 Pre-concentration procedure

As described in chapters 2.1 and 2.2, this is probably the most delicate step in the determination of Ir and Pt. We have made many tests to confirm the validity of the method for Ir and Pt, as described in chapter 2.2. Especially, these tests have shown that the release of Ir and Pt from the PFA Teflon beakers is negligible during the pre-concentration procedure by sub-boiling evaporation. However, this issue is not completely clear in the case of Ir. For instance, preliminary tests made by voluntarily overheating three empty PFA beakers for 15 minutes on a hotplate, evidenced a surprising release of Ir (10 ppq) to the ~1 ml of acidified (0.1 % HNO_3) ultra pure water which was introduced afterwards in the beakers. Of course, it should be kept in mind that such conditions are extreme and are not reached during the pre-

concentrations of the real samples. However, such tests suggest that the walls of the PFA beakers do contain some Ir and that it might eventually be released in particular conditions. It might then be interesting to try to find alternative pre-concentration procedures, for instance based on sublimation [*Tao et al.*, 2001].

6.2.2.4 ICP-SFMS determinations

The Element 2 MS has shown an impressive sensitivity for measuring elements with high atomic weight such as Ir and Pt. However, a traditional problem for ultra trace elements analysis is the lack of adequate certified reference material in which the elements are present at levels more or less similar to those we have in polar snow and ice. Faced with this unsolved problem, a possible strategy could be to organise inter calibration exercises between the most advanced laboratories in the trace elements field such as those which were organized in the past by the U.S. National Science Foundation for trace element in sea water.

Due to the pre-concentration procedure, another new emerging issue concerns the possibility that matrix effects could become surprisingly important even when analysing the ultra pure polar ice matrix. A concentration of ~ 5 ppm of insoluble dust in a typical glacial Greenland sample becomes about 0.5 mg/g if the sample is pre-concentrated (~ x 100) for Ir and Pt analysis. This might not be a negligible matrix. Preliminary tests made by adding various amounts of Ir and Pt to a pre-concentrated sample of fresh Alpine snow have suggested that there might be some matrix effects which could enhance the ICP-SFMS signals.

It is worth to mention that such possible matrix effect could also act positively or negatively during the formation of interfering species such as, in the case of Ir and Pt, the Hf oxides. Hf oxides formation is currently evaluated with Hf

standards prepared from ultra pure water and therefore not subject to any matrix effect. It might be advisable in the future to prepare standards calibration curves, which would better reproduce the matrix of real samples. Such standards solutions could tentatively be obtained by pre-concentrating large quantities of natural matrixes, then by adding the standards. Alternatively it would be worth to test a more absolute analytical method of determination, such as high flux neutron activation analysis on the solid (un-melted) ice samples [*Boutron et al.*, 1984]. This was not possible during our work because of the lack of time. It should, however, be mentioned that we decided to reduce the pre-concentration factors to minimize possible matrix effects.

6.2.3 Trace elements in the EPICA/Dome C ice core

In the future it will be essential to work investigations on the successive interglacial periods, during which the trace element content of the ice is not obscured by a contribution from crustal dust. Of special interest will be the study of the marine isotopic stage 11 (about 400 kyr ago), which was an exceptionally long interglacial stage which characteristics rather similar to our present interglacial [*Epica community members*, 2004]. Also, it will be particularly interesting to study the successive interglacial periods between 430 kyr and 740 kyr ago. During that time period the interglacial periods were less warm but a higher proportion of each climatic cycle was spent in the warm mode [*Epica community members*, 2004].

6.2.4 Isotopes in Antarctic ice cores

In the future, it will be interesting to extend the Pb isotope record obtained in this work to the previous climatic cycles covered by the EPICA/Dome C ice core, back to ~740 kyr BP [*Epica community members*, 2004]. Also, it will be interesting to determine lead isotopes in the Vostok ice core during the last 4 climatic cycles[*Petit et al.*, 1999]. To take full advantage of such data, it will, however, be mandatory to have a better knowledge of the isotopic signature of rock and soil in the different potential source areas in South America, South Africa and Australia, by analysing rock and soil samples from these different areas as was done for Nd and Sr isotopes [*Delmonte et al.*, 2004].

Also, it will be interesting to combine the Pb isotopes data with isotopic data obtained for other elements. Very valuable data have already been obtained for Sr and Nd by Delmonte and co-workers [*Delmonte et al.*, 2004]. Recent analytical improvement open the way for obtaining Sr isotopes variation profile with higher time resolution [*Burton et al.*, 2004; *Burton et al.*, 2002].

Another possibility could be to investigate changes in U isotopes during successive climatic cycles. There are indeed recent indications that U isotopes could be very valuable proxy of climatic changes [*Robinson et al.*, 2004]. Finally, Os isotopes could provide with unique information of past impacts of large rare extraterrestrial bodies [*Turekian*, 1982].

6.2.5 Hg in Antarctic ice cores

In the future it will be important to focus investigations on the successive interglacial periods in the EPICA/Dome C and in the VOSTOK ice core. Special attention should be given to the further study of the mechanism regulating the past

deposition of Hg on continental part of Antarctica in order to determine if Mercury Depletion Events recently registered in the Arctic and in the Antarctic atmosphere are recent phenomena or common episodes occurring under determinate conditions during the past climatic cycles.

REFERENCES

Alvarez, L. W., W. Alvarez, F. Asaro, and H. V. Michel, Extraterrestrial cause for the Cretaceous/Tertiary Extinction, *Science, 208*, 1095-1108, 1980.

Anbar, A. D., D. A. Papanastassiou, and G. J. Wasserburg, Determination of iridium in natural waters by clean chemical extraction and negative thermal ionization mass spectrometry, *Anal. Chem., 69*, 2444-2450, 1997.

Anbar, A. D., G. J. Wasserburg, D. A. Papanastassiou, and P. S. Andersson, Iridium in natural water, *Science, 273*, 1524-1528, 1996.

Anders, E., and N. Grevesse, Abundances of the elements: Meteoritic and solar, *Geochim. Cosmochim. Acta, 53*, 197-214, 1989.

Barbante, C., G. Cozzi, G. Capodaglio, K. Van de Velde, C. Ferrari, A. Veysseyre, C. F. Boutron, G. Scarponi, and P. Cescon, Determination of Rh, Pd, and Pt in polar and alpine snow and ice by double-focusing ICPMS with microcentric nebulization, *Anal. Chem., 71*, 4125-4133, 1999.

Barbante, C., A. Veysseyre, C. Ferrari, K. Van de Velde, C. Morel, G. Capodaglio, P. Cescon, G. Scarponi, and C. F. Boutron, Greenland snow evidence of large scale atmospheric contamination from platinum, palladium and rhodium, *Environ. Sci. Technol., 35*, 835-839, 2001.

Barker, J. L. J., and E. Anders, Accretion rate of cosmic matter from iridium and osmium contents of deep-see sediments, *Geochim. Cosmochim. Acta, 32*, 627-645, 1968.

Berger, A., Milankovitch Theory and Climate, *Rev. Geophys., 26*(4), 624-657, 1988.

Bertsh Mc Grayne, S., Lead-free gasoline and Clair C. Patterson, in *Prometheans in the Lab: Chemistry and the Making of the Modern World*, pp. 169-197, McGraw-Hill, New York, 2002.

Boutron, C. F., A clean laboratory for ultralow concentration heavy metal analysis, *Fresenius J. Anal. Chem., 337*, 482-491, 1990.

Boutron, C. F., M. Leclerc, and N. Risler, Atmospheric trace elments in Antarctic Prehistoric ice collected at a coastal ablation area, *Atmos. Environ., 18*(9), 1947-1953, 1984.

Boutron, C. F., and C. Lorius, Trace metals in Antarctic snow since 1914, *Nature, 277*, 551-554, 1979.

Boutron, C. F., and C. C. Patterson, Lead concentration changes in Antarctic ice during the Wisconsin/Holocene transition, *Nature, 323*(6085), 222-225, 1986.

Boutron, C. F., C. C. Patterson, P. V.N., and N. I. Barkov, Preliminary data on changes of lead concentrations in Antarctic ice from 155,000 to 26,000 years BP, *Atmos. Environ., 21*(5), 1197-1202, 1987.

Burton, G. R., J. P. Candelone, L. Burn, C. F. Boutron, S. Hong, and K. Rosman, Lead and strontium isotope ratios of dust in Greenland ice respond to climatic change, *Submitted to Geophys. Res. Lett.*, 2004.

Burton, G. R., V. I. Morgan, C. F. Boutron, and K. Rosman, High-sensitivity measurments of strontium isotopes in polar ice, *Anal. Chim. Acta, 469*, 225-233, 2002.

Candelone, J. P., S. Hong, and C. F. Boutron, An improved method for decontaminating polar snow and ice cores for heavy metals analysis, *Anal. Chim. Acta, 299*, 9-16, 1994.

Charlson, R. J., J. E. Lovelock, M. O. Andraea, and S. G. Warren, Oceanic phytoplankton, atmospheric sulphur, cloud albedo and climate, *Nature, 326*, 655-661, 1987.

Chisholm, W., K. Rosman, C. F. Boutron, J. P. Candelone, and S. Hong, Determination of lead isotopic ratios in Greenland and Antarctic snow and ice at picogram per gram concentrations, *Anal. Chim. Acta, 311*, 141-151, 1995.

Dansgaard, W., S. J. Johnsen, H. B. Clausen, D. Dahl-Jensen, N. S. Gundestrup, C. U. Hammer, C. S. Hvidberg, and J. P. Steffensen, Evidence for general instability of past climate from a 250- Kyr ice core record, *Nature, 364*, 218-220, 1993.

Delmonte, B., I. Basile-Doelsch, J. R. Petit, V. Maggi, M. Revel-Rolland, A. Michard, E. Jagoutz, and F. E. Grousset, Comparing the Epica and Vostok dust records during the last 220,000 years: stratigraphical correlation and provenance in glacial periods, *Earth-Sci. Rev., 66*, 63-87, 2004.

Epica community members, Eight glacial cycles from an Antarctic ice core, *Nature, 429*, 623-628, 2004.

Evans, N. J., D. C. Gregoire, R. A. F. Grieve, W. D. Goodfellow, and J. Veizer, Use of platinum-group elements for impactor identification: terrestrial impact craters and Cretaceous-Tertiary boundary, *Geochim. Cosmochim. Acta, 57*, 3737-3748, 1993.

Farley, K. A., and D. B. Patterson, A 100-kyr periodicity in the flux of extraterrestrial 3He to the sea floor, *Nature, 378*, 600-603, 1995.

Fresco, J., H. W. Weiss, R. B. Phillips, and R. A. Askeland, Iridium in sea-water, *Talanta, 32*(88), 830-831, 1985.

Gabrielli, P., A. Varga, C. Barbante, C. F. Boutron, G. Cozzi, V. Gaspari, F. Planchon, W. Cairns, S. Hong, C. Ferrari, and G. Capodaglio, Determination of Ir and Pt down to the sub-femtogram per gram level in polar ice by ICP-SFMS using preconcentration and a desolvation system, *J. Anal. At. Spectrom., 19*, 831-837, 2004.

Ganapathy, R., The Tunguska explosion of 1908: Discovery of meteoric debris near the explosion site and at the South Pole, *Science, 220*, 1158-1161, 1983.

Gorlach, U., and C. F. Boutron, Preconcentration of lead, cadmium, copper and zinc in water at the pg/g level by non boiling evaporation, *Anal. Chim. Acta, 236*, 391-398, 1990.

Hildebrand, A. R., and W. V. Boynton, Proximus Cretaceous-Tertiary impact deposits in the Caribbean, *Science, 248*, 843-847, 1990.

Hodge, V., M. Stallard, K. Minoru, and E. D. Goldberg, Determination of platinum and iridium in marine waters, sediments and organisms, *Anal. Chem., 58*, 616-620, 1986.

Hong, S., J. P. Candelone, C. C. Patterson, and C. F. Boutron, Greenland ice evidence of hemispheric lead pollution two millenia ago by Greek and Roman civilization, *Science, 256*, 1841-1843, 1994.

Hong, S., J. P. Candelone, C. C. Patterson, and C. F. Boutron, History of ancient copper smelting pollution during Roman and medieval times recorded in Greenland ice, *Science, 272*, 246-249, 1996a.

Hong, S., J. P. Candelone, C. Turetta, and C. F. Boutron, Changes in natural lead, copper, zinc and cadmium concentrations in central Greenland ice from 8250 to 149,100 years ago: their association with climatic changes and resultant variations of dominant source contribution, *Earth Planet. Sci. Lett., 143*, 233-244, 1996b.

Hong, S., A. Lluberas, and R. F., A clean protocol for determining ultralow heavy metals concentrations: its applications to the analysis of Pb, Cd, Cu, Zn and Mn in Antarctic snow, *Korean J. Pol. Res., 11*, 35-47, 2000.

Hunten, D. M., R. P. Turco, and O. B. Toon, Smoke and dust particles of meteoric origin in the mesosphere and stratosphere, *J. Atmos. Sci., 37*, 1342-1357, 1980.

Imbrie, J., E. A. Boyle, S. C. Clemens, A. Duffy, W. R. Howard, G. Kukla, J. Kutzbach, D. G. Martinson, A. McIntyre, A. C. Mix, B. Molfino, J. J. Morley, L. C. Peterson, N. G. Pisias, N. G. Prell, M. E. Raymo, N. J. Shakmeton, and J. R. Toggweiller, On the structure and origin of major glaciation cycles. Linear responses to Milankovich forcing., *Paleoceanography, 7*, 701-738, 1992.

Jitaru, P., and F. C. Adams, Solid-phase Microextraction and Multicapillary Gas Chromatography Hyphenated to Inductively Coupled Plasma-Time-of-Flight-Mass Spectrometry, *In press J. Chromatography A.*, 2004.

Jouzel, J., J. R. Petit, R. Souchez, N. I. Barkov, V. Y. Lipenkov, D. Raynaud, M. Stievenard, N. I. Vassiliev, V. Verbeke, and F. Vimeux, More Than 200 Meters of Lake Ice Above Subglacial Lake Vostok, Antarctica, *Science, 286*, 2138-2141, 1999.

Kane, T. J., and C. S. Gardner, Lidar observation of the meteoric deposition of mesospheric metals, *Science, 259*, 1297-1300, 1993.

Karner, D. B., J. Levine, R. A. Muller, F. Asaro, M. Ram, and M. R. Stolz, Extraterrestrial accretion from the GISP2 ice core, *Geochim. Cosmochim. Acta, 67*(4), 751-763, 2003.

Knusel, S., D. E. Piguet, M. Schwikowski, and H. W. Gaeggeler, Accuracy of Continuous Ice-Core Trace-Element Analysis by Inductively Coupled Plasma Sector Field Mass Spectrometry, *Environ. Sci. Technol.*, 2003.

Lorius, C., L. Merlivat, J. Jouzel, and M. Pourchet, A 30,000 yr isotope climatic record from Antarctic ice, *Nature, 280*, 644-648, 1979.

Love, S. G., and D. E. Brownlee, Heating and thermal transformation of micrometeoroids entering the Earth's atmosphere, *Icarus, 89*, 26-43, 1991.

Martin, J. H., Glacial-interglacial CO2 change: The iron hypothesis, *Paleoceanography, 5*, 1-13, 1990.

McConnell, J. R., G. W. Lamorey, S. W. Lambert, and K. C. Taylor, Continuous Ice-Core Chemical Analyses Using Inductively Coupled Plasma Mass Spectrometry, *Environ. Sci. Technol., 36*, 7-11, 2002.

Monnin et al, E., Atmospheric CO2 concentrations over the last glacial termination, *Science, 291*, 112-114, 2001.

Muller, R. A., and G. J. MacDonald, Glacial cycles and orbital inclination, *Nature, 377*, 107-108, 1995.

Murozumi, M., T. J. Chow, and D. B. Patterson, Chemical concentrations of pollutant lead aerosols, terrestrial dusts and sea salts in Greenland and Antarctic snow strata, *Geochim. Cosmochim. Acta, 33*, 1247-1294, 1969.

Murphy, D. M., D. S. Thomson, and T. M. J. Mahoney, In situ measurments of organics, meteoric material, mercury, and other elements in aerosol at 5 to 19 kilometers, *Science, 282*, 1664-1669, 1998.

Ng, A., and C. C. Patterson, Natural concentrations of lead in ancient Arctic and Antarctic ice, *Geochim. Cosmochim. Acta, 45*, 2109-2121, 1981.

Nriagu, J. O., The rise and fall of leaded gasoline, *Sci. Total Environ., 92*, 12-38, 1990.

Nriagu, J. O., Automotive lead pollution: Clair Patterson's role in stopping it, in *Clean Hands: Clair Patterson's Crusade Against Environmental Lead Contamination*, edited by C. I. Davidson, pp. 79-92, Nova Science, Commack New York, 1999.

Patterson, C. C., Age of meteorites and the earth, *Geochim. Cosmochim. Acta, 10*, 230-237, 1956.

Patterson, C. C., and D. M. Settle, The reduction of orders of magnitude errors in lead analysis of biological materials and natural waters by evaluating and controlling the extent and sources of industrial lead contamination introduced during sample collection and analysis, *National Bureau of Standards Spec. Publ., 422*, 321-351, 1976.

Patterson, C. C., G. Tilton, and M. Inghram, Age of Earth, *Science, 121*, 69-75, 1955.

Petit, J. R., J. Jouzel, D. Raynaud, N. I. Barkov, J. M. Barnola, I. Basile-Doelsch, M. Bender, J. Chappellaz, M. Davis, G. Delaygue, M. Delmotte, V. M. Kotlyakov, M. Legrand, V. Y. Lipenkov, C. Lorius, L. Pépin, C. Ritz, E. Saltzman, and M. Stievenard, Climate and atmospheric history of the past 420,000 years from the Vostok ice core, Antarctica, *Nature, 399*, 429-436, 1999.

Planchon, F., C. F. Boutron, C. Barbante, E. W. Wolff, G. Cozzi, V. Gaspari, C. Ferrari, and P. Cescon, Ultrasensitive determination of heavy metals at the sub-picogram per gram level in ultraclean Antarctic snow samples by inductively coupled plasma sector field mass spectrometry, *Anal. Chim. Acta, 450*, 193-205, 2001.

Planchon, F., P. Gabrielli, A. Dommergue, P. A. Gauchard, C. Barbante, C. F. Boutron, W. Cairns, G. Capodaglio, P. Cescon, G. Cozzi, C. Ferrari, S. A. Nagorsky, A. Varga, and E. W. Wolff, Direct determination of mercury at the sub-picogram per gram levels in polar snow and ice by ICP-SFMS, *J. Anal. At. Spectrom., 19*, 823-830, 2004.

Planchon, F., K. Van de Velde, K. Rosman, E. W. Wolff, C. Ferrari, and C. F. Boutron, One hundred fifty year record of lead isotopes in Antarctic snow from Coatsland, *Geochim. Cosmochim. Acta, 67*, 693-708, 2003.

Plane, J. M. C., Atmospheric Chemistry of Meteoric Metals, *Chem. Rev., 103*, 4963-4984, 2003.

Plane, J. M. C., A new time-resolved model of the mesospheric Na layer: constraints on the meteor input function, *Atmos. Chem. Phys. Disc., 4*, 39-69, 2004.

Plane, J. M. C., B. J. Murray, X. Chu, and C. S. Gardner, Removal of Meteoric Iron on Polar Mesospheric Clouds, *Science, 304*, 426-428, 2004.

Prather, M. J., and J. M. Rodriguez, Antarctic ozone: meteoric control of HNO3, *Geophys. Res. Lett., 15*(1), 1-4, 1988.

Rasmussen, K., H. B. Clausen, and K. G. W., No iridium anomaly after the 1908 Tunguska impact: evidence from a Greenland ice core, *Meteoritics, 30*, 634-638, 1995.

Rees, D., and D. Bilitza, COSPAR International Reference Atmosphere: 1986, Part II: Middle atmosphere models, *Adv. Space Res., 10*(1), 1990.

Robinson, L. F., G. M. Henderson, L. Hall, and I. Matthews, Climatic Control of Riverine and Seawater Uranium-Isotope Ratios, *Science, 306*, 851-854, 2004.

Rocchia, R., B. P., C. Jehanno, E. Robin, M. de Angelis, and D. Boclet, Search for the Tunguska event relics in the Antarctic snow and new estimation of the cosmic iridium accretion rate, in *Global Catastrophes in Earth History*, vol. 247, edited by S. V. L. and W. P. D., pp. 189-193, 1990.

Russel III, J. M., A. F. Tuck, L. L. Gordley, J. H. Park, S. R. Drayson, J. E. Harries, R. J. Cicerone, and P. Crutzen, Haloe Antarctic observations in the spring of 1991, *Geophys. Res. Lett., 20*(8), 719-722, 1993.

Schuraytz, B. C., D. J. Lindstrom, L. E. Marìn, R. R. Martinez, D. W. Mittlefehldt, V. L. Sharpton, and S. J. Wentworth, Iridium metal in Chicxulub impact melt: forensic chemistry on the K-T smoking gun, *Science, 271*, 1573-1576, 1996.

Takahashi, H., Y. Yokoyoma, E. L. Fireman, and C. Lorius, Iridium content of polar ice and accretion rate of cosmic matter, *Lunar Planet. Sci., 9*, 1131-1133, 1978.

Tao, G., R. Yamada, Y. Fujikawa, A. Kudo, J. Zheng, D. A. Fisher, and R. M. Koerner, Determination of trace amounts of heavy metals in arctic ice core samples using inductively coupled plasma mass spectrometry, *Talanta, 55*, 765-772, 2001.

Turekian, K. T., Potential of 187Os/186Os as a cosmic versus terrestrial indicator in high iridium layers of sedimentary strata, in *Geological implications of impacts of large asteroids and comets on the Earth*, vol. 190, edited by L. T. Shultz and P.H., pp. 243-249, 1982.

Vallelonga, P., K. Van de Velde, J. P. Candelone, C. Ly, K. Rosman, C. F. Boutron, V. I. Morgan, and D. J. Mackey, Recent advances in measurment of Pb isotopes in polar ice and snow at sub-picogram per gram concentrations using thermal ionisation mass spectrometry, *Anal. Chim. Acta, 453*, 1-12, 2002.

Vandal, G. M., W. F. Fitzgerald, C. F. Boutron, and J. P. Candelone, Variations in mercury deposition to antarctica over the past 34,000 years, *Nature, 362*, 621-623, 1993.

Watson, A. J., D. C. E. Bakker, A. J. Ridgwell, P. W. Boyd, and C. S. Law, Effect of iron supply on Southern Ocean CO2 uptake and implications for glacial atmospheric CO2, *Nature, 407*, 730-733, 2000.

Wayne, R. P., Chemistry of Atmospheres. An Introduction to the Chemistry of the Atmospheres of Earth, edited by R. P. Wayne, Oxford University Press, Oxford, 2000.

Wedepohl, K. H., The composition of the continental crust, *Geochim. Cosmochim. Acta, 59*, 1217-1232, 1995.

Wolff, E. W., and E. D. Suttie, Antarctic snow record of Southern Hemisphere lead pollution, *Geophys. Res. Lett., 21*, 781-784, 1994.